



Universidade do Minho
Escola de Engenharia

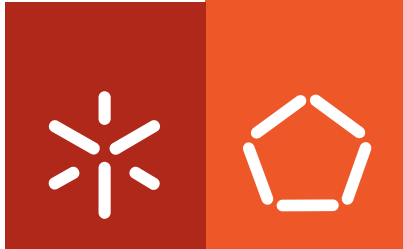
Fábia Karine Andrade

**Development of Structures Based
on Bacterial Cellulose for the
Production of Vascular Prostheses**

Fábia Karine Andrade, **Development of Structures Based on Bacterial Cellulose
for the Production of Vascular Prostheses**

UMinho | 2010

Setembro de 2010



Universidade do Minho
Escola de Engenharia

Fábia Karine Andrade

**Development of Structures Based
on Bacterial Cellulose for the
Production of Vascular Prostheses**

Tese no Programa de Doutoramento em Engenharia Biomédica

Trabalho efectuado sob a orientação do
Doutor Miguel Gama
e da
Doutora Lucília Domigues

Setembro de 2010

É AUTORIZADA A REPRODUÇÃO PARCIAL DESTA TESE APENAS PARA EFEITOS DE INVESTIGAÇÃO, MEDIANTE DECLARAÇÃO ESCRITA DO INTERESSADO, QUE A TAL SE COMPROMETE;

Universidade do Minho, ___/___/_____

Assinatura: _____

À minha querida Mãe,

responsável maior pela minha formação, que sempre me mostrou o valor dos estudos e me ensinou a ter determinação e coragem para vencer as dificuldades. Sempre esteve presente me apoiando, torcendo e acreditando em mim.

Às minhas irmãs Cybelle e Kátia e ao meu pai,

obrigada pelo apoio, carinho, confiança e ajuda durante os momentos de dificuldades.

Ao Bartolomeu,

pelo seu amor, companheirismo e apoio em todos os momentos.

Dedico

Agradecimentos

Agradeço a todas as pessoas que alguma forma me ajudaram na concretização do meu doutoramento. Em especial:

Ao Professor Miguel Gama pela confiança no meu trabalho, orientação, disponibilidade e pelo valioso contributo na elaboração dos artigos e também desta tese.

À professora Lucília Domingues pelo incentivo, disponibilidade e co-orientação deste trabalho.

À professora Raquel Soares pelo apoio, orientação e correcção de artigos desta tese.

À Dra Manuela Carvalho por permitir a realização dos ensaios dos tempos de coagulação no Laboratório de Imuno-hemoterapia do Centro de Trombose e Hemostase do Hospital de São João.

À professora Elisabete Castanheira por me receber em seu laboratório e me ajudar com os ensaios de fluorescência intrínseca do triptofano.

Ao Dr. Duarte N. Paiva e Dr António Peliteiro do São Lázaro Laboratório de Análises Clínicas, Braga – Portugal, pela disponibilidade na coleta de sangue.

Aos seguintes colegas que ajudaram em alguns experimentos dos artigos desta tese: Raquel Costa pela ajuda com ensaios de biocompatibilidade *in vitro*; À Inês Moreira pela ajuda com os ensaios dos tempos de coagulação, à Irina Amorim e profa. Fátima Gartner pelas análise histológicas e ao Nuno Alexandre pela realização e análise dos implantes subcutâneos de celulose.

Aos meus colegas de trabalho: Susana Moreira (uma pessoa sempre disposta à ajudar e ensinar... e como aprendemos com ela!!), Catarina Gonçalves, Vera Carvalho, Renata Pértile, Reinaldo Ramos, David Neri, Orquídea Ribeiro, Sílvia Ferreira, Maria Molinos, Paula Pereira, João Machado, Carla Oliveira, Dina Silvia, Sílvia Pedrosa, Jorge Padrão, Alexandre Leitão e Maria João. Muito obrigada pela agradável amizade, apoio e pelas boas risadas!! Desejo muito sucesso à todos vocês!

Aos colegas do Laboratório de Instalações Piloto (LIP) pela carinho, amizade e por sempre me receberem tão bem em vosso grupo.

Aos vários amigos que fiz nestes 4 anos em Portugal e a quem pude contar em todos os momentos, em especial: Melyssa Negri, Fábio Grassi e o meu afilhado lindo (Henry); Miguel Cerqueira e Tânia Sousa; Augusto Campos (Guga) e Danielly Campos; e Aline Teixeira.

À Coordenação de Aperfeiçoamento de Pessoal de nível Superior (CAPES – Brasil), pelo apoio financeiro.

Summary

Cardiovascular disease is the leading cause of mortality in Western countries. For the reconstruction of arteries with large caliber currently available synthetic grafts offer a reasonable solution and proven clinical efficacy. However, for small sized (<6 mm) grafts these materials generally give poor performance, due to anastomotic intimal hyperplasia and surface thrombogenicity. The production of functional blood vessels by tissue engineering techniques is already possible, however due to the associated costs and lengthy production, the development of new materials appropriated for small diameter blood vessel replacements is still required.

This thesis is a contribute for the improvement of bacterial cellulose for small blood vessel replacements. Among the strategies developed over the years to modify materials for vascular devices, pre-coating with the tripeptide Arg-Gly-Asp (RGD) improves endothelialization thus lowering thrombogenicity. In this work, bifunctional recombinant proteins, with a Cellulose-Binding Module – CBM, from the cellulosome of *Clostridium thermocellum* - and cell binding sequences - RGD, GRGDY – were successfully cloned and expressed in the bacteria *Escherichia coli*. These RGD-containing cellulose-binding proteins were purified and used to coat bacterial cellulose fibres. Bacterial cellulose (BC) secreted by *Gluconacetobacter xylinus* is a material with unique properties and promising biomedical applications. CBMs adsorbs specifically and tightly on cellulose. Thus, they are a useful tool to address the fused RGD sequence (or other bioactive peptides) to the cellulose surface, in a specific and simple way.

In this thesis the effects of chimeric proteins containing a CBM fused to adhesion peptides on the cell adhesion/biocompatibility properties were studied using mouse embryo fibroblasts (3T3) and human microvascular endothelial cells (HMEC) cultures. The results obtained demonstrated that the recombinant proteins containing adhesion sequences were able to significantly increase the attachment and spreading of fibroblasts and HMECs to BC surfaces, specially the RGD sequence. The results also showed that the RGD decreased the ingrowth of the HMEC cells through the BC and stimulated the early formation of cordlike structures by these endothelial cells.

The blood compatibility of native and RGD-modified BC was also studied. The clotting times (aPTT, PT, FT and PRT) and whole blood clotting results demonstrate the hemocompatibility of

BC. A significant amount of plasma protein adsorbed to BC fibres, albumin presenting a higher BC affinity than γ -globulin or fibrinogen. According to analysis carried out by intrinsic tryptophan fluorescence, the BC adsorbed albumin, fibrinogen and γ -globulin do not undergo major conformational modifications. Although the presence of the adhesion peptide on bare-BC surface increases the platelet adhesion, when the material was cultured with human microvascular endothelial cells a confluent cell layer was readily formed, inhibiting the adhesion of platelets.

Once the recombinant protein contains a bacterial CBM, the biocompatibility of native and RGD-CBM treated BC – to analyze whether the presence of the recombinant protein gives rise to any immunologic reaction – was investigated through *in vivo* studies in sheep. The fate of long term subcutaneous BC implants - 32 weeks - was analysed. Histological results showed that BC trigger a biological response typically observed for high surface-to-volume implants. After 1 week of implantation the presence of an inflammatory infiltrate suggests an acute/subacute inflammatory reaction that advance to a chronic inflammation confined to the implantation site and associated to the proliferation of small blood vessels. The presence of giant cells was observed at latter periods (16 and 32 weeks) and a narrow fibrous capsule was present surrounding the implant. BC tubes with small diameter (3mm ID) were produced and its mechanical properties evaluated.

Overall, this work reports the successful functionalization of bacterial cellulose scaffolds with a CBM fused to adhesion peptides, leading to improved blood compatibility and increasing its potential use as blood vessels replacement.

Resumo

As doenças cardiovasculares estão entre as principais causas de morte em países ocidentais. Para a reconstrução de artérias de grande calibre, os enxertos sintéticos actualmente disponíveis oferecem uma solução razoável e com eficácia clínica comprovada. No entanto, como enxertos de pequeno calibre (<6 mm) estes materiais geralmente apresentam mau desempenho, devido a formação de hiperplasia íntima anastomótica e trombogenicidade superficial. A produção de vasos sanguíneos funcionais por meio de técnicas de engenharia de tecidos já é uma realidade, no entanto, devido aos elevados custos e longo tempo de produção, o desenvolvimento de novos materiais adequados para a substituição de vasos sanguíneos de pequeno diâmetro é ainda necessário.

O objectivo geral desta tese foi o melhoramento da matriz de celulose bacteriana (CB) para o seu potencial uso como substituto de pequenos vasos sanguíneos. Entre as estratégias desenvolvidas ao longo dos anos destinadas à modificação de materiais usados como substitutos vasculares, o pré-revestimento com o tripeptídeo Arg-Gly-Asp (RGD) tem melhorado a endotelialização, reduzindo assim a trombogenicidade dos biomateriais. Neste trabalho, proteínas recombinantes bifuncionais, contendo um módulo de ligação à celulose (Cellulose – Binding Module – CBM) – do celulosoma da bactéria *Clostridium thermocellum* - e sequências conhecidas por promover a adesão de células (RGD, GRGDY) foram clonadas e expressas com sucesso na bactéria *Escherichia coli*, sendo posteriormente purificadas e usadas no revestimento de fibras de CB. Os CBMs adsorvem fortemente e especificamente à celulose, assim apresentam-se como uma ferramenta útil para direccionar de maneira simples e específica a sequência RGD (ou outros péptidos bioactivos) às superfícies de celulose.

Nesta tese, os efeitos sobre a adesão celular/biocompatibilidade das proteínas quiméricas produzidas foram estudados usando culturas de fibroblastos de ratinhos (3T3) e células microvasculares humanas (HMEC). Os resultados obtidos demonstraram que as proteínas bifuncionais foram capazes de aumentar significativamente a adesão e o alongamento de fibroblastos e HMECs, além de promover uma distribuição uniforme das células sobre a matriz de celulose. A presença do RGD estimulou a formação antecipada de estruturas tipo-capilares em HMECs, porém diminuiu a invasão destas células na CB.

A hemocompatibilidade da CB nativa e RGD-modificada também foi estudada. Os resultados

mostraram que uma quantidade significativa de proteínas plasmáticas adsorvem às fibras da CB, sendo que a albumina apresentou uma maior afinidade pela CB do que a γ -globulina ou fibrinogênio e que estas mesmas proteínas quando adsorvidas à celulose parecem não sofrer grandes alterações conformacionais. A presença do RGD na superfície da CB não-endotelializada aumentou a adesão de plaquetas, porém quando este material foi revestido com células endoteliais, a adesão de plaquetas foi fortemente inibida.

Uma vez que a proteína recombinante contém um CBM bacteriano, a biocompatibilidade da CB nativa e a tratada com RGD-CBM - para analisar se a presença desta proteína é capaz de originar alguma reação imunológica - foi investigada através de estudos *in vivo*, em ovelhas. Os implantes foram avaliados quanto à reação inflamatória, invasão celular e angiogênese. Os resultados histológicos mostraram que a CB provoca uma resposta biológica tipicamente observada em implantes que apresentam uma grande relação superfície x volume. Uma semana após a implantação a presença de um infiltrado inflamatório sugeriu uma reação inflamatória aguda/subaguda que progrediu para uma inflamação crônica, porém limitada ao local do implante, e associada à proliferação de pequenos vasos sanguíneos. A presença de células gigantes foi observada em períodos tardios e uma cápsula fibrosa delgada estava presente ao redor do implante. Não houve diferença significativa no grau de inflamação entre a CB tratada com RGD-CBM e a nativa. Nesta tese, tubos de CB com pequenos diâmetros foram produzidos e suas propriedades mecânicas avaliadas.

De modo geral, este trabalho relata a funcionalização bem sucedida de matrizes de celulose bacteriana através do uso de peptídeos de adesão ligados a um CBM, resultando em uma melhor hemocompatibilidade e assim, aumentando seu potencial como substitutos de vasos sanguíneos.

Publications

This thesis is based on the following original articles:

Andrade FK, Pertile RAN, Dourado F, Gama FM. Bacterial Cellulose: Properties, Production and Applications. In: Lejeune A, Deprez T, editors. Cellulose: Structure and Properties, Derivatives and Industrial Uses: Nova Science Publishers, Inc., 2010. p. 427-458. (*Adapted* - Chapter 1)

Andrade FK, Moreira SM, Domingues L, Gama FM. Improving the affinity of fibroblasts for bacterial cellulose using carbohydrate-binding modules fused to RGD. J Biomed Mater Res A 2010 Jan;92A(1):9-17. (Chapter 2).

Andrade FK, Costa R, Domingues L, Soares R, Gama M. Improving bacterial cellulose for blood vessel replacement: Functionalization with a chimeric protein containing a cellulose-binding module and an adhesion peptide. Acta Biomater 2010 May 12;6:4034–4041. (Chapter 3).

Andrade FK, Silva JP, Carvalho M, Castanheira EMS, Soares R, Gama M. Studies on the hemocompatibility of Bacterial Cellulose. (*Submitted* - Chapter 4).

Andrade FK, Alexandre N, Amorim I, Gartner F, Mauricio AC, Luís AL, Gama M. Studies on the Biocompatibility of Bacterial Cellulose. (*Work still in progress* - Chapter 5).

Table of contents

Agradecimientosv

Summary.....vii

Resumoix

Publications.....xi

List of Abbreviations.....xv

List of Figures.....xix

List of Table.....xxv

Aims and thesis outline..... 1

CHAPTER 1 – GENERAL INTRODUCTION

Tissue Engineering of small diameter vascular grafts.....5

Bacterial cellulose: properties, production and applications33

CHAPTER 2

Improving the affinity of fibroblasts for bacterial cellulose using carbohydrate – binding modules fused to RGD71

CHAPTER 3

Improving bacterial cellulose for blood vessel replacement: functionalization with a chimeric protein containing a cellulose-binding module and an adhesion peptide89

CHAPTER 4

Studies on the hemocompatibility of bacterial cellulose.....111

CHAPTER 5

Studies on the biocompatibility of bacterial cellulose.....141

CHAPTER 6

General conclusions and future perspectives.....167

List of abbreviations

ADP	Adenosine diphosphate
AMP	Adenosine monophosphate
aPTT	Activated partial thromboplastin time
ATP	Adenosine triphosphate
BC	Bacterial cellulose
BCA	Bicinchoninic acid
BSA	Bovine serum albumin
CBM	Cellulose-binding module
CBS	Calf bovine serum
CipA	Cellulosome integrating protein A
CryoSEM	Cryo-scanning electron microscopy
DAPI	4',6-diamidino-2-phenylindole
DMEM	Dulbecco's modified Eagle medium
DNA	Deoxyribonucleic acid
EC	Endothelial Cell
ECM	Extracellular matrix
ePTFE	expanded poly(tetrafluoroethylene)
FBR	Foreign body reaction
FBS	Foetal bovine serum
FITC	Isothiocyanate
FT	Fibrinogen time
GPa	GigaPascal
GRGDS	Gly-Arg-Gly-Asp-Ser
GRGDY	Gly-Arg-Gly-Asp-Tyr
HE	Haematoxylin – eosin
HFG	Human fibrinogen
His-tag	Polyhistidine-tag
HMWK	High-molecular-weight kininogen
HSA	Human serum albumin
HUVEC	Human endothelial cell

ID	Internal diameter
IG	Human γ -globulin
IPTG	Isopropyl-D-thiogalactopyranoside
kDa	kiloDalton
LDH	Lactic acid dehydrogenase
MPa	MegaPascal
MTS	3-(4,5-dimethylthiazol-2-yl)-5-(3-carboxymethoxyphenyl)-2-(4-sulfophenyl)-2H-tetrazolium)
MW	Molecular weight
NO	Nitric oxide
PBS	Phosphate buffered saline
PC	Protein C
PCR	Polymerase chain reaction
PET	poly(ethylene terephthalate)
PMN	Polymorphonuclear neutrophilic leucocytes
PMSF	Phenylmethylsulfonyl fluoride
PPP	Platelet-poor plasma
PRP	Platelet-rich plasma
PRT	Plasma recalcification time
PT	Prothrombin time
PU	Polyurethane
REDV	Arg-Glu-Asp-Val
RGD	Arg-Gly-Asp
SDS-PAGE	Sodium dodecyl sulfate polyacrylamide gel electrophoresis
SEM	Scanning electron microscopy
SIS	Small intestinal submucosa
SMCs	Smooth muscle cells
TEMED	N,N,N',N'-Tetramethylethylenediamine
TEVs	Tissue engineered vessels
TM	Thrombomodulin
TS	Tensile strength

VEGF	Vascular endothelial growth factor
vWF	Von Willebrand factor
XG	Xyloglucan
YIGSR	Tyr-Ile- Gly-Ser-Arg

List of figures

Chapter 1

Figure 1. The arterial blood vessel (Sarkar et al. 2007 [10])

Figure 2. Metabolic and synthetic functions of endothelial cells: secretion of mediators that are able to influence cellular function throughout the body. LDL, low-density lipoprotein (Galley and Webster, 2004 [9]).

Figure 3. Schematic representation of endothelial functions related to procoagulation and anticoagulation. NO, nitric oxide; PAF, platelet activating factor; PGI₂, prostacyclin; t-PA, tissue plasminogen activator; TXA₂, thromboxane A₂; UK, urokinase; vWF, von Willebrand factor; WPb, Weibel–Palade body; AT III, Antithrombin III. Adapted from Michiels, 2003 [15].

Figure 4. Mechanisms of clotting factor interactions. Clotting is initiated by either an intrinsic or extrinsic pathway with subsequent factor interactions which converge upon a final, common path (Ratner et al., 1996[18]).

Figure 5. Vascular prostheses. (a) Tissue engineering blood vessel (non-exogenous scaffold) produced by L'Heureux and colleagues [55], (b) Dacron, (c) ePTFE.

Figure 6. Endothelial cell interact by integrin family of cell-matrix receptors with the wall bound RGD-sequence and adhere to the vascular graft. Adapted from Walluscheck et al., 1996 [108].

Figure 7. Publications and patents on bacterial cellulose.

Figure 8. Bacterial cellulose pellicle produced by ATCC 10245 *G. xylinus* strain in static culture.

Figure 9. Scanning electron microscopy of bacterial cellulose. Fibroblasts adhered on bacterial cellulose membranes after 24h in culture (Left, 1000x); detail of BC membranes surface (Right, 10.000x).

Chapter 2

Figure 1. *Gluconacetobacter xylinus* (ATCC 53582) cultured on liquid Hestrin-Schramm medium after 7 days. The medium was inoculated with the culture and added to the 24-well polystyrene plate (1 mL/per well) and incubated statically at 30 °C.

Figure 2. Construction of the gene fusion encoding adhesion peptide and the Linker-CBM. (A) Construction containing one copy of the adhesion peptide at the N-terminal of the CBM; (B) Construction containing two copies of the adhesion peptide.

Figure 3. Analysis by SDS-PAGE of recombinant protein expression and nickel column protein purification. 1-

Molecular weight marker (250 kD, 150 kD, 100 kD, 75 kD, 50 kD, 37 kD, 25 kD, 20 kD); 2-Insoluble fraction; 3-Soluble fraction; 4- Column filtrate; 5 to 9-Eluted fraction with 300 mM of Imidazole. (A) CBM; (B) RGD-CBM; (C) RGD-CBM-RGD; (D) GRGDY-CBM; (E) GRGDY-CBM-GRGDY.

Figure 4. Fluorescent microscopy showing the binding of recombinant proteins to cell membranes. The arrows point with respect to some of the fluorescent cells. (A) RGD-CBM; (B) GRGDY-CBM; (C) CBM.

Figure 5. Photographs showing the effect of the recombinant proteins on cell (fibroblasts 3T3) attachment to polystyrene plate. (A) RGD-CBM, (B) RGD-CBM-RGD, (C) GRGDY-CBM, (D) GRGDY-CBM-GRGDY, (E) CBM, (F) Buffer, and (G) Control. The photographs were taken at 1, 5, 24, and 48 h after addition of cells.

Figure 6. MTS assays of fibroblast culture on polystyrene plates treated with the recombinant proteins (CBM, RGD-CBM, RGD-CBM-RGD, GRGDY-CBM, and GRGDY-CBM-GRGDY). The MTS test was developed at 1, 5, 24, and 48 h after addition of cells.

Figure 7. Analysis by SDS-PAGE of the interaction between the recombinant proteins with the cellulose sheets. Line 1, 10, and 11 - Molecular weight marker (250 kD, 150 kD, 100 kD, 75 kD, 50 kD, 37 kD, 25 kD, 20 kD); line 2, 3 - RGD-CBM; line 4, 5 - RGD-CBM-RGD; line 6, 7 - GRGDY-CBM; line 8, 9 - GRGDY-CBM-GRGDY; line 12, 13 - CBM. Lines 3, 5, 7, 9, and 13 represent the proteins after the interaction with BC sheets.

Figure 8. MTS assays of fibroblast culture treated with the recombinant proteins (CBM, RGD-CBM, RGD-CBM-RGD, GRGDY-CBM, and GRGDY-CBM-GRGDY) at the bacterial cellulose pellicles. The MTS test was developed at 2, 24, and 48 h after addition of cells.

Chapter 3

Figure 1: MTS assays of HMEC-1 culture on BC-H pellicles treated with the recombinant proteins (CBM, RGD-CBM, RGD-CBM-RGD, GRGDY-CBM and GRGDY-CBM-GRGDY) and buffer. The MTS assay was developed at 2, 24, 48 hours and 7 days after cells addition. Results are expressed in absorbance values at 490nm.

Figure 2: MTS assays of HMEC-1 culture on BC-L pellicles treated with the recombinant proteins (CBM, RGD-CBM, RGD-CBM-RGD, GRGDY-CBM and GRGDY-CBM-GRGDY) and buffer. The MTS assay was developed at 2, 24, 48 hours and 7 days after cells addition. Results are expressed in absorbance values at 490nm.

Figure 3: MTS assays of HMEC-1 culture on BC-H pellicles treated with CBM, RGD-CBM and buffer. The MTS test was developed at 15, 30, 60, 90 and 120 minutes after addition of cells. Results are expressed in absorbance values at 490nm.

Figure 4: Fluorescence photographs of endothelial cells stained with LIVE/DEAD® Viability/Cytotoxicity Kit for mammalian cells. Live cells are stained in green and dead cells are stained in red. BC-L treated with RGD-CBM

(a), CBM (b) and buffer (c). Controls with cells on polystyrene, live (d) and dead (e). Images were acquired using objectives 40x (scale 50 μ m).

Figure 5: Apoptosis was quantitatively evaluated by the TUNEL assay. The HMEC cells were seeded on the BC-L and after 24h of incubation the TUNEL assay was performed. Bars represent the percentage of apoptotic cells evaluated by the ratio between TUNEL-stained cells and DAPI-stained nuclei in every culture. Experiments were repeated three times with identical results.

Figure 6: Effect of RGD on the HMEC cell invasion through bacterial cellulose pellicles. Invasion was quantified in a double-chamber assay using medium complemented with 20% FBS as a chemoattractant. Bars represent the number of invasive cells.

Figure 7: Images (a), (b) and (c) – optical microscopy photographs showing the effect of the RGD on the assembly of endothelial cells into capillary-like structures. BC-L treated with RGD-CBM (a), CBM (b) and buffer (c). Image was acquired using objective 20x (scale 200 μ m). Image (d) – Fluorescent microscopy image showing HMECs cells cultured at 14 days on BC-L pellicle treated with RGD-CBM recombinant protein. Nuclei were visualized by staining with DAPI (blue) and f-actin with Alexa Fluor 546-phalloidin (red). Image was acquired using objective 20x (scale 100 μ m).

Figure 8: SEM micrographs of bacterial cellulose. BC treated with RGD-CBM (a, b); CBM (c, d) and buffer (e, f). The arrows remark cells with elongated morphology. (a), (c) and (e) scale 50 μ m; (b), (d) and (f) scale 5 μ m.

Figure 9: Immunocytochemical analyses using anti-vWF antibody. The results showed that HMEC cells cultured after 14 days on BC-L treated with recombinant proteins or buffer stained positively for vWF. (a) RGD-CBM, (b) CBM and (c) buffer. Image was acquired using objective 20x (scale 100 μ m).

Chapter 4

Figure 1: Plasma protein adsorption onto the bacterial cellulose membrane untreated or treated with the recombinant proteins (RGD-CBM or CBM) and controls (ePTFE and polystyrene). (a) Platelet-poor plasma; (b) human serum albumin; (c) human γ -globulin and (d) human fibrinogen.

Figure 2: Comparison of the adsorption isotherms for the binding human serum albumin (HSA), human fibrinogen (HFG) and human γ -globulin (IG) on BC.

Figure 3: Percentage of desorbed proteins on BC at each concentration tested after treatment with 1wt% aqueous solution of SDS. Human serum albumin (HSA), human fibrinogen (HFG) and human γ -globulin (IG).

Figure 4: Steady-state fluorescence emission spectra of (a, b) human serum albumin, (c, d) human fibrinogen and (e, f) human γ -globulin adsorbed on BC and in solution. (a, c, e) and (b, d, f) excitation wavelength of 295 nm and 270, respectively, collected from 305 to 400 nm.

Figure 5: Comparison of anticoagulation time (aPTT, PT and FT) of BC membranes untreated or treated with the recombinant protein (RGD–CBM) and the controls (ePTFE, polystyrene and glass microspheres). The coagulation times of PPP non–contacted with the materials (pre–incubation control) were also analysed.

Figure 6: Clotting kinetic profiles of the absorbance at 405nm as a function of time for PPP incubated with polystyrene, BC (hydrated and lyophilized), glass microspheres and ePTFE (a). Citrated PPP (without the addition of calcium) serves as a negative control. The data was averaged over five independent experiments. The half-max time of each profile (b) was calculated as a measure of the clotting time.

Figure 7: The effect of BC, ePTFE, polystyrene and glass microspheres on thrombus formation in whole blood at 0, 5, 15, 25 and 35 min.

Figure 8: Relative number of platelets adhered on ePTFE and BC membrane untreated or treated with the recombinant proteins (RGD–CBM or CBM).

Figure 9: SEM images of BC membrane and ePTFE surface after contact with PRP for 2 hours. Column II (scale bar 5 μ m) is the magnified images of Column I (scale bar 20 μ m).

Figure 10: SEM images of the adhered platelets on endothelialized BC untreated or treated with recombinant proteins and ePTFE. The bare BC and ePTFE were used as controls. The captions without “bare” indicate the cultured HMEC surface. Column II and IV (scale bar 10 μ m) is the magnified images of Column I and II (scale bar 30 μ m), respectively.

Figure 11: Densities of adhered platelets on endothelialized BC untreated or treated with recombinant proteins and ePTFE. The bare BC and ePTFE were used as controls.

Chapter 5

Figure 1. Bacterial cellulose produced by *G. xylinus* (ATCC 53582) grows around the silicon tube, when an air flow is injected through the tube. a) Schematic picture of the cultivation system; b) Bacterial cellulose tube.

Figure 2. MTS assays of fibroblast cultures at the dense or porous side of BC membrane. The MTS assay was developed at 2, 72 and 7 days after cell seeding. Results are expressed as absorbance values at 490 nm.

Figure 3. Fluorescent microscopy images showing fibroblast cultured 7 days on BC pellicle. (a) Dense and (b) porous side of RGD–treated BC; (c) Dense and (d) porous side of untreated BC. Nuclei were visualized by staining with DAPI (blue) and f–actin with Alexa Fluor 546–phalloidin (red). Actin and nuclei combined images were acquired using objectives 10x (scale 200 μ m); Nuclei images were acquired using objectives 20x (scale 100 μ m).

Figure 4. CryoSEM micrographs of bacterial cellulose cultured with fibroblasts after 14 days. (a) Dense and (b) porous side of RGD–treated BC; (c) Dense and (d) porous side of untreated BC. Scale 10 μ m.

Figure 5. CryoSEM micrographs of bacterial cellulose tubes. Visualization through a longitudinal cut of (a) Inner side (b) outer side. Visualization through a transversal cut of (c) Inner side (d) outer side. Scale 60 μm (longitudinal images), scale 10 μm (transversal images).

Figure 6. Tensile stress-strain curves of the lengthwise of BC tubes with an inner diameter and wall thickness of 3 mm and 1 mm, respectively.

Figure 7. Histomorphology of bacterial cellulose membrane implanted subcutaneously in sheep and surrounding tissue reaction. Once there were no significant differences in biological responses by the host, the images represent the results for both groups of the post-implantation times analyzed. (a) 1, (b) 2, (c) 4, (d) 8, (e) 16 and (f) 32 weeks post-implantation. (a, b, c, d), (e) and (f), 40x, 100x and 400x ampliation, respectively (Hematoxylin - eosin staining). The solid arrows indicate the fibrous capsule formation. The dashed arrow on image (f) indicates small blood vessels formation. (*) Bacterial cellulose.

List of tables

Chapter 1

Table 1. Characteristics and desirable features of the ideal vascular graft.

Table 2. Methods for blood vessel replacement.

Table 3. Summary of surface modification to enhance endothelialization (in chronological order).

Table 4. Summary of biomedical applications of bacterial cellulose.

Table 5. Functions of CBMs in CAZyme

Chapter 2

Table 1. PCR primers with the restriction sites NheI (GCTAGC) and XhoI (CTCGAG) used for cloning the gene fusions encoding the adhesion peptide with CBM.

Chapter 4

Table 1: Hemolysis of blood after contact with BC surfaces and ePTFE.

Chapter 5

Table 1. Comparison of the mechanical properties of BC tubes (3mm of inner diameter and 1mm of wall thickness) produced in this present work with BC tubes produced by Putra et al.[48], human arteries and veins and common polymers used as vascular grafts (collagen and PTFE).

Aims and thesis outline

Bacterial cellulose (BC) produced by *Acetobacter* microorganisms, is a glucose polymer with unique properties, including high water holding capacity, high crystallinity, an ultrafine fiber network, and high tensile strength, thus holding great potential for biomedical applications. The aim of this work was the development of a new approach to functionalise BC, through recombinant proteins containing adhesion peptides conjugated with a cellulose binding-module. The use of recombinant proteins containing a CBM domain, exhibiting high affinity and specificity for cellulose surfaces, allows the control on the interaction of this material with cells. To achieve this aim, bifunctional recombinant proteins with CBM – from the cellulosome of *Clostridium thermocellum* – and cell binding sequences (RGD, GRGDY) were cloned and expressed in *Escherichia coli*. Thereafter, the potential use of these recombinant proteins in improving biocompatibility/blood compatibility was studied.

Chapter 1 presents a revision of these subjects, namely 1) The role of endothelium and the tissue engineering of small diameter vascular grafts; 2) properties and biomedical applications of bacterial cellulose.

Chapter 2 describes the strategies used to produce the bifunctional recombinant proteins containing bacterial CBM from *C. thermocellum* fused to a RGD or GRGDY sequences. In this chapter a mouse embryo fibroblasts culture was selected and used in adhesion/biocompatibility *in vitro* assays as animal cells model to test our strategy in modified bacterial cellulose.

Once the general aim of this work is the improvement of BC as scaffold to the production of small vascular graft chapter 3 describes the *in vitro* study of the effect of these chimeric proteins in Human microvascular endothelial cell cultured on BC.

Although BC is promising material for vascular replacements, to our knowledge only very recently a first publication was dedicated to evaluate the thrombogenic properties of this biomaterial. However, further characterization is necessary, not only to confirm the promising hemocompatibility of BC, but also to better understand the BC-blood interaction, through more comprehensive characterization. Thus chapter 4 describes a blood compatibility study of BC.

Biocompatibility is one main requirement for any biomedical material. In chapter 5 we complete the *in vitro* biocompatibility study using fibroblast cultures. Also, the fate of long term subcutaneous implants in sheep – 32 weeks – was analysed to evaluate the *in vivo* biocompatibility of BC membranes. Once the chimeric protein used in this work contains a bacterial CBM the biocompatibility of BC membranes treated with the RGD–CBM protein was investigated. Finally we developed preliminaries studies on the mechanical properties of BC tubes.

In the last chapter of this thesis (chapter 6) are presented the general conclusion of this work and the future perspectives.

Chapter 1

GENERAL INTRODUCTION

Tissue Engineering of small diameter vascular grafts

The prevalence of atherosclerotic arterial disease is increasing in an ageing society [1], the cardiac and peripheral vascular diseases figuring among the major cause of death in the Western world [2]. Vascular grafts are thus required for coronary and peripheral bypass surgeries. Autologous grafts remains the most used treatment, saphenous veins and mammary arteries being preferably used. However, autologous vessels are not available in over 10% of the patients as a result of preexisting vascular disease, amputation or previous harvest for prior vascular procedures. Moreover, a second surgical procedure is needed to obtain the vessel [3, 4].

The ideal vascular graft must meet a number of requirements: appropriate mechanical attributes that mimic the mechanical properties of a native vessel, being capable of withstanding long-term hemodynamic stress without material failure, good suturability and easy handling during the surgical procedure, appropriate permeability to water, solutes and cells. Furthermore, it should exhibit physiological properties such as vasoconstriction/relaxation, induce acceptable postimplantation healing not resulting in inflammation, hyperplasia, or fibrous capsule formation, leading to the integration of the graft into the body. Finally, a fully biocompatible graft should be nonimmunogenic and resistant to both thrombosis and infection [3] (TABLE 1).

Unfortunately, no conduit to date possesses all of these qualities and attributes. Although acceptable patency rates are achievable using current commercially available prosthetic material, such as polyethylene terephthalate (PET, Dacron) or expanded polytetrafluoroethylene (ePTFE), which performs well as large-caliber replacements, small-diameter (less than 6 mm) prosthetic conduits have unacceptably poor patency rate. This is the result of low-flow conditions within a narrow conduit and compliance mismatch between prosthesis and native artery. Intimal hyperplasia and the inherent thrombogenicity of prosthetic materials are further major contributing factors [5].

Table 1. Characteristics and desirable features of the ideal vascular graft.

Biocompatible
No healing disturbances
Non-toxic
Non-allergic
No induction of malignancies
Minimally traumatic to blood compounds
Non-thrombogenic
Resistant to infection
Compliant
Flexible, elastic, without kinking
Resistant to myointimal hyperplasia
Vasoactivity
Appropriate permeability
Easy processing
Adequate physical and chemical properties, mechanical durability
Readily available in a variety of sizes and lengths
No need for special storage or preparation procedures
Easy to suture
Sterilisation
Optional
Capable of local drug delivery
Low costs

(Adapted from Teebken and Haverich, 2002 [6])

The endothelium

The whole circulatory system has a common basic structure and consists of three different layers (FIGURE 1), from innermost to outermost: first, the tunica intima, constituted exclusively of endothelial cells (ECs) which are only one layer thick, supported by a basement membrane and delicate collagenous tissue, is the only layer of vascular tissue which comes into contact with blood; second, an intermediate muscular layer which is named the tunica media, composed of many layers of smooth muscle cells (SMCs) and an outer supporting tissue layer called the tunica adventitia. This last layer is composed primarily of loosely woven collagen fibers and can also contain small capillaries to provide nutrients to the outer layers of the tunica media [7]. Endothelial cells, as the inner lining of blood vessels, are strategically located between circulating blood and blood cells and the vascular smooth muscle [8]. Endothelial cell structure and functional integrity are important in the maintenance of the vessel wall and circulatory function. Furthermore, as a barrier, the endothelium is semi-permeable and regulates the transfer of small and large molecules. Endothelial cells are dynamic and have both metabolic and synthetic functions. They exert significant autocrine, paracrine and

endocrine actions and influence smooth muscle cells, platelets and peripheral leucocytes [9]. Endothelial cells have a main role in maintaining a nonthrombogenic blood – tissue interface and regulate thrombosis, thrombolysis, platelet adherence, vascular tone and blood flow (FIGURE 2). The endothelium is indispensable for body homeostasis; an uncontrolled endothelial cell response is involved in many disease processes, including atherosclerosis, hypertension, pulmonary hypertension, sepsis and inflammatory syndromes. These diseases are related to endothelial injury, dysfunction and activation [9].

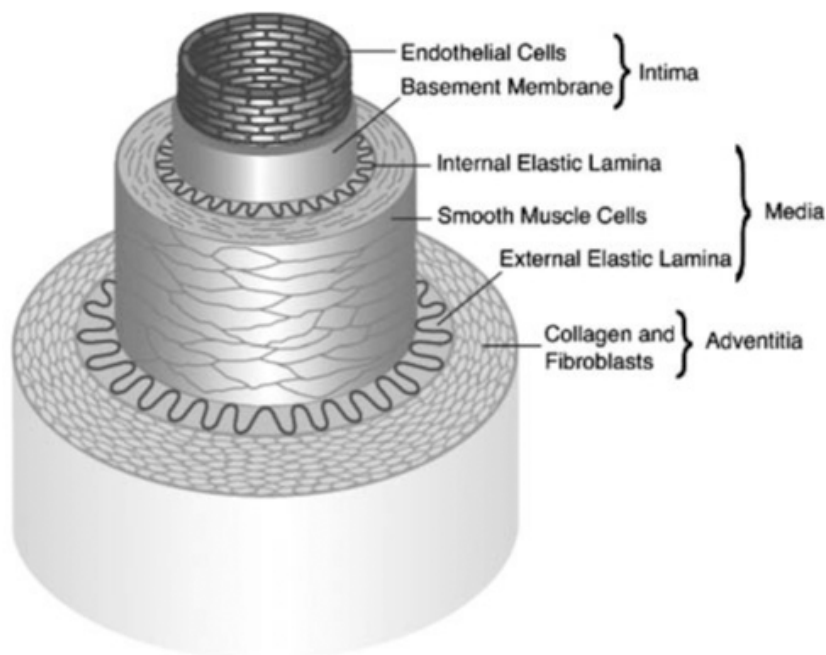


Figure 1. The arterial blood vessel (Sarkar et al. 2007 [10])

Physiological functions of the endothelium:

Anti-thrombotic functions. Under normal conditions the endothelium maintains an equilibrium between the anticoagulant and procoagulant phenotype (FIGURE 3). The anticoagulant activity of the endothelium is geared at restricting the generation of thrombin. At their surface, ECs are lined with a very fine and fragile layer called the glycocalyx, consisting of glycoproteins, glycosaminoglycans and proteoglycans. Globally, the glycocalyx provides an anticoagulant layer because of its negative electrical charge that repels circulating platelets and that allows the interactions with vitamin K-dependent coagulation factors. Also heparan sulfate

and dermatan sulfate, two glyocalyx glycosaminoglycans, potentiate the activity of two anticoagulant enzymes, antithrombin III and heparin cofactor II [11]. ECs produce thrombomodulin (TM) that is either attached to the membrane or released into the circulation. Because TM binds to the same site on thrombin that would normally bind to fibrinogen, platelets or factor V, all of these functions carried out by thrombin are blocked. TM converts thrombin from a procoagulant protease into an anticoagulant and slows down the clotting process. The thrombin/TM complex plays a role as a cofactor in the activation of the zymogen protein C (PC) into activated protein C (APC), which degrades factor V and VIII [12].

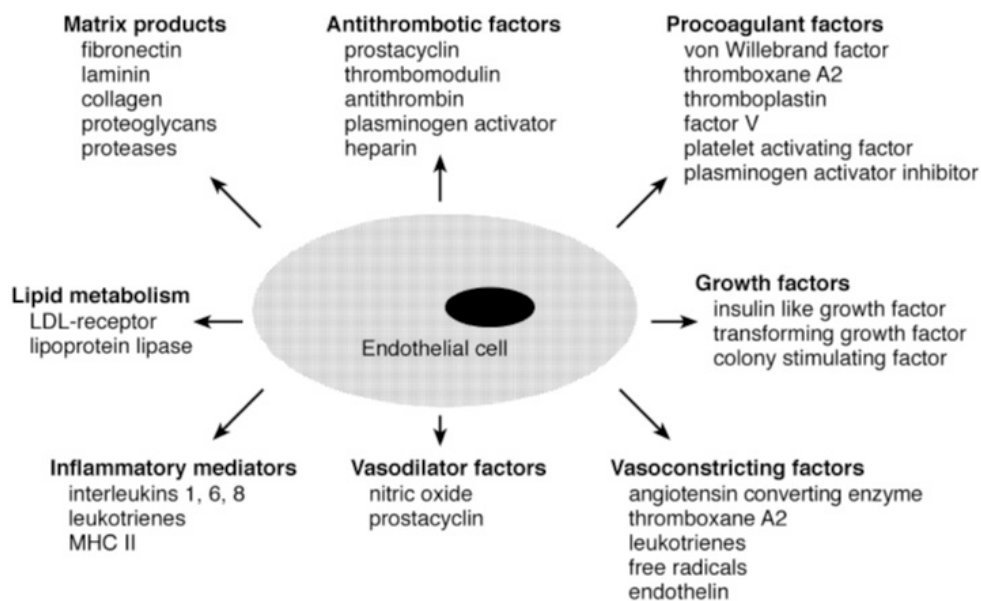


Figure 2. Metabolic and synthetic functions of endothelial cells: secretion of mediators that are able to influence cellular function throughout the body. LDL, low-density lipoprotein (Galley and Webster, 2004 [9]).

In vivo, the initiation of coagulation in response to trauma occurs via the exposure of tissue factors to blood. Tissue factor is the receptor for factor VII and is procoagulant. It is inhibited by tissue factor pathway inhibitor (TFPI), which is synthesized mainly by endothelial cells under basal conditions and is bound to the endothelial cell surface. Tissue factor expression leads to the activation of factor X, which then combines with factor Va to convert prothrombin to

thrombin [13, 14].

The anti-thrombotic functions of ECs also include antiplatelet activity. ECs produce substances such as prostacyclin I₂ (PGI₂) and nitric oxide (NO), both synergistically increase cAMP content in platelets, hence preventing their aggregation. In addition, endothelium also displays ectonucleotidases at its luminal surface. These enzymes hydrolyse ATP and ADP, both potent platelet aggregating agents, into AMP and adenosine [15-17].

Pro-thrombotic functions. The endothelium normally promotes blood fluidity, unless there is an injury. With damage, the normal response is to promote coagulation at the wound site while containing the coagulation response and not allowing it to propagate beyond this site.

At least two mediators released by activated endothelial cells favour platelet activation. The first one is the lipid mediator platelet-activating factor (PAF), synthesized by endothelial cells stimulated by thrombin, histamine, or cytokines. PAF is a potent platelet activator and can promote platelet adhesion to endothelial cells. The second is the von Willebrand factor (vWF) synthesised by EC and stored in vesicles (Weibel-Palade bodies) and secreted upon stimulation by thrombin. Moreover, vWF binds and stabilizes coagulation factor VIII and is a specific factor required for the binding of platelets to exposed extracellular matrix (ECM) components when the vessel wall is damaged [15].

Tissue factor is a glycosylated intrinsic membrane protein that is expressed on the surface of adventitial vascular wall cells and is exposed to flowing blood during vascular injury or endothelial denudation. Endothelial cells do not normally express the primary trigger of the coagulation system, tissue factor. However, when exposed to thrombin, cytokines, or lipopolysaccharides (LPS), endothelial cells synthesize and express tissue factor at their surface. Tissue factor, when bound to factor VIIa, is the major activator of the extrinsic pathway of coagulation [15, 18].

Fibrinolytic activity. During vessel repair a fibrin matrix is formed. The fibrin matrix acts as a barrier preventing further blood leakage and provides a structure for new microvessels to infiltrate in damaged or activated tissue [7]. The fibrinolytic system is responsible for proteolysis and solubilization of the formed clot, allowing its removal. The endothelium participates in fibrinolysis by releasing tissue-type plasminogen activator (t-PA) and urokinase, allowing the transformation of plasminogen into plasmin, which degrades thrombi by digesting

the fibrin network. t-PA is constitutively released while urokinase is only synthesized by activated endothelial cells [11]. It must be noted that the natural inhibitor of t-PA, plasminogen activator inhibitor type 1 (PAI-1) is also constitutively secreted by endothelial cells. The balance of t-PA and PAI-1, which is normally in favor of PAI-1 is also altered by cytokines [19].

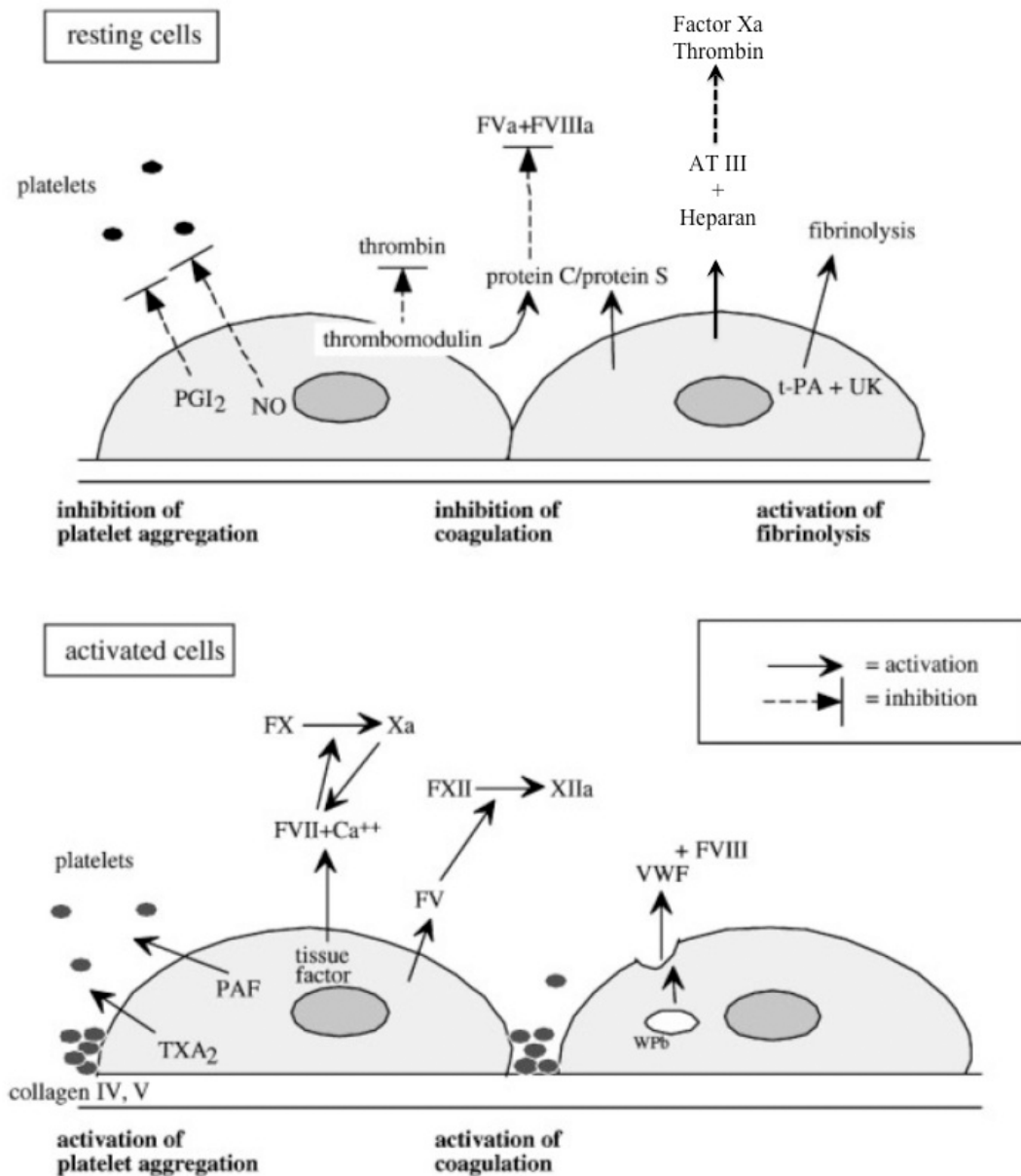


Figure 3. Schematic representation of endothelial functions related to procoagulation and anticoagulation. NO, nitric oxide; PAF, platelet activating factor; PGI₂, prostacyclin; t-PA, tissue plasminogen activator; TXA₂, thromboxane A₂; UK, urokinase; vWF, von Willebrand factor; WPb, Weibel–Palade body; AT III, Antithrombin III. Adapted from Michiels, 2003 [15].

Host defence and inflammation. Endothelial cells play key roles in host defence and inflammation by regulating lymphocyte and leukocyte movement into tissues. At the time of inflammation, due to either tissue injury or infection, several processes occur to facilitate the infiltration of leukocytes into the tissue. Among these are vasodilatation, increased blood flow and release of histamine and inflammatory cytokines. Due to these processes the endothelial cells become activated and interactions with leukocytes occur. The different steps in leukocyte sequestration into the surrounding tissue are tethering, rolling of the leukocyte along the vessel wall, firm adhesion to the endothelial cells, and transmigration through the vascular wall. All these sequential steps in the adhesion cascade are mediated through the intricately regulated expression of adhesion molecules [20].

Regulation of vasomotor tone. The endothelium is a significant contributor to the regulation of vasomotor tone, under the influence of physical and chemical factors originating from the vascular lumen or the surrounding tissues. ECs produce and release vasodilator substances such as NO and prostacyclin, and vasoconstrictor mediators such as endothelin and platelet activating factor (PAF). The production of NO by the endothelium is constitutive and modulated by different stimuli, whereas the synthesis of other mediators (prostacyclin, endothelin and PAF) is inducible [11].

Transport functions. The endothelium is an important barrier to the free passage of molecules and cells from the blood to the underlying interstitium and cells. Specific mechanisms are responsible for the transport of essential circulating blood macromolecules across endothelial cells to the subendothelial space, to meet the metabolic needs of the surrounding tissue cells. In addition, the junctions between endothelial cells (the so called 'tight' junctions) act as a selective barrier to the egress of molecules from the circulation [9].

Angiogenesis. Vascular endothelial growth factor (VEGF) is an angiogenic factor produced by a variety of cells, including endothelial cells, with specific receptors on the endothelium. Angiogenesis – the formation of new blood vessels from pre-existing endothelium – is mediated by VEGF. VEGF contributes to the inflammatory response through stimulation of the release of adhesion molecules, metalloproteinases and NO, via the transcription factor activator protein-1 (AP-1) [9].

Coagulation cascade

Initiation of clotting occurs either intrinsically by surface-mediated reactions, or extrinsically through factors derived from tissues. The two systems converge upon a final common path, which leads to the formation of an insoluble fibrin gel when thrombin acts on fibrinogen. Coagulation proceeds through a “cascade” of reactions by which normally inactive factors become enzymatically active following surface contact, or after proteolytic cleavage by other enzymes. The newly activated enzymes in turn activate other normally inactive precursor molecules. Figure 4 presents a scheme of the clotting factor interactions involved in both the intrinsic and extrinsic systems and their common path.

In the intrinsic system, contact activation refers to reactions following adsorption of contact factors onto a negatively charged surface. This pathway is initiated when factor XII adsorbs to surfaces such as artificial materials, leading to spontaneous cleavage of factor XII into its active form factor XIIa. Factor XIIa converts both prekallikrein and factor XI into their active forms, kallikrein and factor XIa respectively, with high-molecular-weight kininogen (HMWK) as a cofactor. Factor XII, in turn, is a substrate for kallikrein, creating a short reciprocal activation loop, which leads to rapid contact activation. A middle phase of intrinsic clotting begins with the first calcium-dependent step, the activation of factor IX by factor XIa. Factor IXa subsequently activates factor X. Factor VIII is an essential cofactor in the intrinsic activation of factor X, and factor VIII first requires modification by an enzyme, such as thrombin, to exert its cofactor activity. In the presence of calcium, factors IXa and VIIIa form a complex on phospholipid surfaces (as expressed on the surface of activated platelets) to activate factor X. This process is slow in the absence of appropriate phospholipid surfaces and serves to localise the coagulation to the cell surface [18, 21].

The extrinsic system is initiated by the activation of factor VII after interaction with the tissue factor, which is located in the tissue adventitia and comes in contact with blood only after vascular injury. When factor VII interacts with tissue factor, in the presence of calcium ions, factor VII is converted to a serine protease (factor VIIa) by minor proteolysis [22].

The common path begins when factor X is activated by either factor VIIa-tissue factor or by the factor IXa–VIIIa complex. The cofactor V, like factor VIII, is activated by thrombin to factor Va, which together with factor Xa, forms the complex factor Xa-Va that cleaves prothrombin (factor

II) to thrombin in the presence of calcium and phospholipids. Next, thrombin acts on fibrinogen and small peptides from fibrinogen are released. Then, these fibrin monomers polymerize to become a gel. Factor XIII is either trapped within the clot and is activated by thrombin. The factor XIIIa stabilizes the fibrin polymer network and a insoluble fibrin network is formed [18].

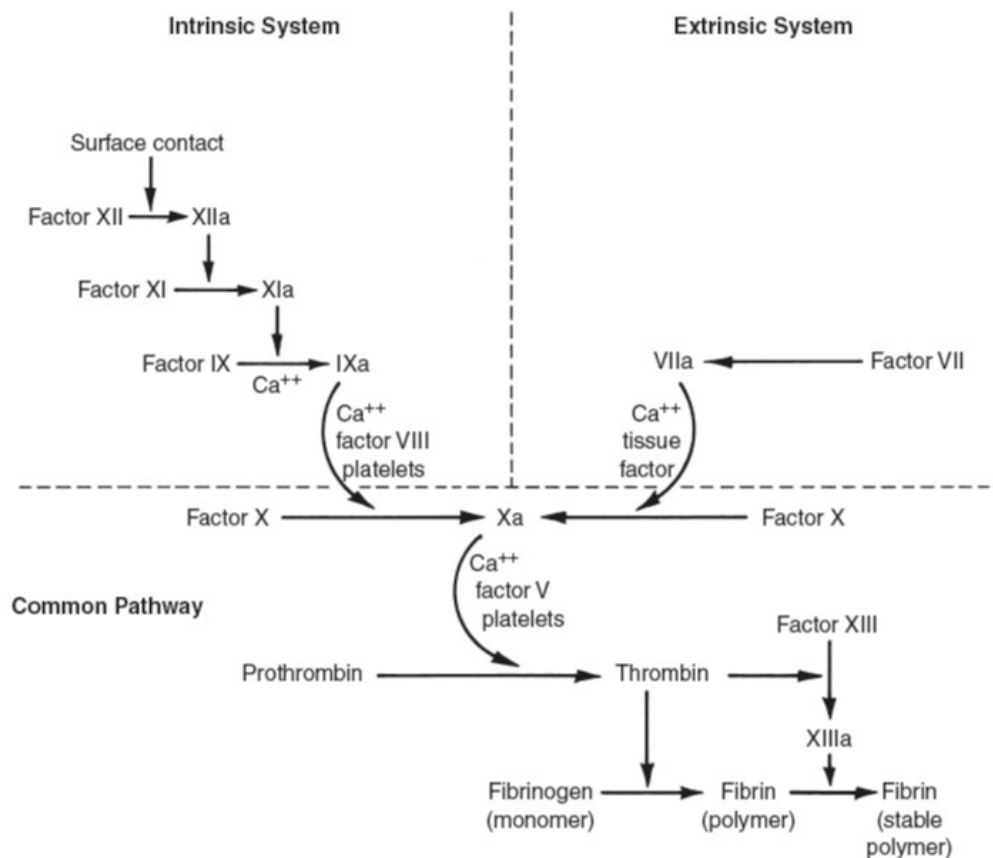


Figure 4. Mechanisms of clotting factor interactions. Clotting is initiated by either an intrinsic or extrinsic pathway with subsequent factor interactions which converge upon a final, common path (Ratner et al., 1996[18]).

Types of vascular grafts

Autografts

Autografts (or autologous graft) are any tissues transplanted from one part of the body to another location in the same individual. The use of venous and to some extent arterial autografts is well established in peripheral vascular surgery. For the reconstruction of small

diameter arteries, as required for lower-extremity bypass and coronary artery bypass grafting procedures, an autologous vein graft is typically used (e.g., saphenous vein); in the case of the coronary artery, an autologous arterial graft may alternatively be used (i.e., internal thoracic artery, gastroepiploic artery, inferior epigastric artery, radial artery) [23, 24]. Although venous and arterial autografts currently yield the best results (Table 2), disadvantages include the need for multiple surgical procedures, with increased risk and cost to the patient. In addition, vein grafts have thin walls that may be damaged when exposed to increased flow and pressure, as the ones present in the arterial circulation. Furthermore, suitable vessels are not available in all patients due to disease, amputation, or previous vessel harvest [25]. Grafting of tubes derived from skin, fascia, pericardium, and dura have been investigated in animal studies and in isolated human cases, and the results were not encouraging due to early thrombosis and aneurysm formation, although autografts from small intestine have shown some promise [6].

Allografts

Fresh or cryopreserved allografts (surgical transplantation of tissue between two genetically dissimilar individuals of the same species) have also been used in the clinic as coronary artery bypass conduits. These grafts are considered superior to artificial prostheses and relatively resistant to infection, enjoy minimal thromboembolic complications, and do not require anticoagulation. Limitations include their reduced availability and durability due to calcification, aneurysmal dilatation, and rupture. Fresh allografts undergo rapid rejection, while cryopreserved allografts have a longer but still limited clinical life [6, 26]. Allografts appear to be a useful choice for (1) the individual with a real need for revascularisation and who is burdened with a limited life expectancy not exceeding the functional life of the allograft, (2) urgent replacement of a major vessel damaged by trauma, [27] in situations where immunosuppression is contraindicated as in an infected surgical field, and (3) in patients whose immune system is already compromised. The allograft probably should not be used (1) simply for the relief of intermittent claudication, (2) in the above mid-calf location, and [27] in other anatomic locations where synthetic grafts perform better [26].

Table 2. Methods for blood vessel replacement.

	Autograft		Allograft	Xenograft	Prosthesis
	Vein	Artery	Different sources	Different sources	Plastic
Authors	[28-32]	[33, 34]	[35-38]	[39, 40]	(Vionion N)[41]; (Teflon)[42]; (Dacron)[43, 44]; (seeded ePTFE)[45]; (Polyurethane)[46].
Examples	Great saphenous vein, arm veins, popliteal vein, superficial femoral vein	Internal and external iliac artery, superficial femoral artery, internal thoracic artery	Artery, great saphenous vein, (Dacron - externally reinforced) umbilical vein, cryopreserved vein segments	Bovine carotid/ internal thoracic artery	Knitted crimped sealed Dacron; externally Reinforced expanded PTFE
Availability	Limited; diameter <1 to >6 mm, segment length <1m	Very limited; diameter, <1 to >8mm segment length cm	Limited/good; diameter 4-6mm, segment length <1 m; special storage (e.g. cooling, liquid nitrogen)	Good; diameter 4-8mm, segment length <40 cm; special storage (e.g. cooling, liquid nitrogen)	Very good; diameter 6 to >30mm, segment length <1m
Long-term results	Complete healing, degeneration and aneurysms are rare, intima hyperplasia	Very good	No complete healing, degenerative disease; calcifications (Dacron reinforcement!); transmission of disease	Degeneration, calcification, intima hyperplasia; transmission of disease (?) - PERV, BSE	Intimal hyperplasia, thrombosis, obstruction, suture aneurysms
5-year patency	~75% (great saphenous vein); ~65% (arm veins)	~95%	~60% (umbilical vein)	~59% (bovine xenografts)	~40% (PTFE); ~80% (EC seeded PTFE)
Compliance mismatch	+	+	(+)	(+)	-
Biocompatibility	+	+	(+)	+	+
Handling	- (preparation, additional wound complications)	- (preparation, additional wound complications)	(+)	(+)	+

Legend: favourable +; less favourable (+); unfavorable - ; PERV = porcine endogenous retro virus; BSE = bovine spongiform encephalitis. Adapted from Teebken and Haverich, 2002 [6].

Xenografts

In contrast to heart valve prostheses, tissue of xenogenic origin for small-diameter vascular grafts is rarely used. In 1964, Rosenberg and colleagues developed arteries derived from bovine sources. These authors created scaffolds, consisting mainly of collagen, by means of enzymatic cellular extraction using a solution of 1% ficin [39]. However, long-term results were not encouraging, due to aneurysm formation, infection, and a high incidence of thrombosis. The antigenicity has a deleterious effect on subsequent endothelialisation. For these reasons use of xenografts cannot be recommended for peripheral vascular reconstruction [6].

Tissue Engineered Grafts

The most common tissue engineering approach involves the use of exogenous scaffolds into which cells are seeded and cultured. These scaffolds provide structural support and allow cell growth, migration, differentiation and cellular ECM production. Ideally, these scaffolds would degrade at the same rate as the natural tissue proliferate and synthesize new ECM. Tissue engineering scaffolds can be made of either natural or synthetic materials.

Natural protein scaffolds. Natural protein scaffolds utilize the components of native ECM and create fully biological grafts. Natural protein scaffolds can be composed of collagen, elastin, fibronectin, or protein hydrogels [47]. Historically, the first adhesive gels were made from collagen [48]. Collagen gels have been shown to yield a high percentage of circumferentially aligned cells, which closely resembles alignment in natural blood vessels. However, these scaffolds do not provide sufficient initial mechanical strength to support normal hemodynamic loading [49]. To improve mechanical properties and increase collagen fiber alignment, collagen has been cross-linked with elastin providing the vessels with a greater elasticity and better mechanical properties [50]. Although the collagen/elastin gels did provide better structural characteristics than pure collagen ones, they still could not withstand the pressures experienced by small diameter arteries [49]. Another advantage is that both collagen and fibrin allow direct cellularization by cell entrapment during the gelation, because this occurs under physiological conditions [3]. On the other hand, natural protein scaffolds are often difficult and expensive to manufacture [47].

Decellularized tissues. After the removal of the original cellular component through sequential protease treatments and detergent extractions, decellularized conduits of natural matrix structures from tissues ranging from cadaveral arteries to umbilical veins and small intestinal submucosa (SIS) xenografts have been tested for their potential to replace vascular matrix and encourage the ingrowth of host cells postimplantation [51]. The use of these natural biomaterials has typically required chemical or physical pretreatment aimed at (1) preserving the tissue by enhancing the resistance of the material to enzymatic or chemical degradation, (2) reducing the immunogenicity of the material, and [27] sterilizing the tissue. Multiple crosslinking techniques have been explored in an attempt to find the ideal procedure to stabilize the collagen-based structure of the tissue while maintaining its mechanical integrity and natural compliance. Decellularized tissues have the advantage of being entirely composed of natural ECM, providing mechanical, chemical and biological advantages over synthetic materials, and thus holding tremendous potential for use in tissue engineering therapies [3].

The decellularization of vascular tissue has the benefit of retaining the structure and composition of a native vessel; however, decellularization can adversely impact the tissue, resulting in reduced ultimate tensile strength and compliance. Significant shrinkage is typically observed in decellularized vessels, presumably as a result of proteoglycans being removed from the tissues by the detergent treatment. Decellularized xenografts undergo aneurysm formation, infection, and thrombosis. In addition, their residual antigenicity can impair subsequent reendothelialization. Another decellularized tissue that has been used for tissue engineering with good deal of success is the matrix derived from small intestinal submucosa (SIS). In addition to the typical ECM components, this scaffold was found to contain a number of growth factors that enhance neovascularization and infiltration of host cells upon implantation [51], promoting site-specific remodeling and regeneration by host [3].

Biodegradable synthetic scaffolds. Synthetic scaffolds serve as temporary structures subsequently replaced by native tissue as they are gradually removed from the implant site through biodegradation [52]. It can be created from a variety of polymers such as polyesters, polyanhydrides, and polyphosphazenes [52]. The most common aim of the use of synthetic polymers as scaffold in tissue engineering is to support tissue growth and remodeling. However, the chemicals and reactions necessary to synthesize these polymer scaffolds are often incompatible with cell survival and cells cannot be directly entrapped during scaffold

formation. Instead, cells must be seeded into the completed scaffolds, posing difficulties in achieving uniform cell distribution and attachment. The scaffold degradation rate must be appropriate to the regrowth of the new tissue, in order to maintain the graft structure and mechanical properties, and to avoid failure [3]. Polyglycolic acid (PGA) is most commonly used as tissue engineering scaffold but is resorbed rapidly. Attempting to improve the mechanical properties and further regulate cell phenotype via interactions with the polymer, numerous other polymers have been copolymerized with PGA, such as poly-L-lactic acid [3]. Although synthetic scaffolds provide initial mechanical strength and structure, compliance mismatch with native vessels has proven difficult to overcome, which can lead to thrombosis formation and failure of the graft [53]. The compliance of vascular grafts once the scaffold has resorbed is the result of cell generated ECM [54]. However, it has been shown that ECM production is inhibited in cells that are in contact with synthetic polymers [50]. This finding has led many researchers to investigate alternatives to synthetic polymer scaffolds.

Non-exogenous scaffolds. Researchers are developing alternative approaches that avoid the use of exogenous scaffolds. In 1998, L'Heureux and colleagues [55] reported a completely biologic vessel generated from human umbilical cord-derived SMCs and ECs, as well as human dermal fibroblasts (FIGURE 5a). Briefly, human SMCs and fibroblasts were grown on culture plates in the presence of elevated ascorbic acid (to induce significant collagen synthesis) to form a sheet with associated extracellular matrix. After sufficient time, the sheet was rolled over a mandrel to form a vascular wall media derived mainly from SMCs. In the same manner, a sheet of skin fibroblast was grown and wrapped around the media to produce the adventitial layer. After maturation, these two layers fused into a single cohesive layer. Then, the tubular support was removed and endothelial cells were seeded in the lumen. The resulting construct showed well-defined multilayer organization in addition to abundant ECM deposition; SMCs demonstrated a reversion to the contractile phenotype by reexpressing desmin (a marker lost under culture condition). The endothelium expressed von Willebrand factor, incorporated acetylated-LDL, produced prostacyclin, and inhibited platelet adhesion *in vitro*, thus exhibiting properties similar to the ones performed by the endothelium of native arteries. These engineered vessels meet the fundamental requirements for grafting: high burst strength (>2000 mm Hg), good surgical handling, suturability, and a functional endothelium. However, although these tissue-engineered blood vessels are more compliant than ePTFE grafts, they are apparently much less compliant than the small-caliber vessels they are designed to replace,

which could potentially lead to complications related to the issue of compliance mismatch, which often leads to anastomotic intimal hyperplasia. In spite of this, short-term grafting experiments in canine model were extremely promising.

In another study from the same group, human tissue engineered vessels (TEVs) were xenografted in immunosuppressed canine model for short term and in immunosuppressed rat and primate models for long-term evaluations [53]. The TEVs were antithrombogenic and mechanically stable though 8 months *in vivo*. It should be noted that in this study, the fabrication process of TEVs differed from the previous study conducted by the same group [55] in the exclusion of the SMC layer, whose early senescence is associated with decreased burst pressures in human models [56]. However, the presence of a smooth muscle-specific α -actin-positive cell population within the TEV suggests the regeneration of vascular media. Moreover, the long time to produce these TEVs (approximately 28 weeks) would limit the application of these vessels in urgent clinical settings. More recently, this group published another study [57] comparing the mechanical properties of completely human TEVs to human saphenous vein and mammary artery. The results demonstrated that the sheet-based tissue engineering approach can consistently produce vessels with mechanical properties similar or superior to those of native vein.

Campbell and co-workers use a method whereby a mandril of foreign material is surgically implanted in the peritoneal cavity of the recipient to induce the growth of tubular tissues [58, 59]. This technique has demonstrated high mechanical strength and good mid-term patency in animal models; because they are grown inside the subject's own body, there is no tissue rejection. However it remains to be seen whether this approach can be repeated in humans.

One approach to creating multilayered constructs more rapidly involves the use of rapid prototyping approaches, including bioprinting. Norotte and colleagues developed a rapid prototyping bioprinting method for scaffold-free small diameter vascular reconstruction. Bioprinting was used to arrange macrofilamentous, sausage-like cell aggregates and acellular agarose rods into tubular vessel-like constructs [60].

Synthetic substitutes

Limited long term success and availability of allografts, which were the first valid vascular replacements, led to the development of synthetic substitutes in the 2nd half of the past century.

Numerous attempts were made using silver, glass, rubber, and so on as grafting materials. A majority of these experiments failed due to early thrombosis, foreign body reaction, or rejection [6]. In 1951, Voorhees and co-workers [27] found that plastic tubes were accepted by the organism as a blood conduit if they had a porous wall and were biocompatible. Materials such as polyester and polypropylene fulfilled these criteria, and artificial conduits were developed as woven or knitted tubes in various forms and sizes.

Dacron and ePTFE. For more than 50 years, Dacron (polyethylene terephthalate) and PTFE (polytetrafluoroethylene) have been used as synthetic vascular prostheses. Both of these molecules are highly crystalline and hydrophobic [5]. Dacron is a thermoplastic polymer resin of the polyester family and is used in synthetic fibers of round cross-section (FIGURE 5b). These fibers are fashioned into multifilament yarns, which can be woven (over-and-under pattern) or knitted (looped fashion) into textile vascular graft fabrics and tubes. A crimping technique (an undulating surface) is sometimes used to increase distensibility and kink-resistance [5]. ePTFE is an expanded polymer which is manufactured by a heating, stretching, and extruding process resulting in a nontextile porous tube composed of irregular-shaped solid membranes ("nodes") (FIGURE 5c). The molecule is relatively biostable, i.e. less prone to deterioration in biological environments than Dacron [61, 62], and the graft surface is electronegative, which minimizes its reaction with blood components. It is characterized by a node-fibril structure, and its average porosity is described by the internodal distance, which is usually 30 to 90 μm . However, the actual available ingrowth spaces between fibrils are much smaller than the internodal distance [5]. In small diameter applications, these two synthetic grafts are highly susceptible to clotting and failure due to a lack of a confluent non-thrombogenic endothelial monolayer. Upon implantation, the luminal surface of the synthetic graft is coated with plasma proteins, and eventually a platelet-fibrin aggregate (pseudointima). This is then covered with an endothelial layer, but only in a 10-15 mm zone from the anastomosis. The pseudointima that is not endothelialized can be subjected to SMC migration and proliferation leading to intimal hyperplasia, or trigger clot formation and thrombosis. Fibrous hyperplasia caused by an over active physiological repair response at the anastomotic site also often leads to failure of the grafts.

Polyurethanes. Polyurethane (PU) is a copolymer that consists of three different monomer types: a diisocyanate hard domain, a chain extender, and a diol soft domain. At physiologic

temperatures, the soft domains provide flexibility, whereas the hard domains impart strength. The most common medical grade polyurethanes are based on soft domains made from polyester, polyether, or polycarbonate [63]. Although PU grafts possess many interesting features, e.g. the presence of a surface that is conducive for seeding, excellent healing, good surgical handling and low suture bleeding, polyurethane grafts have had variable clinically results with a tendency to hydrolytic biodegradation causing aneurysm formation [5]. The latest generation of polycarbonate-based PU is hydrolytically and oxidatively stable, and promoted faster luminal endothelialization and less neointimal formation as small-calibre vascular prostheses [64].

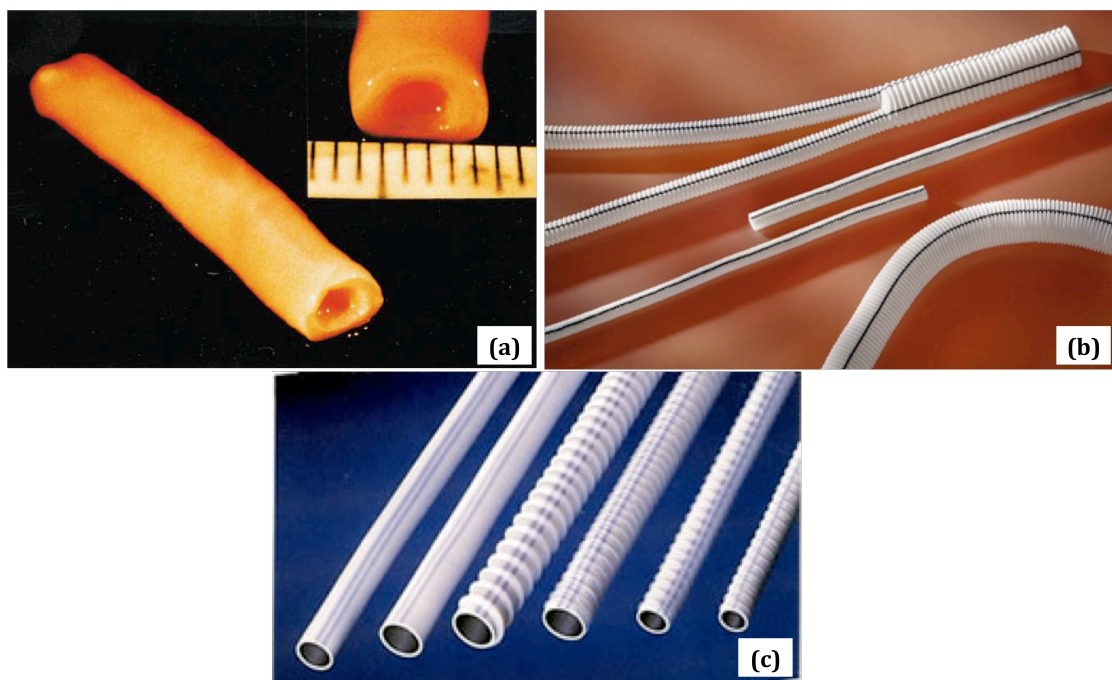


Figure 5. Vascular prostheses. (a) Tissue engineering blood vessel (non-exogenous scaffold) produced by L'Heureux and colleagues [55], (b) Dacron, (c) ePTFE.

Reducing thrombogenicity of vascular grafts

Attempting to produce new biocompatible materials with good performance as vascular conduit, many researchers improved the features of existing synthetic grafts e.g. with regard to surface properties like hydrophilicity and presence of chemical groups, or alternatively by

covalent attachment of bioactive substances, or even the incorporation of autologous vessel wall cells into the vascular graft, where various biological functions of the native vessel are mimicked.

Surface properties modification

This strategy aims the modification of the surface properties of commonly used materials, to minimize reactions at the blood-material/tissue-material interface, avoiding modification of the bulk characteristics. This policy is likely to facilitate introduction of the modified vascular grafts to the market, as less problems with regulatory agencies and acceptance by surgeons are expected.

A film of plasma proteins is immediately deposited on the surface of the vascular graft after the contact with blood, making the foreign material attractive for either platelet adhesion and subsequent platelet aggregation and /or promotion of endothelial cell growth [65-67]. The implant surface qualities are usually described in the categories of texture (roughness), charge (or electrostatic potential) and chemistry. These factors all influence the sequence of protein adsorption and the subsequent platelet adhesion/thrombus formation. Although the mechanism of occlusion and dysfunction of artificial prostheses is multifactorial, all the studies performed suggest that fibrinogen and platelet deposition play a predominant role [67, 68].

The surface electrical charge of vascular graft influences the adhesion of platelets to the graft. It is known that both the blood vessel wall and platelets have electronegative surface charge, which causes their mutual repulsion. Sawyer and colleagues demonstrated that injury to the vessel wall results in the exposition of positively charged material [69]. Although PTFE has a weak negative charge, after implantation a fibrinous layer is formed enhancing the presence of negative charges, contributing to antithrombogenicity and also to antibacterial properties, as those bacteria that are associated with graft infection have electronegative surface properties [70]. A common clinical practice is the coating of PTFE with carbon to increase its electronegativity [71].

Although electronegativity on the graft surface is a prerequisite, this alone will not ensure an antithrombogenic surface, additional surface properties being also critical in determining the platelet reaction. The surface hydrophilicity may confer thromboresistance but that is not to say that all hydrophilic surfaces are thromboresistant [72]. The thrombogenicity of hydrophilic

surfaces has been previously investigated, with variable results. Hydrophilic coatings have been shown to diminish the thrombogenicity of polyurethane catheters [73]. Furthermore, an *in vitro* study demonstrated that hydrophilic surfaces bound less fibrinogen and fewer platelets than did either nonhydrophilic or heparin-coated catheters [74]. However, other studies showed no correlation between hydrophilicity and thromboresistance [75, 76].

Surface properties may be altered by plasma-treatment techniques. Chu and colleagues [77], modified poly(L-lactic acid) (PLLA) with ammonia plasma technique to improve the adhesion of Human endothelial cell (HUVEC) and of rabbit microvascular endothelial cell (RbMVEC). Tseng and Edelman [78] applied amide and amine plasma (butylamine) to ePTFE grafts surfaces using radio frequency glow discharge. The Plasma modified ePTFE vascular grafts showed increased surface hydrophilicity and enhanced the endothelial cell lining under constant and pulsatile flow conditions.

Another approach consists on surface-binding chemical groups. *O*-Carboxymethylchitosan (OCMCS) was covalently immobilized onto ePTFE vascular graft using a photosensitive hetero-bifunctional crosslinking reagent, 4-azidobenzoic acid. The OCMCS-modified PTFE demonstrated good blood-compatibility with reduced fibrinogen adsorption and inhibition of platelet adhesion and activation [79]. Phaneuf and co-workers applied mild hydrolyzation treatment of Dacron with NaOH, which created carboxyl groups at the surface, without significantly decreasing the tensile strength and the sample weight. The introduced groups serve as 'anchor sites' for covalent attachment of plasma albumin to the surface, thus creating a surface with improved biocompatibility [80].

In some other approaches, functional groups were introduced on the surface of the material to immobilize specific proteins. In this way, Chandy et al. [81] modified ePTFE and Dacron with argon plasma and then coated the materials with collagen IV and laminin, subsequently immobilizing bioactive molecules like PGE1, heparin or phosphatidyl choline via the carbodiimide functionalities. The results showed that these biomolecules, immobilized on vascular prostheses, significantly reduced the fibrinogen adsorption and the deposition and spreading of platelets, demonstrating superior biocompatibility. Also PTFE was modified using ammonia plasma or alkylamine plasma to covalently bind collagen, fibronectin or a mixture of both proteins, which improved adhesion of endothelial cells to the surface [82, 83].

Coatings

Porous textile synthetic graft, such as Dacron, are also pervious, sealing being necessary at the time of implantation. Two sealing techniques are known: preclotting of the prosthesis with the patient's own plasma, blood, serum or fibrin glue at the time of implantation, or impregnation of the prosthesis with a bioresorbable substance prior to implantation. Once resorbed, the gap-filling matrices, whether cruoric or proteinic, left in place the porous synthetic structure, which could then be infiltrated by the cicatricial reaction. The preclotting technique consists in making the textile structure of the prosthesis impervious by impregnating it with an adhesive thrombotic matrix. The use of preclotting is as old as textile prostheses [84, 85].

The first sealing molecules used in 1961 were collagen [86], crosslinked or not, and heat-denatured gelatin [87]. Albumin was introduced later on [87].

Collagen. Collagens are the most abundant and ubiquitous proteins in the body of the vertebrates, showing great similitude in all mammals. The collagen molecule is constructed of three helical polypeptide chains that revolve around each other to form a triple helix. Collagen molecules line up by the thousands in regular sequences aligned with their longitudinal axis, thus forming a collagen fibril and these fibrils conglomerate to form a fiber. To be used as a biomaterial, collagen must first be extracted and purified, generally in an acid environment and salt precipitation. It can be prepared in solid form by drying or as a sol (liquid colloidal solution) through dispersion in an acid solution. Collagen is a good choice as impregnant matrix once it is naturally found in connective tissues and has chemotactic properties. [84, 88].

Collagen is advantageous as a sealant since it also improves cell adhesion and migration onto the surface of the prosthesis, thus leading to a better integration with the host tissues [89].

Gelatins. Gelatin is derived from collagen by thermal or chemical processes, applied to destroy the organized structure of water insoluble collagen, to generate a multitude of small hydrosoluble molecules, the gelatin. The production of gelatin requires first the extraction of noncollagenous compounds from the ground tissue, commonly bone or skin, then the transition from collagen to gelatin, and finally the conditioning of gelatin in a dried, solid form. Compared to collagen, the more widespread use of gelatin as an impregnation matrix can be accounted for by its easier production, lower cost, and low thrombogenicity. It replaces collagen in situations where mechanical properties are secondary [84].

Several collagen and gelatin impregnated vascular grafts are nowadays available, some of which have shown to be clinically well tolerated for medium-diameter grafts (5–6 mm) [90]. However, in most of the collagen- and gelatin-coated vascular grafts, glutaraldehyde or formaldehyde is used to crosslink the protein matrix. These crosslinking agents, which are incorporated into the coating, are released during degradation and may evoke cytotoxic reactions [91]. Alternatively, non-toxic carbodiimide can be used to crosslink gelatin in vascular grafts [92].

Albumin. Albumin, synthesized by the liver, is the main plasma protein. Its molecular weight is approximately 69,000 daltons. Albumin can be coagulated and denatured by heat. It can be separated from other plasmatic proteins by either electrophoresis or globulin precipitation in a 27% sodium sulfate solution. Easy production and a low thrombogenicity account for its use in impregnating vascular prostheses [84].

The impregnation has advantage over the preclotting of vascular grafts, once impregnated prostheses are impervious straightaway at the time of implantation, not depending upon the patient's hematologic characteristics (eg. patients under general heparin therapy) and so wards off the risk of preclotting. A reduction in prostheses handling, thanks to suppression of the preclotting stage, may contribute to a decrease in the risk of intraoperative bacterial contamination. On the other hand, some authors have mentioned handling difficulties, which they ascribe to a lack of pliancy in impregnated prostheses [84].

Since crosslinked proteins started to be used to fill the pores of vascular grafts, pre-clotting of the grafts became superfluous. Besides this elementary function, other biological activities have been added to sealants to make them even more useful. The most frequently used additives are anticoagulants and growth factors. More recently, incorporation of antibiotics in sealants has been proposed.

Seeding the surface with endothelial cells

The significant difference in patency between prosthetic and autologous vein grafts could partially be attributed to the presence of viable endothelial cells (ECs) on the luminal surface of autologous veins. These cells are known to prevent thrombosis and intimal hyperplasia actively

and serve as an anticoagulant surface [93]. ECs are therefore interesting as coverage of prosthetic grafts. This is the key rationale behind utilizing autologous ECs to make a hemocompatible artificial polymeric surface that will perform the major functions of an intact healthy endothelium that would normally be found in the blood vessel. This will then provide an anticoagulant and antithrombogenic surface to the circulating blood constituents.

In humans, the natural endothelialization of prosthetic grafts is restricted to a short region around the anastomosis area. Experimental evidence indicated that lack of a confluent EC lining on the surface of prosthetic graft contributes to their failure by thrombosis formation. A cellular engineering approach has been used to overcome this problem by covering *in vitro* the lumen of the graft with ECs, the process known as seeding [94].

There are two types of seeding procedure: one-stage cell seeding, where the endothelial cells of the patient are extracted and immediately used to cover the grafts in the timeframe of the surgical procedure. And the two-stage cell seeding, where after the extraction of the EC from the patient the cells are expanded *in vitro* to obtain a great number of cells to be seeded on the graft (a process known as sodding) before the transplantation. Sodding is needed because many cells are lost from the graft lumen after the pulsatile flow has been restored. The main disadvantage regarding clinical use is that it cannot be used in the emergency situation because of the prolonged cell culture time and the significant chances of failure due to infection of the cells and the inability of the cells to proliferate effectively. In addition, there is the extra cost of a cell culture technician and the need for a cell culture laboratory [94].

The lack of retention of cells can be partly overcome by sodding, but other techniques, involving engineering the lumen to improve cell attachment and retention or stimulate self-endothelialization of the graft have been developed.

Improvement of endothelial cell seeding procedures

Numerous research groups have examined whether modifications of the lumen of the prosthetic graft surface can either stimulate self-endothelialization or improve the attachment and retention of preseeded cells when exposed to arterial flow.

The interaction of ECs with the biomaterial surface has been improved by using different

techniques. One approach consist on promoting non-specific interaction of the cells with the material *via* hydrogen bonding, electrostatic, polar or ionic interactions between the cell membrane and functional chemical groups on the polymers (without any extracellular matrix proteins or their functional parts). In contrast to integrin-mediated cell adhesion, this type of interactions cannot ensure the transmission of adequate signals from extracellular environments into cells and survival of anchorage-dependent cells. If the cells are not able to synthesize and deposit their own ECM molecules in a relatively short time (usually in 24 to 48h after seeding), or they do not have some of these molecules attached on cell membrane, they undergo apoptosis [95].

Functional receptor-mediated and signal-transmitting cell adhesion on a conventional biomaterial is mediated by ECM molecules, such as fibronectin, vitronectin, collagen or laminin [95]. Fibronectin coatings have shown to be the most successful for improving endothelial cell retention. Increased cell attachment is typically seen when fibronectin is used in combination with another protein or ligand [96]. The tripeptide Arg-Gly-Asp (RGD), an amino acid sequence found in many adhesive plasma and extracellular matrix protein, has been used to enhance cell adherence [97-103] (FIGURE 6). Other peptide sequences found to enhance endothelial cell adhesion include YIGSR (Tyr-Ile- Gly-Ser-Arg) [104], derived from laminin and REDV (Arg-Glu-Asp-Val), which is present in a domain of fibronectin and binds endothelial cells selectively, without binding fibroblast, smooth muscle cells, or platelets [105, 106]. The success of this approach has been limited, due to coatings being washed off with high flow rates [94, 107] and, in some cases, poor specificity between the ligand or protein and the cell allows for undesirable platelet adhesion [90].

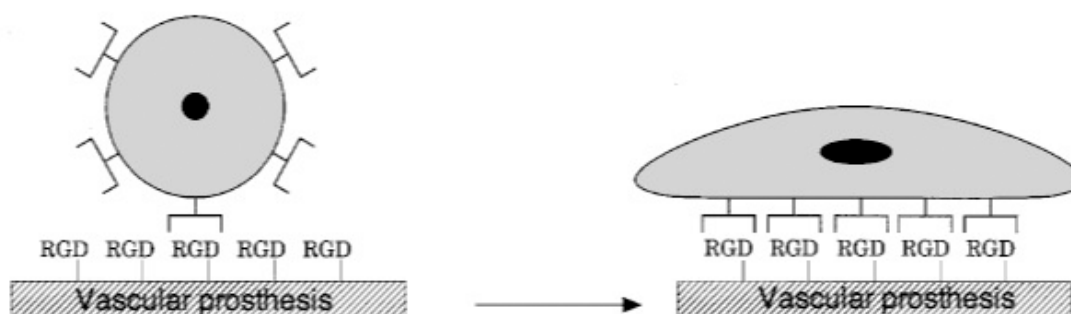


Figure 6. Endothelial cell interact by integrin family of cell-matrix receptors with the wall bound RGD-sequence and adhere to the vascular graft. Adapted from Walluscheck et al., 1996 [108].

Adherent cells are strongly influenced by the mechanical aspects of biomaterials and many studies indicate that micro- and nano-scale mechanical stresses generated by cell-matrix adhesion have significant effects on cellular phenotypic behaviour [109]. Thus, physical methods attempting to the modification of the surface topography of vascular graft have been developed. Gray and colleagues showed that endothelial cells preferentially accumulate on stiffer regions of a poly(dimethylsiloxane) (PDMS) substrate, suggesting that material stiffness may be used to promote preferential endothelial cell adhesion [110]. Goodman and co-workers created a polyurethane scaffold micro-patterned to mimic the natural sub-endothelial extracellular matrix topography [109]. Endothelial cells seeded on these surfaces were found to more closely resemble those attached to the native extracellular matrix, suggesting that mechanical cues from textured surfaces can alter cellular phenotype. Bettinger and co-workers developed a rounded surface topography that was able to promote the alignment and elongation of endothelial cells; this effect was speculated to be a result of the ability of filopodia to sense changes in surface topography [111]. Finally, Daxini and co-workers created a pattern of microchannels with a defined geometry in order to create regions of lowered shear stress to improve the retention of endothelial cells on polyurethane surfaces [112]

Another method used to enhance endothelial cell attachment to a polymer scaffold is the process of flow conditioning by which cells are exposed *in vitro* to flow-induced shear stress post-seeding procedure [113-116]. Results obtained by some groups showed that this enabled enhanced retention of ECs with strengths adequate to withstand physiological shear stresses. Additionally, it has been shown that shear stress influences the phenotype of endothelial cells, including the ability to adhere to a surface, and may be used to control vascular cell differentiation [117]. The various surface modifications undertaken to promote spontaneous and seeded endothelialization are summarized in Table 3.

Cell source

Autologous cells are preferred for prosthetic graft seeding since problems with immunological rejection can be avoided. The veins used in humans are saphenous and external jugular veins. Forearm veins and arteries have also been used, but in less extent [118]. However, despite strong evidence that *in vitro* EC lining improves the patency of small-diameter vascular

prostheses, a major disadvantage of this studies is that a limited number of ECs can be extracted from veins. It takes a 4- to 5- week delay between cell harvest and graft implantation, growth and infection problems can occur, and the costs of cell culture are substantial. Furthermore, seeded cells have been cultured under all sorts of growth factors, inducing the risk of unwanted growth after implantation. To avoid these problems, a search for other cell types and for other EC sources has been started [93].

An alternative source for ECs are cells from the microvessels present in human fat tissue; this source provide large number of cells that can be readily available at the time of surgery. Over the years several sources of fat tissue have been used to obtain ECs, with subcutaneous and mainly the omental fat being the most studied tissues. Cells extracted from omentum have been characterized as mesothelial cells by some authors while others still regard these as endothelial cells. However, both these types of cell have similar functional properties including the release of anticoagulant substances [119]. One disadvantage of extract ECs from fat is that some contaminating cells could be also extracted during the process while cells extracted from vein are pure ECs [94].

In the recent few years, stem cell has become a major cell source for tissue engineering. The merit of utilizing stem cell as a seeding cell source is that those cells are able to self renew and differentiate into mature cells in the proper conditions. Generally there are two types of stem cells based on their origin, the embryonic and adult stem cells. Embryonic stem cells are able to produce all types of cells, while adult stem cells are normally limited to certain lineages. The advantage of choosing the adult instead embryotic stem cells is that the first one can be obtained from patients themselves, which can avoid the immuno-rejection and ethical problems. In addition, adult stem cells are normally limited to certain lineages, which do not have tumorigenic capacity [49].

Adult stems cells are isolated from bone marrow or circulating blood. It is expected that bone marrow cells can differentiate into cells such as fibroblasts, ECs, and SMCs [94]. Endothelial progenitors cells (EPCs) are one type of the adult stem cells that have the capacity to proliferate, migrate and differentiate into mature ECs. EPCs are mainly located in bone marrow and could be mobilized into peripheral blood by certain growth factors, such as granulocyte macrophage colony stimulating factor (GM-CSF) or VEGF. EPCs could be also isolated from umbilical cord blood [49].

Table 3. Summary of surface modification to enhance endothelialization (in chronological order).

Graft	Modified Additive	Study Type	Outcome	Reference
PTFE	P15 peptide	<i>in vitro</i>	↑endothelialisation; ↓IH	[120]
PTFE	Anti-CD34 antibodies	animal model	Rapid endothelialisation; ↑IH	[121]
PTFE	Vascular Endothelial, GF	animal model	↑endothelialisation; ↑IH	[122]
Poly(ether) urethane (Tecothane)	Cholesterol	<i>in vitro</i>	↑endothelialisation and resistance to shear stress; ↑endothelial precursor cell adherence	[123]
PTFE	Poly(amino acid) urethane	animal model	↑endothelialisation	[124]
Fibrin	Endothelial cell GF	<i>in vitro</i>	↑vEC proliferation; ↓early platelet adhesion; ↓late thrombus; ↑patency	[125]
Polyurethaneurea	YIGSR ^a	<i>in vitro</i>	↑endothelialisation; ↑transmural cell migration; ↑hydroxyproline production ^b	[126]
PTFE	Tumorigenic human squamous cell line	animal model	Confluent endothelialisation by 5 weeks	[127]
Dacron, PTFE, polypropylene, silicone, polyurethane	Titanium	<i>in vitro</i>	↑vEC adhesion; no increase in inflammation	[128]
Dacron	Collagen film	<i>in vitro</i>	Confluent endothelialisation	[129]
Dacron	Collagen	animal model	Largely endothelialised and thrombus free at 3 weeks	[130]
Collagen	Heparin	<i>in vitro</i>	↑basic fibroblast growth factor (bFGF) binding and release	[131]
Polyurethane	bFGF/Heparin	animal model	↑endothelialisation, neovascularisation	[132]
PTFE	Nitrogen, oxygen (↑hydrophilicity)	<i>in vitro</i>	↑endothelialisation, ↑plasma protein adsorption	[133]
PTFE	RGD cell adhesion peptide	<i>in vitro</i>	↑immediate vEC adhesion; no long term advantage compared with fibronectin coating	[134]
Dacron	Carbon	<i>in vitro</i>	vEC proliferation	[135]
Polyurethanes and silicones	Extracellular matrix; fibronectin; gluteraldehyde preserved matrix (GPM)	<i>in vitro</i>	GPM provides optimal vEC proliferation	[136]
PTFE	Fibronectin	animal model	↑endothelialisation (both spontaneous and seeded)	[137]

^a Endothelial cell adhesive peptide sequence; ^b Mark of collagen synthesis; GF (growth factor);

vEC (vasculae endothelial cells); IH (intimal hyperplasia). Sarkar et al., 2006 [71].

The advantage of using this source of cells is that they can be easily obtained from peripheral blood of adults by venopuncture rather than by an operation. A disadvantage is that *ex vivo* expansion, takes on average 2 weeks. Besides, the drawbacks of *in vitro* culture are risk of infection, change of phenotype, the need for culture facility, and limitations for emergency situation [93].

Bacterial Cellulose: Properties, Production and Applications

Adapted from: Andrade FK, Pertile RAN, Dourado, F, Gama FM. Bacterial Cellulose: Properties, Production and Applications. In: Lejeune A, Deprez T, editors. Cellulose: Structure and Properties, Derivatives and Industrial Uses: Nova Science Publishers, Inc., 2010. p. 427-458.

Bacterial cellulose (BC) is produced by bacterial strains from the genera *Acetobacter*, *Agrobacterium*, *Pseudomonas*, *Rhizobium* and *Sarcina*, the last one being the only genus of Gram-positive bacteria in this field [138]. Interestingly, only a few bacterial species, taxonomically related to this genus, extracellularly secrete the synthesized cellulose as fibers.

While the first studies on BC were geared towards elucidating the cellulose biosynthetic pathway, BC has quickly developed into a field of study of its own, as observed by the growing number of patents and publications worldwide (Figure 7). Special attention was given to strains from *Gluconacetobacter xylinus* (= *Acetobacter xylinum*), first described by Brown in 1886 [139]. While the secreted cellulose is identical to the one produced by plants, regarding the molecular structure, it is chemically pure, *i.e.* not mixed with non-cellulosic polysaccharides [138, 140-143]. Its unique properties account for its extraordinary physico-chemical and mechanical behaviour, resulting in characteristics that are quite promising for modern medicine and biomedical research [142, 144-148].

1. Biosynthesis, Structure and Properties

The classical medium to culture *G. xylinus* and maximize the growth and cellulose production was described by Hestrin and Schramm. The pH of the medium is 6 and the optimum growth temperature is 30 °C, though the bacteria grow well over a temperature range of 25 to 30°C. The static culture leads to the production of a cellulose pellicle holding bacterial cells floating on the surface medium. In a culture medium aerated by shaking, bacteria grow faster, but less

cellulose, presented as ball-shaped particles, is produced. When *G. xylinus* is cultured on solid medium, the colonies have a dry, wrinkled appearance [149, 150].

The ultrastructure of the cellulose synthesis apparatus is best understood in *G. xylinus*. The cellulose synthase is considered the most important enzyme in the bacterial cellulose biosynthesis.

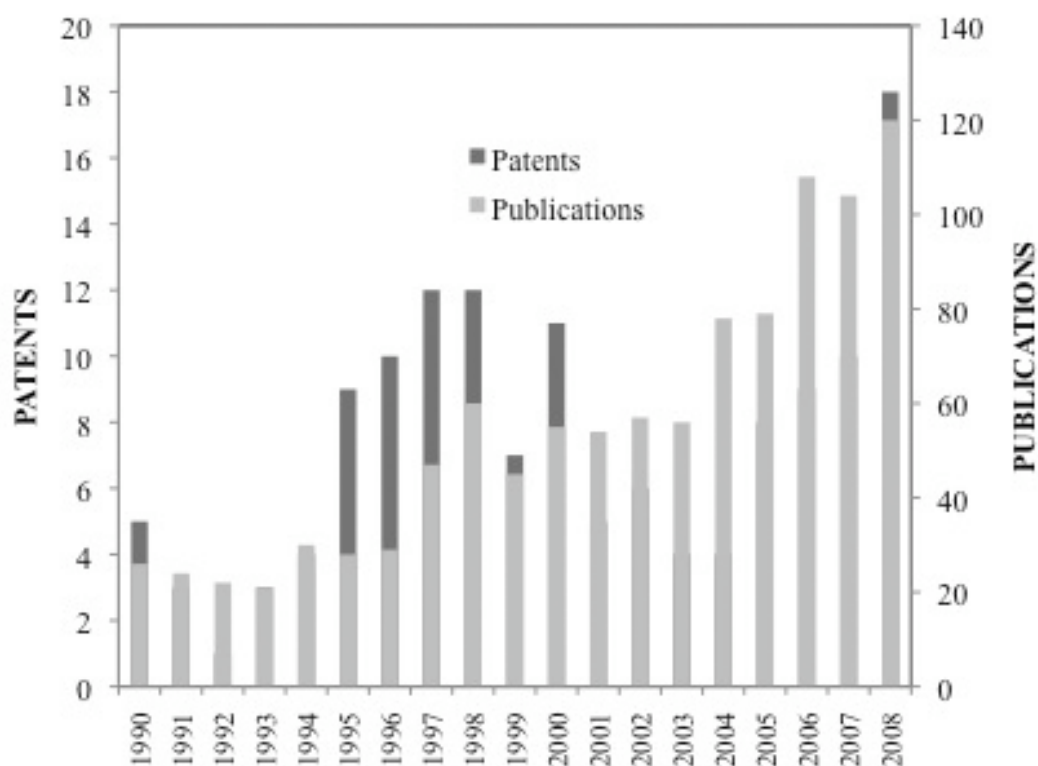


Figure 7. Publications and patents on bacterial cellulose.

The cellulose synthase operon codes protein complexes aligned along the long axis of the cell. Cellulose synthesizing complexes are present in the surface of the bacteria, next to the cell membrane pores where the cellulose fibrils are extruded through, associating with other fibrils and making up the ribbon of crystalline cellulose [138, 143]. Each bacterium synthesizes a cellulosic ribbon with a width ranging from 40 to 60 nm, parallel to the longitudinal axis of the bacterial cell. The ribbon of cellulose is composed of microfibrils with around 1.5 nm thickness, secreted through extrusion sites in the outer membrane of the bacterium. Then, the microfibrils aggregate into 3 to 4 nm microfibrils via crystallization of adjacent glucan chains and finally, together, form the larger cellulosic ribbon [149].

Several studies were developed to clarify the physiologic role of cellulose. As the cellulose matrix is less dense than water, it has been proposed to allow maintaining the bacterial cells in an oxygen-rich environment. Additionally, it allows protecting the bacteria from ultraviolet light, competing microorganisms and heavy-metal ions, while retaining the moisture and allowing nutrient supply by diffusion [142, 148, 150, 151].

As *Gluconacetobacter* microorganisms are mandatory aerobes, under static conditions, BC is synthesized at the air/liquid interface of the culture medium [138, 142]. Other relevant aspects for the BC production are the carbon and nitrogen sources and concentration, the pH and temperature, and the surface area of the fermentation system. All these aspects affect the cellulose production as well as the membrane properties, in static or agitated cell culture. Also, differences in the bacterial strains play an important role in the microstructure and production rate. Figure 8 shows a membrane produced by ATCC 10245 *G. xylinus* strain [138, 142, 152-156].

Besides macroscopic morphological differences, BC produced in static and agitated cultures differs also at various structural levels. While the fibril network remains the same, there are some differences in the structure of the crystals and molecular chains. The crystallinity and cellulose I alpha content, as well as the degree of polymerization, is lower in agitated than in static culture [157].

As referred above, the bacterial and vegetable celluloses have the same molecular structure, both being built up of $\beta(1\rightarrow4)$ -linked D-glucose units. The degree of polymerization is however rather different, about 13000-14000 for plants and 2000-6000 for bacterial cellulose. Both celluloses are highly crystalline; differing in the arrangement of glucosyl units within the unit cells of the crystallites, and several studies suggests that these celluloses are synthesized by enzymatic complexes that differ at the molecular level. Also, this bacterial polysaccharide is secreted free of lignin, pectin, hemicelluloses and other biogenic compounds, which are associated with plant cellulose [138, 142, 158].



Figure 8. Bacterial cellulose pellicle produced by ATCC 10245 *G. xylinus* strain in static culture.

Morphology. The gelatinous BC membrane formed in static culture is characterized by a 3D ultrafine fibrous network structure, containing about 99% water. The randomly assembled ribbon-shaped fibrils are less than 100nm wide and composed of elementary nanofibrils, aggregated in bundles with lateral size of 7-8nm. The crystallinity degree of BC is in the range of 60-90% [159-163]. Crystallographically, BC is a Cellulose I, with 60% α /40% β [148, 163]. The crystallographic molecular arrangement may influence the physical properties, as the allomorphs have different crystal packing, molecular conformation, and hydrogen bonding [159, 163]. In 2006, Sanchavanakit characterized BC pellicles obtained after 48 hours culture: the surface area of the air-dried BC films was 12.6 m²/g, with a pore size distribution ranging from 45 to 600 Å. The pore diameter of the air-dried film was inferior to 0.1 μ m; however, when the air-dried pellicle was swollen with water, at 30 °C, the apparent pore diameter raised to 0.2-1.0 μ m [164]. Due to its high crystallinity and small fiber diameter, BC possess excellent mechanical strength and high surface area when compared to plant derived cellulose [165] and the application and biological function of celluloses are based on its distinct fiber morphology [159].

Mechanical properties. Both the micro and macrostructure of BC are influenced by the growing culture environment and the treatment after synthesis. According to Iguchi, a BC pellicle obtained after 7 days of culture and air-dried at 20 °C and low pressure, presents a Young's modulus of 16.9 GPa, tensile strength of 256 MPa and elongation of 1.7% [148].

However, when a pellicle was dried through the heat-press method described by Iguchi [166] and an excess of pressure (490 – 1960 kPa) was applied, the tensile strength as well as elongation tend to decrease, while the Young modulus remains constant. According to Sanchavanakit (2006), a BC dried film (from a 48h grown culture) with a thickness of 0.12 mm presents a tensile strength and break strain of 5.21 MPa and 3.75%, whereas for the wet films the values are 1.56 MPa and 8.0%, respectively [164]. The high Young's modulus and tensile strength of BC films seems to result from its high crystallinity, high planar orientation of ribbons pressed into a sheet, ultrafine structure, and the complex network of the ribbons [167].

Water holding capacity. BC is highly hydrophilic, holding over 100 times its weight in water. Klemm and colleagues showed that the “never dried” BC has water retention values (WR) in the range of 1000%, drastically decreasing after air-drying to values that can be compared with those of plant cellulose, 106% and 60%, respectively. The method of drying has been shown to affect the BC porosity, freeze-drying (WR of 629%) being reported as the most effective method to preserve the porous structure [142].

Medical Applications

The biocompatible nature of cellulose-based materials, such as oxidized cellulose, regenerated cellulose hydrogels, sponge cellulose and bacterial cellulose, has allowed comprehensive research targeted at medical applications [168-172]. Representative examples BC-based scaffolds for tissue engineering include vascular grafts, cartilage, neural regeneration and wound dressings. Table 4 describes the biomedical application of BC and some results obtained.

The interaction between cells and BC has been investigated by several research groups. In 1993, BC was described as a substrate for mammalian cell culture by Watanabe and colleagues [146]. Adhesion to BC was observed using anchorage-dependent cell lines (L929 mouse fibroblasts, Detroit 551, HEL, mouse 3T3 Swiss, SV40/Balb 3T3, CHO, Human J-111 and Human epidermal Keratinocytes). Modification of the BC surface, to improve the interaction with cells, involved the introduction of electrical charge and adhesive proteins, such as collagen type I, collagen type IV, fibrin, fibronectin or laminin [146].

Table 4. Summary of biomedical applications of bacterial cellulose.

Biomedical Applications	Study	Outcome	References
Cartilage repair	1. <i>In vitro</i> study – BC as scaffolds for chondrocytes culture; 2. Reconstruction and rehabilitation of the nasal framework in rabbits.	1. Growth, cell migration and ingrowth; expression of collagen by the cells; 2. Good integration.	[147, 173, 174]
Vascular grafts	1. <i>In vitro</i> studies were developed to improve BC as scaffold to tissue engineering of vascular grafts; 2. <i>In vivo</i> studies with stents coated with BC (rabbit model); 3. <i>In vivo</i> studies of BC as microvessel endoprosthesis (rats and pig models)	1. Many of the strategies used (e.g. increasing the porosity, improving the mechanical properties, functionalization with adhesion peptides, etc.) improved the adhesion, migration and proliferation of smooth muscle cells or endothelial cell to BC; 2. BC accelerated re-endothelialization of the area covered by the stent, acting as a barrier to the migration of muscle cells; 3. good incorporation in the host tissue without any rejection reaction.	[142, 152, 162, 163, 175-178]
Wound dressing	1. Corneal healing (rabbits); 2. Skin healing (swine); 3. Dural substitute exposed to intact and damaged brain of dogs; 4. Human patients with chronic venous insufficiency and lower-leg ulceration; 5. Repair of chronic lower extremity ulcers in humans; 6. Rabbit's laryngotracheal region.	1. Improved healing; 2. Good performance in healing and adhesion to the wound; 3. Good acceptance of the graft; 4. BC dressings create a protective, hypoxic, moist environment and improved healing. ↓ patients pain; 5. ↓ of time for epithelization and the time for wound closure over standard care; 6. No inflammatory signs.	[179-189]
Dental implants	1. Periodontal disease treatment, dental implants and guided bone regeneration; 2. Biocompatibility evaluation with implantation of BC (Gengiflex®) in rat subcutaneous connective tissue; 3. BC (Gengiflex®) was used for guided tissue regeneration of bone defects in rabbits.	1. Provide a good alternative for guided tissue regeneration; ↑ regeneration of the lesions; 2. BC behaved as a stranger material to the host tissue in comparison to Milipore and Teflon membranes; 3. PTFE presented better results than Gengiflex®.	[190-196]
Nerve regeneration	1. Micronerve reconstruction of rat sciatic nerve using BC tubes (BASYS®); 2. BC tubes (BASYS®) were used as drug depot of neuroregenerative substances; 3. BC sheets to envelop peripheral nerve lesions (dogs); 4. Facial nerves repair (rats) with BC sheets (Biofill®).	1. ↑ regeneration of the functional nerve; the reappearance of acetylcholine as the transmitter of nerve impulses to the executive organ was observed; 2. Improved healing; 3. A moderate fibrous reaction and realignment and axonal growth through the injury were observed. 4. Improve guidance of the nerve fibers, allowing the concentration of neurotrophic factors, which consequently promoted the nerve regeneration.	[142, 197, 198]

The interaction of BC films with human transformed skin keratinocytes and human normal skin fibroblasts was evaluated [164]. The results demonstrated that BC supports the proliferation of both cell types, with no signs of toxicity; the keratinocytes exhibited normal cell proliferation, spreading and also maintained the normal phenotype, while for the fibroblast culture the pattern of cell distribution and stability on BC film was poorer. Moreover, the migration of keratinocytes on a BC film was comparable to that of a polystyrene plate. P ertile and colleagues, in 2007, found a similar behavior when studying the interaction between BC pellicles and skin fibroblasts. Figure 9 shows a detail of the BC network with fibroblast cells adhered on BC membranes [199].

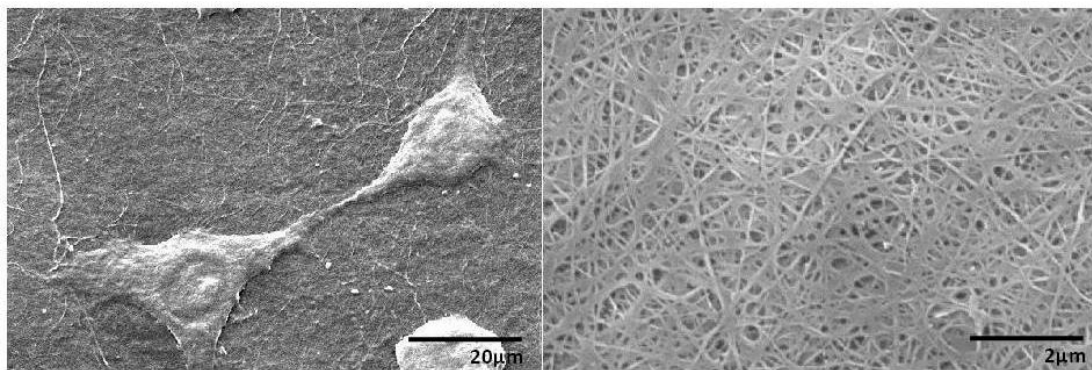


Figure 9. Scanning electron microscopy of bacterial cellulose. Fibroblasts adhered on bacterial cellulose membranes after 24h in culture (Left, 1000x); detail of BC membranes surface (Right, 10.000x).

In an *in vivo* biocompatibility study, BC was subcutaneously implanted in mice, for a period of up to 12 weeks [140]. BC was shown to integrate well into the host tissue, with cells infiltrating the BC network and no signs of chronic inflammatory reaction or capsule formation. The formation of new blood vessels around and inside the implants was also observed, evidencing the good biocompatibility of the biomaterial.

BC as vascular grafts. In 2006, Backdhal and colleagues evaluated BC as a novel biomaterial for the tissue engineered blood vessels [162]. The BC was compared to similar structures of porcine carotid artery (PCA) and expanded-polytetrafluorethylene (ePTFE). The

mechanical properties of the BC rings were comparable to those of PCA, although PCA significantly exceeded BC in both stress and strain at break and Young's modulus. The authors also studied the interaction between BC and smooth muscle cells (SMCs), the compact and porous side of the BC pellicle being separately analyzed. The results showed that, although the attachment and proliferation of SMCs cultured on the compact and porous sides were similar, differences in the morphology were observed. Furthermore, a maximum ingrowth distance on the porous side of 20 μ m and 40 μ m was observed after 1 and 2 weeks, respectively, the more compact side allowing an ingrowth of up to 1-5 μ m depth. The results revealed that the cells could push the nanofibrils aside, while migrating into the cellulose nanofibril network. In 2008, the same research group developed a novel method to prepare three dimensional nanofibril network tubes from BC with controlled microporosity, by placing paraffin wax and starch particles of various sizes in a growing culture of *G. xylinus* [175]. SMCs migrate into this more porous cellulose to a greater depth than in the native BC pellicle. The SMCs produced collagen fibers both in the surface cell layer and further into the scaffolds made with paraffin. However, a mechanical evaluation of the SMC-seeded scaffold was not performed.

The effectiveness of angioplasty using conventional stents was compared to bacterial cellulose coated stents, in a rabbit model, by Negrão *et al.* [176]. The authors showed that BC coated stents do not present adverse events in the angioplastic procedures. Indeed, BC accelerated re-endothelialization of the area covered by the stent, acting as a barrier to the migration of muscle cells, thus representing a promising strategy for the prevention and treatment of restenosis in endovascular procedures.

Bodin *et al.* analyzed the growth of endothelial cells (ECs) in the lumen of BC tubes obtained by culturing the bacteria under different concentrations of oxygen [152]. All tubes had a denser inner side and a more porous outer side. The cross section observation revealed layered tube walls, the number of layers and the yield of cellulose increasing with the oxygen pressure. The cells were able to growth in the tubes, forming a confluent layer after 7 days. The same group developed a novel method to graft the RGD cell adhesion peptide on the cellulose, to enhance cell adhesion [163]. The cellulose was modified with xyloglucan and xyloglucan bearing the GRGDS (Gly-Arg-Gly-Asp-Ser) peptide. The results revealed that the nanocellulose material was homogeneously modified; also, cell adhesion studies confirmed a faster adhesion of endothelial cells on the xyloglucan-GRGDS-modified cellulose.

Klemm *et al.* investigated the application of patented BC tubes (BASYC[®] - BActerialSYnthesized Cellulose) as microvessel endoprosthesis for end-to-end anastomosis procedure, using the carotid artery of a white rat [142]. In this study, four weeks after implantation, the carotid artery-BASYC complex was wrapped up with connective tissue and the BC tube was completely incorporated in the body without any rejection reaction. Putra *et al.* described a simple technique that allows to obtaining a tubular – BC gel with desired length, inner diameter and thickness, along with an oriented fibril structure [177]. This technique requires a shorter cultivation time, as compared to the methodology described by Klemm *et al.*[142]. Over a period of 12 weeks, implanted BC grafts in the carotid artery of pigs showed good *in situ* tissue regeneration without signs of thrombosis, inflammation or fibrotic capsule formation around the implants. The luminal wall of the newly formed tissue showed complete endothelialisation, with a confluent endothelial layer [178].

Improving the Bacterial Cellulose Properties for Biomedical Applications

Biocompatibility is one of the main requirements for any biomedical material. It can be defined as the ability to remain in contact with living tissue without causing any toxic or allergic side effects, simultaneously performing its function [145]. In this context, BC has been modified to further enhance its' biocompatibility. Depending on the envisaged biomedical application, improved cellulose integration with the host tissue, increased degradation *in vivo* or modified mechanical properties, to mimic the tissue to be replaced, are required. Chemical surface modifications, incorporation of bioactive molecules, modification of the porosity and crystallinity, design of 3D structures and nanocomposites, are examples of viable methods to make BC an ideal material for reparative tissue engineering.

The attachment of cells to biomedical materials can be improved by using adhesion molecules, present in the extracellular matrix substances, such as fibronectin, vitronectin, or laminin. The amino acid sequence Arg-Gly-Asp (RGD) has long been recognized for its cellular adhesion function. Bodin *et al.* described a novel method to activate the bacterial cellulose surface with the RGD peptide, to enhance cell adhesion [163]. The adsorption of modified xyloglucan (GRGDS-xyloglucan) increased the BC wettability, which might explain the decreased or even negligible amount of adsorbed protein. Modification with xyloglucan (XG) did not alter the BC

morphology. The water contact angle was lower on BC modified with XG (29 ± 4.8) and XG-GRGDS (32 ± 5.8), when compared to unmodified material (44 ± 5.3). Whitney *et al.* also used xyloglucan to modify BC, in this case incorporating the polysaccharide in the *G. xylinus* culture medium. These authors verified that XG binds to cellulose, altering its crystallinity [200].

In order to improve cell adhesion to BC, Watanabe and co-workers developed several methods of chemical modification, aiming the introduction of electrical charge to the BC membrane [146]. In this context, membranes of trimethyl ammonium betahydroxypropyl-BC (TMAHP – BC), diethyl aminoethyl-BC (DEAE – BC), aminoethyl-BC (AE – BC) and carboxymethyl-BC (CM – BC) were produced. Also, the TMAHP – BC was covered with adhesive proteins (collagen type I, collagen type IV, fibrin, fibronectin or laminin). The new bacterial cellulose substrates favored the adhesion of cells, as compared to the unmodified BC.

Phosphorylation and sulfation of BC matrices were explored by Svensson *et al.* as a means to add surface charges, mimicking the glucosaminoglycans of cartilage tissue *in vivo* [147]. The materials were analyzed for mechanical properties, microstructure and cell–material interactions, in order to assess the potential of this matrix as a scaffold for cartilage tissue engineering. The compressive modulus of the phosphorylated samples increased with the reaction time and was higher than the compressive modulus of native BC. This result was probably due to the more compact structure of the 3D network in the phosphorylated BC. An even more compact network structure was found in sulfated BC, which showed an higher resistance to compressive forces when compared to phosphorylated and native BC. Sulfated – BC had significantly lower Young's modulus than the unmodified BC, resulting in a reduction of the mechanical integrity. The lower strength of sulfated-BC may be due to the prevention of hydrogen bonding between the cellulose chains by the covalently bonded sulfate groups, chain scission by acid hydrolysis, or a combination of both.

It is known that BC properties such as the mechanical strength and permeability can be changed by post production (*ex situ*) treatments [201]. As an example, treatment with sodium hydroxide is widely used to clean the cellulose membranes, after fermentation, for biomedical applications. George *et al.* analyzed the effect of various alkali treatment methods for BC cleaning, such as potassium hydroxide, sodium carbonate and potassium carbonate. According to these authors, any of these chemicals is milder than the sodium hydroxide, better preserving the BC integrity, and improving the tensile strength of the membranes [202].

Backdhal *et al.* developed a method to produce a highly porous BC [175]. The authors added paraffin wax and starch particles of various sizes to the growing culture of *G. xylinus*. Bacterial cellulose scaffolds with different porosities and interconnectivity were prepared through this approach. The partially fused paraffin particles were incorporated throughout the scaffold, while starch particles were found only in the outermost area of the resulting scaffold. This methodology allows the modulation of the porosity, thickness and interconnectivity of tubular BC scaffolds, by varying the porogen size and fermentation conditions. In addition, the porogens can be successfully removed from the BC network.

As *G. xylinus* has been reported to move along cellulose rails while secreting BC, Urakiet *al.* attempted to expand the utilization of BC and developed novel functional biomaterials, through the transformation of BC into a honeycomb-patterned material [203]. Fabrication of such patterned BC structure was possible by controlling the bacterial movement using an agarose film scaffold with honeycomb-patterned grooves, in a humid CO₂ atmosphere. The results suggest that the obtained honeycomb-patterned network is a continuous porous film, built up with highly oriented and I α cellulose microfibrils.

Aiming at the production of a *in vivo* degradable polysaccharide, while exhibiting both chitin- and cellulose-like properties, attempts were made to incorporate *N*-acetylglucosamine (GlcNAc) residues into bacterial cellulose. Ogawa characterized the enzymatic susceptibility of BC containing *N*-acetylglucosamine (N-AcGBC) residues for cellulase, lysozyme and chitinase hydrolysis [204]. The results showed that N-AcGBC possesses high susceptibility for lysozyme (proportional to the GlcNAc content) and cellulase but only slight susceptibility for chitinase. The random distribution of GlcNAc residues on N-AcGBC is responsible for the higher lysozyme reactivity. This approach was also studied by Shirai, who described a *G. xylinus* strain adapted to a medium containing GlcNAc, that was used to prepare a novel cellulosic polysaccharide containing residual GlcNAc [205]. The resulting polysaccharide was lysozyme-susceptible. The amino sugar content in the pellicles was measured after cultivation of the bacteria in the presence of various ammonium salts. Ammonium chloride seems to be the best additive to enhance GlcNAc incorporation, under rotatory and aerobic conditions. The acceleration of GlcNAc incorporation in the presence of ammonium salts seems to be due to the shift of the aminotransferase equilibrium in the presence of a high concentration of ammonium ion. The production of similar polysaccharides was obtained by incubation of *G. xylinus* in a modified

Hestrin – Schramm medium containing lysozyme-susceptible phosphoryl chitin (P-chitin) and D-glucose [206]. Analysis of the culture medium by HPLC showed that the P-chitin is depolymerized to monomeric and oligomeric residues, during the incubation, and these were utilized as a carbon source by the bacteria. Furthermore, monomeric GlcNAc 6-phosphate was also found to enhance the incorporation of GlcNAc residues into the polysaccharide. Also, Ciechanska obtained a modified bacterial cellulose by adding chitosan to the culture medium during the bacterial growth [207]. By FTIR analysis, glucosamine and N-acetylglucosamine units were shown to have been incorporated into the cellulose chain, providing a material with good mechanical properties in the wet state, high moisture-keeping properties, release of oligosaccharides under lysozyme action, and bacteriostatic activity.

Lee and colleagues investigated the flexibility of the BC synthesis apparatus of a *G. xylinus* strain in incorporating different monomers present in culture medium [208]. The bacteria incorporated 2-amino-2-deoxy-D-glucose (glucosamine) and 2-acetamido-2-deoxy-D-glucose (*N*-acetylglucosamine), but not 3-*O*-methyl-D-glucose or 2-deoxy-D-glucose into the exopolymer. The average molar percentage of glucosamine and *N*-acetylglucosamine in the exopolymers amounted to about 18%. The authors suggested that the cellulose synthase and other enzymes involved in the cellulose synthesis have broad specificity. Preliminary analysis of the fibers (cellulose and the new copolymers) by environmental scanning electron microscopy suggested similar gross morphology (*e.g.* diameter and surface smoothness).

Kobayashi *et al.* produced a cellulose-chitin hybrid polysaccharide by enzymatic polymerization, using a chitinase and a cellulase from *Trichoderma viride* [209]. The molecular weight values of the cellulose-chitin hybrid polysaccharides reached 4030 and 2840, which correspond to 22 and 16 saccharide units, respectively. These MW are rather low compared with naturally occurring chitin and cellulose. The produced cellulose-chitin hybrid polysaccharide did not exhibit a crystalline structure and was hydrolyzed *in vitro* by lysozyme. Also, Phisalaphong and Jatupaiboon obtained a nanostructured BC-chitosan composite, by supplementing the BC culture medium with low-molecular-weight chitosan [210]. Films with a denser fibril structure, smaller pore diameter and higher surface area than the native BC were obtained; however no significant influence in the crystallinity and anti-microbial activity were observed.

Another type of BC modification was described in 2008 by Berti *et al.* [211]. This group produced membranes of BC-PHA by mixing BC oligomers with polyhydroxyalkanoates produced by *Ralstonia eutropha* and *Chromobacterium violacium*, obtaining membranes with different surface properties and porosities.

BC Nanocomposites used in Medicine. According to Ajayan *et al.*, nanocomposites can be described as solid structures with nanometer-scale dimensional repeat distances between the different structural phases [212]. These materials typically consist of two or more inorganic/organic phases in some combinatorial form. At least one of the phases or features must be in the nanosize scale. In general, nanocomposite materials demonstrate new and/or improved mechanical, electrical, optical, electrochemical, catalytic or structural properties-

Polyvinyl alcohol (PVA) is a hydrophilic biocompatible polymer with characteristics suitable for biomedical applications. Combined with BC fibres, it has been used to develop biocompatible nanocomposites [213-215]. The PVA-BC nanocomposite is highly anisotropic and its properties make it comparable to heart valve tissue. According to the authors, PVA-BC nanocomposite with specific composition and processing parameters can be obtained to create a custom-designed biomaterial mimetizing the mechanical properties of the tissue to be replaced.

A composite named CollagenBC was developed by Wiegand, by adding collagen type I to the culture medium of BC fermentation, for the treatment of chronic wounds [216]. This composite induces an *in vitro* reduction of protease activity, interleukin concentration and reactive oxygen species, relevant features to support the healing process in chronic wounds. This composite combines the ability of collagen to alter the milieu parameters in chronic wounds, with the excellent BC physical properties. Following the same approach, Zhou and colleagues used a culture medium containing sodium alginate (NaAlg) for the production of BC, obtaining a cellulose with lower cristallinity and a smaller crystallite size [217]. Also, Phisalophon developed a BC-alginate blend exhibiting improved water absorption capacity and water vapor transmission rate combined with a smaller pore size, although the tensile strength and elongation at break of the film decreased [218].

BC is composed of dense microfibrils forming a material with relatively small pore sizes, the pure BC lacking a suitable pore structure essential for tissue engineering scaffolds. In contrast, the hydroxyapatite/BC (Hap/BC) nanocomposite scaffolds combine good mechanical properties with an open pore structure, suitable candidates for tissue engineering applications. With the purpose of evaluating the potential of porous Hap/BC nanocomposite as a bone tissue engineering scaffold, Fang *et al.* performed *in vitro* assays [219, 220] where the proliferation and osteoblastic differentiation of stromal cells derived from human bone marrow (hBMSC) on Hap/BC nanocomposite was investigated. The results showed that the nanocomposites performed better than pure BC, regarding cell adhesion, due to the improved pore sizes and presence of the inorganic component. In addition, the authors demonstrated that the nanocomposites stimulate cell proliferation while enhancing osteoblastic differentiation of hBMSC, without osteogenic reagents. Other authors have also synthesized and characterized BC-hydroxyapatite scaffolds, for bone regeneration [221-223]. Shi and colleagues used an alkaline treatment to optimize the biomimetic mineralization of BC pellicles [172]. Calcium-deficient carbonate hydroxyapatite/BC (CaDHCAp/BC) nanocomposites were synthesized in a 3D network of BC nanofibers. The alkaline treatment improved the mineralization efficiency, making the CaDHCAp/BC a potential biomaterial for bone tissue engineering.

BC is a very attractive material for wound dressings, providing a moist environment for wound regeneration, resulting in a better healing. However, bacterial cellulose itself has no antimicrobial activity to prevent wound infection. To achieve antimicrobial activity, Maneerung *et al.* impregnated BC with silver nanoparticles, by immersing the BC pellicles in a silver nitrate solution [224]. Sodium borohydride was then used to reduce the absorbed silver ion (Ag^+), inside the BC network, to metallic silver nanoparticles. The size and size distribution of the nanoparticles were effectively controlled by adjusting the molar ratio of $\text{NaBH}_4:\text{AgNO}_3$. Under optimal conditions, well dispersed and regular spherical silver nanoparticles were obtained. The freeze-dried silver nanoparticle-impregnated bacterial cellulose exhibited a strong antimicrobial activity against *Escherichia coli* (Gram-negative) and *Staphylococcus aureus* (Gram-positive), bacteria commonly found on contaminated wounds.

Another composite material was recently reported by Charpentier and colleagues: polyester modified with UV/ozone and plasma treatments, bearing improved hydrophilic character, was

coated with BC to produce a new hybrid material that presents potential use in vascular prosthetic devices [225].

Haigler *et al.* added carboxymethylated cellulose (CMC) to the *G. xylinus* culture medium and analyzed the properties of the altered BC produced [226]. The results revealed that an alteration of the ribbon assembly occurs in the presence of CMC, often inducing synthesis of separate, intertwining bundles of microfibrils. Similarly, Tajima incorporated water-soluble polymers such as CMC and methyl cellulose in BC, by incubating *G. xylinus* in a medium containing these polymers [227]. Increased BC production and composites with controllable degradability and mechanical strength were obtained. Also Sakairiet *al.* produced CMC-BC composites by adding CMC to the culture medium [228]. The obtained material had ion exchange ability, with enhanced specific adsorption affinity for lead and uranyl ions, as compared to the original CMC and BC. Using the same approach, Whitney and colleagues [229] added mannan-based polysaccharides to the culture medium, and observed the formation of networks with distinct architecture and modification of other molecular features, such as reduction of crystallinity. A range of different cellulose-associated networks could be formed, depending of the levels of glucomannan and galactomannans added.

Many other studies enlarge the repertoire of different bacterial cellulose composites with potential biomedical application. Different processes were developed to produce BC nanocomposites filled with silica particles, yielding improved elastic modulus and strength, as compared to native BC [230]. Serafica *et al.* produced BC in a rotating disk bioreactor. Several kinds of solid particles (silica gel, iron, aluminum, glass beads, etc) were added to the medium, during gel formation, being trapped to form new classes of composite materials [231]. Other works report the production of BC – nanocomposites, for example BC/starch [232], BC reinforced with cellulose acetate butyrate [233], BC/gluconoxylan blends [234], BC/poly dimethylacrilamide and BC/gelatin [235, 236].

Carbohydrate – Binding Module (CBM)

Carbohydrates are the most abundant biomolecules on Earth and are implicated in intercellular recognition, bacterial and virus infection, metabolism, structural support, energy storage, targeting, attachment, etc. To perform such roles, several carbohydrate-active

(CAZymes) proteins have acquired noncatalytic modules that interact very specifically with mono, oligo, and polysaccharides. In general, these carbohydrate-binding modules (CBM) are autonomous folding without enzymatic activity that brings the catalytic domain in close proximity to the substrate, insuring a prolonged contact and increasing the effective concentration of the enzyme on the target [237, 238].

CAZy (CarbohydrateActive enZyme, <http://www.cazy.org/>) is a database of glycoside hydrolases (GHs), glycosyltransferases (GTs), polysaccharide lyases (PLs), carbohydrate esterases (CEs) and CBMs. These protein groups are further subdivided into a number of families within the groups. In the CAZy database, a CBM is currently defined as a contiguous amino acid sequence within a carbohydrate-active enzyme with a discrete fold having carbohydrate-binding activity. Few works described the occurrence of isolated CBMs, as a single protein [239-241] and CBMs that integrate the cellulosomal scaffoldin proteins [242-244]. The requirement of CBMs existing as modules within larger enzymes sets this class of carbohydrate-binding protein apart from other non-catalytic sugar binding proteins such as lectins and sugar transport proteins.

CBMs may be found in any domain of life and are present in a large variety of enzymes, with different functions and substrate affinities that recognize polysaccharides such as crystalline cellulose, non-crystalline cellulose, chitin, β -1,3-glucans and β -1,3-1,4-mixed linkage glucans, xylan, mannan, galactan and starch [238]. They have been classified based on amino acid similarity into 59 primary structure-based families in the CAZy database. Structures for 44 of the 59 families have been reported and, from its analysis, it is clear that while CBMs vary widely in their carbohydrate specificities, common folds are observed in proteins with different specificities and belonging to different taxonomic groups. CBMs contain from 30 to about 200 amino acids and exist as a single, double, or triple domain and are located at C- or N-terminal, and in a less extent, centrally positioned within the polypeptide chain of proteins. The primary functions of CBMs in CAZyme [237, 238, 245] are described in table 5.

Once the CBMs are independent folding units (allowing it to be expressed in chimeric proteins) and its binding specificities can be controlled using Genetic Engineering technology and in general the attachment matrices for these domains are abundant and inexpensive [245],

Table 5. Functions of CBMs in CAZyme

Proximity effect	CBMs promote the association of the enzyme with the substrate, insuring a prolonged contact, and thereby increasing their effective concentration.
Targeting effect	Fine specificity for polysaccharide substructures.
Nonhydrolytic substrate disruption	Leading to an increase in substrate access and more susceptibility to enzymatic hydrolysis.
Avidity effect	Increases the avidity of the CAZyme for the substrate.

different applications of CBMs have been described: the improvement of fibers in textile and paper industry [246-250]; surface-exposed CBMs can be an efficient means of whole-cell immobilization [251-254]; the recombinant DNA technology allows the production of chimeric proteins containing foreign CBM. Many protein have been expressed fused to CBMs, establishing CBMs as high-capacity purification tags for the isolation of biologically active target from biotechnological products at relatively low cost [250]; Several studies have shown the potential of CBMs for modifying the characteristics of several enzymes through the addition or substitution of a CBM in order to improve the enzyme stability or hydrolytic activity [255]; Other studies involved actual modification of the CBM moiety to match a set of defined reaction conditions, for example, replacing some amino acid in different positions, its possible to obtain a definite pH dependency [256]; Another field for CBM application is bioremediation where, for example, an enzyme capable to degrade or chelate harmful substances to the environment could be expressed with a CBM that enable the anchorage of the enzyme in a support, such as reactors with immobilized enzyme for the detoxification of hazardous organophosphates, heavy metals, etc [257-259]; Finally, CBMs have been used as analytical tools in research and diagnostics, such as probes for protein-carbohydrate interaction and microarrays [238, 245].

Cellulose-binding module from the *Clostridium thermocellum*. The initial event in the cellulose degradation process is the binding of the cellulolytic enzyme(s) or the entire microorganism to the cellulose substrate. This binding is mediated by a separate module that binds to cellulose, a cellulose-binding module (CBM). CBMs appear to play a multiple role in cellulolysis. They often comprise a distinct domain of a free enzyme, linked to one or more catalytic domains (not necessarily cellulases). In some cases, they occur in a discrete subunit,

together with additional non-catalytic domains, which serve to integrate the catalytic subunits into a multifunctional enzyme complex, the cellulosome [260, 261]. Besides targeting cells to cellulose substrate, CBM mediate the non-hydrolytic disruption of cellulose fibers [262].

A cellulose-binding module family-III from the cellulosomal-scaffolding protein A of the bacteria *Clostridium thermocellum* (an anaerobic thermophilic bacterium that excretes large amounts of cellulolytic enzymes of particularly high specific activity) [263] was used to modified structures based on bacterial cellulose in the works developed in this thesis. The enzymatic degradation of cellulose by *C. thermocellum* is mediated by a cellulosome, that consist of discrete multi-functional, multi-enzyme complexe, wherein all the enzymic factors leading to cellulose degradation are physically attached to a central scaffold component (CipA – Cellulosome integrating protein) [242]. The CipA contains cohesin modules, normally in multiple copies, for incorporation of the catalytic domains, including β -(1 \rightarrow 4)-endoglucanases, cellobiohydrolases, hemicellulases and other cellulosomal components. The scaffolding also frequently includes a carbohydrate-binding module (i.e., a cellulose-binding module), through which the complex usually recognizes and binds to the substrate [264, 265]. Family-III CBMs comprise -150 amino acid residues. Currently have 285 members, one with chitin binding ability; the structure of six of these CBM3 is known. They have been identified in many different bacterial enzymes, and in the non-hydrolytic proteins CbpA [243], CipA [266], CipB [267] and CipC [244] which are responsible for the structural organization of the cellulosomes present in *Clostridium cellulovorans* (CbpA), *Clostridium thermocellum* (CipA and CipB from strains ATCC 27405 and YS, respectively), and *Clostridium cellulolyticum* (CipC), respectively.

The crystal structure of a family-III cellulose-binding module (CBM3) from the cellulosomal scaffoldin subunit of *Clostridium thermocellum* was determined by Tormo and colleagues [268]. According to this work the proteic structure forms a nine-stranded β -sandwich with a jelly roll topology and contains a Ca^{2+} binding site. Conserved, surface-exposed residues map into two defined surfaces located on opposite sides of the molecule. On the face that is proposed to bind to crystalline cellulose there is a planar linear strip of aromatic residues (His57, Tyr67 and Trp118) and two polar side chains of aspartic acid (Asp56) and arginine (Arg112). The other conserved residues are contained in a shallow groove, the function of which is currently unknown, and which has not been observed previously in other families of CBMs [268].

References

1. Baguneid MS, Fulford PE, Walker MG. Cardiovascular surgery in the elderly. *J R Coll Surg Edinb* 1999 Aug;44(4):216-221.
2. Gersh BJ, Sliwa K, Mayosi BM, Yusuf S. Novel therapeutic concepts: the epidemic of cardiovascular disease in the developing world: global implications. *Eur Heart J* 2010 Mar;31(6):642-648.
3. Isenberg BC, Williams C, Tranquillo RT. Small-diameter artificial arteries engineered in vitro. *Circ Res* 2006 Jan 6;98(1):25-35.
4. Wang X, Lin P, Yao Q, Chen C. Development of small-diameter vascular grafts. *World J Surg* 2007 Apr;31(4):682-689.
5. Chlupac J, Filova E, Bacakova L. Blood vessel replacement: 50 years of development and tissue engineering paradigms in vascular surgery. *Physiol Res* 2009;58 Suppl 2:S119-139.
6. Teebken OE, Haverich A. Tissue engineering of small diameter vascular grafts. *Eur J Vasc Endovasc Surg* 2002 Jun;23(6):475-485.
7. Hillen F, Melotte V, van Beijnum JR, Griffioen AW. Endothelial Cell Biology. In: Carolyn A. Staton CL, Roy Bicknell, editor. *Angiogenesis Assays*: John Wiley & Sons, Ltd, 2006. p. 1-38.
8. Luscher TF, Barton M. Biology of the endothelium. *Clin Cardiol* 1997 Nov;20(11 Suppl 2):II-3-10.
9. Galley HF, Webster NR. Physiology of the endothelium. *Br J Anaesth* 2004 Jul;93(1):105-113.
10. Sarkar S, Schmitz-Rixen T, Hamilton G, Seifalian AM. Achieving the ideal properties for vascular bypass grafts using a tissue engineered approach: a review. *Med Biol Eng Comput* 2007 Apr;45(4):327-336.
11. Ait-Oufella H, Maury E, Lehoux S, Guidet B, Offenstadt G. The endothelium: physiological functions and role in microcirculatory failure during severe sepsis. *Intensive Care Med* May 5.
12. Esmon CT. Protein C anticoagulant pathway and its role in controlling microvascular thrombosis and inflammation. *Crit Care Med* 2001 Jul;29(7 Suppl):S48-51; discussion 51-42.
13. Lwaleed BA, Bass PS. Tissue factor pathway inhibitor: structure, biology and involvement in disease. *J Pathol* 2006 Feb;208(3):327-339.
14. Broze GJ, Jr. Tissue factor pathway inhibitor. *Thromb Haemost* 1995 Jul;74(1):90-93.
15. Michiels C. Endothelial cell functions. *J Cell Physiol* 2003 Sep;196(3):430-443.
16. Jaffe EA. Physiologic functions of normal endothelial cells. *Ann N Y Acad Sci* 1985;454:279-291.

17. Cines DB, Pollak ES, Buck CA, Loscalzo J, Zimmerman GA, McEver RP, et al. Endothelial cells in physiology and in the pathophysiology of vascular disorders. *Blood* 1998 May 15;91(10):3527-3561.
18. Ratner BD, Hoffman AS, Schoen FJ, Lemons JE. *Biomaterials science: an introduction to materials in medicine*. London, UK: Academic press, 1996.
19. Sidelmann JJ, Gram J, Jespersen J, Klufft C. Fibrin clot formation and lysis: basic mechanisms. *Semin Thromb Hemost* 2000;26(6):605-618.
20. Yadav R, Larbi KY, Young RE, Nourshargh S. Migration of leukocytes through the vessel wall and beyond. *Thromb Haemost* 2003 Oct;90(4):598-606.
21. Mann KG. Biochemistry and physiology of blood coagulation. *Thromb Haemost* 1999 Aug;82(2):165-174.
22. Davie EW, Fujikawa K, Kisiel W. The coagulation cascade: initiation, maintenance, and regulation. *Biochemistry* 1991 Oct 29;30(43):10363-10370.
23. Canver CC. Conduit options in coronary artery bypass surgery. *Chest* 1995 Oct;108(4):1150-1155.
24. Barner HB. Arterial grafting: techniques and conduits. *Ann Thorac Surg* 1998 Nov;66(5 Suppl):S2-5; discussion S25-28.
25. Schmidt CE, Baier JM. Acellular vascular tissues: natural biomaterials for tissue repair and tissue engineering. *Biomaterials* 2000 Nov;21(22):2215-2231.
26. Callow AD. Arterial homografts. *Eur J Vasc Endovasc Surg* 1996 Oct;12(3):272-281.
27. Voorhees AB, Jr., Jaretzki A, 3rd, Blakemore AH. The use of tubes constructed from vinyon "N" cloth in bridging arterial defects. *Ann Surg* 1952 Mar;135(3):332-336.
28. Andros G, Harris RW, Salles-Cunha SX, Dulawa LB, Oblath RW, Apyan RL. Arm veins for arterial revascularization of the leg: arteriographic and clinical observations. *J Vasc Surg* 1986 Nov;4(5):416-427.
29. Carrel A, Guthrie CC. Uniterminal and biterminal venous transplantations. *Surg Gynecol Obstet* 1906;2:266.
30. Goyanes L. Nuevos trabajos de cirugía vascular, substitucion plastica de las arterias por las venas or arterioplastica venosa, aplicada, comoo nuevo metodo, al tratamiento de los aneurismas. *Siglo Med* 1906;53:546-549.
31. Lexer E. Die ideale Operation des arteriellen und des arterioveno Èsen Aneurysmas. *Arch Klin Chir* 1907;83:459-463.
32. Taheri SA. Superficial femoral-popliteal veins and reversed saphenous veins as primary femoropopliteal bypass grafts: a randomized comparative study. *J Vasc Surg* 1987 Dec;6(6):624-625.
33. Jaboulay M, Briau E. Recherches experimentales sur la suture

et la greffe arterielles. Lyon Med 1896;81:97.

34. Faruqi RM, Stoney RJ. The arterial autograft. In: Rutherford RB, editor. *Vascular Surgery*. 5 ed. ed. Philadelphia, Pennsylvania: W. B. Saunders, 2000. p. 532-539.
35. Carrel A. Landmark article, Nov 14, 1908: Results of the transplantation of blood vessels, organs and limbs. By Alexis Carrel. *JAMA* 1983 Aug 19;250(7):944-953.
36. Pirovano MA. Un cas de greffe arterielle. *Press Med* 1911;19:55.
37. Gross RE, Hurwitt ES, et al. Preliminary observations on the use of human arterial grafts in the treatment of certain cardiovascular defects. *N Engl J Med* 1948 Oct 14;239(16):578.
38. Schulze-Bergmann G. Erfahrungen mit der homologen Vene als Arterienersatz im femoropoplitealen Bereich. In: Denck H, Hagmuller GW, editors. IX Jahrestagung der Österreichischen Gesellschaft für Gefäßchirurgie. Wien, Egermann, 1976. p. 157.
39. Rosenberg N, Martinez A, Sawyer PN, Wesolowski SA, Postlethwait RW, Dillon ML, Jr. Tanned collagen arterial prosthesis of bovine carotid origin in man. Preliminary studies of enzyme-treated heterografts. *Ann Surg* 1966 Aug;164(2):247-256.
40. Clarke DR, Lust RM, Sun YS, Black KS, Ollerenshaw JD. Transformation of nonvascular acellular tissue matrices into durable vascular conduits. *Ann Thorac Surg* 2001 May;71(5 Suppl):S433-436.
41. Voorhees AB, Jr., Jaretzki AH, Blakemore AH. The use of tubes constructed from vinyon "N" cloth in bridging arterial defects. *Ann Surg* 1952 Mar;135(3):332-336.
42. Edwards WS. Plastic arterial grafts. In: Thomas AC, editor. Springfield, 1962.
43. DeBakey ME, Jordan GL, Jr., Abbott JP, Halpert B, O'Neal RM. The Fate of Dacron Vascular Grafts. *Arch Surg* 1964 Nov;89:757-782.
44. Parodi JC, Palmaz JC, Barone HD. Transfemoral intraluminal graft implantation for abdominal aortic aneurysms. *Ann Vasc Surg* 1991 Nov;5(6):491-499.
45. Meinhart JG, Deutsch M, Fischlein T, Howanietz N, Froschl A, Zilla P. Clinical autologous in vitro endothelialization of 153 infrainguinal ePTFE grafts. *Ann Thorac Surg* 2001 May;71(5 Suppl):S327-331.
46. Aldenhoff YB, van Der Veen FH, ter Woorst J, Habets J, Poole-Warren LA, Koole LH. Performance of a polyurethane vascular prosthesis carrying a dipyrindamole (Persantin) coating on its luminal surface. *J Biomed Mater Res* 2001 Feb;54(2):224-233.
47. Stegemann JP, Kaszuba SN, Rowe SL. Review: advances in vascular tissue engineering using protein-based biomaterials. *Tissue Eng* 2007 Nov;13(11):2601-2613.
48. Weinberg CB, Bell E. A blood vessel model constructed from collagen and cultured vascular cells. *Science* 1986 Jan 24;231(4736):397-400.
49. Zhang WJ, Liu W, Cui L, Cao Y. Tissue engineering of blood vessel. *J Cell Mol Med* 2007 Sep-Oct;11(5):945-957.

50. Nerem RM, Ensley AE. The tissue engineering of blood vessels and the heart. *Am J Transplant* 2004;4 Suppl 6:36-42.
51. Berglund JD, Galis ZS. Designer blood vessels and therapeutic revascularization. *Br J Pharmacol* 2003 Oct;140(4):627-636.
52. Karande TS, Agrawal M. Functions and Requirements of Synthetic Scaffolds in Tissue Engineering. In: Laurencin CT, Nair LS, editors. *Nanotechnology and Tissue Engineering: The Scaffold*. Boca Raton, FL, 2008. p. 384.
53. L'Heureux N, Dusserre N, Konig G, Victor B, Keire P, Wight TN, et al. Human tissue-engineered blood vessels for adult arterial revascularization. *Nature Medicine* 2006;12(3):361-365.
54. Heydarkhan-Hagvall S, Esguerra M, Helenius G, Soderberg R, Johansson BR, Risberg B. Production of extracellular matrix components in tissue-engineered blood vessels. *Tissue Eng* 2006 Apr;12(4):831-842.
55. L'Heureux N, Paquet S, Labbe R, Germain L, Auger FA. A completely biological tissue-engineered human blood vessel. *FASEB J* 1998 Jan;12(1):47-56.
56. McKee JA, Banik SS, Boyer MJ, Hamad NM, Lawson JH, Niklason LE, et al. Human arteries engineered in vitro. *EMBO Rep* 2003 Jun;4(6):633-638.
57. Konig G, McAllister TN, Dusserre N, Garrido SA, Iyican C, Marini A, et al. Mechanical properties of completely autologous human tissue engineered blood vessels compared to human saphenous vein and mammary artery. *Biomaterials* 2009 Mar;30(8):1542-1550.
58. Chue WL, Campbell GR, Caplice N, Muhammed A, Berry CL, Thomas AC, et al. Dog peritoneal and pleural cavities as bioreactors to grow autologous vascular grafts. *J Vasc Surg* 2004 Apr;39(4):859-867.
59. Campbell JH, Efendy JL, Campbell GR. Novel vascular graft grown within recipient's own peritoneal cavity. *Circ Res* 1999 Dec 3-17;85(12):1173-1178.
60. Norotte C, Marga FS, Niklason LE, Forgacs G. Scaffold-free vascular tissue engineering using bioprinting. *Biomaterials* 2009 Oct;30(30):5910-5917.
61. Guidoin R, Maurel S, Chakfe N, How T, Zhang Z, Therrien M, et al. Expanded polytetrafluoroethylene arterial prostheses in humans: chemical analysis of 79 explanted specimens. *Biomaterials* 1993 Jul;14(9):694-704.
62. Guidoin R, Chakfe N, Maurel S, How T, Batt M, Marois M, et al. Expanded polytetrafluoroethylene arterial prostheses in humans: histopathological study of 298 surgically excised grafts. *Biomaterials* 1993 Jul;14(9):678-693.
63. Ravi S, Qu Z, Chaikof EL. Polymeric materials for tissue engineering of arterial substitutes. *Vascular* 2009 May-Jun;17 Suppl 1:S45-54.
64. Jeschke MG, Hermanutz V, Wolf SE, Koveker GB. Polyurethane vascular prostheses decreases neointimal formation compared with expanded polytetrafluoroethylene. *J Vasc Surg* 1999 Jan;29(1):168-176.

65. Roald HE, Barstad RM, Bakken IJ, Roald B, Lyberg T, Sakariassen KS. Initial interactions of platelets and plasma proteins in flowing non-anticoagulated human blood with the artificial surfaces Dacron and PTFE. *Blood Coagul Fibrinolysis* 1994 Jun;5(3):355-363.
66. Baier RE. Selected methods of investigation for blood-contact surfaces. *Ann N Y Acad Sci* 1987;516:68-77.
67. Vroman L. The life of an artificial device in contact with blood: initial events and their effect on its final state. *Bull N Y Acad Med* 1988 May;64(4):352-357.
68. Joist JH, Pennington DG. Platelet reactions with artificial surfaces. *ASAIO Trans* 1987 Jul-Sep;33(3):341-344.
69. Sawyer PN, Pate JW, Weldon CS. Relations of abnormal and injury electric potential differences to intravascular thrombosis. *Am J Physiol* 1953 Oct;175(1):108-112.
70. Jucker BA, Harms H, Zehnder AJ. Adhesion of the positively charged bacterium *Stenotrophomonas* (Xanthomonas) maltophilia 70401 to glass and Teflon. *J Bacteriol* 1996 Sep;178(18):5472-5479.
71. Sarkar S, Sales KM, Hamilton G, Seifalian AM. Addressing thrombogenicity in vascular graft construction. *J Biomed Mater Res B Appl Biomater* 2007 Jul;82(1):100-108.
72. Kallmes DF, McGraw JK, Evans AJ, Mathis JM, Hergenrother RW, Jensen ME, et al. Thrombogenicity of hydrophilic and nonhydrophilic microcatheters and guiding catheters. *AJNR Am J Neuroradiol* 1997 Aug;18(7):1243-1251.
73. Nagaoka S, Akashi R. Low-friction hydrophilic surface for medical devices. *Biomaterials* 1990 Aug;11(6):419-424.
74. Anderson AB, Tran TH, Hamilton MJ, Chudzik SJ, Hastings BP, Melchior MJ, et al. Platelet deposition and fibrinogen binding on surfaces coated with heparin or friction-reducing polymers. *AJNR Am J Neuroradiol* 1996 May;17(5):859-863.
75. Lin JC, Cooper SL. Surface characterization and ex vivo blood compatibility study of plasma-modified small diameter tubing: effect of sulphur dioxide and hexamethyldisiloxane plasmas. *Biomaterials* 1995 Sep;16(13):1017-1023.
76. Leach KR, Kurisu Y, Carlson JE, Repa I, Epstein DH, Urness M, et al. Thrombogenicity of hydrophilically coated guide wires and catheters. *Radiology* 1990 Jun;175(3):675-677.
77. Chu CFL, Lu A, Liszkowski M, Sipehia R. Enhanced growth of animal and human endothelial cells on biodegradable polymers. *Biochimica Et Biophysica Acta-General Subjects* 1999 Nov 16;1472(3):479-485.
78. Tseng DY, Edelman ER. Effects of amide and amine plasma-treated ePTFE vascular grafts on endothelial cell lining in an artificial circulatory system. *Journal of Biomedical Materials Research* 1998 Nov;42(2):188-198.
79. Zhu AP, Zhang M, Zhang Z. Surface modification of ePTFE vascular grafts with O-carboxymethylchitosan. *Polymer International* 2004 Jan;53(1):15-19.

80. Phaneuf MD, Quist WC, Bide MJ, Logerfo FW. Modification of Polyethylene Terephthalate (Dacron) Via Denier Reduction - Effects on Material Tensile-Strength, Weight, and Protein-Binding Capabilities. *Journal of Applied Biomaterials* 1995 Win;6(4):289-299.
81. Chandy T, Das GS, Wilson RF, Rao GHR. Use of plasma glow for surface-engineering biomolecules to enhance bloodcompatibility of Dacron and PTFE vascular prosthesis. *Biomaterials* 2000 Apr;21(7):699-712.
82. Sipehia R, Martucci G, Barbarosie M, Wu C. Enhanced Attachment and Growth of Human Endothelial-Cells Derived from Umbilical Veins on Ammonia Plasma-Modified Surfaces of Ptfе and Eptfe Synthetic Vascular Graft Biomaterials. *Biomaterials Artificial Cells and Immobilization Biotechnology* 1993;21(4):455-468.
83. Tran CNB, Walt DR. Plasma Modification and Collagen Binding to Ptfе Grafts. *Journal of Colloid and Interface Science* 1989 Oct 15;132(2):373-381.
84. Chakfe N, Bizonne SC, Beaufigeau M, Urban E, Cardon A, Doillon C, et al. Impregnated polyester arterial prostheses: performance and prospects. *Ann Vasc Surg* 1999 Sep;13(5):509-523.
85. Yates SG, Barros D'Sa AA, Berger K, Fernandez LG, Wood SJ, Rittenhouse EA, et al. The preclotting of porous arterial prostheses. *Ann Surg* 1978 Nov;188(5):611-622.
86. Humphries AW, Hawk WA, Cuthbertson AM. Arterial prosthesis of collagen-impregnated Dacron tulle. *Surgery* 1961 Dec;50:947-954.
87. Bascom JU. Gelatin sealing to prevent blood loss from knitted arterial grafts. *Surgery* 1961 Sep;50:504-512.
88. Sai P, Babu M. Collagen based dressings - a review. *Burns* 2000 Feb;26(1):54-62.
89. Madaghiele M, Piccinno A, Saponaro M, Maffezzoli A, Sannino A. Collagen- and gelatine-based films sealing vascular prostheses: evaluation of the degree of crosslinking for optimal blood impermeability. *J Mater Sci Mater Med* 2009 Oct;20(10):1979-1989.
90. Bos GW, Poot AA, Beugeling T, van Aken WG, Feijen J. Small-diameter vascular graft prostheses: current status. *Arch Physiol Biochem* 1998 Apr;106(2):100-115.
91. Huang-Lee LL, Cheung DT, Nimni ME. Biochemical changes and cytotoxicity associated with the degradation of polymeric glutaraldehyde derived crosslinks. *J Biomed Mater Res* 1990 Sep;24(9):1185-1201.
92. Marois Y, Chakfe N, Deng X, Marois M, How T, King MW, et al. Carbodiimide cross-linked gelatin: a new coating for porous polyester arterial prostheses. *Biomaterials* 1995 Oct;16(15):1131-1139.
93. Heyligers JM, Arts CH, Verhagen HJ, de Groot PG, Moll FL. Improving small-diameter vascular grafts: from the application of an endothelial cell lining to the construction of a tissue-engineered blood vessel. *Ann Vasc Surg* 2005 May;19(3):448-456.

94. Seifalian AM, Tiwari A, Hamilton G, Salacinski HJ. Improving the clinical patency of prosthetic vascular and coronary bypass grafts: the role of seeding and tissue engineering. *Artif Organs* 2002 Apr;26(4):307-320.
95. Bacakova L, Filova E, Rypacek F, Svorcik V, Stary V. Cell adhesion on artificial materials for tissue engineering. *Physiological Research* 2004;53:S35-S45.
96. Bhat VD, Truskey GA, Reichert WM. Fibronectin and avidin-biotin as a heterogeneous ligand system for enhanced endothelial cell adhesion. *Journal of Biomedical Materials Research* 1998 Sep 5;41(3):377-385.
97. Cook AD, Hrkach JS, Gao NN, Johnson IM, Pajvani UB, Cannizzaro SM, et al. Characterization and development of RGD-peptide-modified poly(lactic acid-co-lysine) as an interactive, resorbable biomaterial. *Journal of Biomedical Materials Research* 1997 Jun 15;35(4):513-523.
98. Massia SP, Hubbell JA. Human Endothelial-Cell Interactions with Surface-Coupled Adhesion Peptides on a Nonadhesive Glass Substrate and 2 Polymeric Biomaterials. *Journal of Biomedical Materials Research* 1991 Feb;25(2):223-242.
99. Lin HB, Garciaecheverria C, Asakura S, Sun W, Mosher DF, Cooper SL. Endothelial-Cell Adhesion on Polyurethanes Containing Covalently Attached Rgd-Peptides. *Biomaterials* 1992;13(13):905-914.
100. Lin HB, Sun W, Mosher DF, Garciaecheverria C, Schaufelberger K, Lelkes PI, et al. Synthesis, Surface, and Cell-Adhesion Properties of Polyurethanes Containing Covalently Grafted Rgd-Peptides. *Journal of Biomedical Materials Research* 1994 Mar;28(3):329-342.
101. Massia SP, Stark J. Immobilized RGD peptides on surface-grafted dextran promote biospecific cell attachment. *Journal of Biomedical Materials Research* 2001 Sep 5;56(3):390-399.
102. Hsu SH, Sun SH, Chen DCH. Improved retention of endothelial cells seeded on polyurethane small-diameter vascular grafts modified by a recombinant RGD-containing protein. *Artificial Organs* 2003 Dec;27(12):1068-1078.
103. Tiwari A, Kidane A, Salacinski H, Punshon G, Hamilton G, Seifalian AM. Improving endothelial cell retention for single stage seeding of prosthetic grafts: Use of polymer sequences of arginine-glycine-aspartate. *European Journal of Vascular and Endovascular Surgery* 2003 Apr;25(4):325-329.
104. Jun HW, West JL. Modification of polyurethaneurea with PEG and YIGSR peptide to enhance endothelialization without platelet adhesion. *Journal of Biomedical Materials Research Part B-Applied Biomaterials* 2005 Jan 15;72B(1):131-139.
105. Hubbell JA, Massia SP, Desai NP, Drumheller PD. Endothelial Cell-Selective Materials for Tissue Engineering in the Vascular Graft Via a New Receptor. *Bio-Technology* 1991 Jun;9(6):568-572.
106. Massia SP, Hubbell JA. Vascular Endothelial-Cell Adhesion and Spreading Promoted by the Peptide Redv of the Iiics Region of Plasma Fibronectin Is Mediated by Integrin Alpha-4-Beta-1. *Journal of Biological Chemistry* 1992 Jul 15;267(20):14019-14026.

107. Hoenig MR, Campbell GR, Campbell JH. Vascular grafts and the endothelium. *Endothelium* 2006 Nov-Dec;13(6):385-401.
108. Walluscheck KP, Steinhoff G, Kelm S, Haverich A. Improved endothelial cell attachment on ePTFE vascular grafts pretreated with synthetic RGD-containing peptides. *Eur J Vasc Endovasc Surg* 1996 Oct;12(3):321-330.
109. Goodman SL, Sims PA, Albrecht RM. Three-dimensional extracellular matrix textured biomaterials. *Biomaterials* 1996 Nov;17(21):2087-2095.
110. Gray DS, Tien J, Chen CS. Repositioning of cells by mechanotaxis on surfaces with micropatterned Young's modulus. *Journal of Biomedical Materials Research Part A* 2003 Sep 1;66A(3):605-614.
111. Bettinger CJ. Synthesis and microfabrication of biomaterials for soft-tissue engineering. *Pure and Applied Chemistry* 2009 Dec;81(12):2183-2201.
112. Daxini SC, Nichol JW, Sieminski AL, Smith G, Gooch KJ, Shastri VP. Micropatterned polymer surfaces improve retention of endothelial cells exposed to flow-induced shear stress. *Biorheology* 2006;43(1):45-55.
113. Ott MJ, Ballermann BJ. Shear Stress-Conditioned, Endothelial Cell-Seeded Vascular Grafts - Improved Cell Adherence in Response to in-Vitro Shear-Stress. *Surgery* 1995 Mar;117(3):334-339.
114. Isenberg BC, Williams C, Tranquillo RT. Endothelialization and flow conditioning of fibrin-based media-equivalents. *Annals of Biomedical Engineering* 2006 Jun;34(6):971-985.
115. Dardik A, Liu AL, Ballermann BJ. Chronic in vitro shear stress stimulates endothelial cell retention on prosthetic vascular grafts and reduces subsequent in vivo neointimal thickness. *Journal of Vascular Surgery* 1999 Jan;29(1):157-167.
116. Baguneid M, Murray D, Salacinski HJ, Fuller B, Hamilton G, Walker M, et al. Shear-stress preconditioning and tissue-engineering-based paradigms for generating arterial substitutes. *Biotechnology and Applied Biochemistry* 2004 Apr;39:151-157.
117. Riha GM, Lin PH, Lumsden AB, Yao QZ, Chen CY. Roles of hemodynamic forces in vascular cell differentiation. *Annals of Biomedical Engineering* 2005 Jun;33(6):772-779.
118. Tiwari A, Salacinski HJ, Hamilton G, Seifalian AM. Tissue engineering of vascular bypass grafts: role of endothelial cell extraction. *Eur J Vasc Endovasc Surg* 2001 Mar;21(3):193-201.
119. Chung-Welch N, Patton WF, Shepro D, Cambria RP. Human omental microvascular endothelial and mesothelial cells: characterization of two distinct mesodermally derived epithelial cells. *Microvasc Res* 1997 Sep;54(2):108-120.
120. Li C, Hill A, Imran M. In vitro and in vivo studies of ePTFE vascular grafts treated with P15 peptide. *J Biomater Sci Polym Ed* 2005;16(7):875-891.
121. Rotmans JI, Heyligers JM, Verhagen HJ, Velema E, Nagtegaal MM, de Kleijn DP, et al. In vivo cell seeding with anti-CD34 antibodies successfully accelerates endothelialization but

stimulates intimal hyperplasia in porcine arteriovenous expanded polytetrafluoroethylene grafts. *Circulation* 2005 Jul 5;112(1):12-18.

122. Randone B, Cavallaro G, Polistena A, Cucina A, Coluccia P, Graziano P, et al. Dual role of VEGF in pretreated experimental ePTFE arterial grafts. *J Surg Res* 2005 Aug;127(2):70-79.

123. Stachelek SJ, Alferiev I, Choi H, Kronsteiner A, Uttayarat P, Gooch KJ, et al. Cholesterol-derivatized polyurethane: characterization and endothelial cell adhesion. *J Biomed Mater Res A* 2005 Feb 1;72(2):200-212.

124. Wang C, Zhang Q, Uchida S, Kodama M. A new vascular prosthesis coated with polyamino-acid urethane copolymer (PAU) to enhance endothelialization. *J Biomed Mater Res* 2002 Dec 5;62(3):315-322.

125. Santhosh Kumar TR, Krishnan LK. Endothelial cell growth factor (ECGF) enmeshed with fibrin matrix enhances proliferation of EC in vitro. *Biomaterials* 2001 Oct;22(20):2769-2776.

126. Jun HW, West JL. Endothelialization of microporous YIGSR/PEG-modified polyurethaneurea. *Tissue Eng* 2005 Jul-Aug;11(7-8):1133-1140.

127. Kidd KR, Patula VB, Williams SK. Accelerated endothelialization of interpositional 1-mm vascular grafts. *J Surg Res* 2003 Aug;113(2):234-242.

128. Lehle K, Buttstaedt J, Birnbaum DE. Expression of adhesion molecules and cytokines in vitro by endothelial cells seeded on various polymer surfaces coated with titaniumcarboxonitride. *J Biomed Mater Res A* 2003 Jun 1;65(3):393-401.

129. Pollara P, Alessandri G, Bonardelli S, Simonini A, Cabibbo E, Portolani N, et al. Complete in vitro prosthesis endothelialization induced by artificial extracellular matrix. *J Invest Surg* 1999 Mar-Apr;12(2):81-88.

130. Noishiki Y, Ma XH, Yamane Y, Satoh S, Okoshi T, Takahashi K, et al. Succinylated collagen crosslinked by thermal treatment for coating vascular prostheses. *Artif Organs* 1998 Aug;22(8):672-680.

131. Wissink MJ, Beernink R, Poot AA, Engbers GH, Beugeling T, van Aken WG, et al. Improved endothelialization of vascular grafts by local release of growth factor from heparinized collagen matrices. *J Control Release* 2000 Feb 14;64(1-3):103-114.

132. Doi K, Matsuda T. Enhanced vascularization in a microporous polyurethane graft impregnated with basic fibroblast growth factor and heparin. *J Biomed Mater Res* 1997 Mar 5;34(3):361-370.

133. Dekker A, Reitsma K, Beugeling T, Bantjes A, Feijen J, van Aken WG. Adhesion of endothelial cells and adsorption of serum proteins on gas plasma-treated polytetrafluoroethylene. *Biomaterials* 1991 Mar;12(2):130-138.

134. Mazzucotelli JP, Moczar M, Zede L, Bambang LS, Loisanse D. Human vascular endothelial cells on expanded PTFE precoated with an engineered protein adhesion factor. *Int J Artif Organs* 1994 Feb;17(2):112-117.

135. Bernex F, Mazzucotelli JP, Roudiere JL, Benhaiem-Sigaux N, Leandri J, Loisanche D. In vitro endothelialization of carbon-coated Dacron vascular grafts. *Int J Artif Organs* 1992 Mar;15(3):172-180.
136. Zilla P, Fasol R, Grimm M, Fischlein T, Eberl T, Preiss P, et al. Growth properties of cultured human endothelial cells on differently coated artificial heart materials. *J Thorac Cardiovasc Surg* 1991 Apr;101(4):671-680.
137. Seeger JM, Klingman N. Improved in vivo endothelialization of prosthetic grafts by surface modification with fibronectin. *J Vasc Surg* 1988 Oct;8(4):476-482.
138. Jonas R, Farah LF. Production and application of microbial cellulose. *Polymer Degradation and Stability* 1998;59(1-3):101-106.
139. Brown AJ. The chemical action of pure cultivation of bacterial aceti. *Journal of Chemical Society, Transactions* 1886;49:172-187.
140. Helenius G, Backdahl H, Bodin A, Nannmark U, Gatenholm P, Risberg B. In vivo biocompatibility of bacterial cellulose. *J Biomed Mater Res A* 2006 Feb;76A(2):431-438.
141. Vandamme EJ, De Baets S, Vanbaelen A, Joris K, De Wulf P. Improved production of bacterial cellulose and its application potential. *Polymer Degradation and Stability* 1998;59(1-3):93-99.
142. Klemm D, Schumann D, Udhardt U, Marsch S. Bacterial synthesized cellulose - artificial blood vessels for microsurgery. *Progress in Polymer Science* 2001 Nov;26(9):1561-1603.
143. Amano Y, Ito F, Kanda T. Novel cellulose producing system by microorganisms such as *Acetobacter* sp. *Journal of Biological Macromolecules* 2005;5(1):3-10.
144. Czaja W, Krystynowicz A, Bielecki S, Brown RM. Microbial cellulose - the natural power to heal wounds. *Biomaterials* 2006 Jan;27(2):145-151.
145. Czaja WK, Young DJ, Kawecki M, Brown RM. The future prospects of microbial cellulose in biomedical applications. *Biomacromolecules* 2007 Jan;8(1):1-12.
146. Watanabe K, Eto Y, Takano S, Nakamori S, Shibai H, Yamanaka S. A New Bacterial Cellulose Substrate for Mammalian-Cell Culture - a New Bacterial Cellulose Substrate. *Cytotechnology* 1993;13(2):107-114.
147. Svensson A, Harrah T, Panilaitis B, Kaplan D, Gatenholm P. Bacterial cellulose as a substrate for tissue engineering of cartilage. *Abstracts of Papers of the American Chemical Society* 2004 Mar 28;227:U282-U282.
148. Iguchi M, Yamanaka S, Budhiono A. Bacterial cellulose - a masterpiece of nature's arts. *Journal of Materials Science* 2000 Jan;35(2):261-270.
149. Cannon RE, Anderson SM. Biogenesis of Bacterial Cellulose. *Critical Reviews in Microbiology* 1991;17(6):435-447.
150. Hestrin S, Schramm M. Synthesis of Cellulose by *Acetobacter-Xylinum* .2. Preparation of Freeze-Dried Cells Capable of Polymerizing Glucose to Cellulose. *Biochemical Journal* 1954;58(2):345-352.

151. Ross P, Mayer R, Benziman M. Cellulose Biosynthesis and Function in Bacteria. *Microbiological Reviews* 1991 Mar;55(1):35-58.
152. Bodin A, Backdahl H, Fink H, Gustafsson L, Risberg B, Gatenholm P. Influence of cultivation conditions on mechanical and morphological properties of bacterial cellulose tubes. *Biotechnology and Bioengineering* 2007 Jun 1;97(2):425-434.
153. Hwang JW, Yang YK, Hwang JK, Pyun YR, Kim YS. Effects of pH and dissolved oxygen on cellulose production by *Acetobacter xylinum* BRC5 in agitated culture. *Journal of Bioscience and Bioengineering* 1999 Aug;88(2):183-188.
154. Krystynowicz A, Czaja W, Wiktorowska-Jeziarska A, Goncalves-Miskiewicz M, Turkiewicz M, Bielecki S. Factors affecting the yield and properties of bacterial cellulose. *Journal of Industrial Microbiology & Biotechnology* 2002 Oct;29(4):189-195.
155. Kouda T, Yano H, Yoshinaga F. Effect of agitator configuration on bacterial cellulose productivity in aerated and agitated culture. *Journal of Fermentation and Bioengineering* 1997;83(4):371-376.
156. Ramana KV, Tomar A, Singh L. Effect of various carbon and nitrogen sources on cellulose synthesis by *Acetobacter xylinum*. *World Journal of Microbiology & Biotechnology* 2000 Apr;16(3):245-248.
157. Valla S, Ertesvåg H, Tonouchi N, Fjaervik E. Chap.3 - Bacterial Cellulose Production: Biosynthesis and Applications. In: Rehm BHA, editor. *Microbial Production of Biopolymers and Polymer Precursors: Applications and Perspectives*: Horizon Scientific Press, 2009. p. 43-77.
158. Brown RM, Saxena IM. Cellulose biosynthesis: A model for understanding the assembly of biopolymers. *Plant Physiology and Biochemistry* 2000 Jan-Feb;38(1-2):57-67.
159. Klemm D, Heublein B, Fink HP, Bohn A. Cellulose: Fascinating biopolymer and sustainable raw material. *Angewandte Chemie-International Edition* 2005;44(22):3358-3393.
160. Nakagaito AN, Iwamoto S, Yano H. Bacterial cellulose: the ultimate nano-scalar cellulose morphology for the production of high-strength composites. *Applied Physics a-Materials Science & Processing* 2005 Jan;80(1):93-97.
161. Yamanaka S, Watanabe K, Kitamura N, Iguchi M, Mitsunashi S, Nishi Y, et al. The Structure and Mechanical-Properties of Sheets Prepared from Bacterial Cellulose. *Journal of Materials Science* 1989 Sep;24(9):3141-3145.
162. Backdahl H, Helenius G, Bodin A, Nannmark U, Johansson BR, Risberg B, et al. Mechanical properties of bacterial cellulose and interactions with smooth muscle cells. *Biomaterials* 2006 Mar;27(9):2141-2149.
163. Bodin A, Ahrenstedt L, Fink H, Brumer H, Risberg B, Gatenholm P. Modification of nanocellulose with a xyloglucan-RGD conjugate enhances adhesion and proliferation of endothelial cells: Implications for tissue engineering. *Biomacromolecules* 2007 Dec;8(12):3697-3704.

164. Sanchavanakit N, Sangrungraungroj W, Kaomongkolgit R, Banaprasert T, Pavasant P, Phisalaphong M. Growth of human keratinocytes and fibroblasts on bacterial cellulose film. *Biotechnol Prog* 2006 Jul-Aug;22(4):1194-1199.
165. Sokolnicki AM, Fisher RJ, Harrah TP, Kaplan DL. Permeability of bacterial cellulose membranes. *Journal of Membrane Science* 2006 Mar 15;272(1-2):15-27.
166. Iguchi M, Mitsuhashi S, Ichimura K, Nishi Y, Uryu M, Yamanaka S, et al., inventors. Bacterial cellulose-containing molding material having high dynamic strength. US, 1988.
167. Nishi Y, Uryu M, Yamanaka S, Watanabe K, Kitamura N, Iguchi M, et al. The Structure and Mechanical-Properties of Sheets Prepared from Bacterial Cellulose .2. Improvement of the Mechanical-Properties of Sheets and Their Applicability to Diaphragms of Electroacoustic Transducers. *Journal of Materials Science* 1990 Jun;25(6):2997-3001.
168. Fricain JC, Granja PL, Barbosa MA, de Jeso B, Barthe N, Baquey C. Cellulose phosphates as biomaterials. In vivo biocompatibility studies. *Biomaterials* 2002 Feb;23(4):971-980.
169. Entcheva E, Bien H, Yin LH, Chung CY, Farrell M, Kostov Y. Functional cardiac cell constructs on cellulose-based scaffolding. *Biomaterials* 2004 Nov;25(26):5753-5762.
170. Martson M, Viljanto J, Hurme T, Saukko P. Biocompatibility of cellulose sponge with bone. *European Surgical Research* 1998 Nov-Dec;30(6):426-432.
171. Muller FA, Muller L, Hofmann I, Greil P, Wenzel MM, Staudenmaier R. Cellulose-based scaffold materials for cartilage tissue engineering. *Biomaterials* 2006 Jul;27(21):3955-3963.
172. Shi SK, Chen SY, Zhang X, Shen W, Li X, Hu WL, et al. Biomimetic mineralization synthesis of calcium-deficient carbonate-containing hydroxyapatite in a three-dimensional network of bacterial cellulose. *Journal of Chemical Technology and Biotechnology* 2009 Feb;84(2):285-290.
173. Bodin A, Concaro S, Brittberg M, Gatenholm P. Bacterial cellulose as a potential meniscus implant. *Journal of Tissue Engineering and Regenerative Medicine* 2007 Sep-Oct;1(5):406-408.
174. Oliveira RCB, Souza FC, Castro M. Avaliação da resposta tecidual quando da substituição da cartilagem do septo nasal de coelhos por manta de celulose bacteriana. Estudo experimental. *ActaORL* 2007;25(4):267-277.
175. Backdahl H, Esguerra M, Delbro D, Risberg B, Gatenholm P. Engineering microporosity in bacterial cellulose scaffolds. *Journal of Tissue Engineering and Regenerative Medicine* 2008 Aug;2(6):320-330.
176. Negrão SW, Bueno RRL, Guérios EE, Ultramari FT, Faidiga AM, de Andrade PMP, et al. A eficácia do stent recoberto com celulose biosintética comparado ao stent convencional em angioplastia em coelhos. *Revista Brasileira de Cardiologia Invasiva* 2006;14(1):10-19.
177. Putra A, Kakugo A, Furukawa H, Gong JP, Osada Y. Tubular bacterial cellulose gel with oriented fibrils on the curved surface. *Polymer* 2008 Apr 1;49(7):1885-1891.

178. Wippermann J, Schumann D, Klemm D, Kosmehl H, Salehi-Gelani S, Wahlers T. Preliminary Results of Small Arterial Substitute Performed with a New Cylindrical Biomaterial Composed of Bacterial Cellulose. *Eur J Vasc Endovasc Surg* 2009 Feb 19.
179. Alvarez OM, Patel M, Booker J, Markowitz L. Effectiveness of a biocellulose wound dressing for the treatment of chronic venous leg ulcers: Results of a single center randomized study involving 24 patients. *Wounds-a Compendium of Clinical Research and Practice* 2004 Jul;16(7):224-233.
180. Fontana JD, Desouza AM, Fontana CK, Torriani IL, Moreschi JC, Gallotti BJ, et al. Acetobacter Cellulose Pellicle as a Temporary Skin Substitute. *Applied Biochemistry and Biotechnology* 1990 Spr-Sum;24-5:253-264.
181. He A, Fu Y, Li H. [Artificial biological skin for preventing adhesion of repaired tendon in white rats]. *Hunan Yi Ke Da Xue Xue Bao* 1997;22(4):287-290.
182. Mello LR, Feltrin LT, Fontes Neto PT, Ferraz FA. Duraplasty with biosynthetic cellulose: an experimental study. *J Neurosurg* 1997 Jan;86(1):143-150.
183. Osman SA, Souza FC, Doici JE. Estudo experimental sobre a aplicação de película de celulose bacteriana (bionext) em área cruenta de ressecção de concha nasal de coelhos. *ActaORL* 2007;25(4):304-311.
184. Panerari AD, Costa HO, Souza FC, Castro M, Silva L, Sousa Neto OM. Tracheal inflammatory response to bacterial cellulose dressing after surgical scarification in rabbits. *Brazilian Journal of Otorhinolaryngology* 2008 Jul-Aug;74(4):512-522.
185. Pippi NL, Sampaio AJSA. Estudos preliminares sobre o comportamento do Biofill na ceratoplastia lamelar em coelhos. *Revista do Centro de Ciências Rurais* 1990;20(3-4):297-302.
186. Pitanguy I, Salgado F, Maracaja PFD. Utilization of the cellulose pellicle biofill as a biological dressing. *Revista Brasileira de Cirurgia* 1988;78(5):317-326.
187. Portal O, Clark WA, Levinson DJ. Microbial Cellulose Wound Dressing in the Treatment of Nonhealing Lower Extremity Ulcers. *Wounds-a Compendium of Clinical Research and Practice* 2009 Jan;21(1):1-3.
188. Rebello C, Almeida DAD, Lima Jr. EM, Dornelas MDP. Biofill a new skin substitute our experience. *Revista Brasileira de Cirurgia* 1987;77(6):407-414.
189. Wouk AFFF, Diniz JM, Círio SM, Santos H, Baltazar EL, Acco A. Membrana biológica (Biofill) - Estudo comparativo com outros agentes promotores da cicatrização da pele em suínos: aspectos clínicos, histopatológicos e morfométricos. *Archives of Veterinary Science* 1998;3(1):31-37.
190. de Macedo NL, Matuda SM, de Macedo LGS, Monteiro ASF, Valera MC, Carvalho YR. Evaluation of two membranes in guided bone tissue regeneration: histological study in rabbits. *Brazilian Journal of Oral Sciences* 2004;3(8):395-400.

191. dos Anjos B, Novaes AB, Meffert R, Barboza EP. Clinical comparison of cellulose and expanded polytetrafluoroethylene membranes in the treatment of class II furcations in mandibular molars with 6-month re-entry. *Journal of Periodontology* 1998 Apr;69(4):454-459.
192. Novaes AB, Jr., Novaes AB. Bone formation over a TiAl6V4 (IMZ) implant placed into an extraction socket in association with membrane therapy (Gengiflex). *Clinical Oral Implants Research* 1993 Jun;4(2):106-110.
193. Novaes AB, Jr., Novaes AB. Immediate implants placed into infected sites: a clinical report. *International Journal of Oral & Maxillofacial Implants* 1995 Sep-Oct;10(5):609-613.
194. Novaes AB, Jr., Novaes AB. Soft tissue management for primary closure in guided bone regeneration: surgical technique and case report. *International Journal of Oral & Maxillofacial Implants* 1997 Jan-Feb;12(1):84-87.
195. Salata LA, Craig GT, Brook IM. In-Vivo Evaluation of a New Membrane (Gengiflex(R)) for Guided Bone Regeneration (Gbr). *Journal of Dental Research* 1995 Mar;74(3):825-825.
196. Sonohara MK, Greggi SLA. Avaliação da resposta biológica a diferentes barreiras mecânicas, utilizadas na técnica de regeneração tecidual guiada (RTG). *Revista da Faculdade de Odontologia de Bauru* 1994;2(4):96-102.
197. Mello LR, Feltrin Y, Selbach R, Macedo G, Jr., Spautz C, Haas LJ. [Use of lyophilized cellulose in peripheral nerve lesions with loss of substance]. *Arq Neuropsiquiatr* 2001 Jun;59(2-B):372-379.
198. Brancher JA, Torres MF. Reparação microcirúrgica de nervo facial de ratos Wistar por meio de sutura - Parte II. *RSBO* 2005;2(2):34-38.
199. Pértile RAN, Siqueira JM, Rambo CR, Berti FV, do Valle RMR, Porto LM. Interação de cultura celulares com suportes biopoliméricos para aplicações biomédicas. *Exacta* 2007;5(2):343-352.
200. Whitney SEC, Wilson E, Webster J, Bacic A, Reid JSG, Gidley MJ. Effects of structural variation in xyloglucan polymers on interactions with bacterial cellulose. *American Journal of Botany* 2006 Oct;93(10):1402-1414.
201. Clasen C, Sultanova B, Wilhelms T, Heisig P, Kulicke WM. Effects of different drying processes on the material properties of bacterial cellulose membranes. *Macromolecular Symposia* 2006;244:48-58
- 218.
202. George J, Ramana K, Sabapathy S, Bawa A. Physico-mechanical properties of chemically treated bacterial (*Acetobacter xylinum*) cellulose membrane. *World Journal of Microbiology & Biotechnology* 2005 Dec;21(8-9):1323-1327.
203. Uraki Y, Nemoto J, Otsuka H, Tamai Y, Sugiyama J, Kishimoto T, et al. Honeycomb-like architecture produced by living bacteria, *Gluconacetobacter xylinus*. *Carbohydrate Polymers* 2007 May 1;69(1):1-6.

204. Ogawa R, Miura Y, Tokura S, Koriyama T. Susceptibilities of Bacterial Cellulose Containing N-Acetylglucosamine Residues for Cellulolytic and Chitinolytic Enzymes. *International Journal of Biological Macromolecules* 1992 Dec;14(6):343-347.
205. Shirai A, Takahashi M, Kaneko H, Nishimura SI, Ogawa M, Nishi N, et al. Biosynthesis of a Novel Polysaccharide by *Acetobacter-Xylinum*. *International Journal of Biological Macromolecules* 1994 Dec;16(6):297-300.
206. Shirai A, Sakairi N, Nishi N, Tokura S. Preparation of a novel (1->4)-beta-D-glycan by *Acetobacter xylinum* - A proposed mechanism for incorporation of a N-acetylglucosamine residue into bacterial cellulose. *Carbohydrate Polymers* 1997 Mar-Apr;32(3-4):223-227.
207. Ciechanska D. Multifunctional bacterial cellulose/chitosan composite materials for medical applications. *Fibres & Textiles in Eastern Europe* 2004 Oct-Dec;12(4):69-72.
208. Lee JW, Deng F, Yeomans WG, Allen AL, Gross RA, Kaplan DL. Direct incorporation of glucosamine and N-acetylglucosamine into exopolymers by *Gluconacetobacter xylinus* (= *Acetobacter xylinum*) ATCC 10245: Production of chitosan-cellulose and chitin-cellulose exopolymers. *Applied and Environmental Microbiology* 2001 Sep;67(9):3970-3975.
209. Kobayashi S, Makino A, Matsumoto H, Kunii S, Ohmae M, Kiyosada T, et al. Enzymatic polymerization to novel polysaccharides having a glucose-N-acetylglucosamine repeating unit, a cellulose-chitin hybrid polysaccharide. *Biomacromolecules* 2006 May;7(5):1644-1656.
210. Phisalaphong M, Jatupaiboon N. Biosynthesis and characterization of bacteria cellulose-chitosan film. *Carbohydrate Polymers* 2008 Nov 4;74(3):482-488.
211. Berti FV, Rambo CR, Recouvreux DOS, Carminatti CA, Porto LM. Síntese de filmes de PHAS puros e associados com oligômeros de celulose bacteriana para aplicações em biomaterias. In: XXI Congresso Brasileiro de Engenharia Biomédica 2008;1:1-4.
212. Ajayan PM, Schadler LS, Braun PV, editors. *Nanocomposite Science and Technology*. 1 ed. Weinheim: Wiley-VCH, 2003.
213. Millon LE, Wan WK. The polyvinyl alcohol-bacterial cellulose system as a new nanocomposite for biomedical applications. *Journal of Biomedical Materials Research Part B-Applied Biomaterials* 2006 Nov;79B(2):245-253.
214. Millon LE, Mohammadi H, Wan WK. Anisotropic polyvinyl alcohol hydrogel for cardiovascular applications. *Journal of Biomedical Materials Research Part B-Applied Biomaterials* 2006 Nov;79B(2):305-311.
215. Millon LE, Guhadós G, Wan W. Anisotropic polyvinyl alcohol-Bacterial cellulose nanocomposite for biomedical applications. *J Biomed Mater Res B Appl Biomater* 2008 Aug;86B(2):444-452.
216. Wiegand C, Elsner P, Hipler UC, Klemm D. Protease and ROS activities influenced by a composite of bacterial cellulose and collagen type I in vitro. *Cellulose* 2006 Dec;13(6):689-696.

217. Zhou LL, Sun DP, Hu LY, Li YW, Yang JZ. Effect of addition of sodium alginate on bacterial cellulose production by *Acetobacter xylinum*. *J Ind Microbiol Biotechnol* 2007 Jul;34(7):483-489.
218. Phisalaphong M, Suwanmajo T, Tammarate P. Synthesis and characterization of bacterial cellulose/alginate blend membranes. *Journal of Applied Polymer Science* 2008 Mar 5;107(5):3419-3424.
219. Hong L, Wang YL, Jia SR, Huang Y, Gao C, Wan YZ. Hydroxyapatite/bacterial cellulose composites synthesized via a biomimetic route. *Materials Letters* 2006 Jun;60(13-14):1710-1713.
220. Wan YZ, Hong L, Jia SR, Huang Y, Zhu Y, Wang YL, et al. Synthesis and characterization of hydroxyapatite-bacterial cellulose nanocomposites. *Composites Science and Technology* 2006 Sep;66(11-12):1825-1832.
221. Hutchens SA, Benson RS, Evans BR, O'Neill HM, Rawn CJ. Biomimetic synthesis of calcium-deficient hydroxyapatite in a natural hydrogel. *Biomaterials* 2006 Sep;27(26):4661-4670.
222. Bodin A, Gustafsson L, Gatenholm P. Surface-engineered bacterial cellulose as template for crystallization of calcium phosphate. *Journal of Biomaterials Science-Polymer Edition* 2006;17(4):435-447.
223. Grande CJ, Torres FG, Gomez CM, Carmen Bano M. Nanocomposites of bacterial cellulose/hydroxyapatite for biomedical applications. *Acta Biomater* 2009 Jan 31.
224. Maneerung T, Tokura S, Rujiravanit R. Impregnation of silver nanoparticles into bacterial cellulose for antimicrobial wound dressing. *Carbohydrate Polymers* 2008 Apr 3;72(1):43-51.
225. Charpentier PA, Maguire A, Wan WK. Surface modification of polyester to produce a bacterial cellulose-based vascular prosthetic device. *Applied Surface Science* 2006 Jul 15;252(18):6360-6367.
226. Haigler CH, White AR, Brown RM, Cooper KM. Alteration of *In vivo* Cellulose Ribbon Assembly by Carboxymethylcellulose and Other Cellulose Derivatives. *Journal of Cell Biology* 1982;94(1):64-69.
227. Tajima K, Fujiwara M, Takai M, Hayashi J. Synthesis of Bacterial Cellulose Composite by *Acetobacter-Xylinum* .1. Its Mechanical Strength and Biodegradability. *Mokuzai Gakkaishi* 1995;41(8):749-757.
228. Sakairi N, Suzuki S, Ueno K, Han SM, Nishi N, Tokura S. Biosynthesis of heteropolysaccharides by *Acetobacter xylinum* - Synthesis and characterization of metal-ion adsorptive properties of partially carboxymethylated cellulose. *Carbohydrate Polymers* 1998 Dec;37(4):409-414.
229. Whitney SEC, Brigham JE, Darke AH, Reid JSG, Gidley MJ. Structural aspects of the interaction of mannan-based polysaccharides with bacterial cellulose. *Carbohydrate Research* 1998 Feb;307(3-4):299-309.

230. Yano S, Maeda H, Nakajima M, Hagiwara T, Sawaguchi T. Preparation and mechanical properties of bacterial cellulose nanocomposites loaded with silica nanoparticles. *Cellulose* 2008 Feb;15(1):111-120.
231. Serafica G, Mormino R, Bungay H. Inclusion of solid particles in bacterial cellulose. *Applied Microbiology and Biotechnology* 2002 May;58(6):756-760.
232. Grande CJ, Torres FG, Gomez CM, Troncoso OP, Canet-Ferrer J, Martinez-Pastor J. Development of self-assembled bacterial cellulose-starch nanocomposites. *Mater Sci Eng* 2008.
233. Gindl W, Keckes J. Tensile properties of cellulose acetate butyrate composites reinforced with bacterial cellulose. *Composites Science and Technology* 2004 Nov;64(15):2407-2413.
234. Dammstrom S, Salmen L, Gatenholm P. The effect of moisture on the dynamical mechanical properties of bacterial cellulose/glucuronoxylan nanocomposites. *Polymer* 2005 Nov 14;46(23):10364-10371.
235. Nakayama A, Kakugo A, Gong JP, Osada Y, Takai M, Erata T, et al. High mechanical strength double-network hydrogel with bacterial cellulose. *Advanced Functional Materials* 2004 Nov;14(11):1124-1128.
236. Yasuda K, Ping Gong J, Katsuyama Y, Nakayama A, Tanabe Y, Kondo E, et al. Biomechanical properties of high-toughness double network hydrogels. *Biomaterials* 2005 Jul;26(21):4468-4475.
237. Guillen D, Sanchez S, Rodriguez-Sanoja R. Carbohydrate-binding domains: multiplicity of biological roles. *Appl Microbiol Biotechnol* Feb;85(5):1241-1249.
238. Moreira S, Gama M. *Carbohydrate Binding Modules: Functions and Applications*: Nova Science Publishers Inc, 2010.
239. Barral P, Suárez C, Batanero E, Alfonso C, Alché JD, Rodríguez-García MI, et al. An olive pollen protein with allergenic activity, Ole e 10, defines a novel family of carbohydrate-binding modules and is potentially implicated in pollen germination. *Biochem J* 2005;390:77-84.
240. Vaaje-Kolstad G, Horn SJ, van Aalten DMF, Synstad B, Eijsink VGH. The non-catalytic chitin-binding protein CBP21 from *Serratia marcescens* is essential for chitin degradation. *J Biol Chem* 2005;280:28492–28497.
241. Felix M, Diana I, Shaolin C, David BW. Regulation and characterization of *Thermobifida fusca* carbohydrate-binding module proteins E7 and E8. *Biotechnol Bioeng* 2008;100:1066–1077.
242. Kruus K, Lua AC, Demain AL, Wu JH. The anchorage function of CipA (CelL), a scaffolding protein of the *Clostridium thermocellum* cellulosome. *Proc Natl Acad Sci U S A* 1995 Sep 26;92(20):9254-9258.
243. Shoseyov O, Takagi M, Goldstein MA, Doi RH. Primary sequence analysis of *Clostridium cellulovorans* cellulose binding protein A. *Proc Natl Acad Sci U S A* 1992 Apr 15;89(8):3483-3487.

244. Pages S, Belaich A, Tardif C, Reverbel-Leroy C, Gaudin C, Belaich JP. Interaction between the endoglucanase CelA and the scaffolding protein CipC of the *Clostridium cellulolyticum* cellulosome. *J Bacteriol* 1996 Apr;178(8):2279-2286.
245. Shoseyov O, Shani Z, Levy I. Carbohydrate binding modules: biochemical properties and novel applications. *Microbiol Mol Biol Rev* 2006 Jun;70(2):283-295.
246. Kitaoka T, Tanaka H. Novel paper strength additive containing cellulose-binding domain of cellulase. *Journal of Wood Science* 2001;47(4).
247. Yokota S, Matsuo K, Kitaoka T, Wariishi H. Retention and paper-strength characteristics of anionic polyacrylamides conjugated with carbohydrate-binding modules. *BioResources* 2009;4(1):234-244.
248. Yokota S, Matsuo K, Kitaoka T, Wariishi H. Specific interaction acting at a cellulose-binding domain/cellulose interface for papermaking application. *BioResources* 2008;3(4):1030-1041.
249. Cavaco-Paulo A, Morgado J, Andreus J, Kilburn DG. Interactions of cotton with CBD peptides. *Enzyme Microb Technol* 1999;25:639-643.
250. Ramos R, Pinto R, Mota M, Sampaio L, Gama FM. Textile depilling: Superior finishing using cellulose-binding domains with residual enzymatic activity. *Biocatalysis and Biotransformation* 2007;25(1):35-42.
251. Francisco JA, Stathopoulos C, Warren RA, Kilburn DG, Georgiou G. Specific adhesion and hydrolysis of cellulose by intact *Escherichia coli* expressing surface anchored cellulase or cellulose binding domains. *Biotechnology (N Y)* 1993 Apr;11(4):491-495.
252. Lehtio J, Wernerus H, Samuelson P, Teeri TT, Stahl S. Directed immobilization of recombinant staphylococci on cotton fibers by functional display of a fungal cellulose-binding domain. *FEMS Microbiol Lett* 2001 Feb 20;195(2):197-204.
253. Nam J, Fujita Y, Arai T, Kondo A, Morikaw Y, Okada H, et al. Construction of engineered yeast with the ability of binding to cellulose. *J Mol Catalys* 2002;17:197-202.
254. Wang AA, Mulchandani A, Chen W. Whole-cell immobilization using cell surface-exposed cellulose-binding domain. *Biotechnol Prog* 2001 May-Jun;17(3):407-411.
255. Ding M, Teng Y, Yin Q, Zhao J, Zhao F. The N-terminal cellulose-binding domain of EGXA increases thermal stability of xylanase and changes its specific activities on different substrates. *Acta Biochim Biophys Sin (Shanghai)* 2008 Nov;40(11):949-954.
256. Linder M, Nevanen T, Teeri TT. Design of a pH-dependent cellulose-binding domain. *FEBS Lett* 1999 Mar 19;447(1):13-16.
257. Kauffmann C, Shoseyov O, Shpigel E, Bayer EA, Lamed R, Shoham Y, et al. A novel methodology for enzymatic removal of atrazine from water by CBD-fusion protein immobilized on cellulose. *Environ Sci Technol* 2000;34:1292-1296.
258. Wang AA, Mulchandani A, Chen W. Specific adhesion to cellulose and hydrolysis of organophosphate nerve agents by a genetically engineered *Escherichia coli* strain with a

surface-expressed cellulose-binding domain and organophosphorus hydrolase. *Appl Environ Microbiol* 2002 Apr;68(4):1684-1689.

259. Xu Z, Bae W, Mulchandani A, Mehra RK, Chen W. Heavy metal removal by novel CBD-EC20 sorbents immobilized on cellulose. *Biomacromolecules* 2002 May-Jun;3(3):462-465.

260. Lamed R, Setter E, Kenig R, Bayer EA. The cellulosome - a discrete cell surface organelle of *Clostridium thermocellum* which exhibits separate antigenic, cellulose-binding and various cellulolytic activities. *Biotech Bioengng Symp* 1983;13.

261. Lamed R, Bayer EA. The cellulosome of *Clostridium thermocellum*. *Adv Appl Microbiol* 1988;33:1-46.

262. Din N, Gilkes NR, Tekant B, Miller RCJ, Warren RAJ, Kilburn DG. Non-hydrolytic disruption of cellulose fibres by the binding domain of a bacterial cellulase. *BioTechnology* 1991;9:1096-1099.

263. Lamed R, Setter E, Bayer EA. Characterization of a cellulose-binding, cellulase-containing complex in *Clostridium thermocellum*. *J Bacteriol* 1983 Nov;156(2):828-836.

264. Bayer EA, Morag E, Lamed R. The cellulosome—a treasure-trove for biotechnology. *Trends Biotechnol* 1994 Sep;12(9):379-386.

265. Beguin P, Lemaire M. The cellulosome: an exocellular, multiprotein complex specialized in cellulose degradation. *Crit Rev Biochem Mol Biol* 1996 Jun;31(3):201-236.

266. Gerngross UT, Romaniec MP, Kobayashi T, Huskisson NS, Demain AL. Sequencing of a *Clostridium thermocellum* gene (*cipA*) encoding the cellulosomal SL-protein reveals an unusual degree of internal homology. *Mol Microbiol* 1993 Apr;8(2):325-334.

267. Poole DM, Morag E, Lamed R, Bayer EA, Hazlewood GP, Gilbert HJ. Identification of the cellulose-binding domain of the cellulosome subunit S1 from *Clostridium thermocellum* YS. *FEMS Microbiol Lett* 1992 Dec 1;78(2-3):181-186.

268. Tormo J, Lamed R, Chirino AJ, Morag E, Bayer EA, Shoham Y, et al. Crystal structure of a bacterial family-III cellulose-binding domain: a general mechanism for attachment to cellulose. *EMBO J* 1996 Nov 1;15(21):5739-5751.

Chapter 2

Improving the affinity of fibroblasts for bacterial cellulose using carbohydrate – binding modules fused to RGD

Adapted from: Journal of Biomedical Materials Research: Part A 2010; 92A (1): 9-17.

Abstract

The attachment of cells to biomedical materials can be improved by using adhesion sequences, such as Arg-Gly-Asp (RGD), found in several extracellular matrix proteins. In this work, bifunctional recombinant proteins, with a Cellulose-Binding Module – CBM, from the cellulosome of *Clostridium thermocellum* - and cell binding sequences - RGD, GRGDY - were cloned and expressed in *E. coli*. These RGD-containing cellulose binding proteins were purified and used to coat bacterial cellulose fibres. Its effect on the cell adhesion/biocompatibility properties was tested using a mouse embryo fibroblasts culture.

Bacterial cellulose (BC) secreted by *Gluconacetobacter xylinus* (= *Acetobacter xylinum*) is a material with unique properties and promising biomedical applications. CBMs adsorb specifically and tightly on cellulose. Thus, they are a useful tool to address the fused RGD sequence (or other bioactive peptides) to the cellulose surface, in a specific and simple way. Indeed, fibroblasts exhibit improved ability to interact with bacterial cellulose sheets coated with RGD – CBM proteins, as compared with cellulose treated with the CBM, *i.e.*, without the adhesion peptide. The effect of the several fusion proteins produced was analysed.

Introduction

The fundamental premise of tissue engineering is to develop tissue substitutes to restore or improve the function of diseased or damaged human tissues. Many biomaterials have been studied as scaffolds, in which the cells can be seeded, cultured and then, implanted to induce and direct the growth of new, healthy tissue.

The primary function of a scaffold is tissue conduction and, therefore, it must allow cell attachment, migration onto or within the scaffold, cell proliferation and cell differentiation. It must also provide an environment where the cells conserve their phenotype [1]. The successful development of tissue engineering scaffolds requires proper substrates for cell survival and differentiation. The attachment of cells to the biomedical materials can be improved by using adhesion molecules. These molecules, present in the extracellular matrix proteins, regulate the adhesion, migration and growth of cells, by binding to integrin receptors located on the outer cellular membranes [2, 3]. The tripeptide motif RGD was identified 23 years ago by Pierschbacher and Rouslahti as the minimal essential cell adhesion peptide sequence in fibronectin [4]. Since then, cell adhesive RGD sites were identified in many other extracellular matrix (ECM) proteins, including vitronectin, fibrinogen, von Willebrand factor, collagen, laminin, osteopontin, tenascin and bone sialoprotein as well as in membrane proteins, in viral and bacterial proteins, and in snake venoms (neurotoxins and disintegrins) [5]. The RGD sequence is by far the most effective and most often employed peptide sequence used to stimulate cell adhesion on synthetic surfaces, due to its widespread distribution and use throughout the organism, its ability to address more than one cell adhesion receptor, and its biological impact on cell anchoring, behaviour and survival [6]. Incorporation of biomimetic adhesion sites can be used to promote cell adhesion and migration on or within bioactive materials. The selection of which type of cells adhere to a material and their spatial distribution can also be controlled through the selection of the adhesion sites that are incorporated into the bioactive material [7].

In the present study, we analyzed the adhesion of mouse embryo fibroblasts on bacterial cellulose (BC). BC is secreted by *Gluconacetobacter xylinus* (= *Acetobacter xylinum*). It is a material with unique properties, including high water holding capacity, high crystallinity, a

ultrafine fiber network, and high tensile strength [8]. Although chemically identical to plant cellulose, it has a unique fibrillar nanostructure, which determines its extraordinary physical and mechanical properties, characteristics which are quite promising for modern medicine and biomedical research [9]. For example, membranes of bacterial cellulose were used as an artificial skin for temporary covering of wounds and bacterial cellulose tubes were produced as substitution material for blood vessels. BC was also successfully used in periodontal treatments and applied as replacement for dura mater (a membrane that surrounds brain tissue) [8, 9].

A method for producing chimeric proteins, RGD-CBM containing a cellulose-binding module (CBM), was developed. CBMs are discrete protein modules found in a large number of carbohydrases and a few nonhydrolytic proteins [10]. A cellulose-binding domain family III from the cellulosomal-scaffolding protein A of the bacteria *Clostridium thermocellum*, was used in the present work [11]. The main goal was the functionalization of bacterial cellulose aiming its utilization as scaffold in tissue engineering. There are several methodologies to bind adhesion molecules to the biomaterials. However, the use of a CBM, as proposed in this work, is a simple way to direct bioactive peptides to the cellulose surface, avoiding the use of complex peptide chemical grafting. Furthermore, the adsorption of this CBM to BC is specific and very stable. Indeed, the removal of CBM from cellulose can be achieved only using denaturant agents [10]. Thus, the coating of BC with recombinant proteins is stable enough for its practical application in the designed of biomaterials.

The genes encoding these CBM-containing chimeric proteins were cloned, and the proteins expressed and purified. Polystyrene surfaces and bacterial cellulose sheets where “coated” with these RGD-containing proteins, and then used in adhesion/biocompatibility tests, using a mouse embryo fibroblasts culture. Fibroblasts were selected as model animal cells to test our strategy of bacterial cellulose modification, while the polystyrene plate was used as a model surface to test the recognition of the RGDs sequences by the integrins on cells membrane.

Materials and methods

Production of bacterial cellulose

Gluconacetobacter xylinus (ATCC 53582) purchased from the American Type Culture Collection was grown in Hestrin-Schramm medium, pH 5.0. The medium was inoculated with the culture, added to the 24-well polystyrene plate (1 mL/per well) and incubated statically at 30 °C, for 7 days. BC pellicles were purified by 4% SDS treatment at 70 °C, for 12 h followed by 4% NaOH at 70 °C, for 90 min. Samples were autoclaved and stored in PBS pH 7.4, at 4°C, prior to use (FIGURE 1).

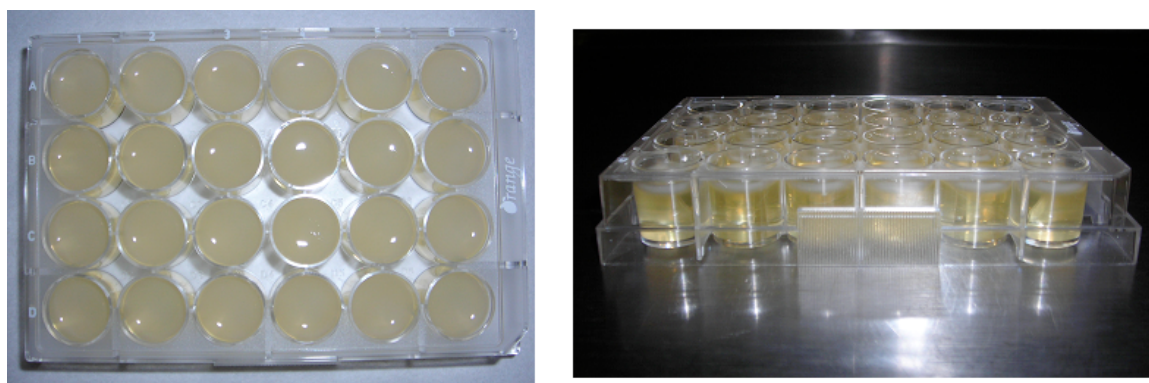


Figure 1. *Gluconacetobacter xylinus* (ATCC 53582) cultured on liquid Hestrin-Schramm medium after 7 days. The medium was inoculated with the culture and added to the 24-well polystyrene plate (1 mL/per well) and incubated statically at 30 °C.

Construction of a gene fusion encoding the adhesion peptide and a CBM

The pET21a vector (Novagen) with the CBM from *C. thermocellum* and a N-terminal linker cloned in the *NheI* and *XhoI* restriction sites was used as template for amplification of the fused genes. The nucleotide sequence of each peptide was determined and the sequences optimized for *E. coli* expression. Peptides were then amplified by PCR with the enzyme Vent DNA polymerase (New England Biolabs) using primers presented in Table 1. Primers included *NheI* and *XhoI* restriction sites, which are shown in bold. PCRs were performed as follows: preheating at 95 °C for 2 min, 40 cycles at 95 °C for 45 s, 53 °C for 45 s and 72 °C for 45s, followed by an elongation at 72 °C for 10 min. The DNA recombinant coding sequences were cloned in pET21a using *E. coli* XL1 Blue (Stratagene) as cloning strain. Clones containing the

recombinant genes were identified by restriction enzyme analysis. Amplified fragments were sequenced to ensure that no mutations had occurred in the PCRs.

The recombinant derivatives were then digested with *NheI* and *XhoI* and the excised products were cloned into the expression vector pET21a (Novagen), previously digested with the same

Table 1. PCR primers with the restriction sites *NheI* (GCTAGC) and *XhoI* (CTCGAG) used for cloning the gene fusions encoding the adhesion peptide with CBM.

Recombinant protein name	Primers
RGD/CBM	Fwd: 5' - CTA GCT AGC AGA GGT GAT ACA CCG ACC AAG GGA G - 3' Rev: 5' - CAC CTC GAG TTC TTT ACC CCA TAC AAG AAC - 3'
GRGDY/CBM	Fwd: 5' - CTA GCT AGC GGT AGA GGT GAT TAT ACA CCG ACC AAG GGA G - 3' Rev: 5' - CAC CTC GAG TTC TTT ACC CCA TAC AAG AAC - 3'
RGD/CBM/RGD	Fwd: 5' - CTA GCT AGC AGA GGT GAT ACA CCG ACC AAG GGA G - 3' Rev: 5' - CAC CTC GAG ATC ACC TCT CGG TTC TTC AGG TTC TGT ACC GCC CGG CGG CGT TCC TTC TTT ACC CCA TAC AAG AAC - 3'
GRGDY/CBM/GRGDY	Fwd: 5' - CTA GCT AGC GGT AGA GGT GAT TAT ACA CCG ACC AAG GGA G - 3' Rev: 5' - CAC CTC GAG ATA ATC ACC TCT ACC CGG TTC TTC AGG TTC TGT ACC GCC CGG CGG CGT TCC TTC TTT ACC CCA TAC AAG AAC - 3'

restriction enzymes. This vector carries a *T7/ac* promoter and includes a C-terminal His6-tag in the recombinant proteins to facilitate purification. The sequence encoding the adhesion peptide (RGD or GRGDY) was annealed with the CBM at the N-terminal, through the N-terminal linker from the CBM containing 40 amino acids. In order to introduce another adhesion sequence at the C-terminal of the CBM, a linker containing 12 amino acids was inserted between the C-terminal of the CBM and the new adhesion sequence (TABLE 1, FIGURE 2).

RGD / GRGDY	Linker1 (40 aa)	CBM	His-Tag	Stop
-------------	-----------------	-----	---------	------

(A)

RGD / GRGDY	Linker1 (40 aa)	CBM	Linker2 (12 aa)	RGD / GRGDY	His-Tag	Stop
-------------	-----------------	-----	-----------------	-------------	---------	------

(B)

Figure 2. Construction of the gene fusion encoding adhesion peptide and the Linker-CBM. (A) Construction containing one copy of the adhesion peptide at the N-terminal of the CBM; (B) Construction containing two copies of the adhesion peptide.

Production and purification of recombinant proteins

High-level expression studies and protein production were carried out in *E. coli* BL21 (DE3) cells grown at 37 °C in LB medium supplemented with ampicillin at 100µg/ml. Cultures were induced at OD₅₉₅ = 0.5 with IPTG (1mM). Five hours after induction the cells were separated from the culture medium by centrifugation at 13,000g. Then, cell pellet was resuspended with buffer A (20mM Tris, 20mM NaCl 5mM CaCl₂ pH 7.4 and phenylmethylsulfonylfluoride (PMSF) 0.1mM) and lysed by sonication. Imidazole was added to a final concentration of 40mM and the pH was adjusted to 7.4. The cell free extract (soluble fraction) was then, collected by centrifugation at 15,000g for 30 minutes, at 4 °C and the His6 – tagged recombinant proteins purified by immobilized metal ion affinity chromatography, using a 5mL nickel His–Trap column (GE Healthcare). Following purification, the proteins were dialyzed against buffer A and stored at -20 °C, prior to use. Samples from purification's different steps and pure protein were analysed by SDS – PAGE using a 12% (W/V) acrylamide gel, Coomassie stained.

Interaction of recombinant proteins with the cells

In order to demonstrate the interaction of the recombinant RGD with cell membrane, the recombinant proteins were chemically conjugated with isothiocyanate (FITC). The fluorescent proteins were added to the wells of 96-well polystyrene plates and the fibroblasts were added in 200µl of DMEM medium with/without serum. The plates were incubated for 1 hour at 37 °C, in atmosphere of 5% CO₂ and 95% humidified air. The cells were observed through fluorescence microscopy.

Effect of the recombinant proteins on the adhesion and spreading of fibroblasts

The mitochondrial activity of the cultured cells was determined using a colorimetric assay, which is related to cell viability. The MTS [3-(4,5-dimethylthiazol-2-yl)-5-(3-carboxymethoxyphenyl)-2-(4-sulfophenyl)-2H-tetrazolium] assay was performed as follows: the purified recombinant proteins were added to the wells of the 96-well polystyrene plates (0.05mg of protein/per well), and left adsorbing to the plate at 4°C, overnight. Unbound

protein was washed out with PBS. In a second test, the adhesion proteins were added to the wells of 24-well polystyrene plates (0.25mg of protein/per well), coated with bacterial cellulose sheets. As referred above, the BC sheets were produced in similar 24-well polystyrene plates, such that they tightly fit in the wells, completely covering the bottom surface. The plates were incubated overnight at 4 °C. Unbound protein was removed and analyzed by SDS – PAGE, then the bacterial cellulose sheets were washed with PBS. The fibroblasts 3T3 were seeded on the polystyrene plate at a density of 4×10^4 cells/per well, in DMEM medium without serum. One hour after the addition of the cells, the wells were washed with PBS and DMEM with serum (10%) was added. The MTS assay and microscope observations of the attached and spreading 3T3 fibroblasts was carried out at 1h, 5h, 24h and 48h after the addition of the cells. In the assay with BC, the fibroblasts 3T3 were seeded at a density of 12×10^4 cells/per well, in DMEM medium without serum. The plates were incubated at 37 °C, in atmosphere of 5% CO₂ and 95% humidified air. Two hours after the addition of the cells, the wells were washed with PBS and DMEM with serum (10%) was added. The MTS assay and microscope observations of the attachment and spreading of 3T3 fibroblasts were carried out at 2h, 24h and 48h after the addition of the cells. The results were obtained from at least 3 different assays, each one with samples in triplicates.

Results

Production and purification of recombinant proteins

The gene fragment encoding RGD–CBM was subcloned into the high-expression vector pET 21a, a plasmid vector containing the T7 promoter and a histidine tag sequence. Four different constructs were made, through the fusion of different peptides with a family 3 CBM from the *Clostridium thermocellum* cellulosome. It has been found, by other authors, that the aminoacids flanking the RGD sequence may affect the affinity of the integrin binding. This interaction may also depend on the peptide exposure, and therefore different constructs were analyzed in this work. Two constructs were made by fusing the RGD or GRGDY sequences at the N – terminal of the linker – CBM. In the other two recombinant constructs a C – terminal linker was designed and an additional RGD or GRGDY sequence was inserted (FIGURE 2). As shown in Figure 3, all the four recombinant fusion proteins (CBM, RGD–CBM, RGD–CBM–

RGD, GRGDY-CBM and GRGDY-CBM-GRGDY) were expressed by *E. Coli* in the soluble fraction. It can also be observed from Figure 3 that the recombinant proteins were isolated to high purity and concentration.

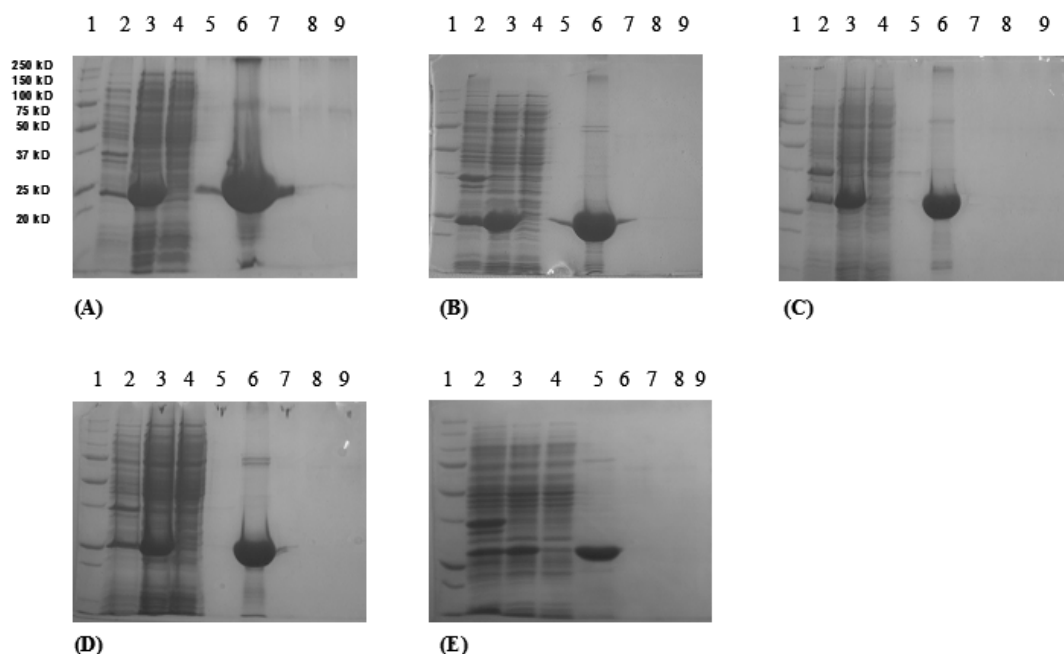


Figure 3. Analysis by SDS-PAGE of recombinant protein expression and nickel column protein purification. 1-Molecular weight marker (250 kD, 150 kD, 100 kD, 75 kD, 50 kD, 37 kD, 25 kD, 20 kD); 2-Insoluble fraction; 3-Soluble fraction; 4- Column filtrate; 5 to 9-Eluted fraction with 300 mM of Imidazole. (A) CBM; (B) RGD-CBM; (C) RGD-CBM-RGD; (D) GRGDY-CBM; (E) GRGDY-CBM-GRGDY.

The interaction of RGD and GRGDY with the cells, in medium with or without serum

The fibroblasts, incubated with the recombinant proteins conjugated with FITC, were observed by fluorescence microscopy. This study was performed to evaluate whether the recombinant proteins are able to interact with the cells through the RGD/GRGDY peptides. When the assays were performed with serum free medium, only the cells treated with RGD-CBM and GRGDY-CBM became fluorescent, as displayed in Figure 4. When medium containing serum was used, no fluorescent cells were observed, due to competition of the serum proteins with RGD/GRGDY

for the integrins on the cell membranes. These results demonstrate the interaction of the RGD/GRGDY with the cells, and furthermore that the CBM does not interact with the cells.

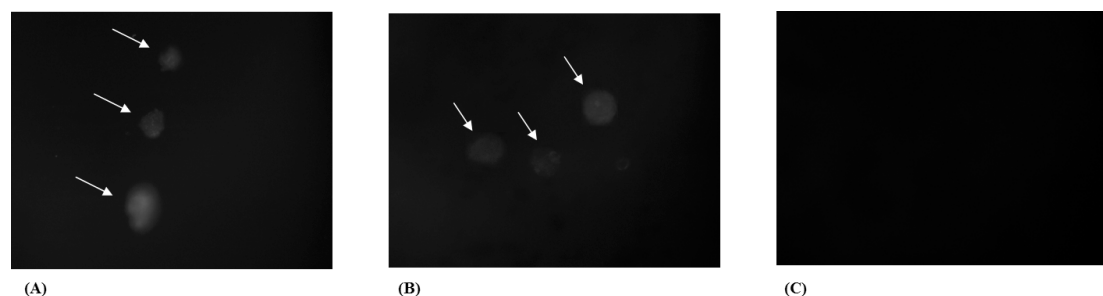


Figure 4. Fluorescent microscopy showing the binding of recombinant proteins to cell membranes. The arrows point with respect to some of the fluorescent cells. (A) RGD/CBM; (B) GRGDY/CBM; (C) CBM.

Attachment of fibroblasts to the polystyrene plate coated with recombinant proteins

In order to test the effect of the recombinant proteins in improving the adhesion and proliferation of fibroblasts, the cell culture polystyrene plates – with non-specifically bound proteins - were used. The polystyrene plates allow the observation of the cells morphology, unlike the bacterial cellulose. In these assays we aimed at observing whether the RGD containing proteins improve the adhesion of fibroblasts and also their effect on the cell differentiation.

The MTS results and microscopic observations showed that the proteins containing the RGD sequence (RGD–CBM and RGD–CBM–RGD) were able to improve the adhesion of fibroblast on polystyrene plates, when compared to the controls (CBM or buffer). Furthermore, the RGD sequence was more effective than GRGDY. The results also showed that, while the protein containing one copy of the GRGDY sequence was able to improve the adhesion of fibroblasts to the polystyrene surface, the protein containing two copies of the GRGDY showed no effect. The fibroblast cells adhered to the wells treated with RGD–CBM and RGD–CBM–RGD showed an elongated morphology one hour after seeding, while the cells on the wells treated with the GRGDY–CBM and GRGDY–CBM–GRGDY and also on the control assays exhibit more spherical morphology (FIGURE 5 and FIGURE 6).

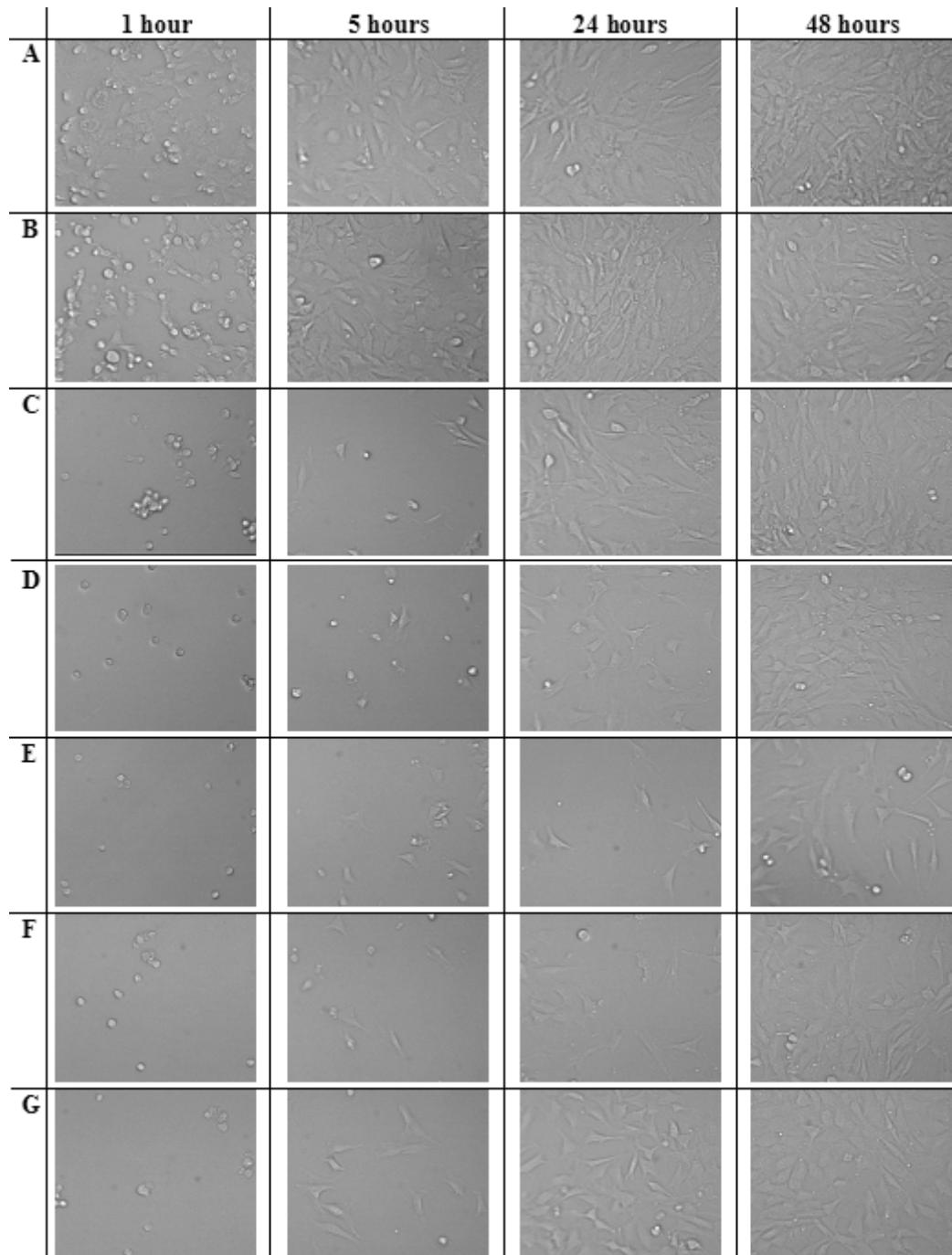


Figure 5. Photographs showing the effect of the recombinant proteins on cell (fibroblasts 3T3) attachment to polystyrene plate. (A) RGD-CBM, (B) RGD-CBM-RGD, (C) GRGDY-CBM, (D) GRGDY-CBM-GRGDY, (E) CBM, (F) Buffer, and (G) Control. The photographs were taken at 1, 5, 24, and 48 h after addition of cells.

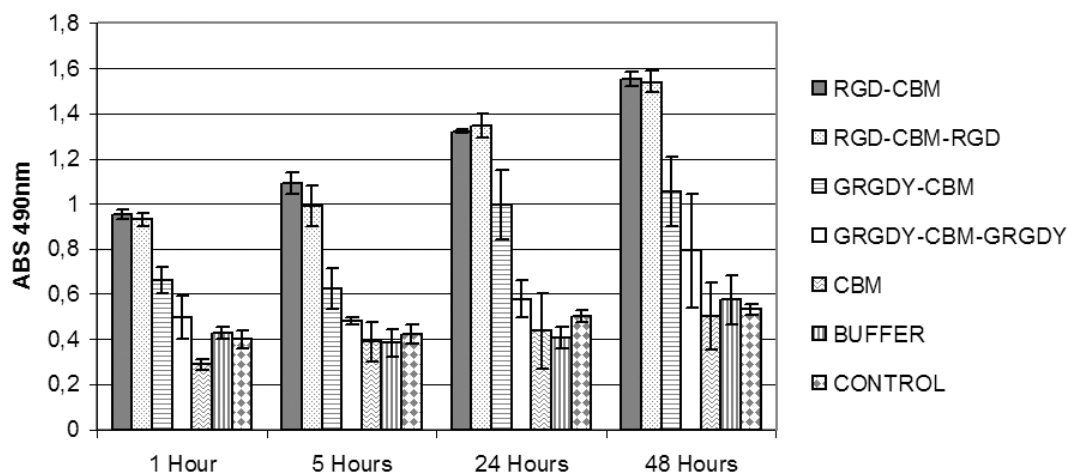


Figure 6. MTS assays of fibroblast culture on polystyrene plates treated with the recombinant proteins (CBM, RGD–CBM, RGD–CBM–RGD, GRGDY–CBM, and GRGDY–CBM–GRGDY). The MTS test was developed at 1, 5, 24, and 48 h after addition of cells.

It is quite clear from the results that the presence of the RGD–CBM, RGD–CBM–RGD and, to lower extent, GRGDY–CBM proteins, adsorbed on the polystyrene cell culture wells, improves the adhesion of fibroblasts.

Attachment of fibroblasts on BC surfaces

The recombinant proteins were added to the bacterial cellulose sheets and left adsorbing overnight. Then, the non-adsorbed protein was removed and analysed by SDS-PAGE electrophoresis. As may be seen in Figure 7, most of the protein adsorbed on the BC fibers. Thus, not only a functional RGD is present in the recombinant proteins, but also the CBM module fully conserves its functionality and ability to bind cellulose.

The adhesion of fibroblasts to BC was improved by the presence of the adsorbed recombinant proteins. Indeed, the results of the MTS test demonstrated that the proteins containing the RGD sequence were able to significantly increase the adhesion of fibroblast to BC surfaces, while the proteins containing the GRGDY sequence had no effect, taking as reference the cellulose treated with the CBM or with buffer. The results also demonstrated that the protein containing one RGD sequence have a stronger effect than the protein containing two RGD sequences (FIGURE 8).

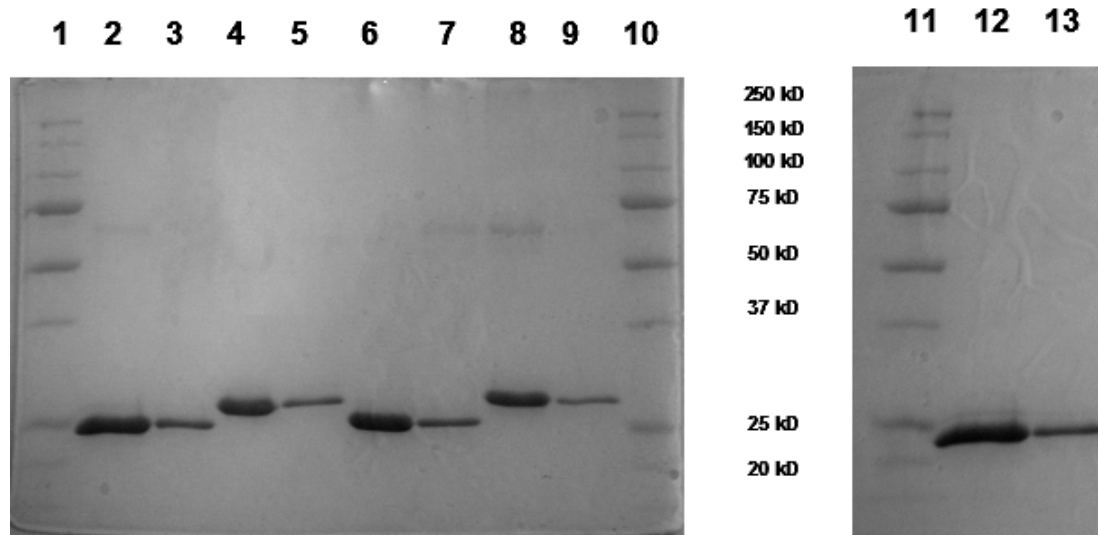


Figure 7. Analysis by SDS-PAGE of the interaction between the recombinant proteins with the cellulose sheets. Line 1, 10, and 11 - Molecular weight marker (250 kD, 150 kD, 100 kD, 75 kD, 50 kD, 37 kD, 25 kD, 20 kD); line 2, 3 - RGD-CBM; line 4, 5 - RGD-CBM-RGD; line 6, 7 - GRGDY-CBM; line 8, 9 - GRGDY-CBM-GRGDY; line 12, 13 - CBM. Lines 3, 5, 7, 9, and 13 represent the proteins after the interaction with BC sheets.

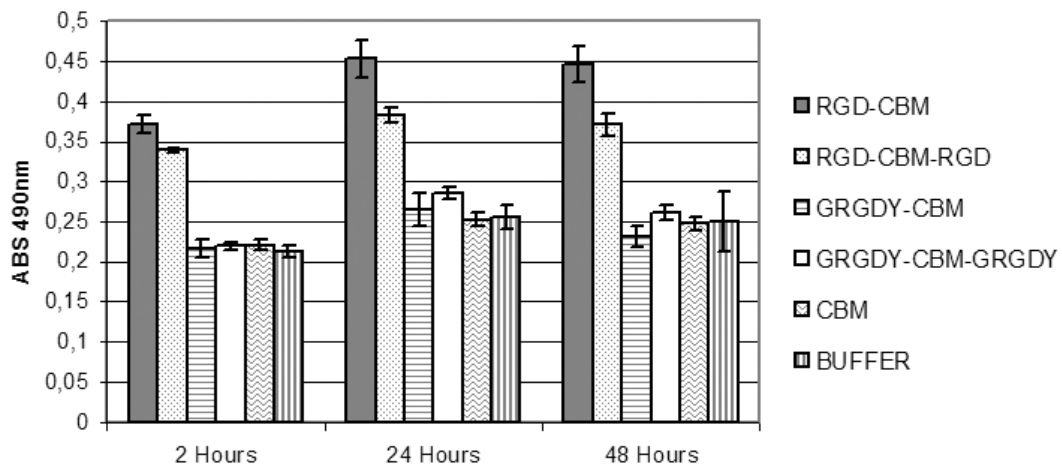


Figure 8. MTS assays of fibroblast culture treated with the recombinant proteins (CBM, RGD-CBM, RGD-CBM-RGD, GRGDY-CBM, and GRGDY-CBM-GRGDY) at the bacterial cellulose pellicles. The MTS test was developed at 2, 24, and 48 h after addition of cells.

Discussion

It is known that the amino acids flanking the RGD sequence can influence (positive or negatively), the interaction of the RGD with the integrins on the cell membrane. Many sequences exhibiting different activities have been described: RGDS, GRGDG, GRGDS, GRGDF, YRGDS, CGRGDSPK, etc[6]. Different cell lines recognize the RGD sequences in a distinct way. In this work, the sequences RGD and GRGDY were fused to a CBM, and the interaction of the recombinant proteins with fibroblasts was analyzed.

The observation of fibroblasts, incubated with the soluble recombinant proteins conjugated with FITC, by fluorescence microscopy, revealed that the integrins interact with the RGD and GRGDY sequences. Different effects are observed in serum and serum-free medium. These differences are probably due to competition of fibronectin and other serum proteins with the RGD/GRGDY – CBM for the integrins on the cell membrane.

The recombinant proteins containing the RGD or GRGDY sequences were able to improve the adhesion of fibroblasts to the polystyrene plate, the CBM alone having no effect. Early cell spreading was also triggered by RGD-CBM and RGD-CBM-RGD proteins, as revealed by the more elongated morphology of the cells one hour after seeding on the polystyrene plates. Similar results have been previously obtained by other authors. Wierzba et al. (1995) produced a recombinant protein containing a RGD sequence at the C-terminus of a CBM from the *Cellulomonas fimi* endoglucanase A (CenA) [12]. This CBM/RGD promoted the attachment of green monkey Vero cell to polystyrene and cellulose acetate. Wang et al. (2006) studied the effect of a protein containing two GRGDS sequences at the N- and C- terminal of a CBM from *Trichoderma koningii*; this recombinant protein improved the adhesion of keratinocytes and dermal fibroblasts when grafted on the petri dish [13].

The proteins containing the RGD sequence significantly increased the adhesion of the fibroblast on the cellulose sheet, as compared to the cellulose treated only with CBM or buffer, while the GRGDY had no effect. The protein containing a single RGD had, surprisingly, a stronger effect on the adhesion of fibroblasts than the protein containing two RGDs. Thus, the effects of RGD vs GRGDY and 1xRGD vs 2xRGD are distinct, depending on whether the proteins are adsorbed on polystyrene or in bacterial cellulose. The affinity of the cells is expected to increase with the concentration of RGD copies. This was the motivation for the production of fusion proteins with

two RGD copies. However, the results demonstrate that there is not a simple and straightforward relation between the RGD surface concentration and the cells adhesiveness and proliferation. Besides concentration, also the exposure, conformation and steric effects may play a role to the RGD-integrin interaction. In fact, it seems that the second RGD or GRGDY brings no further functionality to the proteins. It must be remarked that the presence of a RGD sequence, in a protein, does not guarantee cell attachment activity. Indeed, several hundred proteins contain the RGD tripeptide, but most of these do not have cell attachment activity. To be functional, the RGD sequence must be appropriately exposed, in a conformation that can be recognized by a cell surface receptor [12]. The results obtained in this work consistently showed that, in the assays with BC, the protein containing two RGD sequences had lower activity. The CBM used in this work, from the bacteria *Clostridium thermocellum*, has N- and C- terminals close to each other [11]. Probably, the second linker - containing twelve amino acids, followed by the second adhesion peptide and the hexahistidine tag - at the protein C-terminal interferes with the interaction between the N-terminal RGD or GRGDY with the integrins on the cell membrane. Also, it may be that the presence of a hexahistidine tag, following the RGD, interferes with the exposure of this sequence and its interaction with the integrins. This effect is more relevant with cellulose – where the CBM adsorbs with a specific conformation and orientation - than with the polystyrene plate – where the non-specific adsorption probably leads to random orientation of the molecules. Wierzbka et al. (1995) observed that different cell lines exhibited different patterns of attachment to CBM–RGD, depending on whether it was immobilized on polystyrene plate or cellulose acetate. Vero, COS, HFF, 3T3, 293, and U373 cells attached well to CBM–RGD immobilized on polystyrene or cellulose acetate. CHO, MRC-5, and HEp-2 cells attached to CBM–RGD immobilized on polystyrene, but not to CBM–RGD immobilized on cellulose acetate. BHK and L cells failed to attach to CBM–RGD immobilized on both surfaces. The authors conclude that the adsorption of CBM–RGD to polystyrene plate is nonspecific and presents the RGD in a different configuration or environment, and this may account for differences in the observed cell-binding properties, as observed in this work [14].

Conclusion

Bacterial cellulose is a material with excellent biocompatibility and mechanical properties, thus holding great potential for biomedical applications. In this work, a new approach was developed to functionalise the bacterial cellulose, through recombinant proteins containing adhesion peptides conjugated with a cellulose binding-module. The use of recombinant proteins containing a CBM domain, exhibiting high affinity and specificity for cellulose surfaces, allows the control on the interaction of this material with cells. The CBM may virtually be combined to any biologically active protein for the modification of cellulose-based materials, for *in vitro* or *in vivo* applications. The recombinant proteins containing the RGD or GRGDY sequences were cloned and successfully expressed in fusion with a family 3 CBM of *Clostridium thermocellum* in *E. coli* expression system. The recombinant proteins containing the adhesion peptide were able to promote adhesion and spreading of the cells. Furthermore, the proteins containing the sequence RGD showed a stronger effect than GRGDY on fibroblast cells. The effect of different adhesive sequences seems to depend on the material where they are adsorbed, probably due to conformation effects. Protein models – not in the scope of this work - would probably be useful on helping the design of more effective recombinant proteins.

References

1. Goessler UR, Hormann K, Riedel F. Tissue engineering with chondrocytes and function of the extracellular matrix (Review). *Int J Mol Med* 2004 Apr;13(4):505-513.
2. Plow EF, Haas TA, Zhang L, Loftus J, Smith JW. Ligand binding to integrins. *J Biol Chem* 2000 Jul 21;275(29):21785-21788.
3. Van der Flier A, Sonnenberg A. Function and interactions of integrins. *Cell Tissue Res* 2001 Sep;305(3):285-298.
4. Pierschbacher MD, Ruoslahti E. Cell attachment activity of fibronectin can be duplicated by small synthetic fragments of the molecule. *Nature* 1984;309:30-33.
5. Pfaff E. Recognition sites of RGD-dependent integrins. 1997:101-121. *In* J. A. Eble and K. Kühn (ed.), *Integrin ligand interactions*. R. G. Landes Co., Austin, Tex.
6. Hersel U, Dahmen C, Kessler H. RGD modified polymers: biomaterials for stimulated cell adhesion and beyond. *Biomaterials* 2003 Nov;24(24):4385-4415.
7. Sakiyama-Elbert SE, Hubbell JA. *Functional Biomaterials: Design of novel Biomaterials*. *Annu Rev Mater Res* 2001;31:183-201.
8. Klemm D, Schumann D, Udhardt U, Marsch S. Bacterial synthesized cellulose - artificial blood vessels for microsurgery. *Prog Polym Sci* 2001;26(9):1561-1603.
9. Czaja WK, Yong DJ, Kawecki M, Brown Jr RM. The future prospects of Microbial Cellulose in Biomedical Applications. *Biomacromolecules* 2007;8(1):1-12.
10. Tomme P, Boraston A, McLean B, Kormos J, Creagh AL, Sturch K, et al. Characterization and affinity applications of cellulose-binding domains. *Journal of Chromatography B* 1998;715(1):283-296.
11. Tormo J, Lamed R, Chirino AJ, Morag E, Bayer EA, Shoham Y, et al. Crystal structure of a bacterial family-III cellulose-binding domain: a general mechanism for attachment to cellulose. *Embo J* 1996 Nov 1;15(21):5739-5751.
12. Wierzba A, Reichl U, Turner RFB, Warren RAJ, Kilburn DG. Production and properties of a bifunctional fusion protein that mediates attachment of vero cells to cellulosic matrices. *Biotechnology and Bioengineering* 1995;47(2):147-154.
13. Wang TW, Wu HC, Huang YC, Sun JS, Lin FH. The effect of self-designed bifunctional RGD-containing fusion protein on the behavior of human keratinocytes and dermal fibroblasts. *J Biomed Mater Res B Appl Biomater* 2006 Nov;79(2):379-387.
14. Wierzba A, Reichl U, Turner RFB, Warren RAJ, Kilburn DG. Adhesion of mammalian cells to a recombinant attachment factor, CBM/RGD, analyzed by image analysis. *Biotechnology and Bioengineering* 1995;46(3):185-193.

Chapter 3

Improving bacterial cellulose for blood vessel replacement: functionalization with a chimeric protein containing a cellulose-binding module and an adhesion peptide

Adapted from: Acta Biomaterialia 2010; 12;6:4034–4041.

Abstract

Chimeric proteins containing a cellulose-binding module (CBM) and an adhesion peptide (RGD or GRGDY) were produced and used to improve the adhesion of human microvascular endothelial cells (HMEC) to Bacterial Cellulose (BC). The effect of these proteins on the HMEC-BC interaction was studied. The results obtained demonstrated that the recombinant proteins containing adhesion sequences were able to significantly increase the attachment of HMEC to BC surfaces, specially the RGD sequence. The images obtained by SEM microscopy showed that the cells on the RGD-treated BC present a more elongated morphology, 48h after cell seeding. The results also showed that the RGD decreased the in-growth of the HMEC cells through the BC and stimulated the early formation of cordlike structures by these endothelial cells. Thus, the use of recombinant proteins containing a CBM domain, with high affinity and specificity for cellulose surfaces, allows the control on the interaction of this material with cells. CBM may be combined virtually to any biologically active protein for the modification of cellulose-based materials, for *in vitro* or *in vivo* applications.

Introduction

Cardiovascular disease is the leading cause of mortality in Western countries. Surgical bypass with autologous grafts remains the most used treatment, saphenous veins and mammary arteries being preferably used. However, many patients do not have suitable vessels, due to preexisting vascular disease, amputation or previous harvest for prior vascular procedures. Moreover, a second surgical procedure is needed to obtain the vessel [1, 2]. For the reconstruction of arteries with large caliber, currently available synthetic grafts (e.g.: Dacron, and ePTFE) offer a reasonable solution and proven clinical efficacy. However, for small size (<6 mm) grafts, these materials generally present poor performance, due the anastomotic intimal hyperplasia and surface thrombogenicity [3-5]. This scenario prompts the search for new materials, suitable for the effective replacement of small blood vessels.

Bacterial cellulose (BC) produced by *Acetobacter* organisms is a biomaterial that has gained interest in the field of tissue engineering, due to its unique properties. BC has been studied by several research groups as a scaffold for cartilage [6-8], wound dressing [9, 10], dental implants [11-17], nerve regeneration [18, 19] and vascular grafts [18, 20-23]. The *in vivo* biocompatibility of BC was also evaluated in a study conducted by Helenius and colleagues [24].

Many strategies have been pursued to improve the compatibility and effectiveness of vascular grafts, through the production of unreactive surfaces, the surface modification of existing synthetic grafts (e.g. modifying surface properties, the incorporation of biologically active substances) and coating with autologous cells [4]. Seeding the graft surface with endothelial cells [25] is a quite promising approach; the native vessel is this way mimicked, thereby decreasing thrombosis. However, the high loss of ECs by the restored blood flow after implantation presents a major challenge [4, 26, 27]. The rate and quality of endothelialization of a synthetic vascular graft depends on interaction of EC with these cardiovascular materials. Several approaches have been attempted to increase the EC adhesion on typically non-adhesive polymeric biomaterials used for synthetic vascular grafts [28]. One such approach involves pre-coating with EC specific adhesive glues. The tripeptide Arg-Gly-Asp (RGD), an amino acid sequence found in many adhesive plasma and extracellular matrix protein, has been used to enhance cell adherence. Binding of cells to the RGD-sequence occurs via integrin receptors on the cell membranes. The improvement of the biocompatibility and performance of bacterial cellulose – envisaging its use as small-diameter vascular grafts – by enhancing the

adhesion of human microvascular endothelial cells (HMEC-1), was attempted in this work by coating BC with adhesion peptides.

Many strategies developed to modify the materials used as synthetic grafts (*e.g.*, Dacron, ePTFE, polyurethane) with the adsorption of active substances, like heparin, RGD, albumin-heparin conjugates, dipyridamole, have little or no effect due to the coatings being washed away [27]. In a previous work (presented in chapter 2), we described the production of recombinant proteins containing the adhesion sequences fused to a CBM (cellulose-binding module) [29]. For artificial grafts based on cellulose, the use of a CBM (exhibiting high affinity and specificity for cellulose surfaces) that can virtually be combined to any biologically active protein is an important strategy to avoid losing the biological agents coating the graft.

Materials and methods

Cell culture assays

Human Microvascular Endothelial Cells (HMECs) (kindly provided by Dr João Nuno Moreira, Coimbra University) were used between passages 13 and 22. HMECs were cultured in RPMI 1640 medium (Invitrogen Life Technologies, UK) supplemented with 10% FBS (Invitrogen Life Technologies, UK), 1% penicillin/streptomycin (Invitrogen Life technologies, UK), 1.176 g/L of sodium bicarbonate, 4.76 g/L of Hepes, 1mL/L of EGF and 1 mg/L of hydrocortisone > 98% (Sigma, Portugal), and maintained at 37°C in a humidified 5% CO₂ atmosphere.

Cell attachment, proliferation and viability

Production and purification of recombinant proteins: The recombinant proteins (RGD–CBM, RGD–CBM–RGD, GRGDY–CBM, GRGDY–CBM–GRGDY) have been formerly cloned in *Escherichia coli* and its production and purification was conducted as previously described [29] in chapter 2.

Production of bacterial cellulose and coating with the recombinant peptides: *Gluconacetobacter xylinus* (ATCC 53582 and DSMZ 46604) purchased from the American Type Culture Collection and from the German Collection of Microorganisms and Cell Cultures were grown in Hestrin-

Schramm medium, pH 5.0. The medium was inoculated with the culture, added to the 24-well or 96-well polystyrene plate (1 mL or 0.2mL per well, respectively) and incubated statically at 30 °C, for 5 days (ATCC 53582) or 10 days (DSMZ 46604). BC pellicles were purified by 2% SDS treatment at 60 °C, for 12 h followed by 4% NaOH at 60 °C, for 90 min. Samples were autoclaved and stored in PBS pH 7.4, at 4°C, prior to use. The pellicles produced by the DSMZ 46604 strain (BC – L) presented a thickness of about 0.5mm, while the pellicles produced by the ATCC 53582 strain (BC – H) are approximately 3mm thick. The recombinant proteins were added (0.25mg of protein/per membrane) and left adsorbing to BC for 12 hours, 4 °C. Then, the membranes were washed with phosphate buffered saline (PBS).

HMEC-1 Adhesion and proliferation: The mitochondrial activity of the cultured cells was determined using a colorimetric assay, which is related to cell viability. The MTS [3-(4,5-dimethylthiazol-2-yl)-5-(3-carboxymethoxyphenyl)-2-(4-sulfophenyl)-2H-tetrazolium] assay was performed as follows: BC – H or BC – L membranes treated with the recombinant proteins were added to the wells of 24-well polystyrene plates. As referred above, the BC sheets were produced in similar 24-well polystyrene plates, such that they tightly fit in the wells, completely covering the bottom surface. The HMEC-1 cells were seeded on the BC at a density of 12×10^4 cells/well, in RPMI medium without serum. The plates were incubated at 37 °C, in atmosphere of 5% CO₂ and 95% humidified air. Two hours after the addition of the cells, the wells were washed with PBS and RPMI with 10% Foetal Bovine Serum (FBS) was added. The MTS assay of the adsorbed HMEC-1 cells was carried out to evaluate the adhesion of cells after 2h and proliferation 24h, 48h and 7 days after cell seeding. The results were obtained from at least 3 different assays, each one with samples in triplicates.

In order to evaluate the effect of the RGD on the rate of cell adhesion, a similar assay was performed at 15, 30, 60, 90 and 120 minutes after cell seeding, the non-adherent cells being washed out before running the MTS assay.

Live and dead assay: The viability of the cells coating the cellulose (BC – L), treated or not with the recombinant proteins, was also analyzed with the LIVE/DEAD® Viability/Cytotoxicity Kit for mammalian cells (Invitrogen, UK). This kit provides two-color fluorescence cell viability assay, based on the simultaneous determination of live and dead cells with two probes that measure the intracellular esterase activity and the plasma membrane integrity. This assay employs calcein, a polyanionic dye, which is retained within the living cells, producing green

fluorescence. It also employs the ethidium bromide homodimer dye (red fluorescence), which can enter the cells through damaged membranes, binding to nucleic acids and being excluded by the intact plasma membrane of the living cells. The experiment was developed as described for the MTS assay. The fluorescence microscopy observations of the cells were carried out after 24 hours of incubation. Cells seeded on polystyrene were used as positive control (living cells), and cells further treated with methanol 70% for 30 min were taken as negative control (dead cells). Live and dead assay was also used to analyze the apoptosis event (qualitatively) in combination with the TUNEL assay (quantitatively). Samples were visualized and imaged using a Fluorescent microscope Olympus BX51 (Olympus Portugal SA, Porto, Portugal).

Morphological analysis by fluorescent and SEM microscopy

The BC – L membrane treated with recombinant proteins were seeded with cells as previously described. For fluorescent microscopy, 14 days after cells seeding on BC, the membranes were washed with prewarmed PBS; then, the cells were fixed in 4% formaldehyde (Pierce, Rockford, IL, USA) in PBS, permeabilized with acetone (Sigma) at -20°C , and stained with Alexa Fluor 546-phalloidin (Molecular Probes). Nuclei were visualized by staining with DAPI. Microscopy observations were performed using an Olympus BX51 (Olympus Portugal SA, Porto, Portugal) fluorescence microscope. Fluorescence microscopic observations were carried out only with the BC – L membranes, which allow a proper visualization of the cells due to their thinness. For SEM microscopy, 48 hours after cell seeding the medium was removed and the BC pellicles washed twice with PBS. Next, 1ml of 2.5% glutaraldehyde in PBS was poured into each well, and the materials were maintained at room temperature for 1h, in order to fix the cells on the membrane. Afterwards, the membranes were rinsed with distilled water, and finally dehydrated by successive immersion in a series of ethanol-water solutions (55, 70, 80, 90, 95, 100% v/v), for 30 min each, and allowed to evaporate at room temperature. The surface of the membranes with the adherent cells was observed with scanning electron microscopy (LEICA S 360), after gold-sputtering treatment.

Cell apoptosis

Tunel Assay: HMEC-1 cells (12×10^4 cel/well) were seeded on the BC – L as described for the MTS assay and after 24h of incubation the TUNEL assay (Terminal deoxynucleotidyl transferasemediated deoxyuridine triphosphate nick-end labeling), which examines DNA strand breaks during apoptosis, was performed using the In Situ Cell Death Detection kit (Roche Diagnostics, Basel, Switzerland), according to the manufacturing instructions and as previously described [30]. To facilitate the counting of the total nucleus, the cells were also stained with DAPI.

Cell invasion

To evaluate the RGD effect on the migration of the endothelial cells through the BC a migration chamber and an attractant were used to stimulate the cells migration into the BC. The migration chamber consisted of cell culture inserts with a membrane pore size of $8.0 \mu\text{m}$ in a 24 well plate (BD Biocoat™ Matrigel™ Invasion Chamber, BD, NJ, USA). Initially, HMEC-1 cells were seeded onto BC – L (treated with the recombinant proteins) at a density of 2.5×10^4 cell/well in Medium RPMI without serum. After four hours, 10% FBS serum was added to the wells. The plates were incubated at 37°C in atmosphere of 5% CO_2 and 95% humidified air for 24 hours. In the next day, cell-coated BC pellicles were transferred to the invasion chamber containing medium with 2% FBS. To attract the cells to migrate into the cellulose, 20% FBS were added to the cell culture medium in the wells. Cell cultures were incubated for 72 hours. After conclusion of the experiments, the Matrigel membranes were removed from the inserts with a scalpel. The cellulose and Matrigel membranes were fixed and stained with a methanol – DAPI solution and photographed through fluorescence microscopy. The cells that migrated from the cellulose to matrigel were counted.

Angiogenesis

BC – L pellicles produced in a 24-well polystyrene plate were treated with the recombinant proteins and coated with HMEC cells (4×10^4 cel/well), in serum-free medium for two hours. Then, 10% FBS was added to the wells. The pellicles were incubated for 24 hours at 37°C in

atmosphere of 5% CO₂ and 95% humidified air. Afterwards, the medium was removed and fresh medium with serum (10%) was added. The plates were incubated for four days. To evaluate the effect of the recombinant protein on the morphology and assembly of EC into capillary-like structures when cultured on BC pellicles, the cordlike structures were observed qualitatively in a Leica DM IL inverted microscope (Leica Microsystems, Wetzlar, Germany).

Immunocytochemistry

The cells were grown on BC treated with the recombinant proteins (RGD-CBM or CBM) or buffer for 14 days, then fixed with methanol at -20 °C. To avoid unspecific interactions the cellulose membranes were blocked with BSA 4% in PBS. The Primary antibody was vWF (von Willebrand factor) (1:100) (Chemicon, Hofheim, Germany) and the secondary antibody was an anti-rabbit FITC-conjugated (1:1000) (Santa Cruz Biotechnology, Santa Barbara, USA). The Nuclei were counterstained with DAPI (Sigma Aldrich, Portugal). Cells were observed through fluorescent microscopy (Nikon Eclipse 50i, Japan). The endothelial specificity of the cells was also verified by the uptake of DiI-labelled acetylated low-density lipoprotein (Biomedical Technologies Inc., USA) another specific marker for these cells.

Statistical analyses

All experiments were performed in triplicate. Quantifications are expressed as mean (\pm SD) of 3 independent experiments. Statistical significance of difference between various groups was evaluated by one-way analysis of variance (ANOVA test) followed by the Bonferroni test.

Results

The results of the MTS assay demonstrated that the recombinant proteins containing adhesion sequences were able to increase significantly the attachment of HMEC to BC – H surfaces (FIGURE 1). Two hours after cell seeding, approximately 140-150% and 60-80% more cells adhered to BC treated with the proteins containing the RGD and GRGDY peptides, respectively, when compared to non-treated BC – H.

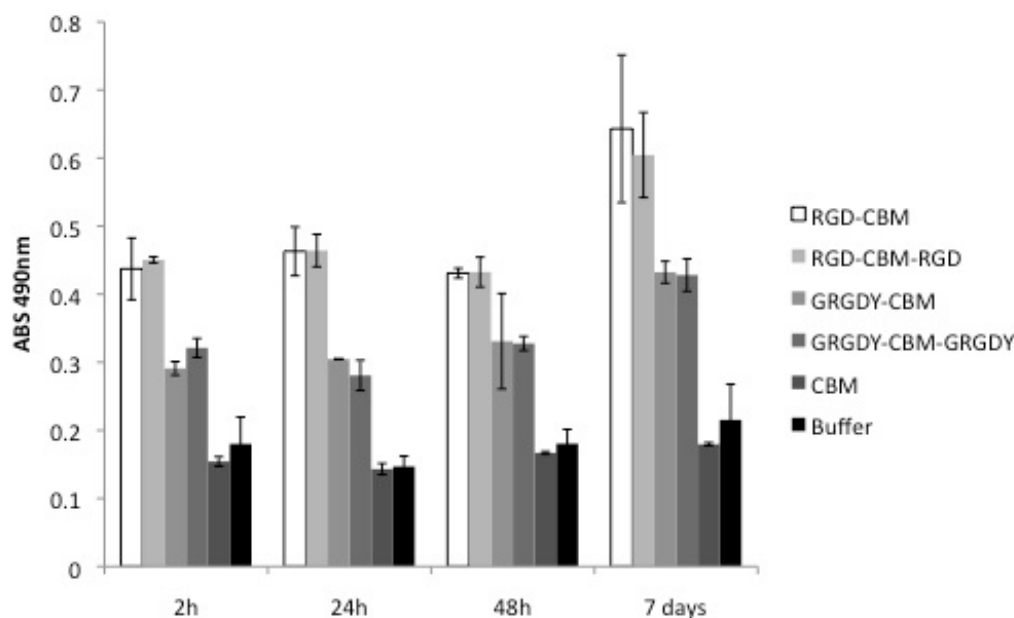


Figure 1: MTS assays of HMEC-1 culture on BC – H pellicles treated with the recombinant proteins (CBM, RGD-CBM, RGD-CBM-RGD, GRGDY-CBM and GRGDY-CBM-GRGDY) and buffer. The MTS assay was developed at 2, 24, 48 hours and 7 days after cells addition. Results are expressed in absorbance values at 490nm.

The results demonstrated that the proteins containing RGD sequence have a stronger effect than the protein containing GRGDY sequences. Moreover, it seems that the presence of a second adhesion sequence at the C-terminal of the protein did not significantly enhance the effect of the recombinant protein when compared with the protein containing only one copy of the peptide. Moreover, the results indicated that the adsorption of the CBM protein to BC – H slightly decreases cell adhesion (FIGURE 1) by 14%. When the assay was developed with BC – L membranes, coated with proteins containing one or two RGD copies, around 108 and 77% more cells adhered to the material than to non-treated BC – L. The proteins containing the GRGDY peptide promoted an increase of only 22-40% of cell adhesion (FIGURE 2). Figure 3 shows that the improvement of cell attachment is significant already 15 minutes after cell seeding. From figures 1 and 2, after 24 and 48 hours following the cell seeding no proliferation is detected, irrespective of the BC membrane or treatment used. However, after 7 days, proliferation is noticeable on BC – H treated with the RGD and GRGDY containing proteins (in contrast with CBM and buffer treated BC-H), while no proliferation is visible when cells were cultured on BC – L.

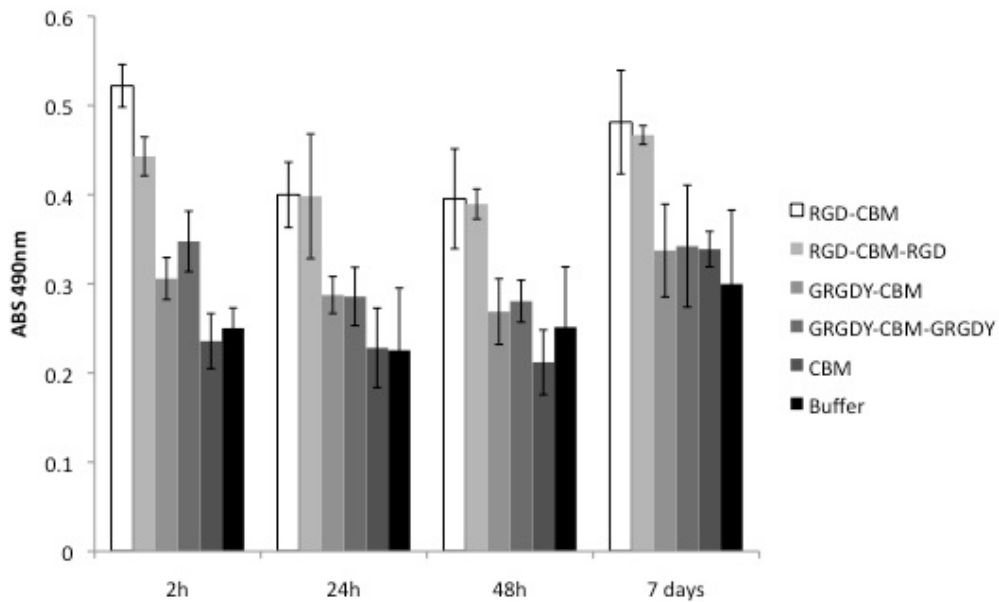


Figure 2: MTS assays of HMEC-1 culture on BC – L pellicles treated with the recombinant proteins (CBM, RGD-CBM, RGD-CBM-RGD, GRGDY-CBM and GRGDY-CBM-GRGDY) and buffer. The MTS assay was developed at 2, 24, 48 hours and 7 days after cells addition. Results are expressed in absorbance values at 490nm.

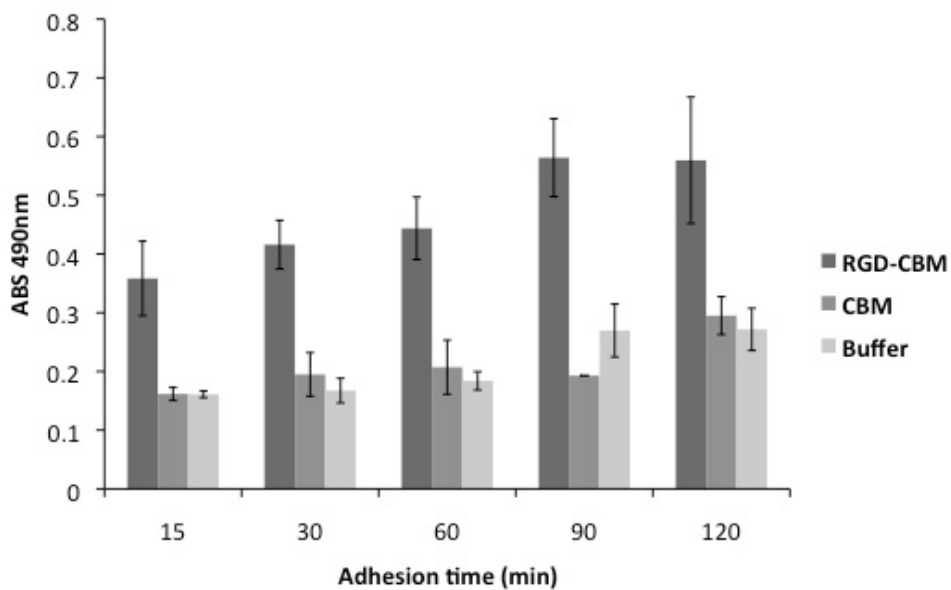


Figure 3: MTS assays of HMEC-1 culture on BC- H pellicles treated with CBM, RGD-CBM and buffer. The MTS test was developed at 15, 30, 60, 90 and 120 minutes after addition of cells. Results are expressed in absorbance values at 490nm.

To estimate the viability of the cells on the protein coated BC, the LIVE/DEAD assay was performed 24 hours after cell adhesion. The fluorescence images obtained show that, irrespective of the treatment, the cells remain viable on the BC pellicle (FIGURE 4). TUNEL assay results corroborated the LIVE/DEAD assay, showing no significant differences between BC pellicles treated with the recombinant proteins (RGD-CBM and CBM) when compared with control (buffer) (FIGURE 5).

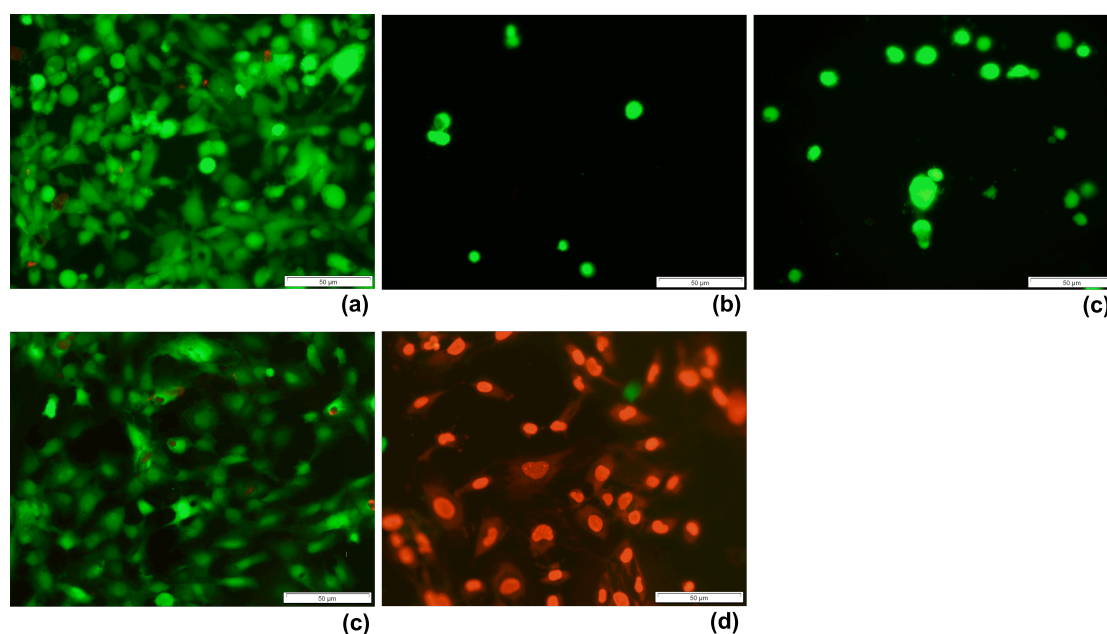


Figure 4: Fluorescence photographs of endothelial cells stained with LIVE/DEAD® Viability/Cytotoxicity Kit for mammalian cells. Live cells are stained in green and dead cells are stained in red. BC-L treated with RGD-CBM (a), CBM (b) and buffer (c). Controls with cells on polystyrene, live (d) and dead (e). Images were acquired using objectives 40x (scale 50 μ m).

We next investigated whether the RGD affects HMEC invasion capacity using a double-chamber assay. The cells were seeded on the BC – L pellicle treated with the RGD, CBM or buffer. The number of migrating cells was then quantified through the double-chamber assay, using serum at 20% as chemoattractant. In comparison to the controls, the RGD decreased the ingrowth of

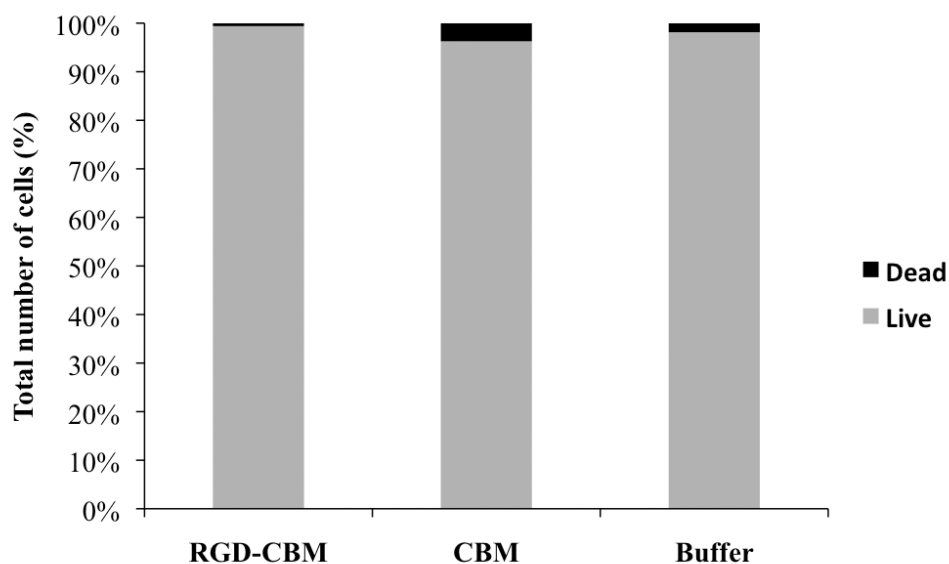


Figure 5: Apoptosis was quantitatively evaluated by the TUNEL assay. The HMEC cells were seeded on the BC – L and after 24h of incubation the TUNEL assay was performed. Bars represent the percentage of apoptotic cells evaluated by the ratio between TUNEL-stained cells and DAPI-stained nuclei in every culture. Experiments were repeated three times with identical results.

the HMEC cells through the BC. A 4- and 2.4-fold increase of the number of cells migrating through the membrane was obtained, respectively for the BC treated with buffer and CBM, taking as reference the BC treated with RGD (FIGURE 6).

Optical Microscopy observation indicated that the RGD stimulated the formation of cellular cordlike structures, at an earlier stage as compared with the other groups. These findings showed that 24 hours after seeding, most of the cells present a round shape in all groups (data no shown). However, after 96 hours, the cells of the RGD treated - BC are more elongated than those on the buffer control, starting to form cordlike structures, while the cell of the CBM group remain round shaped (FIGURE 7). In fact, the structure showed in image (d) from figure 7, obtained by fluorescent microscopy, was found only in the BC surfaces treated with RGD. Details on the morphology of the cells 48 hours after cell seeding were obtained by SEM. The cells on the RGD treated BC presented an elongated shape; in fact, as can be seen in image (a), most of the cells are so elongated that become hardly noticeable on SEM, unlike cells observed on the untreated or CBM treated – BC where most remain rounded (FIGURE 8). The von Willebrand factor expression is a widely used criterion for defining endothelial cell type [31-33], thus to determine whether HMECs cells maintain the endothelial phenotype

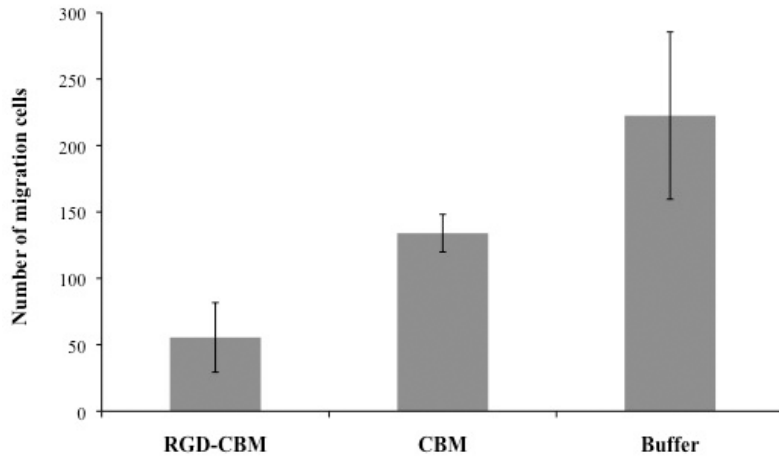


Figure 6: Effect of RGD on the HMEC cell invasion through bacterial cellulose pellicles. Invasion was quantified in a double-chamber assay using medium complemented with 20% FBS as a chemoattractant. Bars represent the number of invasive cells.

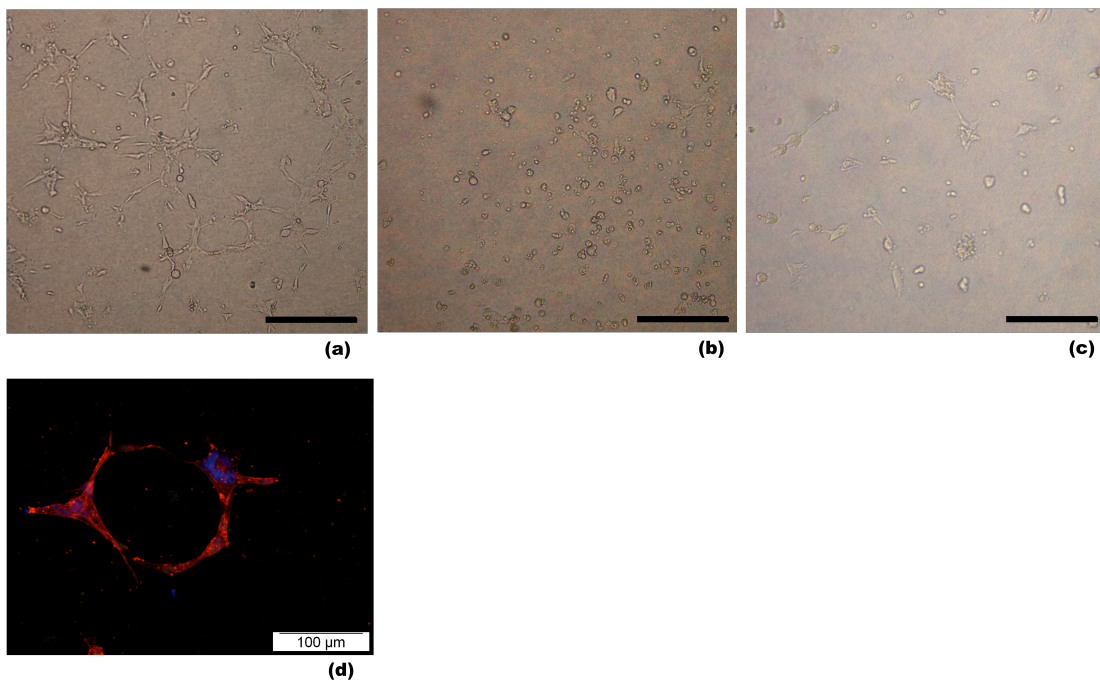


Figure 7: Images (a), (b) and (c) - optical microscopy photographs showing the effect of the RGD on the assembly of endothelial cells into capillary-like structures. BC – L treated with RGD-CBM (a), CBM (b) and buffer (c). Image was acquired using objective 20x (scale 200μm). Image (d) - Fluorescent microscopy image showing HMECs cells cultured at 14 days on BC – L pellicle treated with RGD – CBM recombinant protein. Nuclei were visualized by staining with DAPI (blue) and f-actin with Alexa Fluor 546-phalloidin (red). Image was acquired using objective 20x (scale 100μm).

characteristic after 14 days cultured on BC, the vWF expression was evaluated. Immunocytochemistry results showed that cells grown on BC treated with the recombinant proteins or buffer maintained their positive staining for vWF (FIGURE 9).

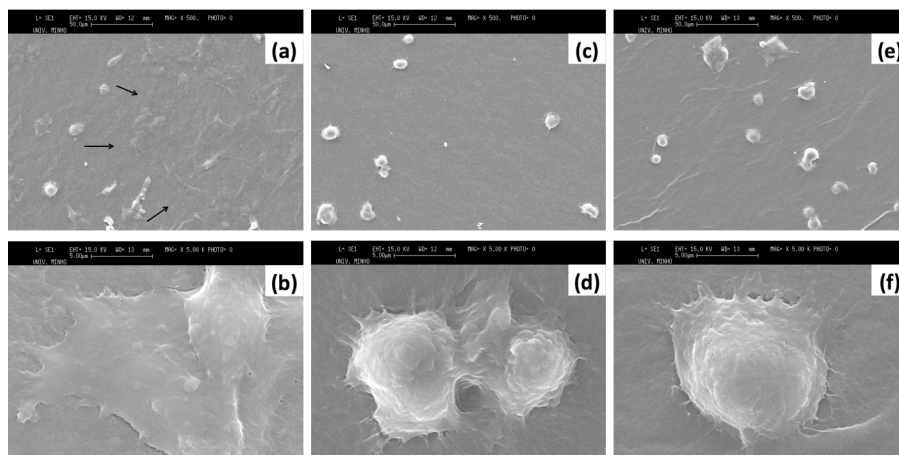


Figure 8: SEM micrographs of bacterial cellulose. BC treated with RGD–CBM (a, b); CBM (c, d) and buffer (e, f). The arrows remark cells with elongated morphology. (a), (c) and (e) scale 50 μ m; (b), (d) and (f) scale 5 μ m.

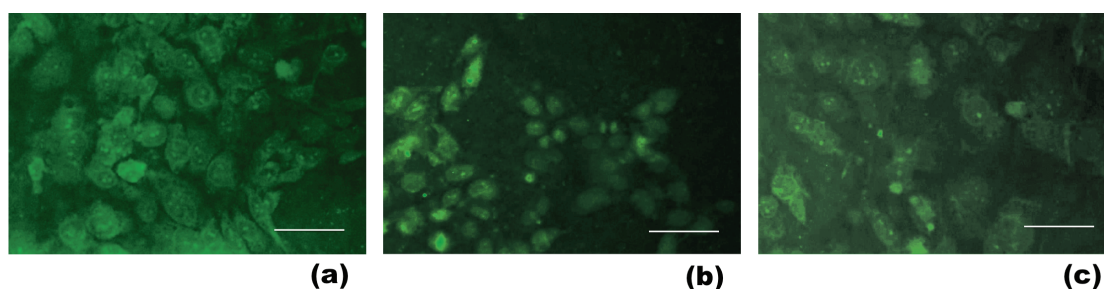


Figure 9: Immunocytochemical analyses using anti-vWF antibody. The results showed that HMEC cells cultured after 14 days on BC–L treated with recombinant proteins or buffer stained positively for vWF. (a) RGD-CBM, (b) CBM and (c) buffer. Image was acquired using objective 20x (scale 100 μ m).

Discussion

Gluconacetobacter xylinus constructs a BC pellicle that presents a denser and flatter surface side and a gelatinous layer on the opposite side [18]. In this study, all the experiments were

conducted on the denser side of both the BC-H and BC-L, because a smooth surface, being similar to the basal membrane of the luminal side of blood vessels, is preferable for the attachment of endothelial cells [20]. Analysis by SEM showed that *G. xylinus* ATCC 53582 produce a thicker and more compact cellulose pellicle than the DSMZ 46604 strain (data not shown). Therefore, the BC-H pellicle presents a smoother surface than the BC-L. This may lead to differences between BC-H and BC-L in the adhesion and proliferation of the cells in the MTS test. The results from the attachment assay were similar to those obtained in our previous work (chapter 2), when fibroblasts were seeded on BC produced by ATCC 53582 strain coated with adhesion peptides [29]. In that previous work, the RGD improved the adhesion of fibroblast onto cellulose and the presence of a second RGD did not enhance the effect of the recombinant protein, probably because the RGD at the C-terminal of the protein was not properly exposed to be recognized by integrins. However, unlike the results with endothelial cells, the GRGDY sequence was not effective on the adhesion of fibroblasts. Apparently, the microvascular endothelial cells adhere stronger than fibroblasts to the recombinant protein containing RGD sequences. Indeed, endothelial cells may have substantially more $\alpha_v\beta_3$ integrin than fibroblasts [34]. The results also demonstrated that pre-coating BC with the RGD-containing protein decreased the incubation time required for adsorption. A short incubation period is particularly important in single-stage seeding as the incubation time is kept to a minimum to fit into the time frame of the surgical procedure [26].

Several works have been developed to improve the interaction of cells to bacterial cellulose [21, 29, 35, 36]. However, only a few studied the migration and ingrowth of cells on BC [20, 21, 37, 38]. The migration of the cells is mediated mainly by integrins, a diverse family of glycoproteins that form heterodimeric receptors for ECM molecules. During migration, cells project lamellipodia that attach to the ECM, and simultaneously break existing ECM contacts at their trailing edge. This allows the cell to pull itself forward. Integrins are essential for cell migration and invasion, not only because they directly mediate adhesion to the extracellular matrix, but also because they regulate intracellular signaling pathways that control cytoskeleton organization, force generation, gene transcription, and survival [39].

Endothelialization may either be developed *ex vivo* or post-implantation, stimulating the ECs (from tissues adjacent to anastomosis or from circulation) to adhere and proliferate on the graft. The rate and quality of a vascular graft endothelialization depends on the cell-material

interaction, leading to functions such as adhesion and migration. Several studies have shown that cell adhesiveness to substratum modulates cell migration on surfaces coated with ECM proteins [25, 40-42]. Our results showed that a small number of cells migrated through the cellulose when compared with the rather large number of cells added (2.5×10^4 cel/well). During invasion, cells release proteases that degrade and remodel the ECM, promoting cell passage through to the stroma and entrance into the new tissue [39]. However, cellulose could not be degraded by animal cells [24] and in order to migrate in a fibrous hydrogel as BC the cells must push the nanofibrils aside when migrating into the cellulose nanofibril network [20]. Probably, the time used in the experiment (72h) was too short to enable cells to migrate through the BC pellicle with around 0.5mm of thickness. Nevertheless, the results obtained allowed the observation that the migration of endothelial cells on BC was decreased by the presence of the RGD. Since adhesion involves receptor/ligand binding, cell migration can be regulated by controlling cell integrin expression level, integrin-ECM binding affinity or substratum ECM surface density. However, if other stimuli are added, such as growth factors that affect signaling processes of the cell, the migration/adhesion relationship can be dramatically altered [43, 44]. The migration rates of cells are influenced by the chemical and physical interaction with the surface of the material. Studies described that cell migration capacity presents a biphasic behavior depending on the attachment strength. Optimal migration speed can be achieved with intermediate strengths of adhesiveness, since when the adhesion to the substratum is weak no traction occurs, so that the locomotion is not possible and the cell spreads poorly. On the other hand, with strong adhesion, cell is well-spread and immobilized, so dynamic disruption of cell-substratum attachments is difficult and locomotion again does not occur [28, 40, 41, 45, 46]. The CBM used in this work presents a great affinity to cellulose and adsorbs in a specific and very stable way. Probably, the amount of protein used in the experiments was great enough as to saturate the surface of the cellulose pellicle with the RGD-containing proteins, promoting an intense affinity of the cells to the substratum and affecting negatively the locomotion through BC. The saturation of the surface of the cellulose pellicle with the RGD-containing proteins is corroborated by the results shown in our previous work (chapter 2) [29]. In order to enhance endothelialization of BC vascular grafts it is important to promote not only the adhesion of endothelial cells, but also to allow migration through the material. The treatment used in this work greatly improved the adhesion, however the migration was negatively affected by the presence of the RGD, because the affinity of

HMEC cells to the material surface became too strong. However, it is probably possible to improve migration of the cells on BC by optimizing the concentration of RGD containing protein, attempting to reach a compromise between adsorption and migration. However, longer experiments are needed to better assess the effect of RGD on cell migration through BC.

The effect of the RGD on HMECs morphology was observed by SEM. The cells on the RGD – coated BC exhibit a more elongated, flattened morphology, while the ones on “bare” BC were round (Fig. 8a and b). The more extended morphology of the HMECs upon interaction with the adhesive peptides is likely driven by the larger number of focal contacts between integrins and RGDs peptides linked to the BC surface. It is well known that a critical RGD density is essential for the establishment of mature and stable integrin adhesions, which, in turn, induce efficient cell migration, spreading and formation of focal adhesions [47-50].

During angiogenesis events, cells must adhere to one another and to extracellular matrix (ECM) to construct and extend new microvessels [51]. Angiogenesis depends not only on growth factors and their receptors, being also influenced by receptors for ECM proteins. Our results showed that the RGD-containing recombinant protein (RGD-CBM protein) stimulated the early formation of cellular cordlike structures by on bacterial cellulose when compared to BC treated with the recombinant protein without the adhesion peptide (CBM protein) or buffer. HMEC-1 cells express $\alpha_v\beta_3$ and $\alpha_v\beta_5$ integrins [52] that can bind an array of ligands such as vitronectin, fibronectin, von Willebrand factor, fibrinogen, osteopontin, thrombospondin, and RGD-containing peptides [51, 53]. Moreover these two complexes also have been identified as having an especially interesting expression pattern among vascular cells during angiogenesis and vascular remodeling.

Immunocytochemistry results showed that cells grown on BC maintained their positive staining for von Willebrand factor (vWF). This glycoprotein is one of the various secretory and membrane-bound molecules produced by the endothelium. The vWF mediates the interaction of platelets with damaged endothelial surfaces at sites of vascular injury and has been long favored as an endothelial-cell marker, once the expression of this factor is highly restricted to endothelial cells, platelets, and megakaryocytes [33].

In the current scenario of regenerative medicine there is a great demand for production of new materials appropriate for small-diameter blood vessel replacements. In this work, bacterial

cellulose, a promising cardiovascular biomaterial, was successfully functionalized. The strategy used aims the improvement of microvascular cell adhesion to BC, through recombinant proteins containing adhesion peptides and a cellulose-binding module. For artificial grafts based on cellulose, the use of a CBM (exhibiting high affinity and specificity for cellulose surfaces) is an excellent feature, once CBM can virtually be combined to any biologically active protein and used to modify the cellulose-based materials. The chimeric proteins were able to enhance endothelial cells adhesion to BC and stimulate angiogenesis. However, the ingrowth of the cell through cellulose was decreased. We believe that an improved migration of the cells on BC will be achieved with intermediary concentration of protein used in this work.

References

1. Isenberg BC, Williams C, Tranquillo RT. Small-diameter artificial arteries engineered in vitro. *Circ Res* 2006 Jan 6;98(1):25-35.
2. Wang X, Lin P, Yao Q, Chen C. Development of small-diameter vascular grafts. *World J Surg* 2007 Apr;31(4):682-689.
3. Conte MS. The ideal small arterial substitute: a search for the Holy Grail? *FASEB J* 1998 Jan;12(1):43-45.
4. Bos GW, Poot AA, Beugeling T, van Aken WG, Feijen J. Small-diameter vascular graft prostheses: current status. *Arch Physiol Biochem* 1998 Apr;106(2):100-115.
5. Zilla P, Bezuidenhout D, Human P. Prosthetic vascular grafts: wrong models, wrong questions and no healing. *Biomaterials* 2007 Dec;28(34):5009-5027.
6. Svensson A, Nicklasson E, Harrah T, Panilaitis B, Kaplan DL, Brittberg M, et al. Bacterial cellulose as a potential scaffold for tissue engineering of cartilage. *Biomaterials* 2005 Feb;26(4):419-431.
7. Oliveira RCB, Souza FC, Castro M. Avaliação da resposta tecidual quando da substituição da cartilagem do septo nasal de coelhos por manta de celulose bacteriana. Estudo experimental. *ACTA ORL/Técnicas em Otorrinolaringologia* 2007;25(4):267-277.
8. Bodin A, Concaro S, Brittberg M, Gatenholm P. Bacterial cellulose as a potential meniscus implant. *J Tissue Eng Regen Med* 2007 Sep-Oct;1(5):406-408.
9. Fontana JD, de Souza AM, Fontana CK, Torriani IL, Moreschi JC, Gallotti BJ, et al. *Acetobacter cellulose pellicle as a temporary skin substitute. Appl Biochem Biotechnol* 1990 Spring-Summer;24-25:253-264.
10. Pippi NL, Sampaio AJSA. Estudos preliminares sobre o comportamento do Biofill na ceratoplastia lamelar em coelhos. *Revista do Centro de Ciências Rurais* 1990;20(3-4):297-302.
11. dos Anjos B, Novaes AB, Jr., Meffert R, Barboza EP. Clinical comparison of cellulose and expanded polytetrafluoroethylene membranes in the treatment of class II furcations in mandibular molars with 6-month re-entry. *J Periodontol* 1998 Apr;69(4):454-459.
12. Novaes AB, Jr., Novaes AB, Grissi MFM, Soares UN, Gabarra F. Gengiflex, an Alkali-Cellulose membrane for GTR: Histologic observations. *Brazilian Dental Journal* 1993;4(2):65-71.
13. Novaes AB, Jr., Novaes AB. Immediate implants placed into infected sites: a clinical report. *Int J Oral Maxillofac Implants* 1995 Sep-Oct;10(5):609-613.
14. Novaes AB, Jr., Novaes AB. Bone formation over a TiAl6V4 (IMZ) implant placed into an extraction socket in association with membrane therapy (Gengiflex). *Clin Oral Implants Res* 1993 Jun;4(2):106-110.

15. Novaes AB, Jr., Novaes AB. Soft tissue management for primary closure in guided bone regeneration: surgical technique and case report. *Int J Oral Maxillofac Implants* 1997 Jan-Feb;12(1):84-87.
16. Salata LA, Craig GT, Brook IM. In-Vivo Evaluation of a New Membrane (Gengiflex(R)) for Guided Bone Regeneration (Gbr). *Journal of Dental Research* 1995;74(3):825-825.
17. Sonohara MK, Gregghi SLA. Avaliação da resposta biológica a diferentes barreiras mecânicas, utilizadas na técnica de regeneração tecidual guiada (RTG). *Revista da Faculdade de Odontologia de Bauru* 1994;2(4):96-102.
18. Klemm D, Schumann D, Udhardt U, Marsch S. Bacterial synthesized cellulose - artificial blood vessels for microsurgery. *Progress in Polymer Science* 2001 Nov;26(9):1561-1603.
19. Brancher JA, Torres MF. Reparação microcirúrgica de nervo facial de ratos Wistar por meio de sutura - Parte II. *Revista Sul-Brasileira de Odontologia* 2005;2(2):34-38.
20. Backdahl H, Helenius G, Bodin A, Nannmark U, Johansson BR, Risberg B, et al. Mechanical properties of bacterial cellulose and interactions with smooth muscle cells. *Biomaterials* 2006 Mar;27(9):2141-2149.
21. Backdahl H, Esguerra M, Delbro D, Risberg B, Gatenholm P. Engineering microporosity in bacterial cellulose scaffolds. *J Tissue Eng Regen Med* 2008 Aug;2(6):320-330.
22. Negrão SW, Bueno RRL, Guérios EE, Ultramari FT, Faidiga AM, de Andrade PMP, et al. A eficácia do stent recoberto com celulose biosintética comparado ao stent convencional em angioplastia em coelhos. *Revista Brasileira de Cardiologia Invasiva* 2006;14(1):10-19.
23. Wippermann J, Schumann D, Klemm D, Kosmehl H, Salehi-Gelani S, Wahlers T. Preliminary results of small arterial substitute performed with a new cylindrical biomaterial composed of bacterial cellulose. *Eur J Vasc Endovasc Surg* 2009 May;37(5):592-596.
24. Helenius G, Backdahl H, Bodin A, Nannmark U, Gatenholm P, Risberg B. In vivo biocompatibility of bacterial cellulose. *J Biomed Mater Res A* 2006 Feb;76(2):431-438.
25. Palecek SP, Loftus JC, Ginsberg MH, Lauffenburger DA, Horwitz AF. Integrin-ligand binding properties govern cell migration speed through cell-substratum adhesiveness. *Nature* 1997 Feb 6;385(6616):537-540.
26. Salacinski HJ, Tiwari A, Hamilton G, Seifalian AM. Cellular engineering of vascular bypass grafts: role of chemical coatings for enhancing endothelial cell attachment. *Med Biol Eng Comput* 2001 Nov;39(6):609-618.
27. Hoenig MR, Campbell GR, Campbell JH. Vascular grafts and the endothelium. *Endothelium* 2006 Nov-Dec;13(6):385-401.
28. Kouvroukoglou S, Dee KC, Bizios R, McIntire LV, Zygourakis K. Endothelial cell migration on surfaces modified with immobilized adhesive peptides. *Biomaterials* 2000 Sep;21(17):1725-1733.

29. Andrade FK, Moreira SM, Domingues L, Gama FM. Improving the affinity of fibroblasts for bacterial cellulose using carbohydrate-binding modules fused to RGD. *J Biomed Mater Res A* 2010 Jan;92A(1):9-17.
30. Costa R, Carneiro A, A. R, Piarraco A, Falcão M, Vasques L, et al. Bevacizumab and ranibizumab on microvascular endothelial cells. A comparative study. *J Cell Biochem* in press.
31. Jaffe EA, Hoyer LW, Nachman RL. Synthesis of von Willebrand factor by cultured human endothelial cells. *Proc Natl Acad Sci U S A* 1974 May;71(5):1906-1909.
32. Monteiro R, Calhau C, Silva AO, Pinheiro-Silva S, Guerreiro S, Gartner F, et al. Xanthohumol inhibits inflammatory factor production and angiogenesis in breast cancer xenografts. *J Cell Biochem* 2008 Aug 1;104(5):1699-1707.
33. Jahroudi N, Lynch DC. Endothelial-cell-specific regulation of von Willebrand factor gene expression. *Mol Cell Biol* 1994 Feb;14(2):999-1008.
34. Joshi P, Chung CY, Aukhil I, Erickson HP. Endothelial cells adhere to the RGD domain and the fibrinogen-like terminal knob of tenascin. *J Cell Sci* 1993 Sep;106 (Pt 1):389-400.
35. Watanabe K, Eto Y, Takano S, Nakamori S, Shibai H, Yamanaka S. A new bacterial cellulose substrate for mammalian cell culture. A new bacterial cellulose substrate. *Cytotechnology* 1993;13(2):107-114.
36. Bodin A, Ahrenstedt L, Fink H, Brumer H, Risberg B, Gatenholm P. Modification of nanocellulose with a xyloglucan-RGD conjugate enhances adhesion and proliferation of endothelial cells: implications for tissue engineering. *Biomacromolecules* 2007 Dec;8(12):3697-3704.
37. Svensson A, Nicklasson E, Harrah T, Panilaitis B, Kaplan DL, Brittberg M, et al. Bacterial cellulose as a potential scaffold for tissue engineering of cartilage. *Biomaterials* 2005 Feb;26(4):419-431.
38. Sanchavanakit N, Sangrungraungroj W, Kaomongkolgit R, Banaprasert T, Pavasant P, Phisalaphong M. Growth of human keratinocytes and fibroblasts on bacterial cellulose film. *Biotechnol Prog* 2006 Jul-Aug;22(4):1194-1199.
39. Hood JD, Cheresh DA. Role of integrins in cell invasion and migration. *Nat Rev Cancer* 2002 Feb;2(2):91-100.
40. DiMilla PA, Barbee K, Lauffenburger DA. Mathematical model for the effects of adhesion and mechanics on cell migration speed. *Biophys J* 1991 Jul;60(1):15-37.
41. DiMilla PA, Stone JA, Quinn JA, Albelda SM, Lauffenburger DA. Maximal migration of human smooth muscle cells on fibronectin and type IV collagen occurs at an intermediate attachment strength. *J Cell Biol* 1993 Aug;122(3):729-737.
42. Lauffenburger DA, Horwitz AF. Cell migration: a physically integrated molecular process. *Cell* 1996 Feb 9;84(3):359-369.
43. Maheshwari G, Brown G, Lauffenburger DA, Wells A, Griffith LG. Cell adhesion and motility depend on nanoscale RGD clustering. *J Cell Sci* 2000 May;113 (Pt 10):1677-1686.

44. Maheshwari G, Wells A, Griffith LG, Lauffenburger DA. Biophysical integration of effects of epidermal growth factor and fibronectin on fibroblast migration. *Biophys J* 1999 May;76(5):2814-2823.
45. Wacker BK, Alford SK, Scott EA, Das Thakur M, Longmore GD, Elbert DL. Endothelial cell migration on RGD-peptide-containing PEG hydrogels in the presence of sphingosine 1-phosphate. *Biophys J* 2008 Jan 1;94(1):273-285.
46. Cox EA, Huttenlocher A. Regulation of integrin-mediated adhesion during cell migration. *Microsc Res Tech* 1998 Dec 1;43(5):412-419.
47. Heilshorn SC, Liu JC, Tirrell DA. Cell-binding domain context affects cell behavior on engineered proteins. *Biomacromolecules* 2005 Jan-Feb;6(1):318-323.
48. Kurihara H, Nagamune T. Cell adhesion ability of artificial extracellular matrix proteins containing a long repetitive Arg-Gly-Asp sequence. *J Biosci Bioeng* 2005 Jul;100(1):82-87.
49. Cavalcanti-Adam EA, Volberg T, Micoulet A, Kessler H, Geiger B, Spatz JP. Cell spreading and focal adhesion dynamics are regulated by spacing of integrin ligands. *Biophys J* 2007 Apr 15;92(8):2964-2974.
50. Singer, II, Kazazis DM, Scott S. Scanning electron microscopy of focal contacts on the substratum attachment surface of fibroblasts adherent to fibronectin. *J Cell Sci* 1989 May;93 (Pt 1):147-154.
51. Bischoff J. Cell Adhesion and Angiogenesis. *Cell adhesion in vascular Biology: J. Clin. Invest.*, February 1997. p. 373-376.
52. Xu Y, Swerlick RA, Sepp N, Bosse D, Ades EW, Lawley TJ. Characterization of expression and modulation of cell adhesion molecules on an immortalized human dermal microvascular endothelial cell line (HMEC-1). *J Invest Dermatol* 1994 Jun;102(6):833-837.
53. Eliceiri BP, Cheresh DA. The role of alphav integrins during angiogenesis: insights into potential mechanisms of action and clinical development. *J Clin Invest* 1999 May;103(9):1227-1230.

Chapter 4

Studies on the hemocompatibility of bacterial cellulose

Abstract

Vascular grafts must gather a complex and vast number of attributes, namely good mechanical properties and an appropriate post implantation healing response. Among the strategies developed over the years to modify materials for vascular devices, pre-coating with the tripeptide Arg-Gly-Asp (RGD) improves endothelialization thus lowering thrombogenicity. In the present work, the blood compatibility of native and RGD-modified bacterial cellulose (BC) was studied. Although this is a rather promising material for vascular replacements, to our knowledge only very recently a first publication was dedicated to this subject.

The clotting times (aPTT, PT, FT and PRT) and whole blood clotting results demonstrate the good hemocompatibility of BC. A significant amount of plasma protein adsorbed to BC fibres, albumin presenting a higher BC affinity than γ -globulin or fibrinogen. According to analysis carried out by intrinsic tryptophan fluorescence, the BC adsorbed albumin, fibrinogen and γ -globulin do not undergo major conformational modifications. Although the presence of the adhesion peptide on bare-BC surface increases the platelet adhesion, when the material was cultured with human microvascular endothelial cells a confluent cell layer was readily formed, inhibiting the adhesion of platelets. As a general conclusion, both native and RGD-modified BCs may be classified as hemocompatible materials, since they showed to be non-hemolytic and the whole blood coagulation studies shows that the results are comparable to those produced by currently available materials for blood replacements.

Introduction

Biocompatibility refers to the ability of a biomaterial to perform with an appropriate host response in a specific situation [1]. It is well known that blood-contacting surfaces may activate the coagulation and complement systems, as well as trigger cellular responses [2, 3]. Thus, blood-contacting biomaterials and artificial organs, such as artificial blood vessels, pumps and artificial hearts, require improved blood compatibility for clinical uses. In addition, vascular grafts must bear both good mechanical attributes and post implantation healing responses. However, vascular substitutes currently available (e.g. Polyurethane, Dacron and ePTFE) still do not fully achieve these ideals, thrombogenicity hampering their use as small-diameter (<6 mm) arterial substitutes. Vascular graft failure is mainly caused by thrombosis/thromboembolism, infections, intimal fibrous hyperplasia and poor mechanical performance [4]. These problems arise from the fact that, after half a century of research and implant of cardiovascular devices, no material has been found to be truly blood-compatible [5].

While developing materials for blood-contacting devices, researchers have primarily focused their attention on hydrophobic polymers, such as Teflon, silicones and polyethylene, which have good mechanical properties and optimal surface lubricity for applications as catheters and shunts [6]. However, these materials have strong affinity for proteins, like fibrinogen, that adsorb on the surface, forming a monolayer that promotes platelets adhesion. These events are associated with coagulation factors activation and thrombus formation [7, 8]. Also, highly hydrophobic materials generally retard wound healing due to very slow tissue ingrowth [9].

Bacterial Cellulose (BC) is a highly hydrophilic material and according to several research groups a promising arterial substitute [10-14]. This biomaterial, produced by *Acetobacter* microorganisms, is a glucose polymer with unique properties, including high water holding capacity, high crystallinity, ultrafine fiber network, and high tensile strength [13]. Several authors addressed the potential use of BC as scaffold, for tissue engineering applications, given its harmless interaction with mammalian cells [15-18], and *in vivo* good integration with host tissues, showing no signs of chronic inflammatory or foreign body reactions [19].

The biomedical devices conceived to perform in contact with blood are often surface modified using active substances like heparin, to reduce thrombogenicity. However, the limited success of surface treatments for improved blood compatibility has encouraged researchers to pursue

other strategies. Instead of designing materials that avoid indiscriminately the problematic interaction with blood proteins and platelets, the incorporation of molecules that can stimulate the adhesion and colonization of endothelial cell (EC) has been investigated [20]. It is known that ECs covering the lumen of vessels actively inhibit thrombosis and intimal hyperplasia, also serving as anticoagulant surface [21, 22]. Therefore, the formation of an EC layer on the luminal surface of prosthetic grafts is highly desirable. The endothelialization of the graft may either be developed *ex vivo*, or post-implantation, stimulating the ECs (from tissues adjacent to anastomosis or from circulation) to adhere and proliferate on the graft. The rate and quality of a vascular graft endothelialization depends, of course, on the cell-material interaction. Several approaches have been used, attempting to increase the EC adhesion on typically non-adhesive polymeric biomaterials used for synthetic vascular grafts [23]. One such approach, that involves pre-coating the material with the tripeptide Arg-Gly-Asp (RGD), an amino acid sequence found in many adhesive plasma and extracellular matrix proteins, has been used to enhance cell adherence. Binding of cells to the RGD-sequence occurs via integrin receptors on the cell membranes. In a previous work, we described the production of recombinant proteins containing the adhesion sequences fused to a CBM (cellulose-binding module) [18] (chapter 2). For artificial grafts based on cellulose, the use of a CBM (a protein exhibiting specific high affinity for cellulose surfaces) may be a facile and smart strategy to avoid losing the biological agents coating the graft when the blood flow is restored, after implantation. In the same lines, we have also shown [24] that the presence of RGD sequences significantly increases the adhesion of human microvascular cells (HMECs) on BC (chapter 3). Thus, RGD sequence could be used to improve the endothelialization of vascular substitutes based on bacterial cellulose. However, although envisaging the graft coverage with ECs, the blood compatibility of both the bare native and RGD-modified bacterial cellulose must be also characterized.

To our knowledge, only one study conducted by Fink et al. [25] evaluated the thrombogenic properties of vascular graft tubes based on BC and compared with commercial vascular grafts of poly(ethylene terephthalate) (PET) and expanded poly(tetrafluoroethylene) (ePTFE). The results showed that the BC material did not induce plasma coagulation to any great extent and in comparison with PET and ePTFE, the BC material performed very well and was found to induce the least and slowest activation of the coagulation cascade. Further characterization is necessary, not only to confirm the promising hemocompatibility of BC, but also to better understand the BC-blood interaction, through more comprehensive characterization.

Materials and Methods

Production of bacterial cellulose

Gluconacetobacter xylinus (ATCC 53582) purchased from the American Type Culture Collection was grown in Hestrin-Schramm medium, pH 5.0. The medium was inoculated with the culture, added to the 24-well polystyrene plate (1 ml per well) and incubated statically at 30 °C, for 5 days. BC pellicles were purified by 2% sodium dodecyl sulfate (SDS) treatment at 60 °C, for 12 h, followed by 4% NaOH at 60 °C, for 90 min. Samples were autoclaved and stored in phosphate buffered solution (PBS) pH 7.4, at 4°C, prior to use. The pellicle produced in a 24-well polystyrene plate presented a diameter of 15.5mm.

Production and purification of recombinant proteins

The recombinant proteins RGD – CBM and CBM have been formerly cloned in *Escherichia coli* and its production and purification was conducted as described in our previous work [18] (chapter 2).

Surface modification with CBM and RGD-CBM proteins

The surface modification of BC was developed as previously described [18] (chapter 2). The purified recombinant proteins were added to the wells of 24-well polystyrene plates (0.25mg of protein/per well), coated with bacterial cellulose sheets produced in similar 24-well polystyrene plates. The plates were incubated overnight at 4 °C. Unbound protein was removed and the BC pellicles were washed with PBS and used in the *in vitro* blood compatibility assays.

Preparation of blood samples

Whole blood was collected from healthy donors with vacuum blood-collection tubes of 1.8ml, containing sodium citrate buffer solution 3.2% (0,109 mol/l). The citrated whole blood was immediately centrifuged for 15 min (300g, 4 °C) and the citrated platelet-rich plasma (PRP)

was collected. Citrated platelet poor plasma (PPP) was also prepared from the whole blood, by centrifugation for 15 min at 2000g, 4 °C.

Determination of the amount of adsorbed plasma proteins

Plasma protein adsorption on the membrane surface was evaluated as follows. Disk-shaped BC pellicles (1.88 cm², ~ 2.4mg), previously incubated with the recombinant proteins (RGD-CBM and CBM) or buffer, were immersed in PPP (0.5ml per pellicle) diluted (1:2) with a phosphate-buffered solution (PBS, pH 7.4), at 37 °C for 3 hours. Expanded tetrafluoroethylene (MAXIFLO™ ePTFE Vascular Prosthesis, Vascutek Ltda, Scotland) samples (1.4 cm², ~ 114 mg) were used as a control. The unbound fraction (supernatant) of plasma proteins was then collected. The total protein in the PPP and supernatants were quantified using the micro-BCA method (Pierce); the protein concentration was calibrated with bovine serum albumin solution (Applichem Biochemica, Darmstadt, Germany).

Albumin, fibrinogen and Human γ -globulin adsorption on BC

Disk-shaped BC pellicles – untreated or previously treated with the recombinant proteins and also the control materials (ePTFE – 1.4 cm² and polystyrene plate – 1.88 cm²) – were immersed in phosphate buffered solution (PBS, 0.02M, pH 7.4) of (1) 5mg/ml human serum albumin (HSA), (2) 1mg/ml Human γ -globulin (IG) or (3) 0.3mg/ml human fibrinogen (HFG), for 120 min at 37°C [26, 27]. The concentrations of the tested proteins were chosen to reflect a 10-fold dilution of their levels in blood.

In another study, to evaluate the affinity of HSA, HFG and IG for bacterial cellulose, adsorption isotherms of these proteins on BC were developed as follows: untreated BC membranes were immersed (0.5ml) in two-fold dilution series of protein solutions (with concentrations ranging from 10mg/ml to 0.078125 mg/ml) and shaken for 60 min, 37°C. After the removal of the supernatant and rinsing the membranes five times with PBS, 0.5ml of 1wt% aqueous solution of SDS was added; the samples were then shaken for 60min at room temperature, to remove the proteins adsorbed on the membranes. Both the concentration in the supernatant and the desorbed protein recovered after washing were quantified using the micro-BCA method

(Pierce). The protein concentration was calibrated with bovine serum albumin solution (Applichem Biochemica, Darmstadt, Germany). The amount of adsorbed protein on the BC membrane was calculated through the difference between the initial protein and the protein from supernatant.

Determination of conformational changes of adsorbed proteins

Intrinsic tryptophan fluorescence was used to evaluate the conformational changes of albumin, fibrinogen and γ -globulin adsorbed on bacterial cellulose. BC pellicles were immersed in phosphate buffered solution (PBS, 0.02M, pH 7.4) of (1) 1mg/ml human serum albumin (HSA), (2) 1mg/ml Human γ -globulin (IG) or 1mg/ml human fibrinogen (HFG), for 60 min at 37°C, then the pellicles were washed five times with PBS to removed unbound proteins. Fluorescence measurements were performed using a Fluorolog 3 spectrofluorimeter[®], equipped with double monochromators in both excitation and emission. Fluorescence spectra were corrected for the instrumental response of the system. Emission spectra were measured by exciting the sample at 295 nm or 270 nm and collecting the emitted fluorescence from 305 to 400 nm. Protein solutions of HSA, IG and HFG were used as controls.

Coagulation Times

BC membranes, treated either with the recombinant protein (RGD-CBM) or buffer, were incubated with 0.5ml of PPP, at 37 °C for 1h. The activated Partial Thromboplastin Time (aPTT), Prothrombin Time (PT) and Fibrinogen Time (FT) of the PPP were determined, as described below, using an automated coagulation analyser (STA-R Evolution[®], Diagnostica STAGO, France). The polystyrene plate, ePTFE, glass coverslips and glass microspheres (with 0.10mm of diameter) were used as controls. The coagulation times of PPP non-contacted with the materials were also analysed, as a control. The comparison of coagulation times (aPTT, PT and FT) of endothelialized polymers were also tested. For the description of the methods used in cell culture, please see item "Platelet adhesion to BC covered with human microvascular endothelial cells" from materials and methods.

Activated partial thromboplastin time: The aPTT is a simple and highly reliable measurement of the capacity of blood to coagulate through the intrinsic coagulation pathway and the effect of the biomaterial on possible delay of the process. After contacting the materials, 50µl of the PPP was removed and then activated by addition of 50µl of Pathromtin SL® (Siemens Healthcare Diagnostics, Marburg, Germany). This reagent contains silicon dioxide particles, plant phospholipids, sodium chloride and HEPES, pH 7.6. Then, immediately after adding calcium chloride 0.025M (50µl, 37°C), the time for initiation of clot formation was measured by using an automated coagulation analyser (STAR Evolution®, Diagnostica STAGO, France).

Prothrombin time: Prothrombin time was measured to assess BC-induced deferment, interdiction or activation of the extrinsic coagulation pathway. After contact with the materials, 50µl of the PPP was removed and then 100µl of Thromborel® S (Siemens Healthcare Diagnostics, Marburg, Germany) – a reagent containing human placental thromboplastin with calcium chloride – was added. Immediately, the time for initiation of clot formation was detected by using an automated coagulation analyser (STAR Evolution®, Diagnostica STAGO, France).

Fibrinogen time: In the presence of excess thrombin, the coagulation time of a plasma sample is inversely proportional to the fibrinogen concentration. Thus, to assess the effect of BC interaction with the fibrinogen plasma, FT was developed. After contact with the materials, 100µl of the PPP was removed and then human thrombin (STA Fibrinogen, Diagnostica Stago/Roche Diagnostics, Mannheim, Germany) was added. Immediately afterwards the time for initiation of clot formation was detected by using an automated coagulation analyser (STAR Evolution®, Diagnostica STAGO, France).

Measurement of plasma recalcification profiles

The measurement of plasma recalcification time was analyzed through the adapted method described by Motlagh et al. [28]. Blood was drawn from healthy adult volunteers into citrated tubes (as described above) and centrifuged at 2000g in order to obtain the PPP. BC samples were incubated with 0.5ml of PPP, at 37 °C for 1h. Then 100µl of citrated PPP were transferred to the wells of a 96-well plate. Controls consisted of polystyrene plate (exposed to

PPP with and without CaCl_2), ePTFE and glass microspheres. Following the addition of PPP, 100ml of 0.025M CaCl_2 was added to each well (except the negative control with no Ca^{+2}). The plate was then immediately placed in a 96-well plate reader, where the kinetics of the clotting process due to recalcification were monitored by measuring the absorbance at 405nm (every 30 s for 30 min) at 37 °C. In calculating the mean absorbance at each time point, tested samples treated with PPP from 5 different donors were averaged per sample. The clotting time to reach half maximal absorbance was calculated and analyzed.

Quantification of whole blood clotting time

The thrombogenicity of BC was evaluated using a whole blood kinetic clotting time method, as previously described [28]. Samples of the tested materials were used per time point. Briefly, the clotting reaction was activated with the addition of 850 μl CaCl_2 (0.1M) to the 8.5 ml sample of citrated blood. A 100 μl volume of the activated blood was carefully added to BC lyophilized samples, which were placed in the wells of a 12-well plate. Glass microspheres, ePTFE and polystyrene were used as controls. All samples were incubated at room temperature for 0, 5, 15, 25 and 35. At the end of each time point, the samples were incubated with 2.5ml of distilled water for 5 min. Each well was sampled in triplicate (200 μl each) and transferred to a 96-well plate. The red blood cells that were not trapped in a thrombus were lysed with the addition of distilled water, thereby releasing hemoglobin into the water for subsequent measurement. The concentration of hemoglobin in solution was assessed by measuring the absorbance at 540nm using a 96 well plate reader. The size of the clot is inversely proportional to the absorbance value.

Evaluation of Platelet Adhesion

Bare-BC membranes, treated with the recombinant proteins or buffer, were placed in contact with 0.5ml of human PRP and incubated for 2h. Then, the supernatant was removed and the BC pellicles washed twice with PBS. Next, 0.7ml of 2.5% glutaraldehyde in PBS was poured into each well, and the materials were maintained at room temperature for 1h, in order to fix the blood components on the membrane. Afterwards, the membranes were rinsed with

distilled water, and finally dehydrated by successive immersion in a series of ethanol-water solutions (55, 70, 80, 90, 95, 100% v/v), for 30 min each, and allowed to evaporate at room temperature. The surface of the membranes with adsorbed platelets was observed with scanning electron microscopy (LEICA S 360), after gold-sputtering treatment.

In a parallel assay, the number of platelets adhered on the bare-BC membranes was determined by the lactic acid dehydrogenase (LDH) activity method [29]. The PRP (0.4 ml) was placed in contact with BC membranes, in the 24-wells, and allowed to stand for 90 min at 37 °C. The samples were washed twice. In order to release the intracellular LDH, adhered platelets were lysed with 0.3ml of Triton X-100 (0.1%) for 45min, at 37 °C. Then, the supernatant was used to determine the LDH activity as follows: The supernatant (0.050ml) was added to a tube containing 1.5 ml of solution I (50mM phosphate, 0.63 mM piruvate (Sigma), pH 7.5) and 0.025ml of solution II (11.3mM β -NADH (Sigma), 119 mM sodium bicarbonate), and homogenised. Recording of the enzymatic reaction kinetics started promptly, reading the absorbance at 340nm (Jasco V-550) for 120s, at 25 °C. The initial reaction rate was determined as the slope of the graph obtained plotting the optical density vs reaction time, at time zero. The LDH calibration curve was obtained by measuring the enzymatic activity of a set of samples with a known concentration of platelets, under the same conditions as above. The ePTFE was used as a reference material.

Platelet adhesion to BC covered with human microvascular endothelial cells

Cell culture: Human Microvascular Endothelial Cells (HMECs) were cultured in RPMI 1640 medium (Invitrogen Life Technologies, UK) supplemented with 10% FBS (Invitrogen Life Technologies, UK), 1% penicillin/streptomycin (Invitrogen Life technologies, UK), 1.176 g/L of sodium bicarbonate, 4.76 g/L of Hepes, 1mL/L of EGF and 1 mg/L of hydrocortisone > 98% (Sigma, Portugal), and maintained at 37 °C in a humidified 5% CO₂ atmosphere.

As previously described [24] (chapter 3), the HMEC-1 cells were seeded on the BC and ePTFE (control) at a density of 12×10^4 cells/well, in RPMI medium without serum. The plates were incubated at 37 °C, in atmosphere of 5% CO₂ and 95% humidified air. Two hours after the addition of the cells, the wells were washed with PBS and RPMI with 10% Foetal Bovine Serum (FBS) was added. The cells were allowed to grow on BC for 14 days.

Platelet adhesion: 0.5ml of human PRP was loaded on the HMECs proliferated on BC and ePTFE, and incubated for 2h at 37 °C in a humidified 5% CO₂ atmosphere. Then, the supernatant was removed and the BC pellicles washed twice with PBS. Next, 0.7ml of 2.5% glutaraldehyde in PBS was poured into each well, and the materials were maintained at room temperature for 1h, in order to fix the blood components on the membrane. Afterwards, the membranes were rinsed with distilled water, and finally dehydrated at 30 °C. The surface of the membranes with adsorbed platelets was observed with scanning electron microscopy (Nova NanoSEM 200, The Netherlands), after gold-sputtering treatment. By counting the number of adhered platelets on the sample surfaces, the platelet adhesion densities were determined for each kind of sample. On each sample, five different areas (19x10³ μm²) were selected [30]. The bare polymers (BC and ePTFE) that were incubated with RPMI with 10% Foetal Bovine Serum for 14 days were used as controls.

Hemolysis

Hemolysis studies were conducted according to the procedures described in *American Society for Testing and Materials* (ASTM F756-00, 2000). BC samples with 1.88 cm² were equilibrated in PBS (Ca and Mg free), and then transferred to a tube containing 7 ml of PBS (Ca and Mg free). Then, 1 ml of diluted blood (hemoglobin concentration of 10mg/ml) was added. The material was maintained in contact with the blood for 3h, at 37 °C, in a water bath. The tubes were gently inverted twice every 30 min to promote the BC-blood contact. Afterwards, the membranes were removed and the diluted blood centrifuged at 750g, 15 min. The hemoglobin was determined adding 1 ml of the supernatant to 1 ml of Drabkin 's reagent (Sigma); after 15 min, the absorbance at a wavelength of 540nm was read (Jasco V-550). The hemoglobin concentration (HC) was determined using a calibration curve prepared with human hemoglobin (Sigma) and was calculated by the equation: $HC = A \times F \times d$ (A, Absorbance; F, Slope of the hemoglobin curve; d, dilution). The hemolytic index (HI) was obtained by the equation $HI = 100 \times (\text{concentration of hemoglobin released in supernatant}) / (\text{total hemoglobin concentration in tube})$. As reference materials, ePTFE and PBS (negative control) and ultra pure water (positive control) were used.

Results and Discussion

Protein adsorption

It is well known that protein adsorption and denaturation are responsible for triggering hemostasis and specifically the contact pathway, upon blood-biomaterial contact. While albumin is considered non-thrombogenic, other plasma proteins are. Hence, in this section, the BC affinity and surface denaturation of the three more abundant plasma proteins was analysed. The total plasma protein adsorption was measured after incubation of the BC pellicles in diluted plasma for 3 hours. The results obtained showed that the amount of protein adsorbed on BC surface is not influenced by the treatment with recombinant proteins (CBM or RGD-CBM) and also that BC membranes adsorbed approximately 1.7 – 1.8 mg of protein per mg of BC, while only 0.01 mg of protein adsorbed per mg of ePTFE, the reference material (FIGURE 1a). It is well known that the protein adsorption is significantly influenced by surface characteristics, such as hydrophilicity, topography, charge, or chemistry [8]. The gelatinous BC membrane formed in static culture is characterized by a 3D ultrafine fibrous network structure, containing about 99% water [13]; it is, thus, a highly hydrophilic material. Proteins adsorb preferentially on hydrophobic than hydrophilic surfaces, once more energy is necessary to remove the water molecules from hydrophilic than from hydrophobic surfaces. The adhesion forces on hydrophobic substrates have been shown to be dependent on the structural rigidity of the protein, while on the hydrophilic substrates both the protein and surface charge are more important [31]. Therefore, it has been reported that polymers with a hydrophilic surface adsorb low amounts of serum proteins, having low thrombogenic potential [8, 32]; however, the large surface area of the nanofibrous network of BC allows the binding of a large quantity of protein. However, the amount of plasma protein adsorbed on a surface is by itself not enough to draw conclusions regarding the blood compatibility, its identity and conformation (which may change over time following adsorption) being also important [33]. When a material comes in contact with blood, immediately proteins adsorb to the material surface. These initially adsorbed proteins may be displaced by a series of others, all within a few minutes. At least two or three of these proteins, namely fibrinogen, fibronectin and immunoglobulins, plays an important role when adsorbed, since platelets or leukocytes will adhere to these proteins through specific receptors [34].

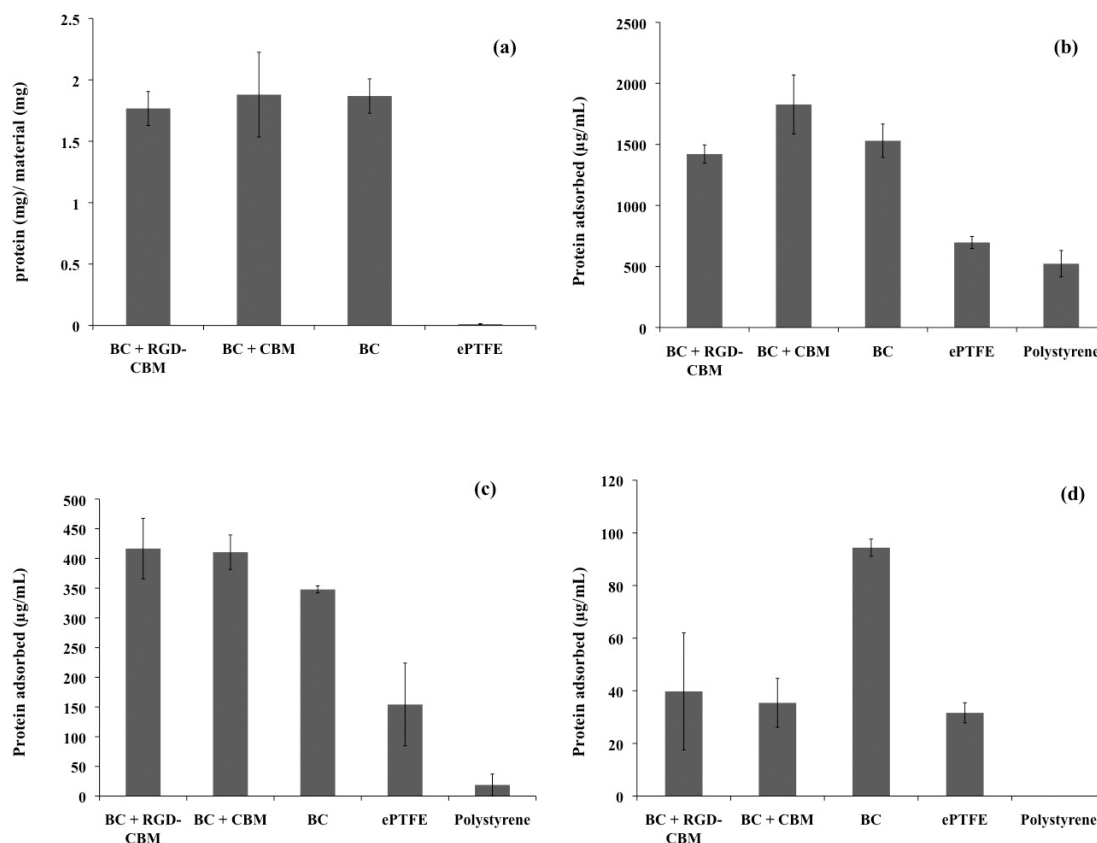


Figure 1: Plasma protein adsorption onto the bacterial cellulose membrane untreated or treated with the recombinant proteins (RGD-CBM or CBM) and controls (ePTFE and polystyrene). (a) Platelet-poor plasma; (b) human serum albumin; (c) human γ -globulin and (d) human fibrinogen.

Platelets adhesion follows, mediated by the proteins initially adsorbed on the surface. Therefore, in the present work, the BC affinity for plasma proteins human albumin, fibrinogen and immunoglobulin, corresponding respectively to 60, 4% and 20% of the total plasma protein was analysed, attempting to better understand the nature of the platelet adhesion on BC surfaces, since it is known that plasma protein adsorption is a key phenomenon in determining the thrombogenicity of the materials. In a first experiment BC membranes were immersed in pure solutions of HSA, HFG or IG - the concentrations of the tested proteins were chosen to reflect a 10-fold dilution of their levels in blood. The results obtained show that the presence of recombinant proteins (CBM and RGD-CBM) decreased the adsorption of fibrinogen on BC, an effect not observed in the case of albumin and immunoglobulin (FIGURE 1b-d). We believe that the recombinant proteins on the BC surface interfere more significantly in the case of fibrinogen because its concentration (0.3mg/ml) was lower than that of albumin (5mg/ml) and

γ -globulin (1mg/ml). The lower concentration explains also why a different amount of adsorbed protein is not observed when using the PPP (FIGURE 1a).

The adsorption isotherms (FIGURE 2) shows that, for the same concentration, the amount of adsorbed HSA, HFG and IG on BC-untreated are similar; however, when the membranes were treated with 1wt% aqueous solution of SDS, a higher amount of fibrinogen desorbed from the BC than albumin or immunoglobulin was observed (FIGURE 3). This result showed that the BC affinity of the tested proteins follows the order albumin > γ -globulin > fibrinogen. These are interestingly results since, fibrinogen, fibronectin and γ -globulin pre-coating, even at low levels, causes an increase of platelet adhesion. The opposite effect has been described for surfaces coated with albumin [34, 35].

Determination of conformational changes of adsorbed proteins

Conformational changes always occur, following unfolding, to different extent depending on the protein, exposing previously hidden amino acid sequences. This remodeling of the protein surface can trigger the activation of processes such as the blood coagulation cascade.

The intrinsic fluorescence of tryptophan, tyrosine and to a lesser extent phenylalanine is a sensitive probe of conformational changes because the intensity and Stokes' shift of the fluorescence depends on local environment of the fluorophore [36]. The unfolding of human serum proteins albumin, fibrinogen and γ - globulin were studied by measuring the intrinsic fluorescence intensity at a wavelength of excitation corresponding to tryptophan's or tyrosine's fluorescence. For an excitation of 295 nm tryptophan is the only aromatic amino acid to absorb light. For an excitation of 274 nm there is a transfer of energy from the excited tyrosine to tryptophan, which also corresponds to a single emission peak [37, 38].

Figure 4 shows the fluorescence spectra at excitation wavelengths of 295 and 270 nm. Irrespective of the protein analyzed or the excitation wavelength used, the proteins adsorbed on BC exhibit no conformational changes, taking as reference the protein in solution. These results are a promising prospect regarding BC as vascular implants. Once proteins cover the surface of implants, host cells no longer contact the underlying foreign-body material but only the protein-coated surface.

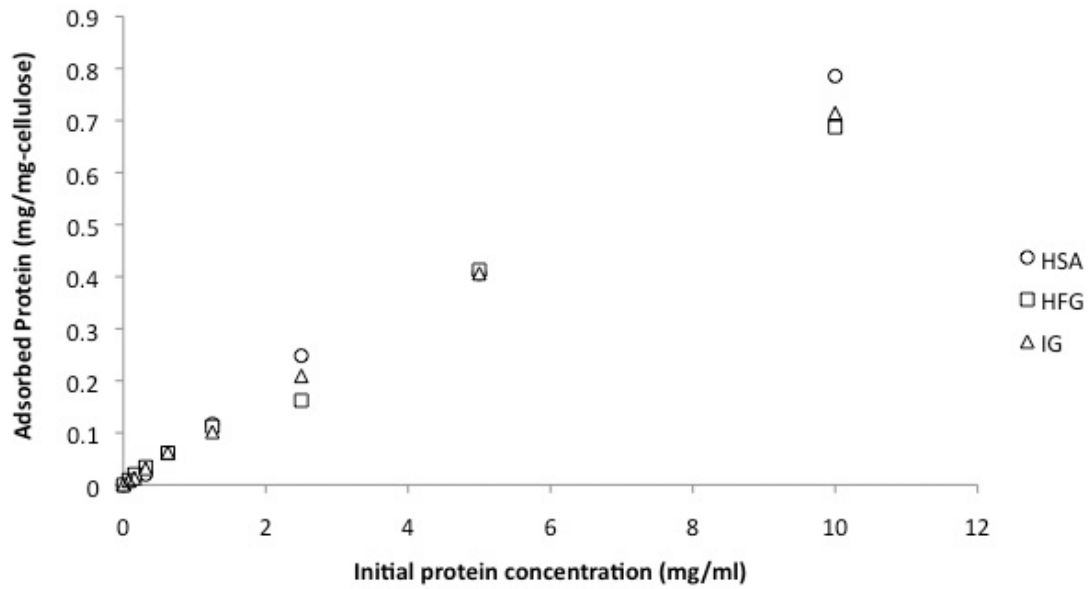


Figure 2: Comparison of the adsorption isotherms for the binding human serum albumin (HSA), human fibrinogen (HFG) and human γ -globulin (IG) on BC.

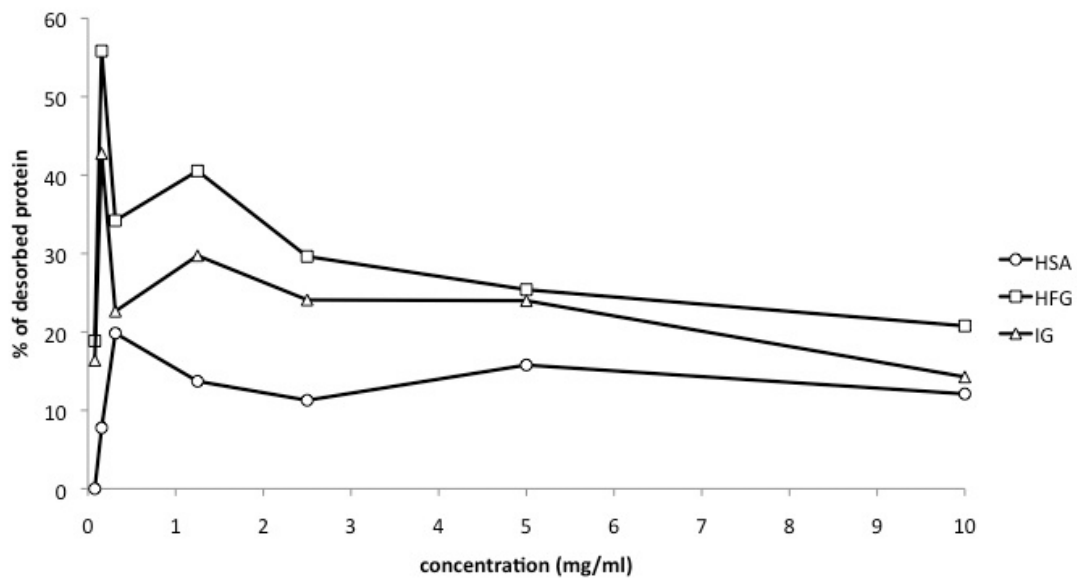


Figure 3: Percentage of desorbed proteins on BC at each concentration tested after treatment with 1wt% aqueous solution of SDS. Human serum albumin (HSA), human fibrinogen (HFG) and human γ -globulin (IG).

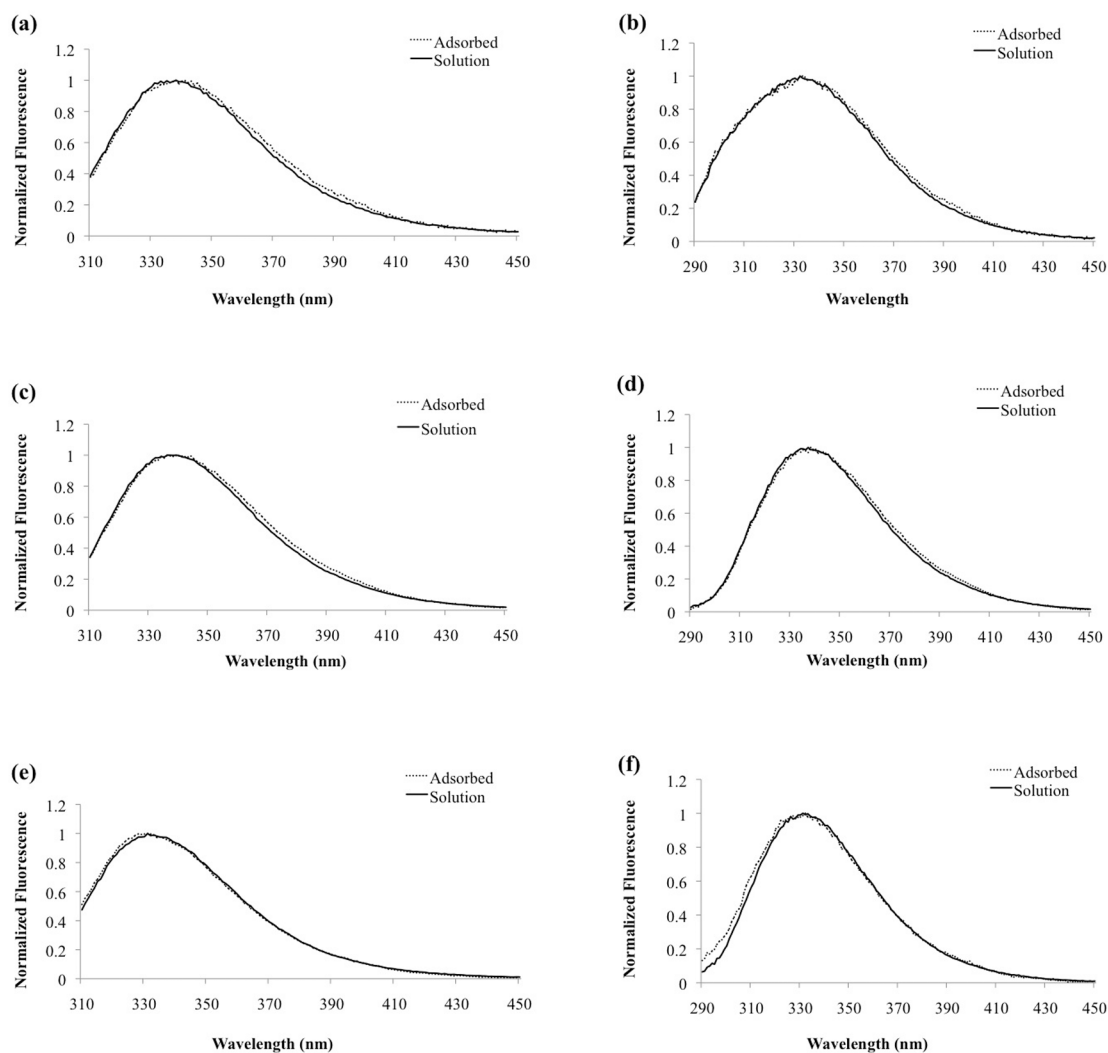


Figure 4: Steady-state fluorescence emission spectra of (a, b) human serum albumin, (c, d) human fibrinogen and (e, f) human γ -globulin adsorbed on BC and in solution. (a, c, e) and (b, d, f) excitation wavelength of 295 nm and 270, respectively, collected from 305 to 400 nm.

The adsorbed protein layers rather than the foreign material itself may stimulate or inhibit further biochemical processes. Platelet adhesion and activation is strongly influenced not only by the adhesion but especially by the conformation change, namely of the adsorbed fibrinogen. The dissolved, native fibrinogen, does not bind to the adhesion receptors of platelets unless these are appropriately stimulated. When the fibrinogen adsorbed to a surface and a conformational change occur some amino acids previously hidden inside the molecule becomes exposed and able to interact with the platelet receptors [31, 36, 39, 40]. Also, it is well known that platelet adhesion and spreading do not occur on an albumin-coated surface, and that with increasing degree of albumin denaturation, platelet adhesion and activation are

enhanced [40]. Although a highly hydrophilic material, BC adsorbs a large amount of plasma protein due to the large surface area; however, these proteins remain their native conformation once adsorbed, hence are not expected to become a factor of adhesion and activation of platelets.

Blood coagulation

The coagulation cascade consists of three pathways: contact activation (intrinsic), tissue factor (extrinsic), and the final common pathway of factor X, thrombin and fibrin. Although they are initiated by distinct mechanisms, the two converge on a common pathway that leads to clot formation. The formation of a thrombus or a clot in response to an abnormal vessel wall in the absence of tissue injury is the result of the intrinsic pathway. Fibrin clot formation in response to tissue injury is the result of the extrinsic pathway [41]. When biomaterials are in contact with blood, plasma proteins are instantaneously adsorbed onto the surface and coagulation factors or platelets will then be activated, starting a series of cascade reactions and leading to blood coagulation [42]. Interference with the coagulation cascade can be indicated by alterations of a series of plasma coagulation assays: aPTT, PT and FT. APTT and PT are used to examine mainly the intrinsic and extrinsic pathway, respectively. FT measures how much fibrinogen converts into fibrin clot, by action of thrombin [43]. The results showed that the BC polymer, irrespective of the presence of RGD peptide covering the surface, presented similar plasma clotting times (FT, aPTT and PT) comparable to the ones obtained for the negative controls (plasma incubated in the absence of tested materials or with polystyrene) (FIGURE 5). In fact, none of the tested materials were able to alter the fibrinogen or extrinsic factors content (or even activate the extrinsic factors) present in PPP, as no differences were detected in FT and PT, respectively.

To study the blood compatibility of a material, important information can be obtained through the evaluation of its effect on the intrinsic (contact) coagulation pathway. In the intrinsic pathway, activation of factor XII occurs when blood comes into contact with a surface containing negative charges (eg, the wall of a glass tube). This process is called "contact activation" and still requires the presence of other plasma components: pre-kallikrein (a serine

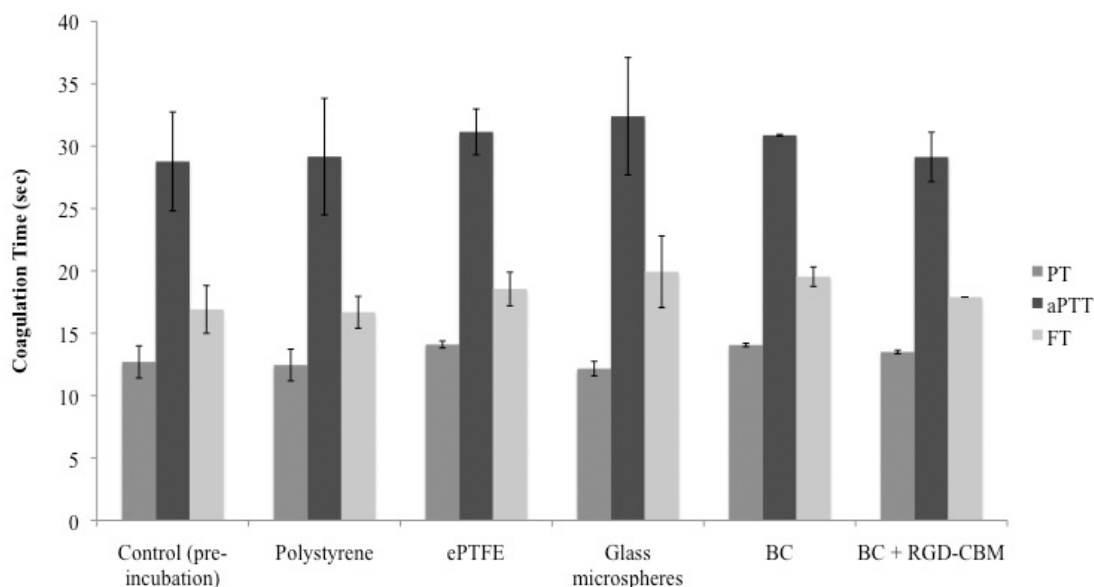


Figure 5: Comparison of anticoagulation time (aPTT, PT and FT) of BC membranes untreated or treated with the recombinant protein (RGD-CBM) and the controls (ePTFE, polystyrene and glass microspheres). The coagulation times of PPP non-contacted with the materials (pre-incubation control) were also analysed.

protease) and high molecular weight kininogen (a non-enzymatic cofactor) [44]. Several authors used the aPTT test to evaluate the blood compatibility of materials [45-48]. In this test an aliquot of platelet-poor plasma is incubated with a factor XII activator (i.e., silica, celite, kaolin, micronized silica, ellagic acid, etc.), a reagent containing phospholipid (partial thromboplastin) and CaCl_2 . Although aPTT is appropriated to detect antithrombogenic activity such as in materials with heparinised surfaces [48, 49], this method should not be used when aiming to detect the activation of the contact pathway (as often shown in the literature). Indeed, the effect of the material can be masked by the reagent used for the test, which already contains an activating substance, as described above. This effect explains the similar aPTT results for the all tested materials described in the present work.

The coagulation assays (FT, PT and aPTT) were also carried out using the endothelialized materials and no significant differences in the coagulation time values were observed between the tested materials (data not shown). Similar results were obtained by Liu et al. [46], when comparing the bare and endothelialized poly(D,L-lactide-*co-beta*-malic acid) (PLMA) polymer modified with the GRGDS sequence. Also, this may indicate that the cells seeded on polymers showed a balance of procoagulant and anticoagulant activities, which would not be displaced to either side without certain stimuli, as is the case for ECs in their normal state [46].

For the evaluation of the BC blood compatibility, specifically to ascertain whether the activation of the contact pathway occurs, the plasma recalcification time (PRT) and whole blood clotting time tests were carried out. Plasma recalcification profiles serve as a measure of the intrinsic coagulation system [28, 34]. The absorbance increases as the plasma becomes more turbid, correlating with the formation of a clot. A rightward shift of the curve indicates a slower clotting time; whereas, a leftward shift of the curve indicates a faster one. Citrated platelet poor plasma (without the addition of CaCl_2) serves as a negative control, as it should not form a clot. In the kinetic profiles the plasma incubated with glass microspheres produced the more leftward curve while the ePTFE produced the more rightward curve, and the others materials tested presented kinetics profiles between these two controls (FIGURE 6a). The plasma incubated with BC treated with RGD-CBM and untreated BC presented similar curves (data not showed). The clotting time to reach half-maximal absorbance (half-max time) was measured for each surface (FIGURE 6b). The half-max time for glass microsphere (2.826 ± 0.13 min) was significantly lower than that for BC (3.92 ± 0.161 min) or BC treated with RGD-CBM (3.725 ± 0.202 min, data not showed), followed by polystyrene (5.896 ± 0.154 min), lyophilized BC (5.908 ± 0.141 min) and ePTFE (6.725 ± 0.117 min). Taken together, the shift of the kinetic profile (Fig. 6a) and the half-maximal absorbance clotting time (Fig. 6b) results, the order of the lower to higher coagulative materials is glass microspheres < untreated and RGD-CBM treated BC < polystyrene and lyophilized BC < ePTFE. We believe that the difference between the hydrated BC and the lyophilized BC is due to reduction of the porosity, and consequently of the surface area, of the cellulose after the lyophilization process [13].

Whole blood was used to assess clotting times. In this assay, higher absorbance values correlate with improved thromboresistance of the material. The results showed that, after 15 min of calcium addition, the percentage of blood coagulation was 87, 57, 9.3 and 8.6% for glass microspheres, lyophilized BC, ePTFE and polystyrene, respectively. At each time point measured, blood incubated with glass had a significantly higher coagulation percentage, while the polystyrene presented the lower values. In general, the BC presented a clotting time higher than the glass microsphere and lower than the ePTFE and polystyrene (FIGURE 7). Although lyophilized BC induces a faster blood coagulation than ePTFE, this may be the result of the larger surface area, a parameter quite difficult to control in these experiments, which directly influence the blood-material interaction.

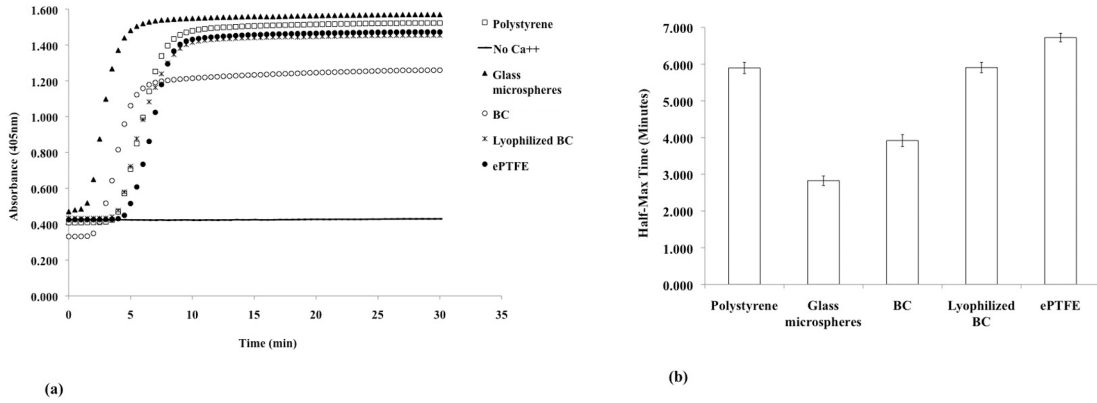


Figure 6: Clotting kinetic profiles of the absorbance at 405nm as a function of time for PPP incubated with polystyrene, BC (hydrated and lyophilized), glass microspheres and ePTFE (a). Citrated PPP (without the addition of calcium) serves as a negative control. The data was averaged over five independent experiments. The half-max time of each profile (b) was calculated as a measure of the clotting time.

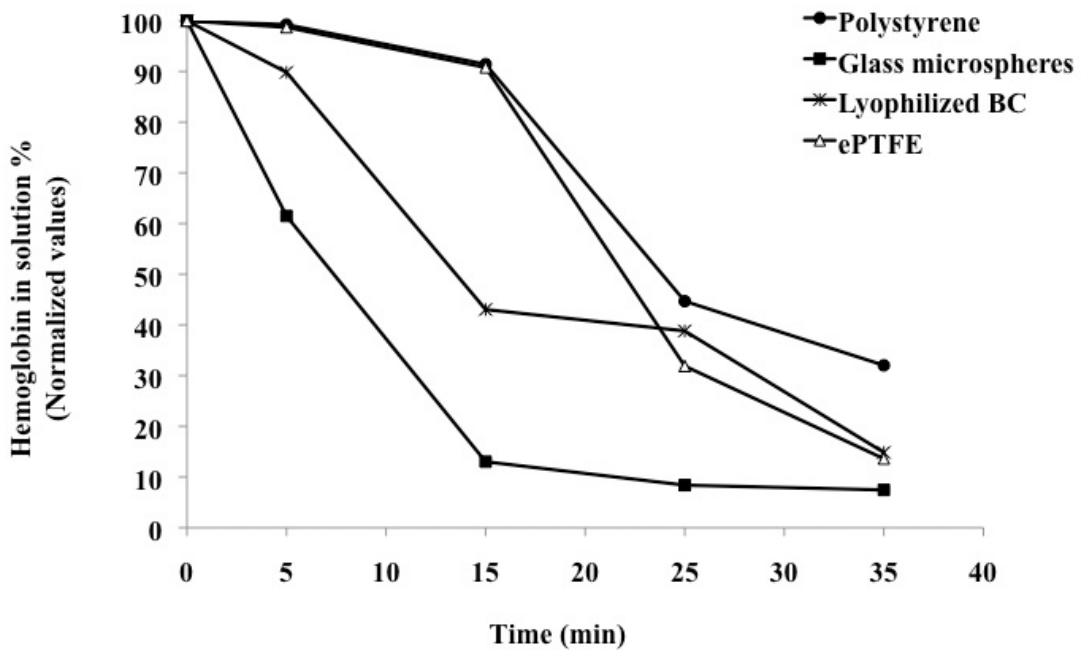


Figure 7: The effect of BC, ePTFE, polystyrene and glass microspheres on thrombus formation in whole blood at 0, 5, 15, 25 and 35 min.

Platelet adhesion

When blood contacts a foreign material, such as artificial vessel, catheter or a hemodialyzer, plasma proteins readily adsorb onto the material surfaces. Stimulation of adhesion of platelets, white blood cells and some red blood cells onto the plasma protein layer may follow. After adhesion and aggregation, platelets release materials such as ADP and ATP, thereby inducing more platelet aggregation on the surface. Finally, a non-soluble fibrin network or thrombus is formed [47]. Thus, platelet adhesion on BC is an important test for the evaluation of blood compatibility. Figure 8 shows the relative number of platelet adhered to the ePTFE and BC surfaces. The lactic acid dehydrogenase (LDH) activity method [29] was used for platelet quantification. The untreated and the CBM-treated BC adsorbed approximately 15% and 16%, respectively, of the platelets added to the pellicle during the assay, while the reference material (ePTFE) adsorbed only 6%. However, when BC was pre-treated with RGD-CBM, the amount of platelets adhered increased to 34%.

The adhesion of platelets to BC may be driven by the adsorption of plasma protein and clearly, the RGD peptide increases the platelets adhesion by two-fold. Thus, the results demonstrate that the RGD was able to recognize the platelet integrin $\alpha_{IIb}\beta_3$, leading to platelet adhesion, which is in agreement with results previously reported by Hansson et al. [50].

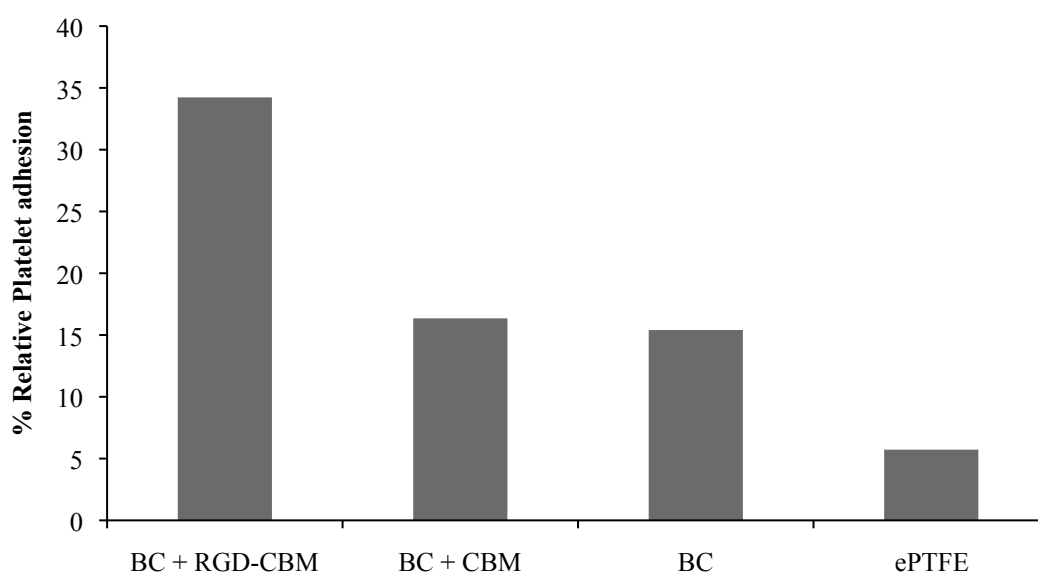


Figure 8: Relative number of platelets adhered on ePTFE and BC membrane untreated or treated with the recombinant proteins (RGD-CBM or CBM).

Figure 9 shows SEM images of the platelets adhered to the materials tested. As can be seen, these results are in agreement with the LDH assay (FIGURE 8). The platelets adhered to ePTFE present pseudopodia, indicating that they might have been activated. In the case of BC, it is difficult to identify elongations of the adhered platelets, due to the fibrous structure of the material.

The platelet adhesion on endothelialized polymer was also studied. As demonstrated in our previous work [24] (chapter 3) after 14 days, only the BC treated with RGD-CBM was able to form a confluent endothelial cell layer when compared with the untreated or CBM-treated BC. The SEM images from figure 10 shows that the presence of an endothelial layer on the RGD-treated BC significantly decreases the platelet adhesion, when compared with bare-BC. Once HMECs were not able to form a confluent layer on untreated or CBM-treated BC, platelets were still able to adhere to the gaps between the cells. Few platelets adhered to ePTFE, and also HMEC cells attached and proliferated poorly on this material. The densities of adhered platelets on endothelialized polymers are shown in figure 11 and as can be seen the number of platelets on RGD-treated BC reached similar values to the reference material. Although the presence of RGD increased the platelet adhesion on bare-BC, it may be used to cover the BC grafts with ECs before implantation. This strategy has been successfully reached by other authors [30, 46] that observed fewer platelets adhering to surfaces covered with endothelial cells. ECs are antithrombogenic, the glycocalyx preventing platelets from adhering; production of nitric oxide and prostacyclin also inhibit platelet adhesion, aggregation and cause blood vessel dilatation. In addition, endothelium also displays ectonucleotidases at its luminal surface. These enzymes hydrolyze ATP and ADP, both potent platelet aggregating agents, into AMP and adenosine [51, 52].

Hemolysis

The results of hemolysis quantification over incubation of blood with BC membranes and ePTFE are shown in table 1. As negative and positive controls, blood was incubated in an isotonic solution (PBS buffer) and ultra pure water, respectively. It may be observed that hemolysis occur in less than 2% of the red cells, thus BC is classified as a nonhemolytic material, since, according to the *American Society for Testing and Materials* (ASTM F756-00, 2000), a material may be classified as nonhemolytic (0-2% of hemolysis), slightly haemolytic (2-5% of hemolysis) and haemolytic (>5% of hemolysis). However, the evaluation of the

haemolytic character for materials are subject to consideration of the nature of tissue contact, duration of contact, and surface area to body ratios, and the nature of device.

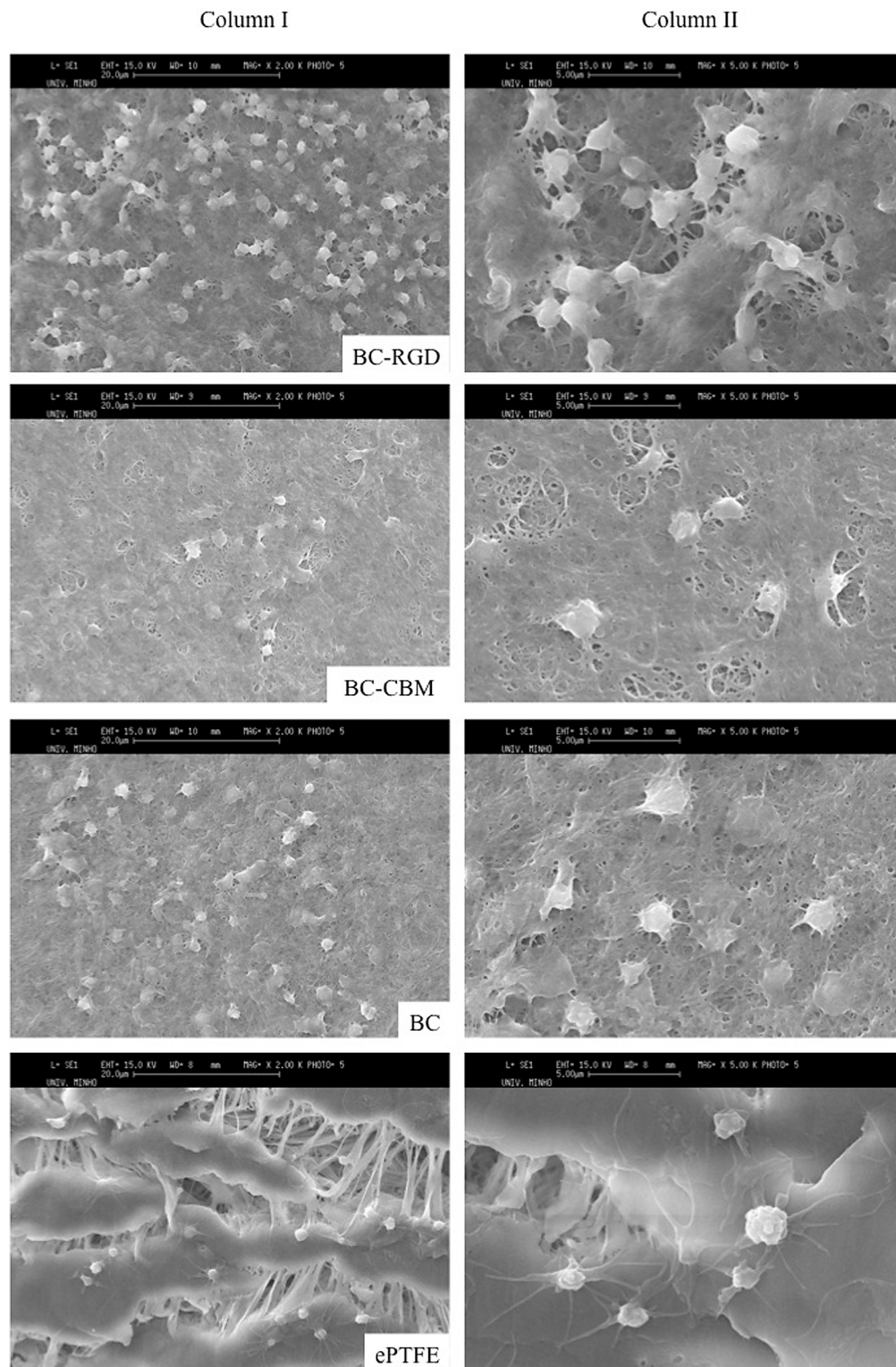


Figure 9: SEM images of BC membrane and ePTFE surface after contact with PRP for 2 hours. Column II (scale bar 5µm) is the magnified images of Column I (scale bar 20µm).

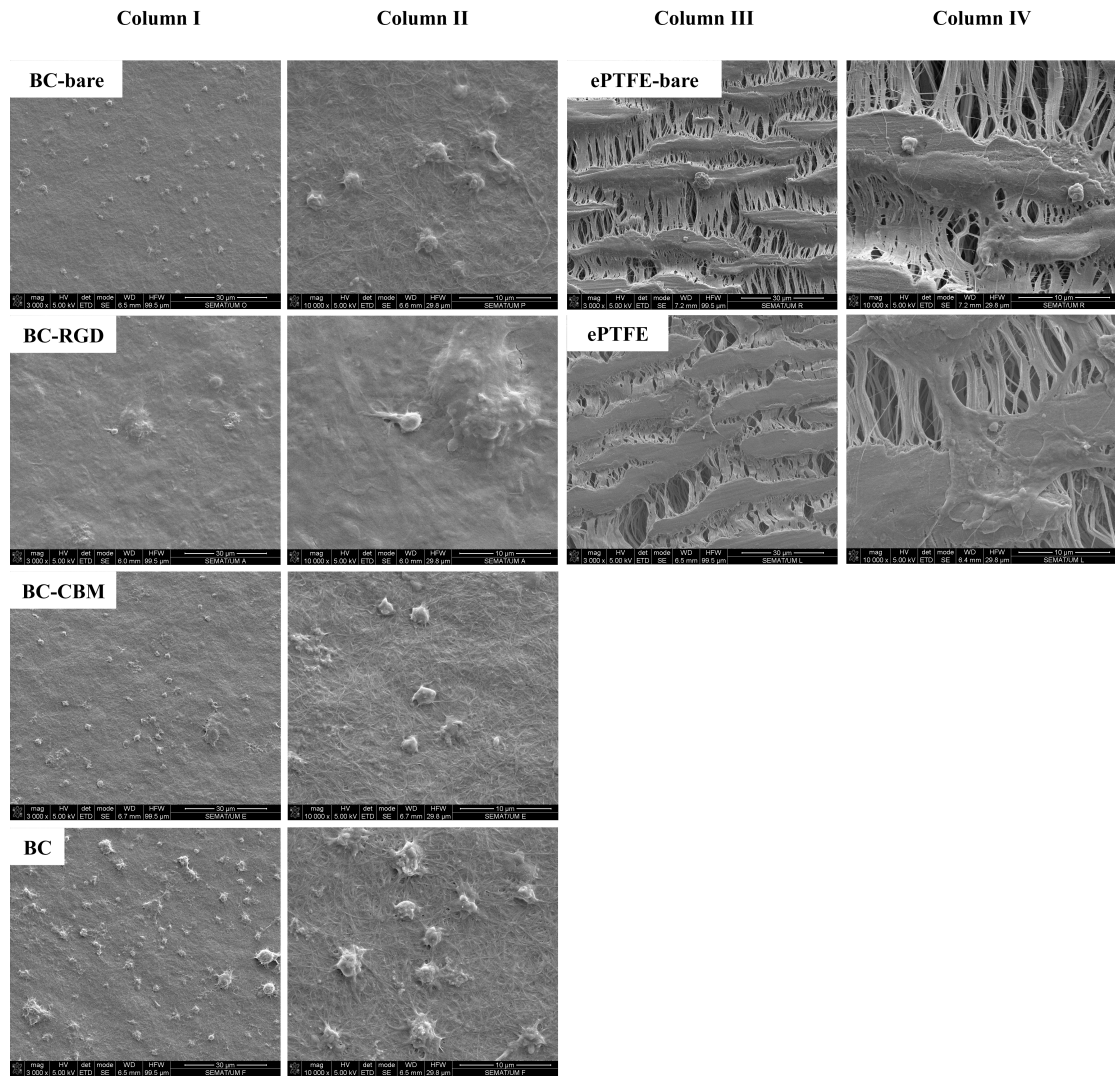


Figure 10: SEM images of the adhered platelets on endothelialized BC untreated or treated with recombinant proteins and ePTFE. The bare BC and ePTFE were used as controls. The captions without “bare” indicate the cultured HMEC surface. Column II and IV (scale bar 10 μ m) is the magnified images of Column I and II (scale bar 30 μ m), respectively.

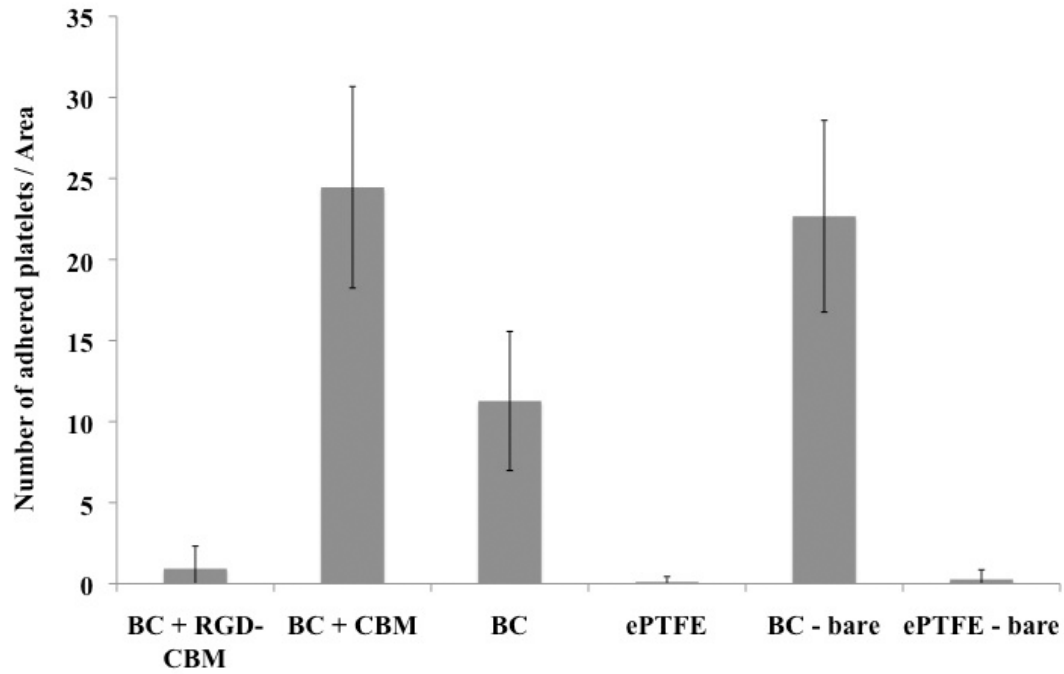


Figure 11: Densities of adhered platelets on endothelialized BC untreated or treated with recombinant proteins and ePTFE. The bare BC and ePTFE were used as controls.

Table 1: Hemolysis of blood after contact with BC surfaces and ePTFE.

Sample	Hemolytic index (%)
Ultra pure water	99.3
PBS buffer	1.43
BC + RGD-CBM	1.63
BC + CBM	1.42
BC	1.43
ePTFE	1.85

Conclusions

The blood compatibility of BC has not been systematically investigated. In this report, the adhesion of plasma protein and platelets and blood coagulation on bare and endothelialized BC surfaces was studied. The results showed that BC presents good hemocompatibility, the blood coagulation studies shows that the results are comparable to those produced by currently available materials for blood replacements and that the adsorption of total plasma protein was not influenced by the presence of recombinant proteins bearing the peptide RGD, although decreasing the adhesion of fibrinogen on pure solutions. Besides adsorption isotherm studies showed that BC presented a higher affinity for albumin than immunoglobulin or fibrinogen. Results also showed that the presence of RGD on BC polymer increased platelet adhesion, however when endothelial cells were cultured on RGD-treated BC, a confluent cell layer was formed and almost no platelets adhered to the material, thus the improvement of BC blood-compatibility through modification with adhesion peptides seems to be an interesting strategy in cases where cellulose grafts were previous covered with endothelial cells.

References

1. Williams DF. Definitions in Biomaterials. In: Williams DF, editor. Proceedings of a Consensus Conference of the Europeans Society For Biomaterials March 3-5, 1986; Chester, England: Elsevier, 1987.
2. Vroman L. The importance of surfaces in contact phase reactions. *Semin Thromb Hemost* 1987 Jan;13(1):79-85.
3. Colman RW, Schmaier AH. Contact system: a vascular biology modulator with anticoagulant, profibrinolytic, antiadhesive, and proinflammatory attributes. *Blood* 1997 Nov 15;90(10):3819-3843.
4. Padera RF, Schoen FJ. Cardiovascular Medical Devices. In: Ratner BD, Hoffman AS, Schoen FJ, Lemons JE, editors. *Biomaterials Science*. San Diego, CA: Elsevier, Academic Press, 2004. p. 470-494.
5. Ratner BD. The catastrophe revisited: blood compatibility in the 21st Century. *Biomaterials* 2007 Dec;28(34):5144-5147.
6. Postaire E. *Les matières plastiques à usage pharmaceutique: Médicales Internationales*, 1991.
7. Tsai WB, Grunkemeier JM, Horbett TA. Human plasma fibrinogen adsorption and platelet adhesion to polystyrene. *Journal of Biomedical Materials Research* 1999 Feb;44(2):130-139.
8. Hoffman AS. Blood Biomaterial Interactions - an Overview. *Advances in Chemistry Series* 1982(199):3-8.
9. Njatawidjaja E, Kodama M, Matsuzaki K, Yasuda K, Matsuda T, Kogoma M. Hydrophilic modification of expanded polytetrafluoroethylene (ePTFE) by atmospheric pressure glow discharge (APG) treatment. *Surface & Coatings Technology* 2006 Oct 5;201(3-4):699-706.
10. Backdahl H, Helenius G, Bodin A, Nannmark U, Johansson BR, Risberg B, et al. Mechanical properties of bacterial cellulose and interactions with smooth muscle cells. *Biomaterials* 2006 Mar;27(9):2141-2149.
11. Backdahl H, Esguerra M, Delbro D, Risberg B, Gatenholm P. Engineering microporosity in bacterial cellulose scaffolds. *J Tissue Eng Regen Med* 2008 Aug;2(6):320-330.
12. Negrão SW, Bueno RRL, Guérios EE, Ultramari FT, Faidiga AM, de Andrade PMP, et al. A eficácia do stent recoberto com celulose biosintética comparado ao stent convencional em angioplastia em coelhos. *Revista Brasileira de Cardiologia Invasiva* 2006;14(1):10-19.
13. Klemm D, Schumann D, Udhardt U, Marsch S. Bacterial synthesized cellulose - artificial blood vessels for microsurgery. *Progress in Polymer Science* 2001 Nov;26(9):1561-1603.

14. Wippermann J, Schumann D, Klemm D, Kosmehl H, Salehi-Gelani S, Wahlers T. Preliminary results of small arterial substitute performed with a new cylindrical biomaterial composed of bacterial cellulose. *Eur J Vasc Endovasc Surg* 2009 May;37(5):592-596.
15. Watanabe K, Eto Y, Takano S, Nakamori S, Shibai H, Yamanaka S. A new bacterial cellulose substrate for mammalian cell culture. A new bacterial cellulose substrate. *Cytotechnology* 1993;13(2):107-114.
16. Svensson A, Nicklasson E, Harrah T, Panilaitis B, Kaplan DL, Brittberg M, et al. Bacterial cellulose as a potential scaffold for tissue engineering of cartilage. *Biomaterials* 2005 Feb;26(4):419-431.
17. Sanchavanakit N, Sangrungraungroj W, Kaomongkolgit R, Banaprasert T, Pavasant P, Phisalaphong M. Growth of human keratinocytes and fibroblasts on bacterial cellulose film. *Biotechnol Prog* 2006 Jul-Aug;22(4):1194-1199.
18. Andrade FK, Moreira SM, Domingues L, Gama FM. Improving the affinity of fibroblasts for bacterial cellulose using carbohydrate-binding modules fused to RGD. *J Biomed Mater Res A* 2010 Jan;92A(1):9-17.
19. Helenius G, Backdahl H, Bodin A, Nannmark U, Gatenholm P, Risberg B. In vivo biocompatibility of bacterial cellulose. *J Biomed Mater Res A* 2006 Feb;76(2):431-438.
20. Chen SA, Sawchuk RJ, Brundage RC, Horvath C, Mendenhall HV, Gunther RA, et al. Plasma and lymph pharmacokinetics of recombinant human interleukin-2 and polyethylene glycol-modified interleukin-2 in pigs. *J Pharmacol Exp Ther* 2000 Apr;293(1):248-259.
21. Davie EW. Biochemical and molecular aspects of the coagulation cascade. *Thromb Haemost* 1995 Jul;74(1):1-6.
22. Gimbrone MA, Jr., Bevilacqua MP, Cybulsky MI. Endothelial-dependent mechanisms of leukocyte adhesion in inflammation and atherosclerosis. *Ann N Y Acad Sci* 1990;598:77-85.
23. Kouvrakoglou S, Dee KC, Bizios R, McIntire LV, Zygourakis K. Endothelial cell migration on surfaces modified with immobilized adhesive peptides. *Biomaterials* 2000 Sep;21(17):1725-1733.
24. Andrade FK, Costa R, Domingues L, Soares R, Gama M. Improving bacterial cellulose for blood vessel replacement: Functionalization with a chimeric protein containing a cellulose-binding module and an adhesion peptide. *Acta Biomater* 2010 May 12;6:4034-4041.
25. Fink H, Faxalv L, Molnar GF, Drotz K, Risberg B, Lindahl TL, et al. Real-time measurements of coagulation on bacterial cellulose and conventional vascular graft materials. *Acta Biomater* 2009 Mar;6(3):1125-1130.
26. Higuchi A, Shirano K, Harashima M, Yoon BO, Hara M, Hattori M, et al. Chemically modified polysulfone hollow fibers with vinylpyrrolidone having improved blood compatibility. *Biomaterials* 2002 Jul;23(13):2659-2666.
27. Higuchi A, Sugiyama K, Yoon BO, Sakurai M, Hara M, Sumita M, et al. Serum protein adsorption and platelet adhesion on pluronic-adsorbed polysulfone membranes. *Biomaterials* 2003 Aug;24(19):3235-3245.

28. Motlagh D, Yang J, Lui KY, Webb AR, Ameer GA. Hemocompatibility evaluation of poly(glycerol-sebacate) in vitro for vascular tissue engineering. *Biomaterials* 2006 Aug;27(24):4315-4324.
29. Tamada Y, Kulik EA, Ikada Y. Simple method for platelet counting. *Biomaterials* 1995 Feb;16(3):259-261.
30. Chen YM, Tanaka M, Gong JP, Yasuda K, Yamamoto S, Shimomura M, et al. Platelet adhesion to human umbilical vein endothelial cells cultured on anionic hydrogel scaffolds. *Biomaterials* 2007 Apr;28(10):1752-1760.
31. Sagvolden G, Giaever I, Feder J. Characteristic Protein Adhesion Forces on Glass and Polystyrene Substrates by Atomic Force Microscopy. *Langmuir* 1998;14:5984-5987.
32. Chen J, Yang L, Nho YC, Hoffman AS. Preparation of Blood Compatible Hydrogels by Preirradiation Grafting Techniques. In: Ashammakhi N, Reis R, Chiellini F, editors. *Topics in Tissue Engineering*, 2008.
33. Ishihara K, Fukumoto K, Iwasaki Y, Nakabayashi N. Modification of polysulfone with phospholipid polymer for improvement of the blood compatibility. Part 2. Protein adsorption and platelet adhesion. *Biomaterials* 1999 Sep;20(17):1553-1559.
34. Vroman L. The life of an artificial device in contact with blood: initial events and their effect on its final state. *Bull N Y Acad Med* 1988 May;64(4):352-357.
35. Sivaraman B, Latour RA. The Adherence of platelets to adsorbed albumin by receptor-mediated recognition of binding sites exposed by adsorption-induced unfolding. *Biomaterials* 2010;31:1036-1044.
36. Ballet T, Boulange L, Brechet Y, Bruckert F, Weidenhaupt M. Protein conformational changes induced by adsorption onto material surfaces: an important issue for biomedical applications of material science. *Bull Pol Ac: Tech* 2010;58(2):303-315.
37. Permyakov EA, Burstein EA. Some aspects of studies of thermal transitions in proteins by means of their intrinsic fluorescence. *Biophys Chem* 1984 May;19(3):265-271.
38. Yengo CM, Chrin L, Rovner AS, Berger CL. Intrinsic tryptophan fluorescence identifies specific conformational changes at the actomyosin interface upon actin binding and ADP release. *Biochemistry* 1999 Nov 2;38(44):14515-14523.
39. Steiner G, Tunc S, Maitz M, Salzer R. Conformational changes during protein adsorption. FT-IR spectroscopic imaging of adsorbed fibrinogen layers. *Anal Chem* 2007 Feb 15;79(4):1311-1316.
40. Tanaka M, Motomura T, Kawada M, Anzai T, Kasori Y, Shiroya T, et al. Blood compatible aspects of poly(2-methoxyethylacrylate) (PMEA)-relationship between protein adsorption and platelet adhesion on PMEA surface. *Biomaterials* 2000 Jul;21(14):1471-1481.
41. Jetsy J, Nemerson Y, McGraw-Hill NY. The pathways of blood coagulation. In: E. Beutler MAL, B.S. Coller, T.J. Kipps, editor. *Williams Hematology*. 5th ed. New York: McGraw-Hill, 1995. p. 1227-1238.

42. Gorbet MB, Sefton MV. Biomaterial-associated thrombosis: roles of coagulation factors, complement, platelets and leukocytes. *Biomaterials* 2004 Nov;25(26):5681-5703.
43. Kung FC, Yang MC. Effect of conjugated linoleic acid immobilization on the hemocompatibility of cellulose acetate membrane. *Colloids Surf B Biointerfaces* 2006 Jan 15;47(1):36-42.
44. Franco RF. Fisiologia da coagulação, anticoagulação e fibrinólise. Simpósio: Hemostasia e Trombose jul./dez. 2001; Medicina, Ribeirão Preto. p. 229-237.
45. Amarnath LP, Srinivas A, Ramamurthi A. In vitro hemocompatibility testing of UV-modified hyaluronan hydrogels. *Biomaterials* 2006;27 1416–1424.
46. Liu Y, Wang W, Wang J, Wang Y, Yuan Z, Tang S, et al. Blood compatibility evaluation of poly(D,L-lactide-co-beta-malic acid) modified with the GRGDS sequence. *Colloids Surf B Biointerfaces* 2010;75:370-376.
47. Lin WC, Yu DG, Yang MC. Blood compatibility of thermoplastic polyurethane membrane immobilized with water-soluble chitosan/dextran sulfate. *Colloids Surf B Biointerfaces* 2005 Aug;44(2-3):82-92.
48. Lin WC, Tseng CH, Yang MC. In-vitro hemocompatibility evaluation of a thermoplastic polyurethane membrane with surface-immobilized water-soluble chitosan and heparin. *Macromol Biosci* 2005 Oct 20;5(10):1013-1021.
49. Lin WC, Liu TY, Yang MC. Hemocompatibility of polyacrylonitrile dialysis membrane immobilized with chitosan and heparin conjugate. *Biomaterials* 2004 May;25(10):1947-1957.
50. Hansson KM, Tosatti S, Isaksson J, Wettero J, Textor M, Lindahl TL, et al. Whole blood coagulation on protein adsorption-resistant PEG and peptide functionalised PEG-coated titanium surfaces. *Biomaterials* 2005 Mar;26(8):861-872.
51. Heyligers JM, Arts CH, Verhagen HJ, de Groot PG, Moll FL. Improving small-diameter vascular grafts: from the application of an endothelial cell lining to the construction of a tissue-engineered blood vessel. *Ann Vasc Surg* 2005 May;19(3):448-456.
52. Michiels C. Endothelial cell functions. *J Cell Physiol* 2003 Sep;196(3):430-443.

Chapter 5

Studies on the biocompatibility of bacterial cellulose

Abstract

The production of functional blood vessels by tissue engineering techniques being already possible, it must be acknowledged that, due to the associated costs and lengthy production, the development of new materials appropriated for small diameter blood vessel replacements is still required. Bacterial cellulose is a promising material for this application, given its excellent biocompatibility and mechanical properties. In the present work, BC tubes with small diameter (3mm ID) were produced and its mechanical properties evaluated. The functionalization of BC membranes using a chimeric protein containing a cellulose – binding module (CBM) and the adhesion peptide Arg-Gly-Asp (RGD) improves interaction with cells – work previously developed in our lab; Since the recombinant protein contains a bacterial CBM, the biocompatibility of native and RGD-CBM treated BC – to analyse whether the presence of the recombinant protein gives rise to any immunologic reaction – was now investigated through *in vitro* and *in vivo* studies. BC was implanted subcutaneously in the sheep for 1, 2, 4, 8, 16 and 32 weeks. Implants were evaluated regarding the inflammatory reaction, cell in-growth and angiogenesis. Histological results showed that BC trigger a biological response typically observed for high surface-to-volume implants (e.g., fabrics medical devices). After 1 week the presence of an inflammatory infiltrate suggests an acute/subacute inflammatory reaction that advances to a chronic inflammation confined to the implantation site and associated to the proliferation of small blood vessels. The presence of giant cells was observed at latter periods (16 and 32 weeks) and a narrow fibrous capsule was present surrounding the implant. There were no significant differences on the inflammation degree between the BC coated with the recombinant protein RGD-CBM and the native BC.

The CryoSEM analysis showed that the BC tubes present a denser luminal side and a porous outer side; no orientation of the fibrils network was observed. Fluorescence microscopy reveals

that apart from increasing cell adhesion, the presence of RGD stimulates an even cell distribution, while cells coating the untreated BC seem to form aggregates. Furthermore, cells observed on the RGD treated – BC present a more elongated morphology. Mechanical test results showed that small-diameter BC tube produced by our group possess an elasticity higher than that of human arteries and veins.

Introduction

Tissue engineering and regenerative medicine aim at promoting the regeneration of diseased or damaged human tissues. Biomaterials are used as scaffolds in which cells and/or growth factors are seeded, cultured, and implanted to induce and direct the growth of new, healthy tissue [1]. Among the biomaterials used, natural polymers represent one of the most attractive options, since being similar to biological macromolecules, may avoid the stimulation of chronic inflammation or immunological reactions and toxicity, often detected with synthetic polymers. Although several groups described the successful production of tissue engineered blood vessels [2-7], it must be recognized the cost and long time required for its production. Furthermore, the long culture time required brings about the question of the safety, due to possible cell differentiation. Therefore, using a material with good mechanical properties, allowing cell colonization, may provide a “mixed” tissue engineered/artificial prosthesis approach, allowing a prompt utilization and good tissue integration.

Bacterial cellulose (BC) is a pure form of cellulose secreted by bacteria such as *Gluconacetobacter xylinus*. It is a material with unique properties, including high water holding capacity, high crystallinity, ultrafine fiber network, high tensile strength and the possibility to be shaped into three-dimensional (3D) structures during synthesis [8]. This set of features makes BC a promising material for the production of scaffolds in tissue engineering. In fact, several research groups studied the use of BC as a scaffold for cartilage [9, 10], wound dressing [11, 12], dental implants [13-19], nerve regeneration [20, 21] and vascular grafts [22, 24-28].

Inflammation, wound healing, and foreign body response are generally considered as parts of the tissue or cellular host responses to injury and implantation of a biomaterial in the body. This involves injection, insertion, or surgical implantation, all of which injure the tissues or organs involved. The sequence of local events following implantation is: injury, acute inflammation, chronic inflammation, granulation tissue, foreign body reaction and fibrosis/fibrous capsule development [22]. The degrees to which the homeostatic mechanisms are perturbed and pathophysiologic conditions created and resolved are a measure of the host reaction to the biomaterial and may ultimately determine its biocompatibility.

Biocompatibility is one main requirement for any biomedical material. It can be defined as the ability to remain in contact with living tissue without causing any toxic or allergic side effects, simultaneously performing its function [23]. In this context, BC has been modified to further enhance biocompatibility. Depending on the envisaged biomedical application, improved

cellulose integration with the host tissue, increased degradation *in vivo* or modified mechanical properties, to mimic the tissue to be replaced, are required. Many BC modification studies, such as chemical surface modifications [24-26], incorporation of bioactive molecules [27], modification of porosity and crystallinity [28], design of 3D structures [29], modification of BC composition [30-32] and production of nanocomposites [33-36], enlarge the repertoire of bacterial cellulose as a potential material for biomedical application.

The functionalization of BC tubes using bioactive peptides was previously successfully developed in our research group, envisaging its application for vascular replacements. The attachment of cells to biomedical materials can be improved by using adhesion molecules, such as fibronectin, vitronectin, or laminin. These molecules, present in the extracellular matrix proteins, regulate the adhesion, migration and growth of cells, by binding to integrin receptors located on the outer cellular membranes. The amino acid sequence Arg-Gly-Asp (RGD) has been recognized as the minimal essential cell adhesion peptide sequence present in these proteins. In a previous work we described the production of recombinant proteins containing RGD sequences fused to a CBM (cellulose-binding module) [37] (chapter 2). The use of a CBM (a protein exhibiting high adsorption affinity and specificity for cellulose surfaces) fused with biologically active peptides, allow a simple and effective approach to decorate the BC surface. This concept was further demonstrated using human microvascular endothelial cells [38] (chapter 3). The chimeric proteins were able to enhance endothelial cell adhesion to BC and stimulate angiogenesis.

Very few studies on the *in vivo* biocompatibility of BC have been published. Helenius and colleagues [39] reported the histological analysis of subcutaneously implanted BC, in mice, for a period of up to 12 weeks. BC was shown to integrate well into the host tissue, with cells infiltrating the BC network and no signs of chronic inflammatory reaction or capsule formation. The formation of new blood vessels around and inside the implants was also observed, evidencing the good biocompatibility of the biomaterial. In another study, Klemm *et al.* [20] investigated the application of patented BC tubes (BASYS[®] - BActerialSYnthesized Cellulose) as microvessel endoprosthesis, using the carotid artery of a white rat. In this study, four weeks after implantation, the carotid artery-BASIC complex was wrapped up with connective tissue and the BC tube was completely incorporated in the body without rejection. Following the same approach, but this time in the carotid artery of pigs over a period of 12 weeks, BC grafts showed good *in situ* tissue regeneration, without signs of thrombosis, inflammation or fibrotic

capsule formation around the implants. The luminal wall of the newly formed tissue showed complete endothelialisation, with a confluent endothelial layer [40].

To further explore the potential of BC for tissue engineering blood vessels, in this work we investigate the mechanical properties of BC tubes and the *in vivo* and *in vitro* biocompatibility of BC membranes. The fate of long term subcutaneous implants in sheep - 32 weeks - was analysed. Implants were evaluated in aspects of chronic inflammation, foreign body reaction responses, cell in-growth and angiogenesis. Once the chimeric protein used in this work contain a bacterial CBM – a cellulose-binding domain family III from the cellulosomal-scaffolding protein A of the bacteria *Clostridium thermocellum* – also the *in vivo* biocompatibility of BC membranes treated with the RGD-CBM protein was investigated. Furthermore, the *in vitro* biocompatibility was evaluated using 3T3 mouse embryo fibroblast cultures. Viability, morphology and cell in-growth were analysed by MTS [3-(4,5-dimethylthiazol-2-yl)-5-(3-carboxymethoxyphenyl)-2-(4-sulfophenyl)-2H- tetrazolium] assay, fluorescence and CryoSEM microscopy.

Material and Methods

Production of Bacterial Cellulose

Gluconacetobacter xylinus (ATCC 53582) purchased from the American Type Culture Collection was grown in Hestrin-Schramm medium, pH 5.0. The medium was inoculated with the culture, added to the 24-well polystyrene plate (1 ml per well) and incubated statically at 30 °C, for 5 days. BC pellicles were purified by 2% SDS treatment at 60 °C, for 12 h, washed with distilled water until complete removal of SDS and immersed in 4% NaOH at 60 °C, for 90 min. After neutralization with distilled water the samples were autoclaved and stored in phosphate buffered solution (PBS) pH 7.4, at 4°C, prior to use. The pellicle produced in a 24-well polystyrene plate presented a diameter of 15.5mm.

Preparation of tubular BC: the experimental set-up used for the production of BC tubes (FIGURE 1) was autoclaved and the Hestrin-Schramm medium was inoculated and added to the system. A layer of sterilized oil was placed surfacing the culture medium, to reduce the growth of the bacteria at the air-liquid interface. The silicon tube is permeable to oxygen, allowing the growth of the strictly aerobic bacteria next to the tub wall. To avoid the formation of air bubbles on the surface of the silicon tube – leading to irregularly shaped BC tubes – the

system was first connected to an air bomb during 4 days in an open circuit. After the formation of a thin BC pellicle, the air bomb was disconnected and pure oxygen was injected at 0,5 bar for 14 days and allowed the production of a BC tube with (3mm of inner diameter). Then, the BC tubes were removed from the silicon mould and treated with a 4% NaOH solution, at 60 °C, for 12 hours. The purified BC was then neutralized with filtered distilled water, autoclaved and stored in phosphate buffered solution (PBS) pH 7.4, at 4°C, prior to use.

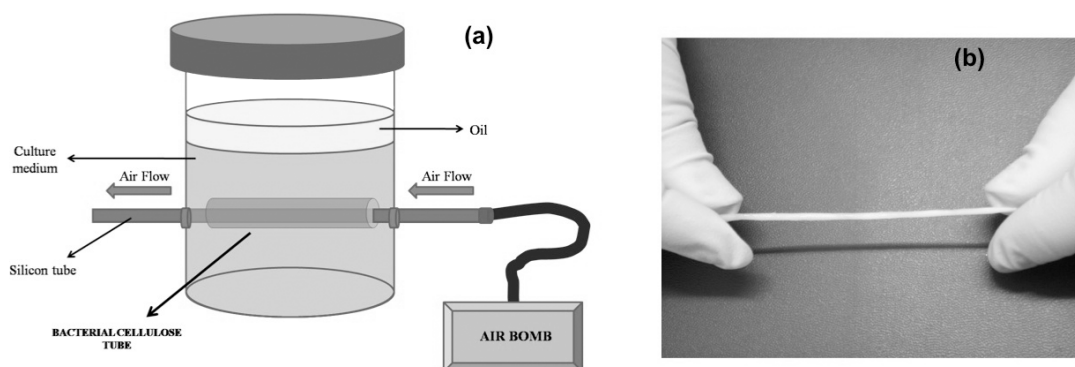


Figure 1. Bacterial cellulose produced by *G. xylinus* (ATCC 53582) grows around the silicon tube, when an air flow is injected through the tube. a) Schematic picture of the cultivation system; b) Bacterial cellulose tube.

Surface modification of BC with RGD-CBM protein

The recombinant protein RGD – CBM has been formerly cloned in *Escherichia coli* and its production and purification was conducted as described in our previous work [37] (chapter 2). For surface modification of BC, the purified recombinant protein was added to the wells of 24-well polystyrene plates (0.25mg of protein/per well), coated with bacterial cellulose sheets produced in similar 24-well polystyrene plates. The plates were incubated overnight at 4 °C. Unbound protein was removed and the BC pellicles were washed with PBS and used in the *in vitro* and *in vivo* biocompatibility assays.

Fibroblast adhesion and proliferation

The mitochondrial activity of the cultured cells was determined using a colorimetric assay, commonly used as a measure of cell viability. The MTS [3-(4,5-dimethylthiazol-2-yl)-5-(3-carboxymethoxyphenyl)-2-(4-sulfophenyl)-2H-tetrazolium] assay was performed as follows: the purified recombinant proteins were added to the wells of the 24-well polystyrene plates (0.25

mg of protein/per well), coated with bacterial cellulose sheets. As referred earlier, the BC sheets were produced in similar 24-well polystyrene plates, such that they tightly fit in the wells, completely covering the bottom surface. The fibroblasts 3T3 were seeded at a density of 12×10^4 cells/per well, in DMEM medium without serum. Two hours after the addition of the cells, the wells were washed with PBS and DMEM with serum (10%) was added. The MTS assay of the attached and spreading 3T3 fibroblasts was carried out at 2, 72 and 7 days after the addition of the cells. The plates were incubated at 37°C, in atmosphere of 5% CO₂ and 95% humidified air. The results were obtained from at least three different assays, each one with samples in triplicates.

Morphological analysis by fluorescent microscopy

After 2h, 72 and 7days of cell seeding on BC - untreated or treated with the RGD-CBM protein –the membranes were washed with pre-warmed PBS; then, the cells were fixed in 4% formaldehyde (Pierce, Rockford, IL, USA) in PBS, permeabilized with acetone (Sigma) at – 20°C, and stained with Alexa Fluor 546-phalloidin (Molecular Probes). Nuclei were visualized by staining with DAPI. Microscopy observations were performed using an Olympus BX51 (Olympus Portugal SA, Porto, Portugal) fluorescence microscope.

Cryo-Scanning Electron Microscopy (CryoSEM)

CryoSEM presents a valuable technique for the visualization of materials that have a high water content, whose structure might be altered or destroyed by dehydration and cross linking. After 14 days of cell seeding on BC – untreated or treated with the RGD-CBM protein – the membranes were washed with pre-warmed PBS; then, the cells were fixed in 2.5% glutaraldehyde in PBS. Samples were washed in ultrapure water and a piece of BC membrane was placed between two miniature rivets on a vacuum transfer rod and the sample was slam-frozen in a nitrogen slush and transferred to the cryostat chamber, which was maintained at - 150 °C. The top rivet was flicked off to produce a fractured surface, the ice was sublimed at - 90 °C during 2 minutes (for visualization of fibers on the dense side of BC) or 4 minutes (for visualization of fibers on the porous side of BC), and then fractured surface was coated with gold/palladium. Afterwards, the sample was transferred to the microscope chamber, which was also maintained at - 150 °C and examined at 15 kV using a working distance of 15 mm.

The samples were analyzed by use of a CryoSEM (Model Gatan ALTO 2500) at CEMUP (Centre for materials characterization from the University of Porto).

For visualization of the fibers from the BC tube, the tube samples were cut longitudinally and transversely. The transversal section was fractured and sublimed during 10 minutes. The longitudinal section was not fractured and the sublimation time was 30 minutes.

Mechanical properties: Young´s modulus (E) tensile strength (TS) and elongation-at-break (ϵ %)

TS, E and ϵ % were measured with an Instron Universal Testing Machine (Model 4500, Instron Corporation, USA). The initial grip separation was set at 15 mm and the crosshead speed was set at 5 mm/min. TS is the stress needed to break a sample and was calculated by dividing the maximum load (N) by the initial cross-sectional area (m^2) of the specimen, the TS is expressed in MPa. E is the initial slope of the stress-strain curve and expressed in MPa. ϵ % is the strain on a sample when it breaks. It was calculated as the ratio of the increased length to the initial length of a specimen (15 mm) and expressed as a percentage. BC tube was stretched in lengthwise direction and a total of fifteen tubes were used in the test.

In vivo biocompatibility studies

Experimental groups: 18 adult female white merino sheep weighing approximately 60 kg were random allocated to two groups of 6 animals each. One group (group 1) of animals was implanted with bacterial cellulose discs with 1.5 cm diameter and treated with the recombinant protein (RGD-CBM), a second group (group 2) was implanted with untreated BC discs.

Anaesthesia and surgical procedures: The animals were solids fastened for 48 hours prior to the surgical procedure. An intravenous catheter of 20G was placed at the cephalic vein. The anesthetic protocol consisted in xylazine (0.2 mg/Kg, intravenous) as tranquilizer. For inducing anesthesia, sodium thiopental was used at a dosis of 15 mg/Kg intravenous. The anesthetic maintenance was done with isoflurane at 2% via endotracheal intubation carried by 100% oxygen with a flow of 2L/min.

For surgery, sheep were placed in sternal recumbence over a tilted table so that the animal´s head and neck are always lower than the stomach to reduce risks of aspiration pneumonia. The wool was clipped in roughly square areas and the skin was aseptic prepared with

iopovidone. The incisions were made over the dorsal area, starting over the last ribs and ending just cranially to the sacrum. These 3 cm length incisions, 3 on the left side e two on the right one, were made parallel and 4 cm off the midline. A minimum distance of 3 cm was kept between incisions. After exposing the dorsal muscles, the BC tubes were inserted under the skin, distally to the midline, subsequently, the skin was closed with a Supramid® USP1 suture and the ewes were transferred to straw yards (4 m x 3 m) after surgery. The skin sutures were not removed in order to localize the implant site.

Collection of implants and histological procedures: The implants and the surrounding tissue were collected after a peripheral infiltration of 2% lidocaine, at 1, 2, 4, 8, 16 e 32 weeks post-implantation. Two samples were collected in each animal, randomly selected in each experimental group at the previously reported temporal points. The samples were fixed in 10% formalin, paraffin-embedded, cut in 2 µm and stained with hematoxylin and eosin (HE) for histological evaluation.

Histological evaluation: The biological response parameters were assessed in the implant/tissue interface with three high power fields (x400) by at least two pathologists, for each sample and recorded in an appropriated formulary. Among the biological response parameters all were evaluated according to the ISO standard 10993-6 (annex E) and included: the extent of fibrosis/fibrous capsule (layer in micrometres) and inflammation; the degeneration as determined by changes in tissue morphology; the number and distribution from the material/tissue interface of the inflammatory cell types, namely polymorphonuclear neutrophilic leucocytes (PMN), lymphocytes, plasma cells, eosinophils, macrophages and multinucleated cells; the presence, extent and type of necrosis; other tissue alterations such as vascularization, fatty infiltration and granuloma formation; the material parameters such as fragmentation and/or debris presence, form and location of remnants of degraded material.

Results and discussion

***In vitro* studies on the BC-cell interactions**

When cultivated in static culture *G. xylinus* constructs a cellulose network much denser on the culture medium/air interface than on the opposite side [20, 41]. The results of the MTS test (FIGURE 2) showed that there were no significant differences on the fibroblast adhesion to the porous or dense side of BC and also that the cells proliferated equally well on both sides, as

previously reported by Backdahl and colleagues [41], in a study using human smooth muscle cells (SMC). The effect of the recombinant protein (RGD – CBM) on the adhesion of fibroblasts to BC was previously discussed [37] (chapter 2). Fluorescence microscopy allows, in this work, the observation of more details of the cell-BC interaction. Figure 3 show that, apart from increasing cell adhesion – as previously observed using the MTS assay – the presence of RGD stimulates a uniform distribution of the cells, important to improve the endothelialization of the graft, while cells coating the untreated BC seems to form aggregates (the images containing only the nuclei labelled on figure 3 allow a better visualization of this effect). There were no differences on the morphology of the fibroblast cultured on porous and denser side of the membrane.

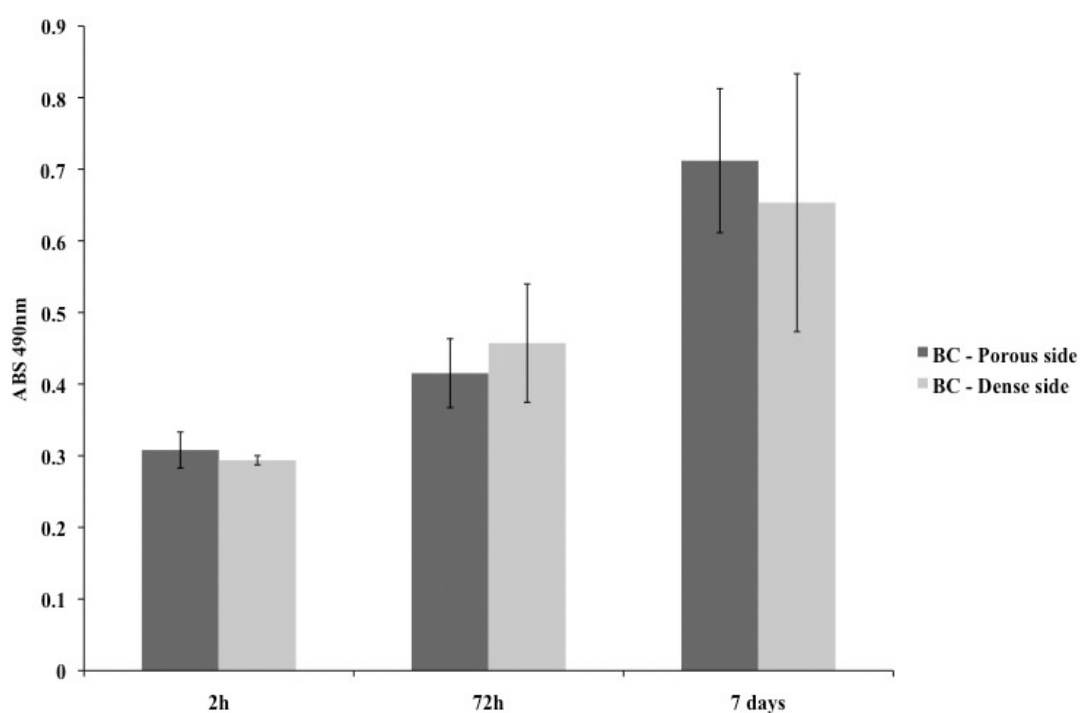


Figure 2. MTS assays of fibroblast cultures at the dense or porous side of BC membrane. The MTS assay was developed at 2, 72 and 7 days after cell seeding. Results are expressed as absorbance values at 490 nm.

The CryoSEM results (FIGURE 4) showed that cells on RGD-treated BC present a more elongated morphology than the ones covering the untreated pellicle, irrespective of the side analysed. The more extended morphology of fibroblasts upon interaction with the adhesive peptides is likely driven by the greater number of focal contacts between integrins and RGD-containing peptides linked to the BC surface. It is well known that a critical RGD density is

essential for the establishment of mature and stable integrin adhesions, which, in turn, induce efficient cell migration, spreading and formation of focal adhesions [42-45].

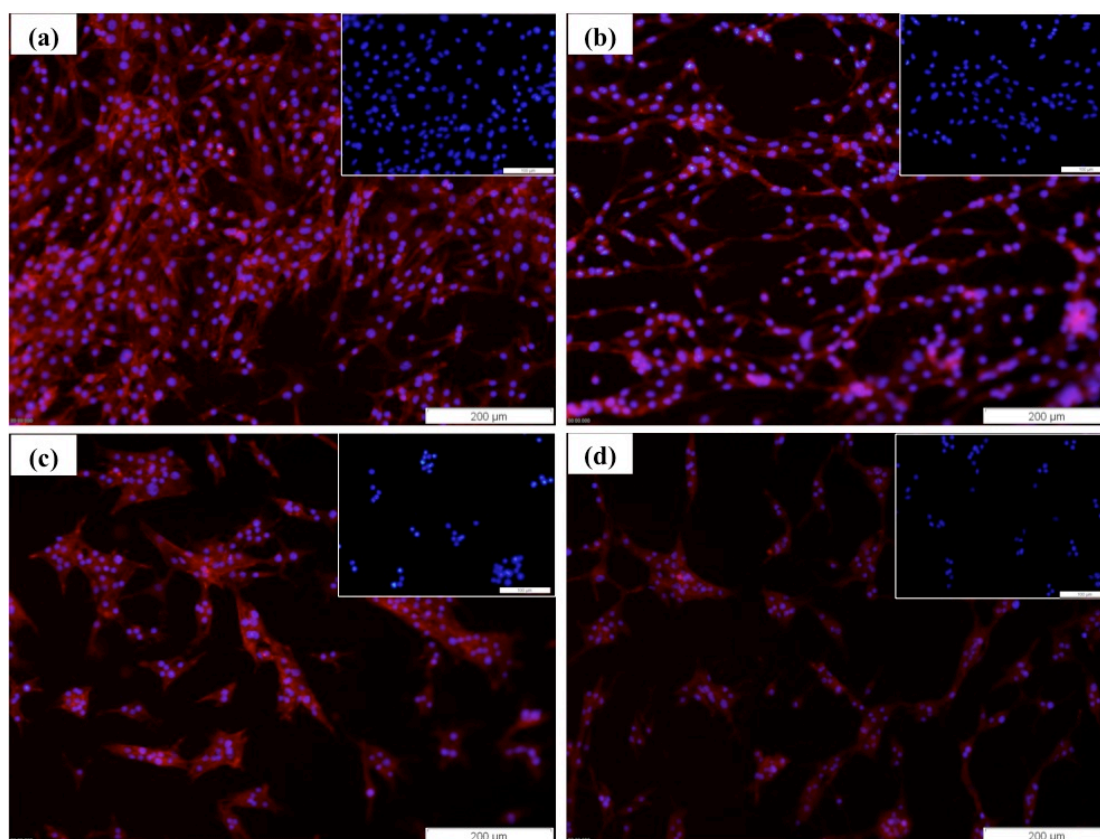


Figure 3. Fluorescent microscopy images showing fibroblast cultured 7 days on BC pellicle. (a) Dense and (b) porous side of RGD-treated BC; (c) Dense and (d) porous side of untreated BC. Nuclei were visualized by staining with DAPI (blue) and f- actin with Alexa Fluor 546-phalloidin (red). Actin and nuclei combined images were acquired using objectives 10x (scale 200 μ m); Nuclei images were acquired using objectives 20x (scale 100 μ m).

The migration of cells is mediated by integrins, a diverse family of glycoproteins that form heterodimeric receptors for extracellular matrix (ECM) molecules. During migration, cells project lamellipodia that attach to the ECM and simultaneously break existing ECM contacts at their trailing edge. This allows the cell to pull itself forward [46]. Animal cells cannot degrade cellulose [39] and must push the nanofibrils aside while migrating into the cellulose network [41]. The CryoSEM technique was also used for visualization of cell ingrowth in BC scaffold. The results showed that after 14 days of culture the cells could not migrate through the BC fibers, once only cells on the surface were found. However, it has been demonstrated that cells

may migrate through BC membranes. Andrade et al. [38] (chapter 3) and Backdahl et al. [41] demonstrated the ingrowth of human microvascular endothelial cells (HMECs) and SMC, respectively, through BC network using an invasion chamber where an attractant (serum, growth factor, etc...) is used to stimulate the cells to grow into the BC - in both cases the cells were able to invade the fibrous cellulose matrix.

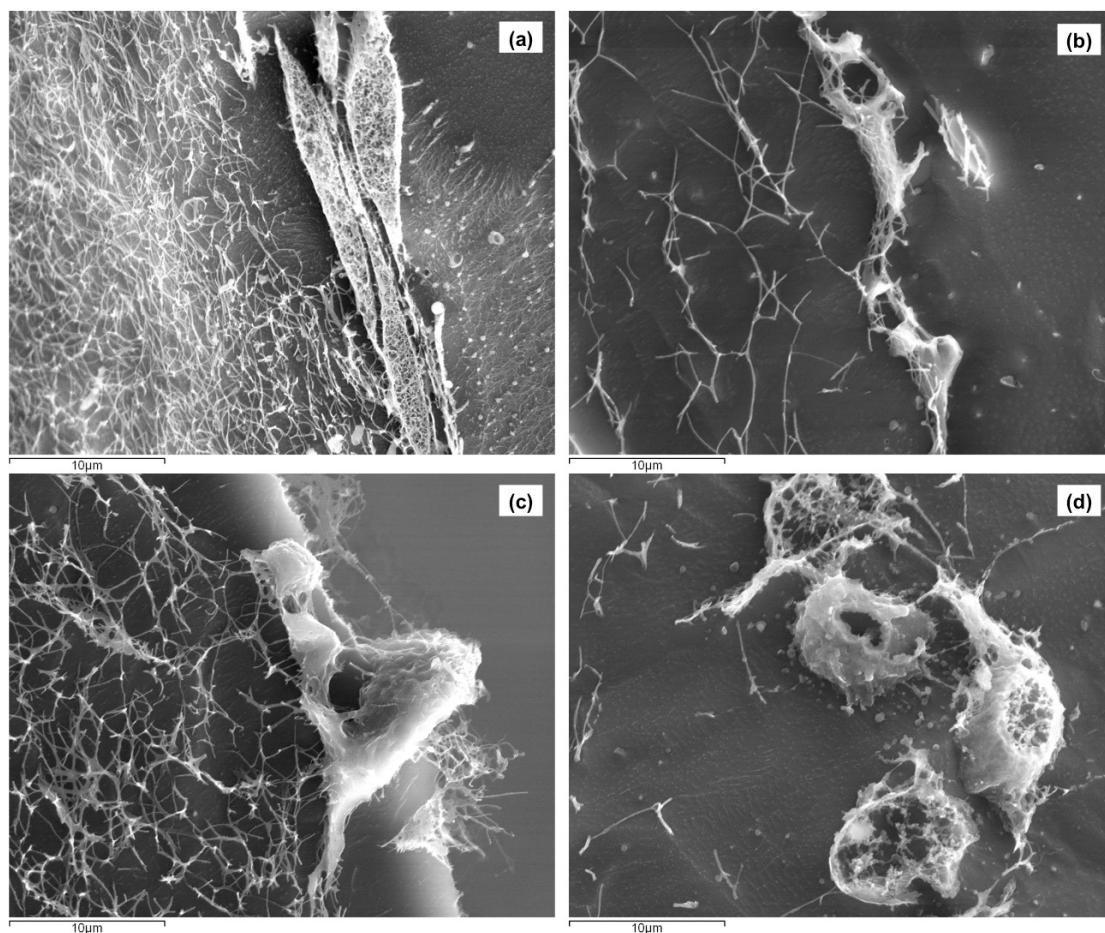


Figure 4. CryoSEM micrographs of bacterial cellulose cultured with fibroblasts after 14 days. (a) Dense and (b) porous side of RGD-treated BC; (c) Dense and (d) porous side of untreated BC. Scale 10µm.

Mechanical properties of the BC tubes; structural details (CryoSEM)

The production of BC tubes using different techniques has been described in the literature, for example:(1) a cylindrical glass matrix is immersed in a large volume and tubular BC is produced in the culture medium that enters between the outer and inner matrices. In this case the oxygen is supplied through the second opening that opens to the air surface [20]. This approach is not feasible for the production of long tubular BC structures. (2) Another technique

was developed by Putra et al. [47]; the authors used a silicone tube (an oxygen-permeable material) as a mould. The culture medium is poured into a silicone tube and the both edges were sealed. The *G. xylinus* produce BC gel all around the interface between the inner surface of silicone tube and the culture medium, which leads the formation of a BC tube with a more porous structure on the luminal side than the outer side. (3) Gatenholm and his group [41, 48, 49] produced BC tubes submerging silicone tubes in a glass tube containing culture medium. One of the edges was sealed and at the other edge gas was inlet through the support. The *G. xylinus* produce BC gel all around the interface between the outer surface of silicone tube and the culture medium. The experimental set-up used in this work for the production of BC tubes (FIGURE 1) is similar to the one used by the Gatenholm group and produces a BC tube with a smoother and denser luminal side and a more porous outer side (FIGURE 5). According to Backdahl et al. [41] a smoother luminal surface, being similar to the basal membrane of the luminal side of blood vessels, is preferable for the attachment of endothelial cells while a porous outer side probably will facilitated the integration with the host tissue. The CryoSEM results also showed that, unlike the tubes produced by Putra et al. [47], no orientation of the fibrils network was observed. According to Putra and co-workers the degree of orientation of the fibrils depended on the diameter of the curvature of the silicone mould. An increase in the diameter of curvature led to a decrease in the degree of BC fibril orientation. Since, in the present study, the bacteria grow on the outer side of the silicone tube (hence, with lower curvature), this probably affected the direction of the fibril secretion by the *G. xylinus*.

The Young's modulus (E) of the BC tube was evaluated. Higher values of E are associated with a greater vessel wall stiffness. The BC tube produced in this work presented a more elastic structure in the lengthwise, *i.e.*, lower E (0.25 ± 0.07 MPa) than human arteries and veins and much lower than collagen and PTFE, two common polymers used as vascular grafts (TABLE 1). The value reported by Putra and colleagues [47] is, also along the length of the tube, even more elastic (lower E), these differences are probably due to the different cellulose density/thickness. Typical plots of wall stress *versus* strain in BC tube segments are shown in Figure 6. The BC-tube produced in this work presented an $\epsilon\%$ of $31 \pm 4.4\%$, a value higher than presented by collagen (10%) and lower than PTFE (200–400).

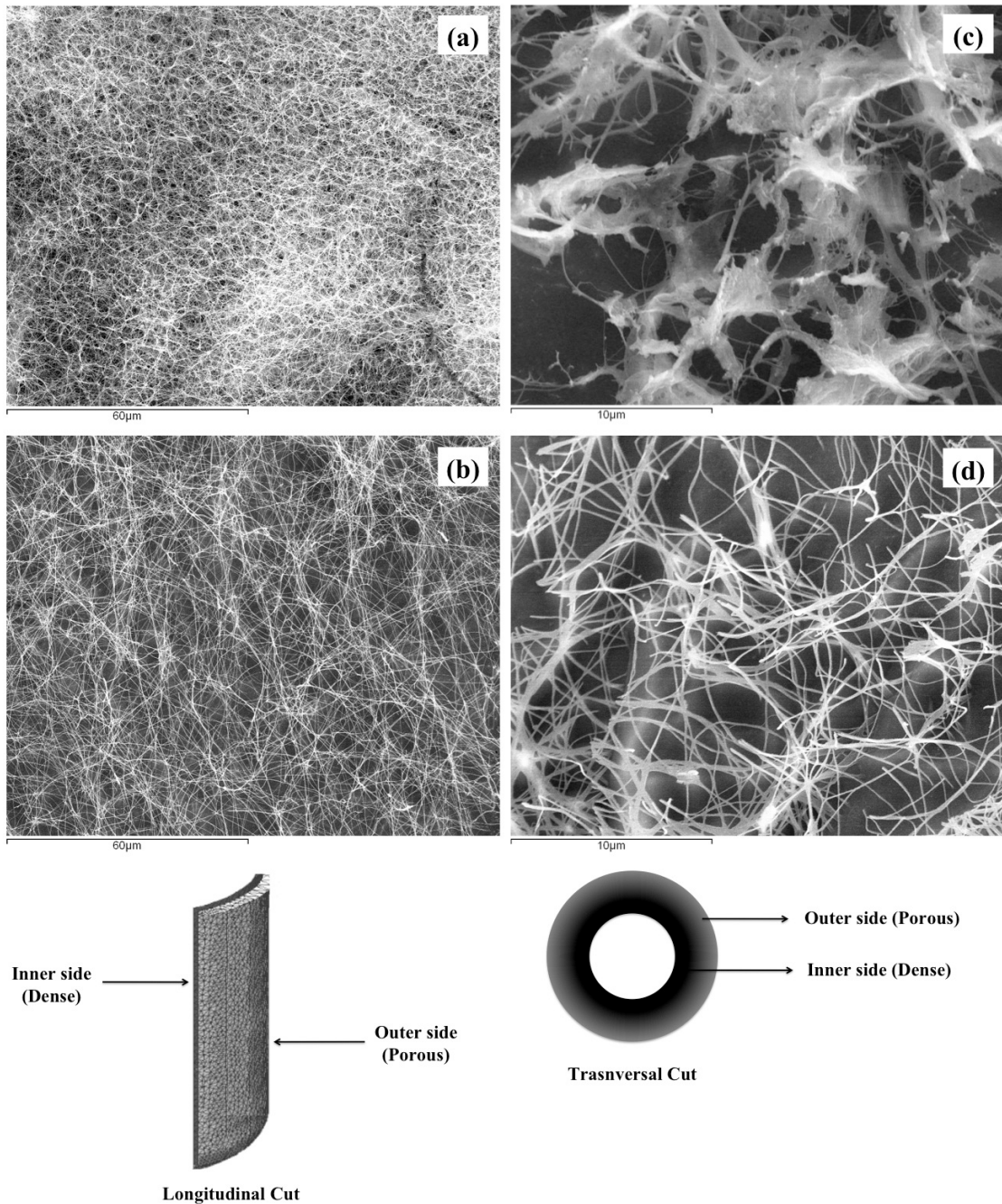


Figure 5. CryoSEM micrographs of bacterial cellulose tubes. Visualization through a longitudinal cut of (a) Inner side (b) outer side. Visualization through a transversal cut of (c) Inner side (d) outer side. Scale 60µm (longitudinal images), scale 10µm (transversal images).

The TS from our BC-tube was 0.19 ± 0.03 MPa, a value lower than the one obtained by Putra and colleagues (0.59 MPa) [47]. Again, although the values are in the same order of magnitude, the different properties may be assigned to variable thickness of the tubes. The TS

values for the BC tubes (obtained in our lab and described by Putra and colleagues [47]) are one order of magnitude lower than the ones reported for human arteries and veins (TABLE 1).

Table 1. Comparison of the mechanical properties of BC tubes (3mm of inner diameter and 1mm of wall thickness) produced in this present work with BC tubes produced by Putra et al.[47], human arteries and veins and common polymers used as vascular grafts (collagen and PTFE).

	Young's Modulus (MPa)	Tensile Strength (MPa)	Elongation (%)	References
BC – tube	0.25	0.19	31	*
BC – tube	0.06	0.59	-	[47]
Arteries	1.54	1.57	-	[50, 51]
Veins	3.11	2.65 – 3.3	-	[50, 51]
Collagen	1000	50 – 100	10	[52]
PTFE	400	14 – 35	200 – 400	[52]

* BC tubes produced in this work.
- Not described.

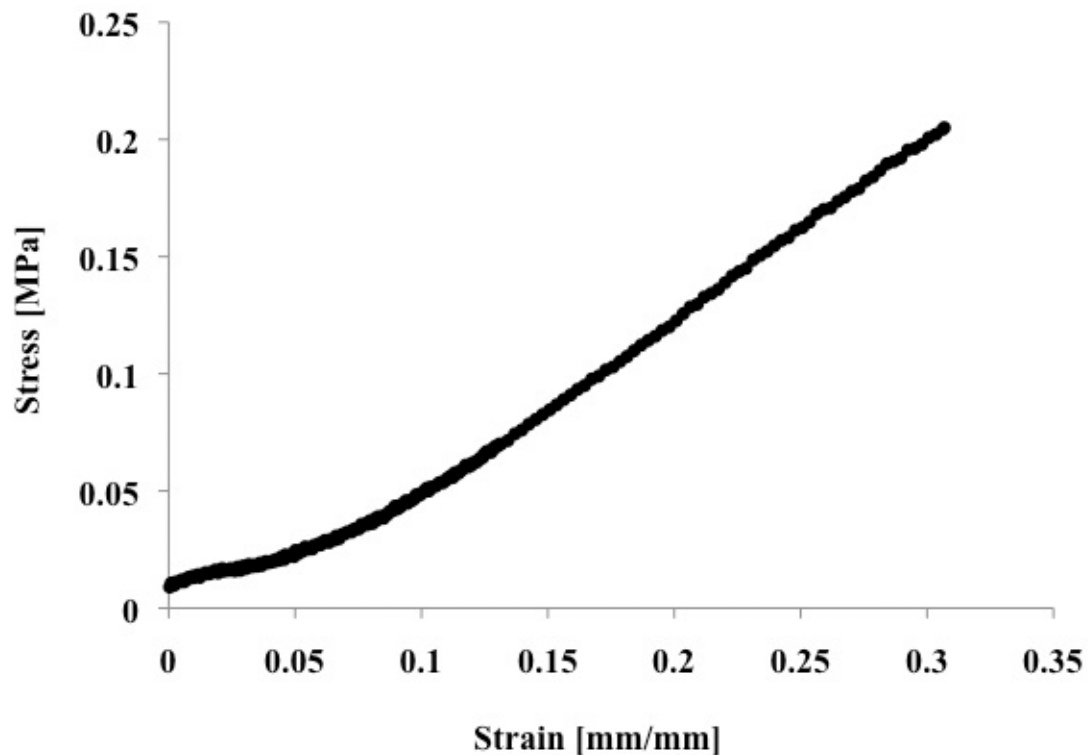


Figure 6. Tensile stress-strain curves of the lengthwise of BC tubes with an inner diameter and wall thickness of 3 mm and 1 mm, respectively.

According to Sanchavanakit and colleagues, a BC dried film (from a 48h grown culture) with a thickness of 0.12 mm presents a tensile strength and break strain of 5.21 MPa and 3.75%, whereas for the reswollen films the values are 1.56 MPa and 8.0%, respectively [53]. McKenna and colleagues reported a TS value of wet bacterial cellulose sheet grown between 48h – 96h of 1.1 - 2.2 MPa, $\epsilon\%$ of 16 - 27% and E 10 - 14 MPa [54]. The BC production as well as the mechanical properties are influenced by the carbon and nitrogen sources and concentration, the pH and temperature, time of cultivation, the surface area of the fermentation system, the type of cultivation system (e.g. static or agitated cell culture) and differences in the bacterial strains. Also, the treatment after synthesis influenced the properties of BC membranes [8].

The mechanical properties of the BC tubes produced using the method adopted in this work are inferior to the properties of both the commercial BC grafts available and of the natural blood vessels. Therefore, a different method for the production of the tubes, allowing a thicker BC wall is required (ongoing work). On the other hand, the impregnation of the porous cellulose matrix with blood before implantation may provide significant improvement on the mechanical properties.

***In vivo* biocompatibility studies**

Implanted medical devices must perform, improving quality of life of the patients. However, some implants ultimately develop complications (adverse patient – device interactions) leading to the graft failure, and thereby may cause harm to or death of the patient. The complications associated to medical devices are largely due to the materials – tissue interactions, including both the effects of the implant on the host tissues, as well as the effects of the host tissues on the implant [52]. This way, much of the research is directed towards the search for biomaterials that are able to provide best performance.

As a promising material for small vascular grafts, bacterial cellulose was evaluated in terms of its *in vivo* biocompatibility. The effect of the recombinant protein containing a bacterial domain on the biocompatibility of BC was also examined. Bacterial cellulose membranes with 1.5 cm diameter coated or not with the RGD-CBM, were subcutaneously implanted in the sheep. The implants and the surrounding tissue were collected at 1, 2, 4, 8, 16 e 32 weeks post-implantation.

The histological observation showed that at 1 week post-implantation there was a predominance of polymorphonuclear leukocytes (PMN) and macrophage infiltrate at the

implant – tissue junction in both groups 1 and 2, suggesting an acute/subacute inflammatory reaction (FIGURE 7a).

In the 2nd week post-implantation an increase in macrophages, plasma cells and lymphocytes infiltration associated to a proliferation of small blood vessels was compatible with a chronic inflammation. The persistence of the inflammatory stimuli (BC membranes) led to a change from acute to chronic inflammation [55]. This chronic inflammation response was confined to the implantation site (FIGURE 7b).

During the initial 4 weeks of observation, lymphocytes and macrophages were the most represented cells for both groups. The type of cell infiltrate and the increased neovascularisation, always surrounding the implant area were compatible with a chronic inflammation (FIGURE 7c). Macrophages must be considered in the development of immune responses to synthetic biomaterials by presenting antigen to immuno competent cells such as lymphocytes and plasma cells [56]. The macrophage is probably the most important cell in chronic inflammation because of the great number of biologically active products expressed by these cells [56]. Among these, growth factors are responsible for the growth of fibroblasts and blood vessels observed in both groups at the 4 week pos-implantation.

8 weeks past implantation a marked decrease in inflammation grading was detected in both experimental groups (FIGURE 7d). These findings can be related to the formation of granulation tissue, the hallmark of healing inflammation, consisting in the proliferation of fibroblasts, macrophages and vascular endothelial cells and a decrease in inflammatory cells such as PMN and lymphocytes.

The foreign body reaction (FBR), consisting mainly of macrophages and/or foreign body giant cells infiltration at the tissue-implant interface associated to the different degrees fibrosis (i.e. fibrous encapsulation) were observed at latter periods (16 and 32 weeks) of the experimental process (FIGURE 7e and 7f). With biocompatible materials, the composition of the foreign body reaction in the implant site may be controlled by the surface properties of the biomaterial, the form of the implant and the relationship between the surface area of the biomaterial and the volume of the implant [57, 58]. High surface-to-volume implants such as the BC membranes will have higher counts of macrophages and foreign body giant cells in the tissue-implant surface than will smooth-surface implants, which will have fibrosis as a significant component of the implant site.

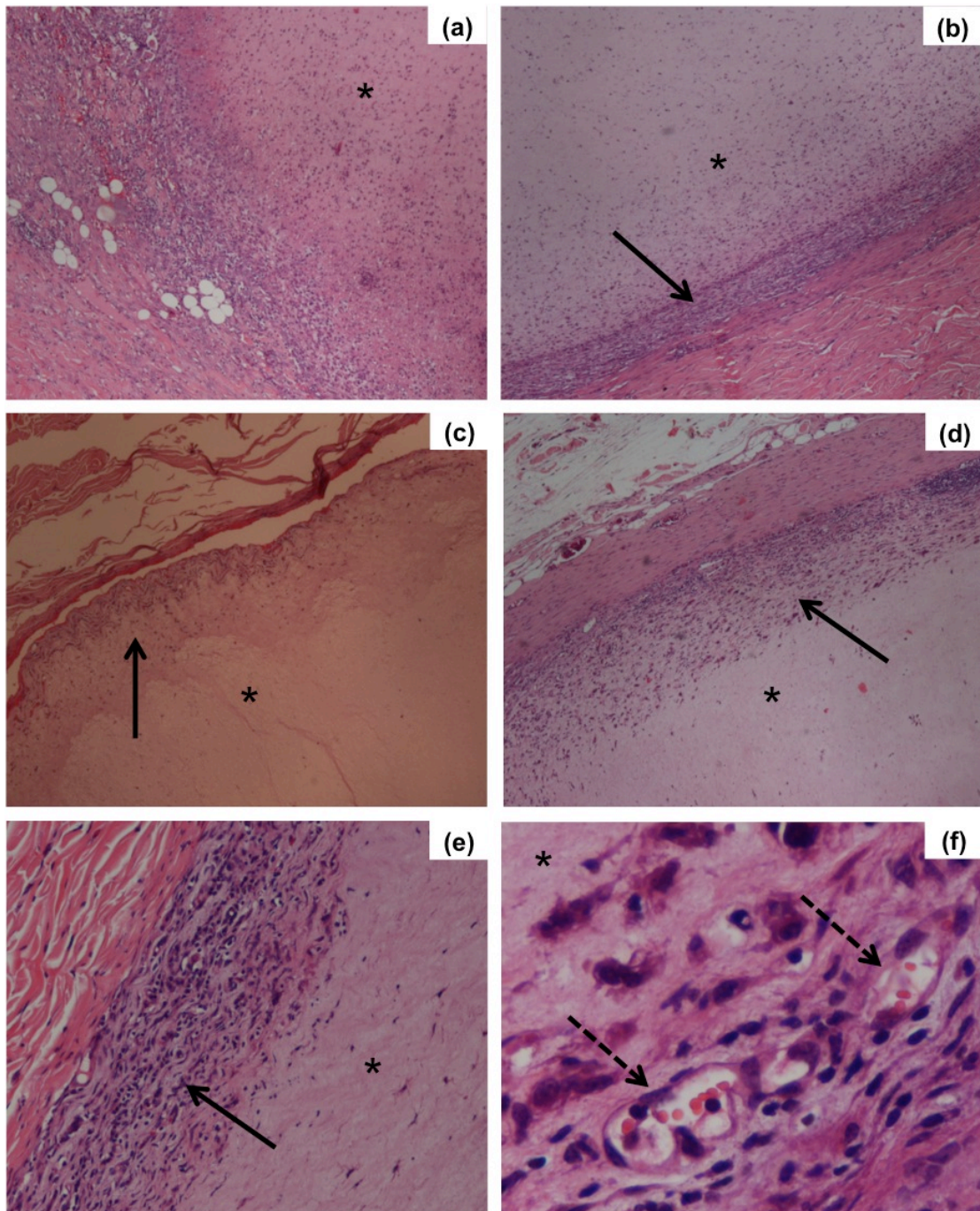


Figure 7. Histomorphology of bacterial cellulose membrane implanted subcutaneously in sheep and surrounding tissue reaction. Once there were no significant differences in biological responses by the host, the images represent the results for both groups of the post-implantation times analyzed. (a) 1, (b) 2, (c) 4, (d) 8, (e) 16 and (f) 32 weeks post-implantation. (a, b, c, d), (e) and (f), 40x, 100x and 400x ampliation, respectively (Hematoxylin - eosin staining). The solid arrows indicate the fibrous capsule formation. The dashed arrow on image (f) indicates small blood vessels formation. (*) Bacterial cellulose.

Most biomaterials of potential clinical interest typically elicit the foreign body reaction, a special form of nonspecific inflammation. The major role of the neutrophil in acute inflammation is to remove foreign materials and bacteria from the injury site through phagocytose (engulfment, followed by the killing or degradation) [59]. The form and topography of the surface of the biomaterial determine the composition of the foreign-body reaction. Relatively flat and smooth surfaces such as that found on breast prostheses have a foreign body reaction that is composed of a layer of macrophages one to two cells in thickness. Relatively rough surfaces such as those found on the outer surfaces of expanded poly tetrafluoroethylene (ePTFE) or Dacron vascular prostheses have a foreign-body reaction composed of macrophages and foreign body giant cells at the surface. Fabric materials generally have a surface response composed of macrophages and foreign body giant cells, with varying degrees of granulation tissue subjacent to the surface response. A material in a phagocytosable form (i.e., powder or particulate) may provoke a different degree of inflammatory response than the same material in a nonphagocytosable form (i.e., film) [52].

Multinucleated giant cells (formed by the fusion of monocytes and macrophages in an attempt to phagocytose the material with a size greater than the own cell) in the vicinity of a foreign body are generally considered evidence of a more severe FBR, however it is not uncommon to see very large foreign-body giant cells containing large numbers of nuclei on the surface of biomaterials, in fact the components of the FBR (giant cells and granulation tissue) may persist at the tissue-implant interface for the lifetime of the implant [22, 52]. Sonohara and Gregghi compared the biological response of Millipore membrane, Teflon and Gengiflex (a product based on bacterial cellulose) after subcutaneous implantation in rats for an experimental period of 30 days. The histological results showed that none of the material tested induced intense reaction with the host. The presence of a discrete to moderate giant cells infiltrate was observed for Millipore membrane and Teflon, in case of Gengiflex the framework was moderate to intense. [60]

Mårtson et al. [61] implanted a high purity cellulose sponge (Cellspan®) in the subcutaneous tissue of rats from 1 to 60 weeks. In that study, a mild foreign body reaction was observed at 16 weeks post-implantation, in agreement with the observation made in the present study, at the same temporal point [61]. Mårtson et al. described a decrease in the volume of amorphous cellulose implants that can be attributed to a degradation by, probably, a combination of chemical, biological and mechanical processes. At the latter stages of the

current assay (16 and 32 weeks), a change in the shape of the membrane was observed, which may be assigned to similar events, but our data do not allow an objective position regarding the possible degradation of the BC implants.

Only a few studies addressed so far the *in vivo* biocompatibility of BC. Helenius and colleagues [39] reported the histological analysis of subcutaneously implanted BC, in mice, for a period of up to 12 weeks. BC was shown to integrate well into the host tissue, with cells infiltrating the BC network and no signs of chronic inflammatory reaction or capsule formation. The formation of new blood vessels around and inside the implants was also observed, evidencing the good biocompatibility of the biomaterial.

Mendes and coworkers implanted BC subcutaneously in mice for 90 days, the results showed that the microbial cellulose membrane was found to be nonresorbable and induced a mild inflammatory response, suggesting that the membrane was well tolerated by the organism [62].

Esguerra and colleagues used another animal model to evaluate the biocompatibility of BC, polyglycolic acid and expanded polytetrafluorethylene; these materials were implanted in a dorsal skinfold chambers of Syrian golden hamsters. The authors used intravital fluorescence microscopy, histology, and immunohistochemistry to analyze the biocompatibility, neovascularization, and incorporation of each material over a time period of 2 weeks. Histology results showed that the inflammatory response to BC is similar to that of ePTFE and PGA. However angiogenesis in BC is slower and less well developed than the other materials tested [63].

Testing always leads to experimental variability, particularly tests in living systems. It should be noted that the different results obtained until now with BC implants, may be explained by the different animal species used and the different methodology applied in assessing the inflammatory reaction.

Generally, fibrosis (i.e., fibrous encapsulation) surrounds the biomaterial, isolating the implant and foreign-body reaction from the local tissue environment [52]. Our results showed that BC implants present a narrow fibrous capsule for both groups tested. The thickness of the fibrous capsule around implants placed subcutaneously has been used as a measure of the “biocompatibility” of materials. Hence, overall, from the present work, a classification of BC as a biocompatible material may be drawn. However, it is important to note that materials yielding acceptable tissue compatibility in one implantation site might yield unfavourable results in

another site [52]. Thus, to employ BC as a biomedical scaffold for artificial blood vessels requires additional compatibility studies, in which the BC is subjected to the environment that exists in the grafting site in the vasculature.

Figure 7 shows the histological photographs of bacterial cellulose membrane implanted subcutaneously in sheep and surrounding tissue reaction. Once there were no significant differences in biological responses by the host for untreated or RGD-CBM treated BC, the images represent the results for both groups of the post-implantation times analyzed. Analysis of the histological sections by light microscopy shows the maturation of the granulation tissue, with a inflammatory infiltrate of mainly polymorphonuclear cells and lymphocytes and no capsule at 1 week pos-implantation, leading the formation of a mature fibrous capsule surround the implant and presence of newly formed vessels at 32 weeks pos-implantation.

Significant differences of inflammation degree between the two groups were not observed. Although the adhesion peptide (RGD) present on BC membranes (group 2) could potentially interact with monocytes/macrophages (these cells express $\alpha_v\beta_3$ integrin) [22], influencing the adhesion and chemotaxis of these cells, a more intense infiltration of inflammatory cells was not observed.

Conclusion

Our data indicate that BC triggers a biological reaction typical of high surface-to-volume implants with an acute/subacute inflammatory reaction after 1 week pos-implantation that advance to a mild chronic inflammation confined to the implantation site and associated with neovascularisation. The presence of giant cells was observed at latter periods and a narrow fibrous capsule was present surrounding the implant. There were no significant differences on the inflammation degree between the BC coated with the recombinant protein RGD-CBM and the native BC.

The CryoSEM analysis showed that the BC tubes present a denser luminal side and a porous outer side; no orientation of the fibrils network was observed. Fluorescence microscopy reveals that apart from increasing cell adhesion, the presence of RGD stimulates the elongation and an even cell distribution, while cells coating the untreated BC are rounded and seems to form aggregates. Mechanical test results showed that small-diameter BC tube produced by our group possess an elasticity higher than human arteries and veins.

References

1. Langer R, Vacanti JP. Tissue engineering. *Science* 1993 May 14;260(5110):920-926.
2. Konig G, McAllister TN, Dusserre N, Garrido SA, Iyican C, Marini A, et al. Mechanical properties of completely autologous human tissue engineered blood vessels compared to human saphenous vein and mammary artery. *Biomaterials* 2009 Mar;30(8):1542-1550.
3. L'Heureux N, Dusserre N, Konig G, Victor B, Keire P, Wight TN, et al. Human tissue-engineered blood vessels for adult arterial revascularization. *Nat Med* 2006 Mar;12(3):361-365.
4. L'Heureux N, Paquet S, Labbe R, Germain L, Auger FA. A completely biological tissue-engineered human blood vessel. *FASEB J* 1998 Jan;12(1):47-56.
5. L'Heureux N, Germain L, Labbe R, Auger FA. In vitro construction of a human blood vessel from cultured vascular cells: a morphologic study. *J Vasc Surg* 1993 Mar;17(3):499-509.
6. Chue WL, Campbell GR, Caplice N, Muhammed A, Berry CL, Thomas AC, et al. Dog peritoneal and pleural cavities as bioreactors to grow autologous vascular grafts. *J Vasc Surg* 2004 Apr;39(4):859-867.
7. Campbell JH, Efendy JL, Campbell GR. Novel vascular graft grown within recipient's own peritoneal cavity. *Circ Res* 1999 Dec 3-17;85(12):1173-1178.
8. Andrade FK, Pertile RAN, F. D, M. GF. Bacterial Cellulose: Properties, Production and Applications. In: Lejeune A, Deprez T, editors. *Cellulose: Structure and Properties, Derivatives and Industrial Uses*: Nova Science Publishers, Inc., 2010. p. 427-458.
9. Svensson A, Nicklasson E, Harrah T, Panilaitis B, Kaplan DL, Brittberg M, et al. Bacterial cellulose as a potential scaffold for tissue engineering of cartilage. *Biomaterials* 2005 Feb;26(4):419-431.
10. Oliveira RCB, Souza FC, Castro M.
11. Fontana JD, de Souza AM, Fontana CK, Torriani IL, Moreschi JC, Gallotti BJ, et al. *Acetobacter cellulose pellicle as a temporary skin substitute*. *Appl Biochem Biotechnol* 1990 Spring-Summer;24-25:253-264.
12. Pippi NL, Sampaio AJSA. Estudos preliminares sobre o comportamento do Biofill na ceratoplastia lamelar em coelhos.
13. dos Anjos B, Novaes AB, Jr., Meffert R, Barboza EP. Clinical comparison of cellulose and expanded polytetrafluoroethylene membranes in the treatment of class II furcations in mandibular molars with 6-month re-entry. *J Periodontol* 1998 Apr;69(4):454-459.
14. Novaes AB, Jr., Novaes AB, Grissi MFM, Soares UN, Gabarra F. Gengiflex, an Alkali-Cellulose membrane for GTR: Histologic observations. *Brazilian Dental Journal* 1993;4(2):65-71.

15. Novaes AB, Jr., Novaes AB. Immediate implants placed into infected sites: a clinical report. *Int J Oral Maxillofac Implants* 1995 Sep-Oct;10(5):609-613.
16. Novaes AB, Jr., Novaes AB. Bone formation over a TiAl6V4 (IMZ) implant placed into an extraction socket in association with membrane therapy (Gengiflex). *Clin Oral Implants Res* 1993 Jun;4(2):106-110.
17. Novaes AB, Jr., Novaes AB. Soft tissue management for primary closure in guided bone regeneration: surgical technique and case report. *Int J Oral Maxillofac Implants* 1997 Jan-Feb;12(1):84-87.
18. Salata LA, Craig GT, Brook IM. In-Vivo Evaluation of a New Membrane (Gengiflex(R)) for Guided Bone Regeneration (Gbr). *Journal of Dental Research* 1995;74(3):825-825.
19. Sonohara MK, Greggi SLA.
20. Klemm D, Schumann D, Udhardt U, Marsch S. Bacterial synthesized cellulose - artificial blood vessels for microsurgery. *Progress in Polymer Science* 2001 Nov;26(9):1561-1603.
21. Brancher JA, Torres MF.
22. Anderson JM, Rodriguez A, Chang DT. Foreign body reaction to biomaterials. *Semin Immunol* 2008 Apr;20(2):86-100.
23. Czaja WK, Young DJ, Kawecki M, Brown RM. The future prospects of microbial cellulose in biomedical applications. *Biomacromolecules* 2007 Jan;8(1):1-12.
24. Watanabe K, Eto Y, Takano S, Nakamori S, Shibai H, Yamanaka S. A New Bacterial Cellulose Substrate for Mammalian-Cell Culture - a New Bacterial Cellulose Substrate. *Cytotechnology* 1993;13(2):107-114.
25. Svensson A, Harrah T, Panilaitis B, Kaplan D, Gatenholm P. Bacterial cellulose as a substrate for tissue engineering of cartilage. *Abstracts of Papers of the American Chemical Society* 2004 Mar 28;227:U282-U282.
26. Pertile RAN, Andrade FK, Alves Jr C, Gama M. Surface modification of bacterial cellulose by nitrogen-containing plasma for improved interaction with cells. *Carbohydrate Polymers* 2010 Oct; 82(3):692-698.
27. Bodin A, Ahrenstedt L, Fink H, Brumer H, Risberg B, Gatenholm P. Modification of nanocellulose with a xyloglucan-RGD conjugate enhances adhesion and proliferation of endothelial cells: Implications for tissue engineering. *Biomacromolecules* 2007 Dec;8(12):3697-3704.
28. Backdahl H, Esguerra M, Delbro D, Risberg B, Gatenholm P. Engineering microporosity in bacterial cellulose scaffolds. *Journal of Tissue Engineering and Regenerative Medicine* 2008 Aug;2(6):320-330.
29. Uraki Y, Nemoto J, Otsuka H, Tamai Y, Sugiyama J, Kishimoto T, et al. Honeycomb-like architecture produced by living bacteria, *Gluconacetobacter xylinus*. *Carbohydrate Polymers* 2007 May 1;69(1):1-6.

30. Ogawa R, Miura Y, Tokura S, Koriyama T. Susceptibilities of Bacterial Cellulose Containing N-Acetylglucosamine Residues for Cellulolytic and Chitinolytic Enzymes. *International Journal of Biological Macromolecules* 1992 Dec;14(6):343-347.
31. Lee JW, Deng F, Yeomans WG, Allen AL, Gross RA, Kaplan DL. Direct incorporation of glucosamine and N-acetylglucosamine into exopolymers by *Gluconacetobacter xylinus* (=Acetobacter xylinum) ATCC 10245: Production of chitosan-cellulose and chitin-cellulose exopolymers. *Applied and Environmental Microbiology* 2001 Sep;67(9):3970-3975.
32. Kobayashi S, Makino A, Matsumoto H, Kunii S, Ohmae M, Kiyosada T, et al. Enzymatic polymerization to novel polysaccharides having a glucose-N-acetylglucosamine repeating unit, a cellulose-chitin hybrid polysaccharide. *Biomacromolecules* 2006 May;7(5):1644-1656.
33. Fang B, Wan YZ, Tang TT, Gao C, Dai KR. Proliferation and Osteoblastic Differentiation of Human Bone Marrow Stromal Cells on Hydroxyapatite/Bacterial Cellulose Nanocomposite Scaffolds. *Tissue Eng Part A* 2009 Jan 12.
34. Grande CJ, Torres FG, Gomez CM, Carmen Bano M. Nanocomposites of bacterial cellulose/hydroxyapatite for biomedical applications. *Acta Biomater* 2009 Jan 31.
35. Millon LE, Guhados G, Wan W. Anisotropic polyvinyl alcohol-Bacterial cellulose nanocomposite for biomedical applications. *J Biomed Mater Res B Appl Biomater* 2008 Aug;86B(2):444-452.
36. Phisalaphong M, Suwanmajo T, Tammarate P. Synthesis and characterization of bacterial cellulose/alginate blend membranes. *Journal of Applied Polymer Science* 2008 Mar 5;107(5):3419-3424.
37. Andrade FK, Moreira SM, Domingues L, Gama FM. Improving the affinity of fibroblasts for bacterial cellulose using carbohydrate-binding modules fused to RGD. *J Biomed Mater Res A* 2010 Jan;92(1):9-17.
38. Andrade FK, Costa R, Domingues L, Soares R, Gama M. Improving bacterial cellulose for blood vessel replacement: Functionalization with a chimeric protein containing a cellulose-binding module and an adhesion peptide. *Acta Biomater* May 14.
39. Helenius G, Backdahl H, Bodin A, Nannmark U, Gatenholm P, Risberg B. In vivo biocompatibility of bacterial cellulose. *J Biomed Mater Res A* 2006 Feb;76(2):431-438.
40. Wippermann J, Schumann D, Klemm D, Kosmehl H, Salehi-Gelani S, Wahlers T. Preliminary results of small arterial substitute performed with a new cylindrical biomaterial composed of bacterial cellulose. *Eur J Vasc Endovasc Surg* 2009 May;37(5):592-596.
41. Backdahl H, Helenius G, Bodin A, Nannmark U, Johansson BR, Risberg B, et al. Mechanical properties of bacterial cellulose and interactions with smooth muscle cells. *Biomaterials* 2006 Mar;27(9):2141-2149.
42. Heilshorn SC, Liu JC, Tirrell DA. Cell-binding domain context affects cell behavior on engineered proteins. *Biomacromolecules* 2005 Jan-Feb;6(1):318-323.

43. Kurihara H, Nagamune T. Cell adhesion ability of artificial extracellular matrix proteins containing a long repetitive Arg-Gly-Asp sequence. *J Biosci Bioeng* 2005 Jul;100(1):82-87.
44. Cavalcanti-Adam EA, Volberg T, Micoulet A, Kessler H, Geiger B, Spatz JP. Cell spreading and focal adhesion dynamics are regulated by spacing of integrin ligands. *Biophys J* 2007 Apr 15;92(8):2964-2974.
45. Singer, II, Kazazis DM, Scott S. Scanning electron microscopy of focal contacts on the substratum attachment surface of fibroblasts adherent to fibronectin. *J Cell Sci* 1989 May;93 (Pt 1):147-154.
46. Hood JD, Cheresh DA. Role of integrins in cell invasion and migration. *Nat Rev Cancer* 2002 Feb;2(2):91-100.
47. Putra A, Kakugo A, Furukawa H, Gong JP, Osada Y. Tubular bacterial cellulose gel with oriented fibrils on the curved surface. *Polymer* 2008;49(7):1885-1891.
48. Backdahl H, Esguerra M, Delbro D, Risberg B, Gatenholm P. Engineering microporosity in bacterial cellulose scaffolds. *J Tissue Eng Regen Med* 2008 Aug;2(6):320-330.
49. Bodin A, Backdahl H, Fink H, Gustafsson L, Risberg B, Gatenholm P. Influence of cultivation conditions on mechanical and morphological properties of bacterial cellulose tubes. *Biotechnol Bioeng* 2007 Jun 1;97(2):425-434.
50. Pukacki F, Jankowski T, Gabriel M, Oszkinis G, Krasinski Z, Zapalski S. The mechanical properties of fresh and cryopreserved arterial homografts. *Eur J Vasc Endovasc Surg* 2000 Jul;20(1):21-24.
51. Purinya BA, Knets IV, Kas'yanov VA. Autogenous vein transplants in reconstructive vascular surgery. *Mekh Polim* 1975;1:153-159.
52. Ratner BD, Hoffman AS, Schoen FJ, Lemons JE. *Biomaterials science: an introduction to materials in medicine*. London, UK: Academic press, 1996.
53. Sanchavanakit N, Sangrungraungroj W, Kaomongkolgit R, Banaprasert T, Pavasant P, Phisalaphong M. Growth of human keratinocytes and fibroblasts on bacterial cellulose film. *Biotechnol Prog* 2006 Jul-Aug;22(4):1194-1199.
54. McKenna BA, Mikkelsen D, Wehr JB, Gidley MJ, Menzies NW. Mechanical and structural properties of native and alkali-treated bacterial cellulose produced by *Gluconacetobacter xylinus* strain ATCC 53524. *Cellulose* 2009;16:1047-1055.
55. Gallin J, Synderman R. *Inflammation: Basic Principles and Clinical Correlates*. 3rd ed. Philadelphia, 1999.
56. Johnston RB, Jr. Current concepts: immunology. Monocytes and macrophages. *N Engl J Med* 1988 Mar 24;318(12):747-752.
57. Rae T. The macrophage response to implant materials- with special reference to those used in orthopedics. *Crit Rev Biocompatibility* 1986;2:97-126.

58. Greisler H. Macrophage-biomaterial interactions with bioresorbable vascular prostheses. *ASAIO Trans* 1988 Oct-Dec;34(4):1051-1059.
59. Babensee JE, Anderson JM, McIntire LV, Mikos AG. Host response to tissue engineered devices. *Adv Drug Deliv Rev* 1998 Aug 3;33(1-2):111-139.
60. Sonohara MK, Greggi SLA. Avaliação da resposta biológica a diferentes barreiras mecânicas, utilizadas na técnica de regeneração tecidual guiada (RTG). *Revista da Faculdade de Odontologia de Bauru* 1994;2(4):96-102.
61. Martson M, Viljanto J, Hurme T, Laippala P, Saukko P. Is cellulose sponge degradable or stable as implantation material? An in vivo subcutaneous study in the rat. *Biomaterials* 1999 Nov;20(21):1989-1995.
62. Mendes PN, Rahal SC, Pereira-Junior OC, Fabris VE, Lenharo SL, de Lima-Neto JF, et al. In vivo and in vitro evaluation of an *Acetobacter xylinum* synthesized microbial cellulose membrane intended for guided tissue repair. *Acta Vet Scand* 2009;51:12.
63. Esguerra M, Fink H, Laschke MW, Jeppsson A, Delbro D, Gatenholm P, et al. Intravital fluorescent microscopic evaluation of bacterial cellulose as scaffold for vascular grafts. *J Biomed Mater Res A* Apr;93(1):140-149.

Chapter 6

General conclusions and future perspectives

This work consisted in the functionalization of structures based on bacterial cellulose with recombinant proteins containing a cellulose-binding module fused to an adhesion peptide and the study of the potential application of this biomaterial as blood vessel replacement. The results obtained showed that the recombinant proteins containing the RGD or GRGDY sequences were cloned and successfully expressed in fusion with a family 3 CBM of *Clostridium thermocellum* in *Escherichia coli* expression system. The recombinant proteins containing the adhesion peptide were able to promote adhesion and spreading of the fibroblasts; besides, the presence of RGD stimulates the elongation and an even cell distribution, while cells coating the untreated BC are rounded and seem to form aggregates. Furthermore, the proteins containing the sequence RGD showed a stronger effect than GRGDY on these cells. However, it seems that the second RGD or GRGDY brings no further functionality to the proteins, probably because the RGD sequence at the C-terminus of the peptide was not exposed in such a way as to be recognized by integrins. The chimeric proteins were able to enhance endothelial cells adhesion to BC and stimulate angiogenesis. However, the ingrowth of the cell through cellulose was decreased. We believe that an improved migration of the cells on BC will be achieved with an intermediary concentration of the protein used in this work. Immunocytochemistry results showed that cells grown on BC maintained their positive staining for vWF. This glycoprotein is one of the various secretory and membrane-bound molecules produced by the endothelium and has long been favored as an endothelial cell marker.

Blood compatibility studies showed that BC presents good hemocompatibility. Namely, the whole blood coagulation studies shows that the results are comparable to those produced by currently available materials for blood replacements. Taking in consideration the – presumably – much larger surface area of BC, and the possibility of having this material endothelialized (not possible with Dacron or ePTFE), the results may be considered very promising. The

adsorption of total plasma protein was not influenced by the presence of recombinant proteins (RGD-CBM), although decreasing the adhesion of fibrinogen on pure solutions. Adsorption isotherm studies showed that BC presents a higher affinity for albumin than immunoglobulin or fibrinogen. The presence of RGD on BC polymer increased platelet adhesion; however, when endothelial cells were cultured on RGD-treated BC, a confluent cell layer was formed and almost no platelets adhered to the material. Thus, the improvement of BC blood-compatibility through modification with adhesion peptides seems to be an interesting strategy as long the cellulose grafts are previously covered with endothelial cells. Nevertheless, a further characterization of the hemocompatibility is advised for future work, namely using methods for the detection of the specific activation of coagulation factors related to the contact activation pathway.

In vivo biocompatibility studies indicate that BC triggers a biological reaction typical of high surface-to-volume implants. There were no significant differences on the inflammation degree between the BC coated with the recombinant protein RGD-CBM and the native BC. The CryoSEM analysis showed that the BC tubes present a denser luminal side and a porous outer side; no orientation of the fibrils network was observed. Preliminary mechanical test results showed that small-diameter BC tube produced by our group possess an elasticity higher than human arteries and veins. However, the tensile strength was significantly lower as compared to the one exhibited by natural vessels, and therefore a method to produce tubes with improved mechanical properties is already in progress in our laboratory.

The modification of BC with the CBM technique is far from limited to the adhesion peptide. Other active groups and growth factors could be fused to the CBM domain. Also once platelets adhered to exposed RGD peptides, other peptides more specific to ECs, or different combinations of peptides should be explored. Future modifications of BC could include heparinisation to produce not only a blood compatible but also an antithrombogenic surface. Some research could be directed to the production of a more porous BC tubes that allows the in-growth of endothelial cells. In fact, our lab is currently developing a different method for the production of the tubes, with thicker and porous wall thus, improving the quality and mechanical properties of BC tubes.

The realization of *in vivo* experiments is mandatory for the effective evaluation of BC as a blood vessel substitute. These assays started indeed in the course of this work, however it has been

not possible to conclude the experiments in due time. Among other issues, evaluation of the thrombogenicity in *in vivo* conditions, suturability, mechanical performance, endothelialisation, etc, must be evaluated (assays are already ongoing).